Structural Approach to Discriminate Planar Shapes

Claude-Marie Lafforgue

A Thesis

in

The Department

of

Computer Science

Presented in Partial Fulfillment of the Requirements

for the Degree of Master of Computer Science at

Concordia University

Montréal, Québec, Canada

January 1994

ISBN 0-315-90876-9

ABSTRACT

Structural Approach to Discriminate Planar Shapes

Claude-Marie Lafforgue

This thesis explores a way to use syntactic contour information primitives described by a set of twelve basic topological configurations to encode the emerging geometric patterns of a planar shape into an ordered sequence or string of features for the purpose of recognition. Feature strings generated from training data are used to construct a digital search tree for each class of objects to be recognized. In linguistic analogy, a figure can be thought of as a "word" (path), the concatenation of shape patterns composing it as "syllables" (sequence of vertices) and the shape relations themselves as "letters" (nodes). The recognition process is then analogous to matching a word in a set of dictionaries. Statistical information is gathered at each tree vertex and this knowledge is used in a classifier. Without knowledge of the mechanics of the probabilistic process which generates feature strings, a function discriminating feature strings in different trees can only be approximated. Extensive experimental results are presented and a method to extract canonically formed substructures of the planar shapes is proposed in order to reduce the representation of classes. Further developments to the basic methodology are discussed and suggested.

ACKNOWLEDGMENTS

A warm, heart felt thank you to an exceptional group of friends, for their patience and understanding, soon to be Dr. Henry Polley, Dr. Marc Comeau and Mr. Roberto Girolami. Henry, for sharing your insight in Parallel Computer Architecture, your programming expertise, but most of all, "thank you for the sockets"!!! My dear Marc, your mathematical intuition was invaluable as were your revisions and encouragement. Rob, my friend, for helping me in the final stages of preparation, when time was of the essence, I wish to express my gratitude.

Dr. Pervez Ahmed, my initial supervisor, to you I extend my appreciation for suggesting the starting point of this work with the use of your edges and their relationships. My only regret is that you are not here at the final stage of my thesis.

Soon to be Dr. Raymond Legault, thank you for helping me get started with the contour extraction phase and always being available to answer my questions.

Dr. Suen, thank you for taking over supervision after Dr. Ahmed's departure, and most of all thank you for your support and your unshakeable belief in me.

I would also like to mention the financial contribution of the Fondation Desjardins for the grant I received in the academic year 1990-1991. Becoming the beneficiary of this subsidy was a great honor, as I was competing with four hundred and one candidates coming from both the master's level and the doctoral level within the Province of Québec.

For these contributions, words cannot express...

DEDICATION

I would like to dedicate this thesis to my family, for believing in me and encouraging me ... always. I love you. Also to the memory of my granny Berthe Dazé (nee Dagenais). I miss you.

EPIGRAM

This is the end of something old,
Or the beginning of something new,
A mark in time,
A statement of self, myself,
A period of transition ...
The conclusion
Of an era.

TABLE OF CONTENTS

LIST OF FIGURES xi
LIST OF TABLES xv
LIST OF NOTATIONS xvii

CHAPTER 1

INTRODUCTION

1.1 Introduction 1
1.2 Motivation for this Research 4
1.3 Proposed Recognition Scheme 5
1.4 Thesis Outline 6
1.5 Database 6

CHAPTER 2

PREPROCESSING

2.1 Introduction 10
2.2 Edge Smoothing 10
2.3 Small Random Cavities 12
2.4 Connectivity 13

CHAPTER 3

CONTOUR EXTRACTION

3.1 Introduction 18
3.2 Edge Types and Edge-to-Edge Relationships 18
3.3 Extraction of Components and Edges 22
3.4 Contour Extraction from Edge Chains 28

CHAPTER 4

FEATURE EXTRACTION

4.1 Introduction 31
4.2 Processing of Outer and Inner Contours 31
4.3 Selection of Reference Points 32
4.4 Feature String 35
4.5 Superimposed Edge Points 43
4.6 Treatment of Holes 47

CHAPTER 5

CLASSIFICATION ALGORITHM

5.1 Introduction 52
5.2 A Simple Representation, a Trie 52
5.3 Probability Distribution of the Classes 60
5.4 Goodness of Fit Measure 66
5.5 Decision Making Process 68

CHAPTER 6

PRELIMINARY STATISTICAL INFORMATION

6.1 Introduction 71
6.2 Hole Statistics 71
6.3 Relation Counts and Relative Frequencies 72
6.4 Quadrant Parameters 84
6.5 Statistical Parameters of the Tries 97

CHAPTER 7

EXPERIMENTAL RESULTS

7.1 Introduction 100
7.2 Experimental Results 100
7.3 Analysis of Errors 112
7.4 Sensitivity of Recognition 123

7.5 Observation of a Sample 131
7.6 Goodness of Fit of the Samples in Appendix A 137
7.7 Comparison to other Recognition Schemes 154

CHAPTEP 8

DISTRIBUTED PROCESSING

8.1 Introduction 157
8.2 Implementation 158

CHAPTER 9

CONCLUSION AND FUTURE DEVELOPMENTS

9.1 Introduction 161
9.2 Summary and Contributions 161
9.3 Discussion 165
9.4 Descriptive Shape Strings 167
9.5 The "Sliding Window" Technique 168
9.6 Conclusion 186

REFERENCES 188

APPENDIX A

SAMPLES FROM THE DATA SET

A.1 Samples of Zero 197
A.2 Samples of One 198
A.3 Samples of Two 199
A.4 Samples of Three 200
A.5 Samples of Four 201
A.6 Samples of Five 202
A.7 Samples of Six 203
A.8 Samples of Seven 204
A.9 Samples of Eight 205
A.10 Samples of Nine 206

APPENDIX B

FEATURE VECTORS

B.1 Feature Strings for Digit 0 208
B.2 Feature Strings for Digit 1 210
B.3 Feature Strings for Digit 2 211
B.4 Feature Strings for Digit 3 216
B.5 Feature Strings for Digit 4 218
B.6 Feature Strings for Digit 5 222
B.7 Feature Strings for Digit 6 224
B.8 Feature Strings for Digit 7 227
B.9 Feature Strings for Digit 8 228
B.10 Feature Strings for Digit 9 234

APPENDIX C

TREES

C.1 Tree for Digit 0 238
C.2 Tree for Digit 1 239
C.3 Tree for Digit 2 240
C.4 Tree for Digit 3 241
C.5 Tree for Digit 4 242
C.6 Tree for Digit 5 243
C.7 Tree for Digit 6 244
C.8 Tree for Digit 7 245
C.9 Tree for Digit 8 246
C.10 Tree for Digit 9 247

SUBTREES

C.11 First Level Subtrees for Digit 0 249
C.12 First Level Subtrees for Digit 1 251
C.13 First Level Subtrees for Digit 2 254
C.14 First Level Subtrees for Digit 3 256
C.15 First Level Subtrees for Digit 4 258
C.16 First Level Subtrees for Digit 5 261
C.17 First Level Subtrees for Digit 6 264
C.18 First Level Subtrees for Digit 7 267
C.19 First Level Subtrees for Digit 8 270
C.20 First Level Subtrees for Digit 9 274

LIST OF FIGURES

CHAPTER 1

INTRODUCTION

1.1 Some Tools for a Pattern Recognition Tool Kit 2
1.2 Example of Run-Length Code 8
1.3 Conceptual Representation of the Data Acquisition Phase 9

CHAPTER 2

PREPROCESSING

2.1 Edge Smoothing Templates 11
2.2 Example of Small Random Cavities 13
2.3 Adjacency 14
2.4 8-Connectivity Closes Holes 14
2.5 Hole Split into 4 Small Holes 15
2.6 Contour Tracing 17

CHAPTER 3

CONTOUR EXTRACTION

3.1 Basic Edge Definition (Horizontal Scan) 19
3.2 Twelve Possible Shapes 21
3.3 Binary Image of a Sample of Digit 2 23
3.4 The Various States 24
3.5 Digit 2, Pattern 109, Horizontal Scanning (Vertical Edges) 26
3.6 Digit 2, Pattern 109, Vertical Scanning (Horizontal Edges) 27
3.7 Digit 2, Pattern 109, Horizontal Scanning 29
3.8 Digit 2, Pattern 109, Vertical Scanning 30

CHAPTER 4

FEATURE EXTRACTION

4.1 Bolded Reference Points of Digit 2 Pattern 109 33
4.2 Reference Points and Point Number 34
4.3 Superimposed Scans and Counter-Clockwise Extraction of Reference Points 38
4.4 Equivalent Shape Strings in our Data Sets 39
4.5 Grid with Quadrant Numbers 40
4.6 Reference Points Localized in a 4x3 Quadrant Configuration and the Generated Feature String 41
4.7 Reference Points Localized in a 3x3 Quadrant Configuration and the Generated Feature String 42
4.8 Digit 1, Pattern 111, Training A, Horizontal Scanning 44
4.9 Digit 1, Pattern 111, Training A, Vertical Scanning 45
4.10 Digit 0 with a Detailed Inner Contour, Horizontal Scan 50
4.11 Digit 0 with a Detailed Inner Contour, Vertical Scan 51

CHAPTER 5

CLASSIFICATION ALGORITHM

5.1 A Trie 54
5.2 Trie Representation of Digit 1 56
5.3 Preorder Numbering for a Trie 58
5.4 Passage Count Relation for a General Trie Node 59
5.5 Portion of the Intersection of the Distributions of $\mathcal{T}_c$ and $\mathcal{T}_d$ 63
5.6 Learning the Distribution of $\mathcal{T}_c$ through Training 64
5.7 Variables Used by the Decision Making Process 70

CHAPTER 6

PRELIMINARY STATISTICAL INFORMATION

6.1 Relation Histograms for Digits 0 and 1 79
6.2 Relation Histograms for Digits 2 and 3 80
6.3 Relation Histograms for Digits 4 and 5 81
6.4 Relation Histograms for Digits 6 and 7 82
6.5 Relation Histograms for Digit 8 and 9 83

6.6 Quadrant Averages and Shading for Digit 0 86
6.7 Quadrant Averages and Shading for Digit 1 87
6.8 Quadrant Averages and Shading for Digit 2 88
6.9 Quadrant Averages and Shading for Digit 3 89
6.10 Quadrant Averages and Shading for Digit 4 90
6.11 Quadrant Averages and Shading for Digit 5 91
6.12 Quadrant Averages and Shading for Digit 6 92
6.13 Quadrant Averages and Shading for Digit 7 93
6.14 Quadrant Averages and Shading for Digit 8 94
6.15 Quadrant Averages and Shading for Digit 9 95
6.16 Quadrant Averages and Shading over all Sample Data : " The Slant Phenomenon " 96

CHAPTER 7

EXPERIMENTAL RESULTS

7.1 Recognition Graphs 109
7.2 Substitution Graphs 111
7.3 Confusion Plots for Samples of Digit 0 113
7.4 Confusion Plots for Samples of Digit 1 114
7.5 Confusion Plots for Samples of Digit 2 115
7.6 Confusion Plots for Samples of Digit 3 116
7.7 Confusion Plots for Samples of Digit 4 117
7.8 Confusion Plots for Samples of Digit 5 118
7.9 Confusion Plots for Samples of Digit 6 119
7.10 Confusion Plots for Samples of Digit 7 120
7.11 Confusion Plots for Samples of Digit 8 121
7.12 Confusion Plots for Samples of Digit 9 122
7.13 Recognition Rates of Digits with all Inner Contours versus those with a Limited Number of Inner Contours 124
7.14 Recognition Rates in Various Grids 126
7.15 Digit Recognition Rates in Various Grids 130
7.16 Digit 5, Pattern 178 from TrB, Horizontal Scanning 132
7.17 Digit 5, Pattern 178 from TrB, Vertical Scanning 133

CHAPTER 8

DISTRIBUTED PROCESSING

8.1 Distributed Processing Architecture 159

CHAPTER 9

CONCLUSION AND FUTURE DEVELOPMENTS

9.1 Canonical Tree Model 172
9.2 Relation Histograms in Clusters for Digits 0 and 1 180
9.3 Relation Histograms in Clusters for Digits 2 and 3 181
9.4 Relation Histograms in Clusters for Digits 4 and 5 182
9.5 Relation Histograms in Clusters for Digits 6 and 7 183
9.6 Relation Histograms in Clusters for Digits 8 and 9 184

LIST OF TABLES

CHAPTER 4

FEATURE EXTRACTION

4.1 Extended Sample Set Sizes 46

CHAPTER 5

CLASSIFICATION ALGORITHM

5.1 Feature Strings for Digit 1 55

CHAPTER 6

PRELIMINARY STATISTICAL INFORMATION

6.1 Average Hole Count per Digit 72
6.2 Counts of Horizontal Relations 73
6.3 Count of Vertical Relations 74
6.4 Average Numbers of Horizontal Relations per String 74
6.5 Average Numbers of Vertical Relations per String 75
6.6 Statistics on the Number of Relations in a String 76
6.7 Relative Frequencies of the Horizontal Relations 77
6.8 Relative Frequencies of the Vertical Relations 77
6.9 Decreasing Sequence of Sets 78
6.10 Relation Count per Quadrant for each Digit in a 4x3 Grid 84
6.11 Relation Count per Quadrant for each Digit in a 3x3 Grid 85
6.12 Tabulated Trie Outlook 98
6.13 Number and Percentage of Nonleaf Terminals 99

CHAPTER 7

EXPERIMENTAL RESULTS

7.1 Results for Training Set A in a 4x3 Quadrant Frame 102
7.2 Results for Training Set B in a 4x3 Quadrant Frame 103
7.3 Results for the Testing Set in a 4x3 Quadrant Frame 104
7.4 Results for Training Set A in a 3x3 Quadrant Frame 105
7.5 Results for Training Set B in a 3x3 Quadrant Frame 106
7.6 Results for the Testing Set in a 3x3 Quadrant Frame 107
7.7 Total Number of Matches Per Digit per Set for 4x3 Quadrants 108
7.8 Total Number of Matches Per Digit per Set for 3x3 Quadrants 108
7.9 Total Number of Errors Per Digit per Set for 4x3 Quadrants 110
7.10 Total Number of Errors Per Digit per Set for 3x3 Quadrants 110
7.11 Error Analysis (Normalization to 486+600=1086) 112
7.12 Minimum and Maximum String Lengths 125
7.13 Height/Width Ratio 128
7.14 Best Matches Generated by our String in a 4x3 Grid 135
7.15 Best Matches Generated by our String in a 3x3 Grid 136
7.16 Comparison Table 155

CHAPTER 9

CONCLUSION AND FUTURE DEVELOPMENTS

9.1 Clusters of Size ≥ 10 170
9.2 Canonical Feature Vectors 174
9.3 Counts of Horizontal Relations in the Clusters 175
9.4 Counts of Vertical Relations in the Clusters 175
9.5 Statistics of the Number of Relations in a String in a Cluster 176
9.6 Relative Frequencies of Horizontal Relations in the Clusters 177
9.7 Relative Frequencies of Vertical Relations in the Clusters 177
9.8 Decreasing Sequence of Selected Canonical Sets 178
9.9 Decreasing Sequence of Original Sets 179

LIST OF NOTATIONS

Database

Tr	Training set
Tr_A	Training set A composed of 2000 samples, i.e. 200 samples per class
Tr_B	Training set B with similar characteristics to Tr_A
$Ext(T_c)$	Extended sample set size for class c which contains all 400 samples coming from each class, i.e., of the union of Tr_A and Tr_B

$$Tr_A = \sum_{s=1}^{2000} Tr_{A_s} = \sum_{i=0}^{9}\left(\sum_{j=1}^{200} Tr_{A_j}\right)$$

Edge Types and Relationships

e_k^m	edge of type m with sequence number k, where $1 \leq m \leq 4$ and $k \geq 1$
HR_i	horizontal scan, relation number i for the selected reference point, where $1 \leq i \leq 12$
VR_j	vertical scan, relation number j for the selected reference point, where $1 \leq j \leq 12$

Classification Algorithm

$Pass_j$	passage count for the jth string in the clump, $j = 1, ..., n$
$Term_j$	terminal count for the jth string in the clump, $j = 1, ..., n$
Rem_j	remaining number of occurences of training strings terminating within the proper subtree, i.e., not including the root, $Rem_j \geq 0$
T_c	trie for class c
s_i	passage count for nodes $i = 0, 1, ..., \lvert T_c \rvert - 1$
t_i	terminal count for nodes $i = 0, 1, ..., \lvert T_c \rvert - 1$ where $t_i = 0$ when node i is a nonterminal and $t_i = Term_j$ when node j is the jth terminal node
$\mathscr{T}_c$	universel trie for class c representing the sample space of all possible class c feature strings
F_c	arbitrary feature string for class c
$\mathscr{T}_{ck}$	subtree of $\mathscr{T}_c$ rooted at node k
$F_x = \mathscr{T}_{ck}$	means that a feature string F_x from an unknown class x terminates at node k of $\mathscr{T}_c$
$F_x \in \mathscr{T}_{ck}$	means that a feature string F_x from an unknown class x terminates at some node within the subtree $\mathscr{T}_{ck}$
$P(F_x = \mathscr{T}_{ck})$	probability of feature string terminating at node k in $\mathscr{T}_c$
$P(F_x \in \mathscr{T}_{ck})$	accumulated distribution of feature strings with a prefix terminating at node k in associated $\mathscr{T}_c$
$F_c^i \in \mathscr{T}_{ck}$	event in the matching process

$\{F_c^i \in T_{ck_i}\}_{i=1,\ldots,u}$

set of strings in T_c with a minimum number of differing relations

w_{k_i} relative frequency of the ith event in $\{F_c^i \in T_{ck_i}\}_{i=1,\ldots,u}$

s_{k_i} passage count of the node k_i in T_c

Q_X quadrant string associated to each feature string F_X, localizing each shape relation of F_X in some grid quadrant of the image

$Q_x(\ell)$ quadrant associated with the ℓth shape relation in F_X

$Q_c^i(\ell)$ averaged quadrant for the ℓth shape relation in a string $F_c^i \in T_c$ against which F_X is compared

$D_c^i(\ell)$ quadrant distances $|Q_x(\ell) - Q_c^i(\ell)|$, where $\ell = 1, \ldots, \text{length}(Q_c^i(\ell))$

$D_c^i(F_x)$ distance between strings F_X and F_c^i

$B_c^i(F_x)$ termination attribute "term bias" which adjusts the relative frequency measure $W_c^i(F_x)$ for strings F_X terminating at nonterminals in T_c

$E_c(F_X)$ goodness of fit measure

$E_c^i(F_x)$ goodness of fit between the incoming string F_X and the string F_c^i in T_c

M_{ck}	minimum number of misses that occur in the subtrie T_{ck} during traversal
m_{ck}	binary variable in the subtrie T_{ck}, which indicates whether or not a miss occurs at node k, i.e., $m_{ck} = 1$ if a miss occurs at node k and $m_{ck} = 0$, otherwise
d_{ck}	quadrant distance measure for relations compared at node k in the subtrie T_{ck}
D_{ck}	variable used to accumulate the distance measure for the best path in T_{ck}
W_{cn_j}	relative frequency associated with node $n_j \in T_{cj}$
B_{cn_j}	terminal bias associated with node $n_j \in T_{cj}$

Statistical Information

H COUNTS	counts of individual horizontal relations H_1, H_2, H_3, H_4, H_5, H_6, H_7, H_8, H_9, H_{10}, H_{11}, H_{12}
V COUNTS	counts of individual vertical relations V_1, V_2, V_3, V_4, V_5, V_6, V_7, V_8, V_9, V_{10}, V_{11}, V_{12}
n_{ijk}	frequency count of the individual shape feature k for string j of digit i
p_{ijkm}	step position of an mth occurrence of relation k for string j of digit i
q_{ijkm}	quadrant coefficient at p_{ijkm}
W_{ik}	relative frequency of relation k of digit i

CHAPTER 1

INTRODUCTION

1.1 Introduction

Increasingly popular in the world of solving complex pattern recognition problems, is the use of hybrid methodologies integrating multiple paradigms. The following statement appeared in [KANA72] and was taken from [KANA93]:

> "It is now recognized that the key to pattern recognition problems does not lie wholly in learning machines, statistical approaches, spacial filtering, heuristic programming, formal linguistic approaches, or in any particular solution which has been vigorously advocated by one or another group during the last one and a half decades as the solution to the pattern recognition problem."

A statement made by Marvin Minsky in 1991 was also stated in the same article:

> In the 1960's and 1970's students frequently asked, "Which kind of representation is best", and I usually replied that we'd need more research before answering. But now I would give a different reply: "To solve really hard problems, we'll have to use several different representations."

Later in the same article Minsky continues:

"It is time to stop arguing over which type of pattern-classification technique is best because that depends on our context and goal. Instead we should work at a higher level of organization and discover how to build managerial systems to exploit the different virtues and evade the different limitations of each of these ways of comparing things."

Figure 1.1 displays some of the tools currently available in the pattern recognition tool kit, and some of the problems to which these tools have been applied [KANA93].

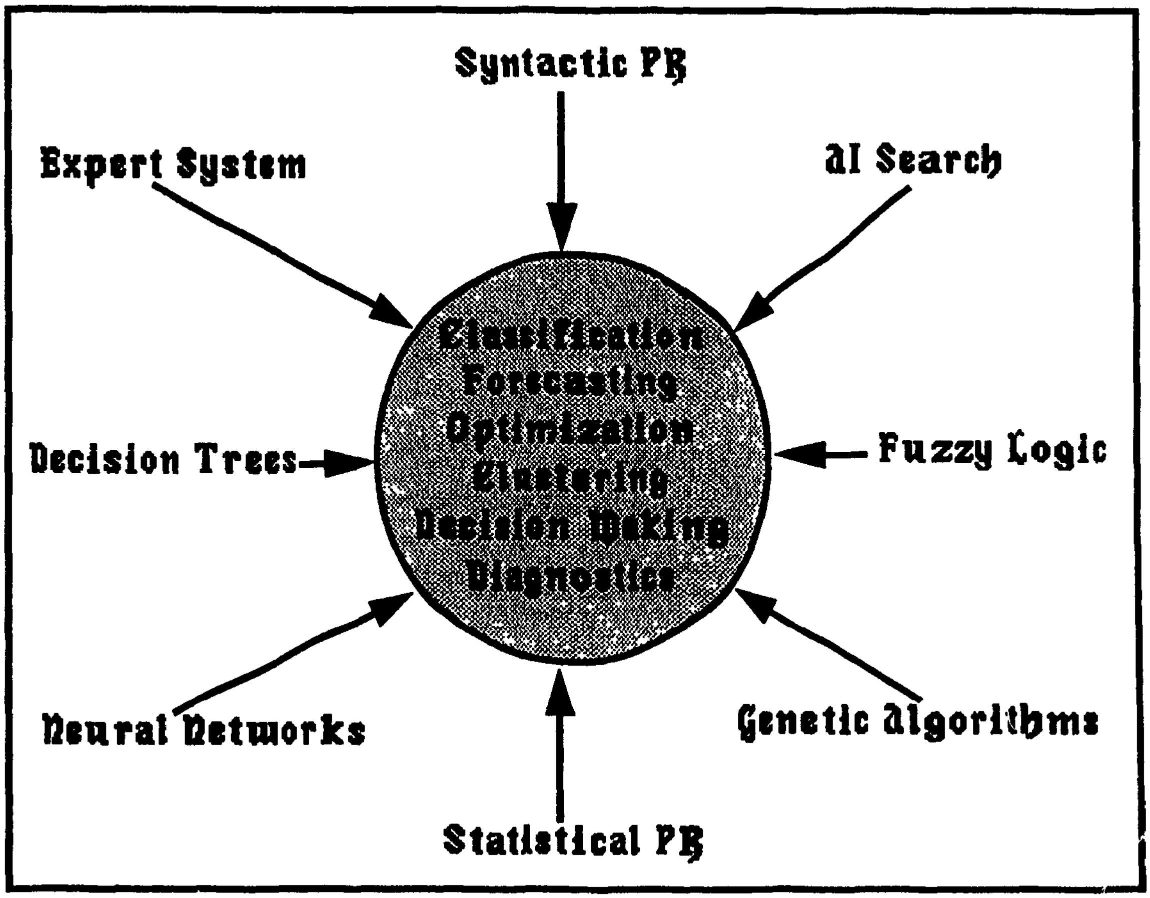

Figure 1.1 Some Tools for a Pattern Recognition Tool Kit

The statistical and the structural approaches are two general methods used for the process of pattern recognition [ENCY93]. In a purely statistical approach, a multi-dimensional *feature space* is partioned into decision regions. An unknown pattern is assigned the label of the class region containing its *feature vector*. The statistical approach requires a probability measure and general distance measures over the feature space in order to define decision regions. Structural approaches use a small set of pattern *primitives* as features and examine the relationships among them in order to determine how patterns arise from their primitives. Statistical and other discriminating information may be incorporated in the classification procedure. A large part of structural pattern recognition, known as syntactic pattern recognition, uses language theory to describe the composition of the patterns in terms of their primitives through the production rules of some underlying grammar.

An introduction to the area of statistical or decision-theoretic pattern recognition can be found in the texts [CHEN73], [YOCA74], [FUKU72] and the collection of papers on statistical methods [DEKI82]. For an introduction to the area of structural and syntactic pattern recognition, the reader is referred to the texts [FUKS82], [PAVL77], [FUKS74]. Structural characterizations of patterns in terms of primitives are many and varied as there is a multitude of possible features which may be extracted or derived as pattern primitives. Geometric features such as strokes, bars, hooks, arches, loops, cross points, end points and the like have typically been used as the basis for pattern recognition schemes [CHER88], [BERT82], [SUEN82], [YHGR81], [PAVL76], [FREE62].

A historical review of the research in pattern recognition covering the period from 1968 to 1974 can be found in [KANA74]. Some of the major areas of research in pattern recognition are discussed in the text [DEKI86] and some excellent surveys on the state of the art can be found in the papers [MOSY92], [TASW90], [SUEN82]. Implementation issues for pattern recognition systems are the focus of the collection of papers [SIMO89]. Most recently, the paper [LESR93] contains a performance comparison of a number of pattern recognition algorithms using various approaches.

1.2 Motivation for this Research

This thesis evolves from Pervez Admed's Ph.D. Thesis on the recognition of handwritten zip codes by edge detection. In his work, Ahmed implements a new approach to extract structural features such as holes, simple cavities and end points based on contour information. He uses a relational data-model to organize the information related to each shape and applies a fuzzy-set-theoretic technique along with this structural approach, to identify unknown characters.

The prime objective of this research is to develop a system capable of identifying planar shapes. Our method is based on edge classification and the relationships resulting from the concatenation of edges serve as a basis for a statistical approach. A second objective of this work is to gather statistical information and infer some of the properties of this feature-based representation of handwritten numerals.

The shapes used were connected but otherwise unconstrained handwritten numerals and we applied our system to the identification of these unknown characters. The proposed scheme can be adapted to different sets of planar shapes, such as the ASCII character set, machine parts, or arbitrary sets of objects, by incorporating minor modifications. Such alterations to the methodology would be incurred due to the presence of detached elements if any.

The construction of the model is oriented towards a self-training approach where associated weights are modified rather than the underlying rules. Similar regions of planar shapes are clustered as occurrences of successive edge relations by this approach.

Due to the large variety of shapes, sizes, stroke, thicknesses and orientations within each class, the database must be representative of the population for this scheme to perform well.

The implementation is done on a simulated distributed computing environment in order to mimic high performance speeds required for real time recognition.

1.3 Proposed Recognition Scheme

Preprocessing techniques have been applied to all the character images considered. The use of contour tracing for feature extraction is the principal starting point for this work. Contours are scanned both horizontally and vertically in order to retain sufficient descriptive information, and special reference points are selected and identified by shape relations. These pattern primitives are incorporated in a shape-string feature vector and associated with each one of these basic elements is specific statistical information characterizing the shape relations.

This knowledge is expressed with the use of decision trees (refer to Appendix C) with their nodes representing the relations extracted at specific (x,y) coordinates, which we will call the selected reference points.

These search trees are called *tries* and were originally introduced by Fredkin in 1960 [STAN80]. The reference points, associated with shape relations, are the tree nodes where statistical properties of structural features are introduced. This collection of trees represents our knowledge base.

The statistics gathered are used to create a probabilistic framework underlying the recognition scheme.

1.4 Thesis Outline

Chapter 2 contains the smoothing templates used for data enhancement and describes the connectivities used for contour following. Chapter 3 details the basic edge definition and shape topologies presented in [AHME86], [AHSU87]. Edge extraction is introduced and the scans are discussed. Chapter 4 deals with feature extraction and string definition. The classification algorithm is presented in Chapter 5. All preliminary statistical information is put forth in Chapter 6 and Chapter 7 introduces the experimental results. The simulated multiple processor architecture implemented is illustrated in Chapter 8 and in Chapter 9, we propose further developments to the basic methodology.

1.5 Database

The data used for this proposed recognition scheme was originally collected from the dead letter envelopes by the U.S. Postal Services at different American locations and served to create the first U.S. zipcode database of the Concordia University OCR research team.

The region of the paper where the characters (patterns) were written was optically scanned so as to preserve the pattern as a two-dimensional array whose values were represented by 16 shades of gray from white to black on a 64x224 grid of 0.153 mm^2 elements. The obtained resolution was approximately 166 DPI.

These images were enhanced iteratively and when a proper threshold was derived, dimensionality reduction from 16 levels of gray to 2 was established. The picture was now black and white, a condition called binarization referring to the 2 levels of gray. Segmentation was effected when five body regions (5 numbers) per zipcode were attained providing us with single-body region binary images. The resulting numerals were run-length encoded. An example of run-length code follows in Figure 1.2. The first two numbers represent the row and column sizes. These values are followed by alternations of white and black pixel counts per row. If a row starts by a black pixel, the count will start by 0. When a sum of these values is equal to the number of columns, we know that we have passed to the next row.

```
. . * * * . .      2 3 2
. * * * * * .      1 5 1
* * . . . * *      0 2 3 2
* * . . . * *      0 2 3 2
* * * * * * *      0 7
. . * * * * .      2 4 1
. . * * . . .      2 4 1
. . * * . . .      2 2 3
                   2 2 3

Run-lengthcode:
8 7 2 3 2 1 5 1 0 2 3 2 0 2 3 2 0 7 2 4 1 2 4 1 2 2 3 2 2 3
```

Figure 1.2 Example of Run-Length Code

The conceptual representation of the data acquisition phase can be seen in Figure 1.3.

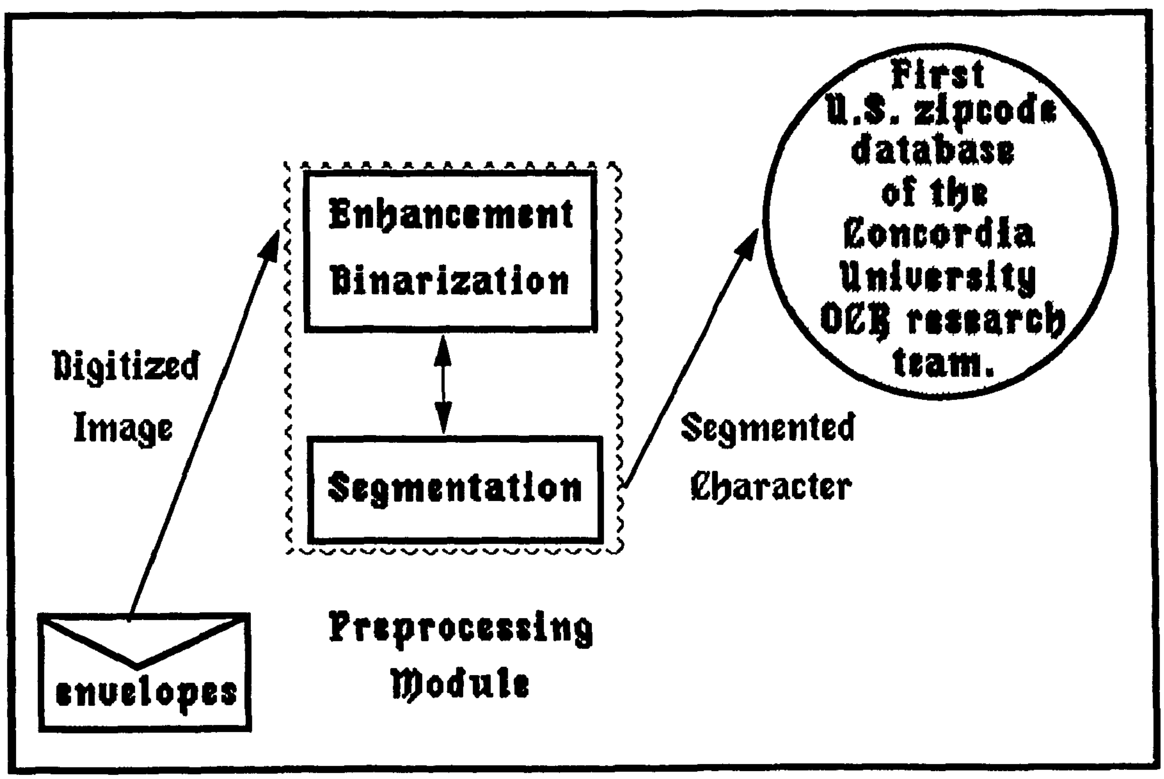

Figure 1.3 Conceptual Representation of the Data Acquisition Phase

The zip codes used were handwritten and totally unconstrained. There were, therefore, numerous styles and sizes for each character. Assuming each envelope came from a different source, we have many writers and a large variety of writing instruments used on a wide range of paper quality and color.

The OCR research team of Concordia University prepared three standard sets of 2000 digits, each incorporating 200 samples for each numeral or class. Two sets are used for training while one is used as the testing set.

CHAPTER 2

PREPROCESSING

2.1 Introduction

It is important to preserve the truly descriptive features of a contour, but it is also necessary to make an effort to remove insignificant characteristics that exist due to digitization, ink flow, paper quality, etc. As we revealed in Section 1.5, significant enhancement was done before data acquisition at the time the database was generated. The additional preprocessing effected prior to the feature extraction phase shall be presented in this chapter.

2.2 Edge Smoothing

Prior to edge extraction, smoothing is performed based on template matching [NALS90], which is briefly described here.

Let us define a component list as a sequence of similar pixels in a row. These may either be background pixels "." or object pixels "*". For further reference, we will label the various cases (using "*" for object pixel, "." for background and "?" for either, i.e. object or background).

Preprocessing is effected by a smoothing window which slides over the area of the image and modifies its pixels according to a given rule for each window template. Figure 2.1 illustrates the various templates. When the image in the window matches one of the templates, the center pixel is either filled with a "*", becoming part of the object, or deleted by replacing it with a ".", becoming part of the background. Five templates are used for filling and eight are used for deleting.

Templates for filling:

```
? * ?     ? * .     . * ?     ? * ?     . . .
* . *     * . .     . . *     * . *     * . *
? * ?     ? * .     . * ?     . . .     ? * ?
(F1)      (F2)      (F3)      (F4)      (F5)
```

Templates for deletion

```
. . ?     . . *     * . .     ? . .
. * *     . * *     * * .     * * .
. . *     . . ?     ? . .     * . .
(D1)      (D2)      (D3)      (D4)

* * ?     . . .     . . .     ? * *
. * .     . * .     . * .     . * .
. . .     * * ?     ? * *     . . .
(D5)      (D6)      (D7)      (D8)
```

Figure 2.1 Edge Smoothing Templates

Edge smoothing is essentially a filtering operation which makes edge extraction more efficient.

2.3 Small Random Cavities

In an attempt to remove meaningless small cavities due to "salt-pepper" (random) noise, etc., the following approach has been proposed. Patterns are scanned both horizontally and vertically. All the filling and deletion of pixels is done during the horizontal scanning as all symmetries are examined by our smoothing templates. If we perform 90-, 180- and 270-degree rotations of F2, D1 and D2, we obtain all other F and D patterns seen in Figure 2.1.

The component lists of interest to us are the ones comprised of object pixels "*". These lists are checked for smoothing. Looking at the following line, there are two object component lists:

. . * * * * . . . * * * * . . .

The pixels affected by the first component list, i.e. the ones that will be checked, are indicated by a ?:

. ? ? * * ? ? . . * * * * . . .

As can be seen, only four pixels may be affected. It is important to note that if a component starts or ends at a picture boundary, it's bordering neighbour is considered to be a background pixel. Once an object component list (or black run) has been located, its end pixels, as well as their neighbouring background pixels are checked by template matching. In this way, we avoid moving a small 3x3 window over every single pixel.

The component lists for the first and last rows are treated in a particular way: components which are separated by less than a few background pixels are merged; the actual number of background pixels depends on image size.

This removes a number of small random cavities which represent the overwhelming majority of the insignificant features appearing randomly along the contours of our database numerals. Figure 2.2 gives us an example of this type of situation.

```
             1                                  1
    123456789012345678                 123456789012345678

 1  .*****************              1  .*****************
 2  ******************              2  ******************
 3  ******************              3  ******************
 4  ............*****.              4  ............*****.
 5  ..........*******.              5  ..........*******.
 6  ........********..              6  ........********..
 7  ......**********..              7  ......**********..
 8  .....**********...              8  .....**********...
 9  ...**********.....              9  ...**********.....
10  ..**************..             10  ..**************..
11  ..****************             11  ..****************
12  ...*.*.*.*********             12  ...*.*.*.*********
13  ...........*******             13  ...........*******
14  . ...........*****.            14  ............*****.
15  ...........*****..             15  ...........*****..
16  ..**......*****...             16  ..**......*****...
17  .**......*****....             17  .**......*****....
18  ***....******.....             18  ***....******.....
19  ***********.......             19  ***********.......
20  **********........             20  **********........
21  .*******..........             21  .*******..........
22  ..*****...........             22  ..*****...........
```

Figure 2.2 Example of Small Random Cavities

2.4 Connectivity

In order to define the contours of a binarized object, we need the notions of pixel adjacency and connectivity. In the Cartesian coordinate system, a point can be considered *adjacent* to either 4 or 8 surrounding points as shown in Figure 2.3. These two adjacencies are known as 4-adjacency and 8-adjacency, respectively. Two pixels are said to be *connected* if their points are adjacent. Hence, we have the notion of 4-connectivity and 8-connectivity for 4-adjacent and 8-adjacent pixels, respectively.

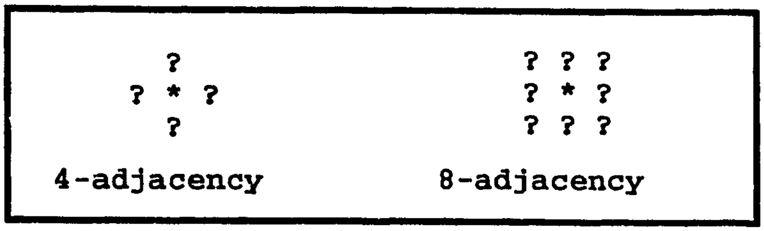

Figure 2.3 Adjacency

The use of 8-connectivity for the foreground improves contour quality and helps in preserving continuity. This connectivity helps in closing holes (Figure 2.4) that would otherwise remain open but creates a few split holes (Figure 2.5) [LESU89] and useless small holes. These potential problems are detected and avoided by the deletion of a single pixel.

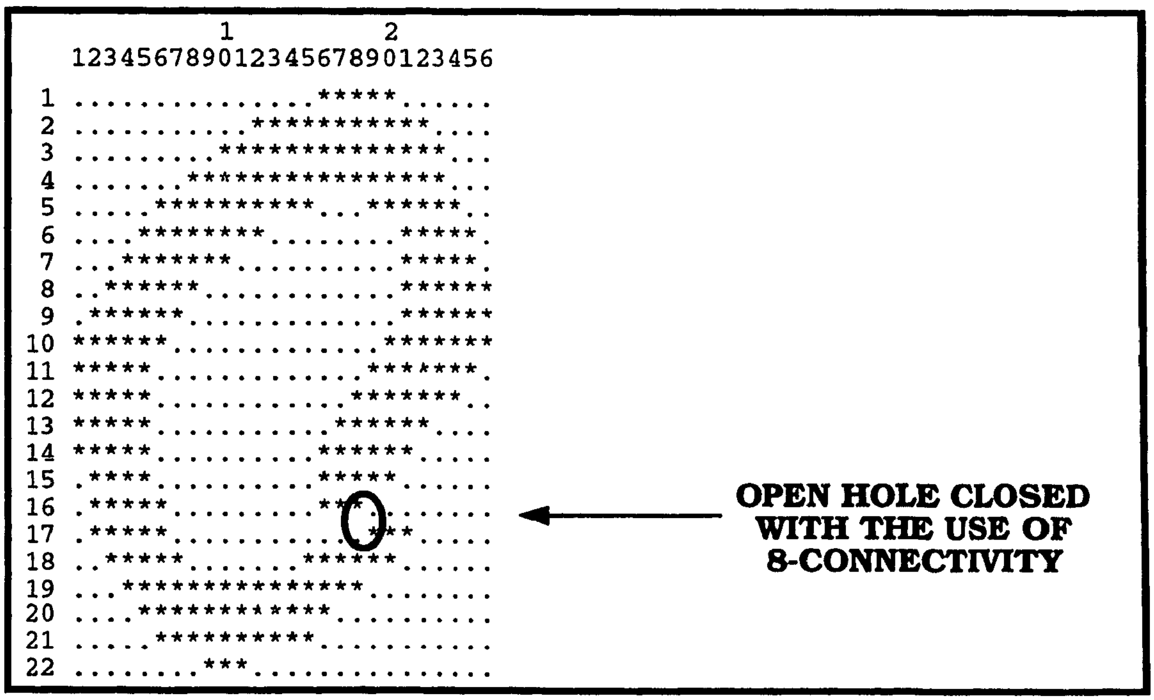

Figure 2.4 8-Connectivity Closes Holes

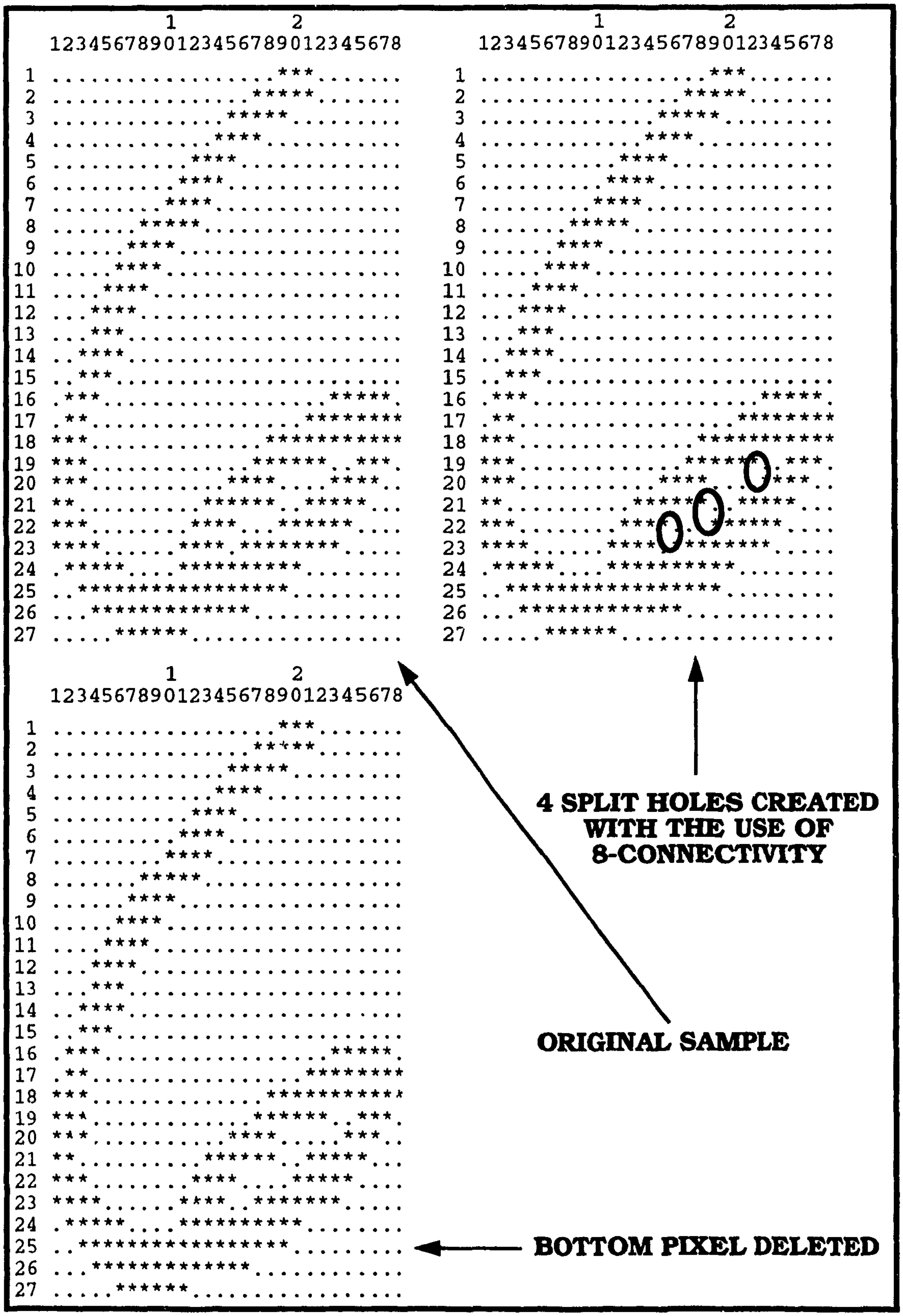

Figure 2.5 Hole Split into 4 Small Holes

In the following figure (Figure 2.6), we notice what happens when we apply alternating connectivities (Figure 2.6 B-C) as well as equivalent ones (Figure 2.6 D-E) when tracing the contours of the foreground and background.

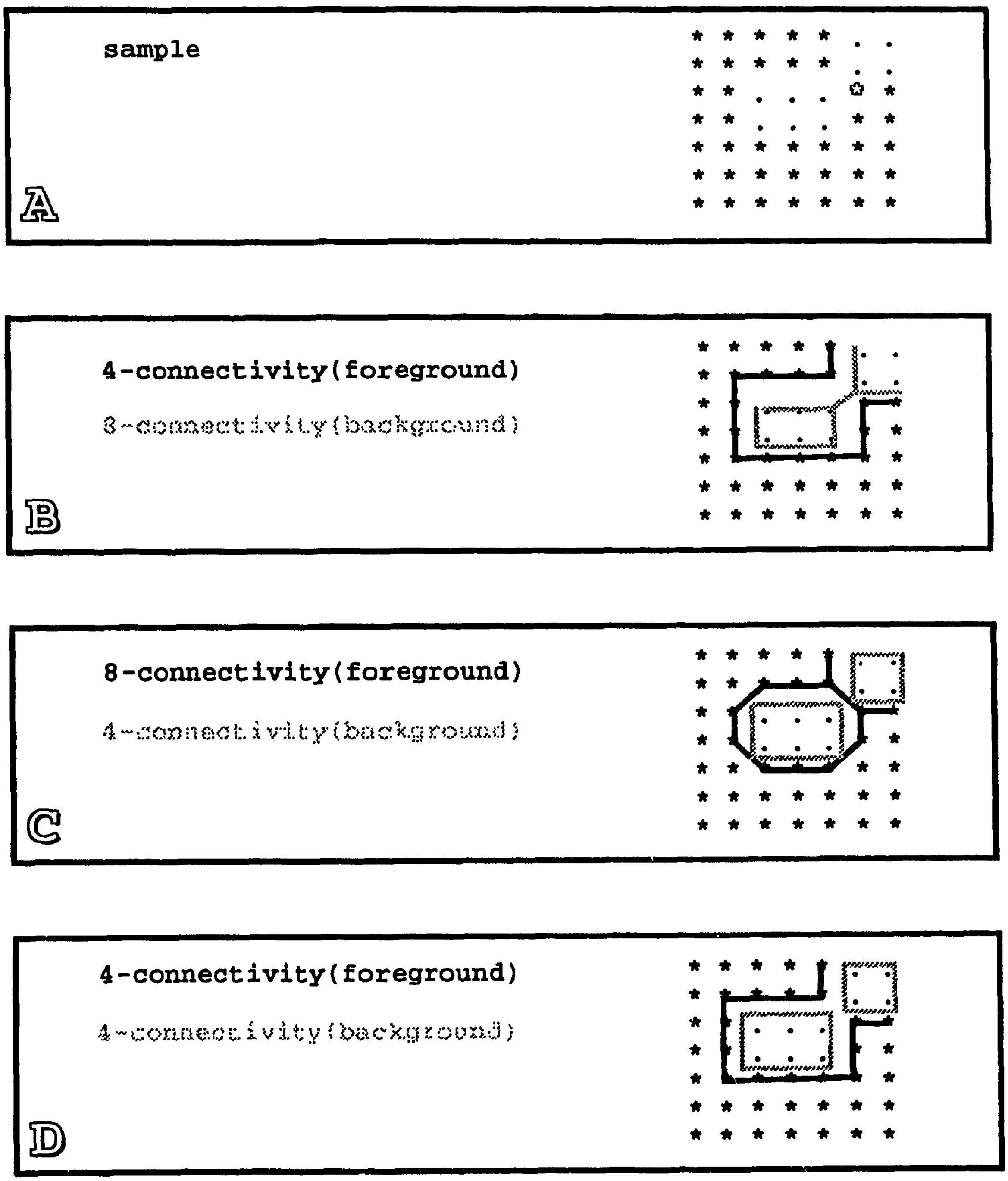

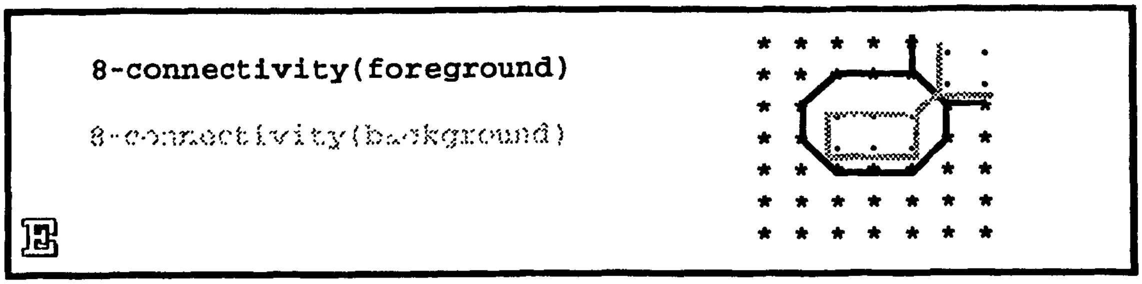

Figure 2.6 Contour Tracing

8-connectivity in the foreground (Figure 2.6 C) provides us with a much smoother foreground contour than 4-connectivity. As can be seen, pairing 8-connectivities (Figure 2.6 B-C) presents us with a paradox, i.e. the foreground and background contours may intersect, yet they should always be disjoint. In other words, we have joined the holes but we have also combined the image.

Since the object is more important to us than the background, we decided to use 8-connectivity for the foreground and 4-connectivity for the background. To minimize the number of split holes which may occur, as shown in Figures 2.5 and 2.6, whenever we encounter such a situation when extracting contours, as will be discussed in the next chapter, we delete a pixel. In order to remove the split in the hole created in Figure 2.6 C, we removed the pixel outlined in Figure 2.6 A.

CHAPTER 3

CONTOUR EXTRACTION

3.1 Introduction

A brief discussion of edges and edge relationships is first given, followed by a description of our coordinate system and the line components examined and connected while scanning an object region. The edge extraction implementation ensues and the application of these edges to define a contour is then explained.

3.2 Edge Types and Edge-to-Edge Relationships

Edges play an important role in the description and the analysis of a binary pattern and are discovered while scanning. An edge is the transition from a white region to a black one or vice-versa.

There are four basic types of edges (Figure 3.1) [AHME86]: outer left (e_i^1), outer right (e_j^2), inner left (e_k^3) and inner right (e_l^4). We have attached a subscript notation to Ahmed's basic edge type definition. Edges are always created and terminated in pairs and they are numbered (subscript parameter) from top to bottom and left to right, based on the point of their first appearance. Pairs of edges connect to define various topological features of the contours they describe.

The concatenation relationships considered in this implementation are *head-to-head* (X), that is the head of an edge can only be connected to the head of another edge or *tail-to-tail* (-) where the tail of an edge is connected to the tail of another edge. The starting $(e_1^1 \times e_2^2)$ and splitting $(e_3^3 \times e_4^4)$ points of a body region are referred to as the "heads" of an edge and the ending $(e_1^1 - e_5^3)$ and merging $(e_3^3 - e_4^4)$ points as the "tails" of an edge. They occur as a result of the *detection* or the *split* of a body region and terminate with the *ending* or the *merging* of two areas of a body region.

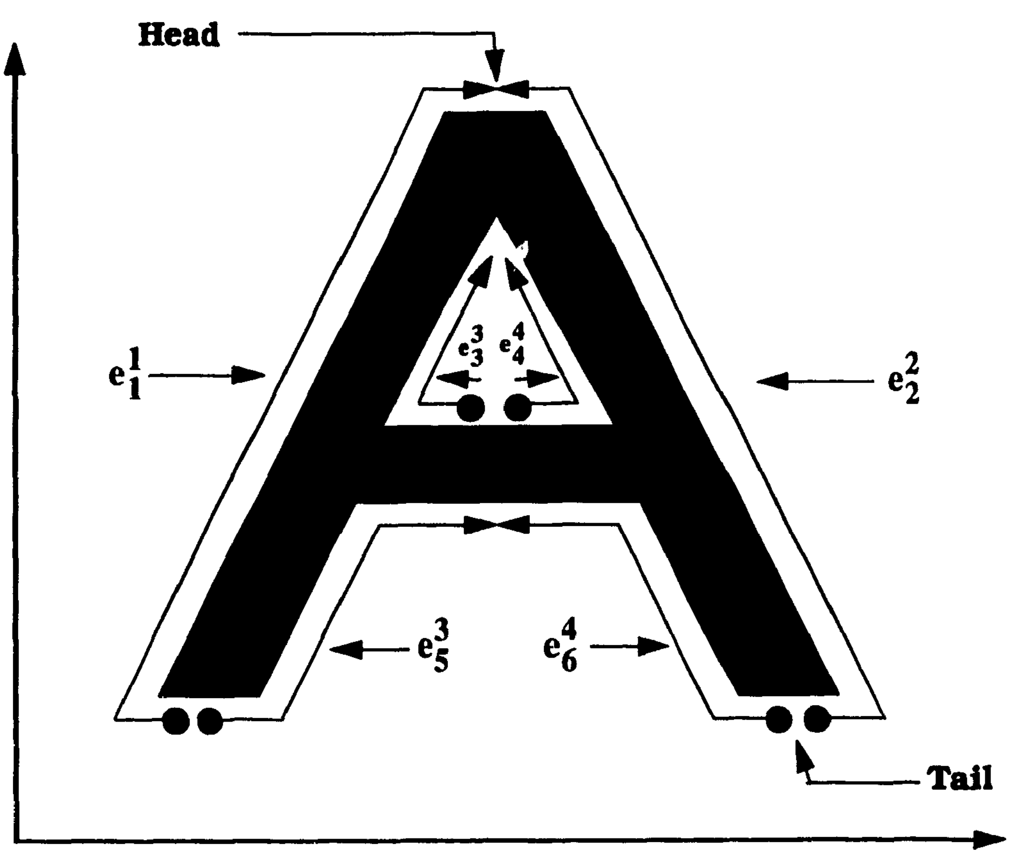

Figure 3.1 Basic Edge Definition (Horizontal Scan)

All the possible pattern configurations formed by the concatenation of two edges are depicted in the following figure (Figure 3.2) [AHME86]. The shaded area is part of the body region while the background is white. Note that R_{11} and R_{12} are holes and blobs formed by the concatenation of two relations R_7 and R_8, R_1 and R_2.

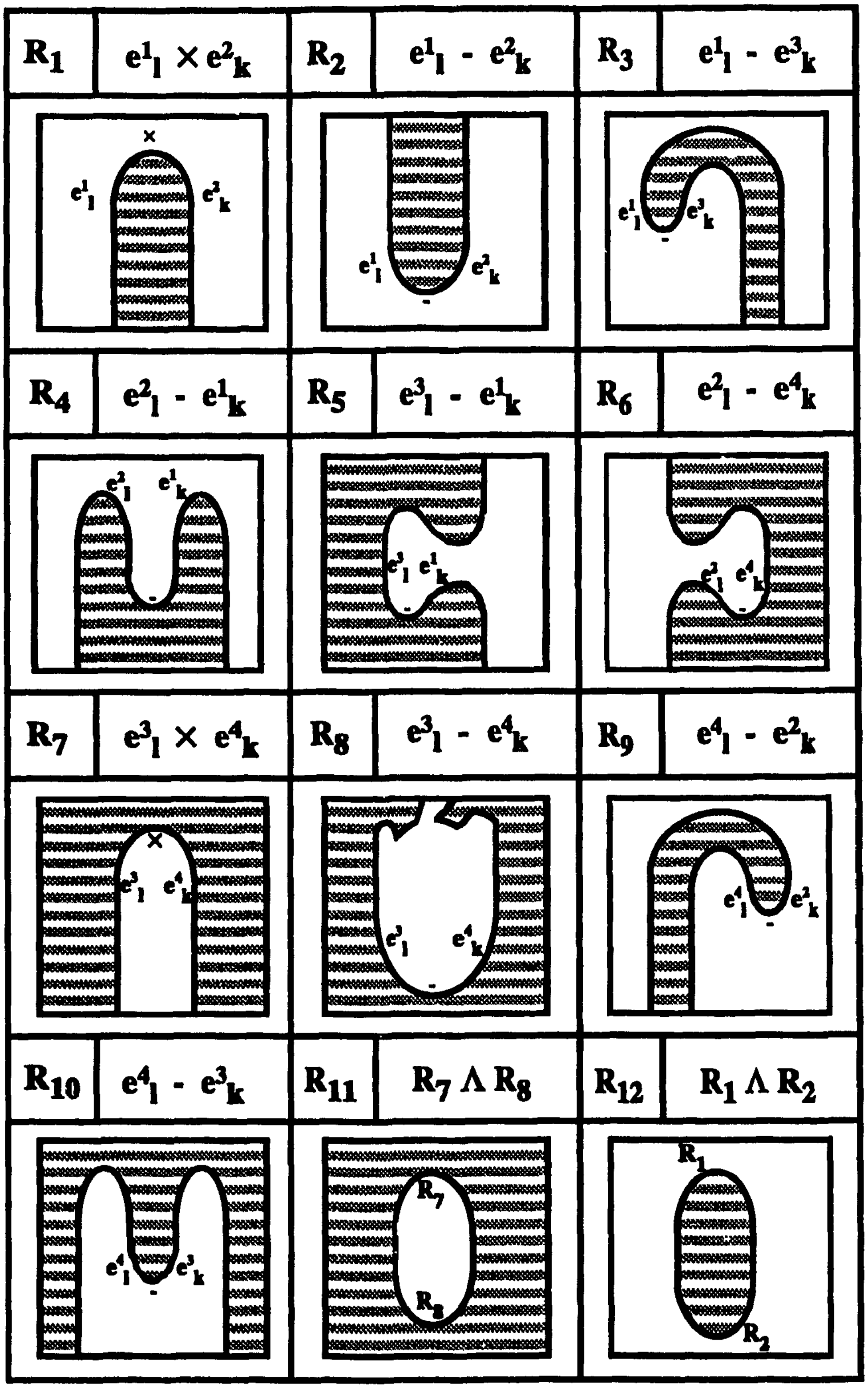

Figure 3.2 Twelve Possible Shapes

This figure was reproduced from Ahmed's thesis. Ahmed used only a horizontal scan throughout his work, so this figure should be observed from top to bottom.

These are the different shape topologies we will encounter throughout this research.

3.3 Extraction of Components and Edges

The samples used in this work have been set in the smallest possible rectangle enclosing them (bounding box), i.e. there are no empty rows or columns around the patterns unless certain pixels were deleted by the smoothing operation. As we examine the next figure (Figure 3.3), we observe that there are 34 rows, each comprised of one or more black runs. These object components are the ones we will refer to when we use the word components. Both the leftmost and rightmost pixels of a component are associated with a different edge. Scanning horizontally, we proceed row by row and check the connectivity of the components of the current row with those of the previous one. This is how the edge types are determined. In the case of the vertical scan, we advance column by column starting with the one on the extreme right of the frame. As we start scanning the body region, we extract the first component which is not yet connected.

```
             1         2         3         4
    12345678901234567890123456789012345678901
 1  ....................**********...........
 2  .................**************..........
 3  .................***************.........
 4  .................****************........
 5  .............................****........
 6  ..............................***........
 7  ..............................****.......
 8  ..............................****.......
 9  ..............................****.......
10  ..............................****.......
11  .............................****........
12  .............................****........
13  .............................****........
14  ............................****.........
15  ............................****.........
16  ...........................****..........
17  ...........................****..........
18  ..........................****.........**
19  .........................*****.......****
20  .........................****......****..
21  ........................*****....****....
22  .......**.............******....****.....
23  .....*******.........******..******......
24  ...******************************........
25  ..****....*********************..........
26  ..***.........***************............
27  .***..........**********.................
28  .***..........*******....................
29  .**.........*******......................
30  ***.......********.......................
31  ***...**********.........................
32  .*************...........................
33  .************............................
34  ..*******................................
```

Figure 3.3 Binary Image of a Sample of Digit 2

Our work makes use of Ahmed's [AHME86] edge-extraction method but it is implemented differently. It is based on sequential horizontal and vertical scanning of the image. The various states seen in Figure 3.4 (new start, continuation, split, merge, termination) are established directly by inspecting two consecutive rows during the scanning process.

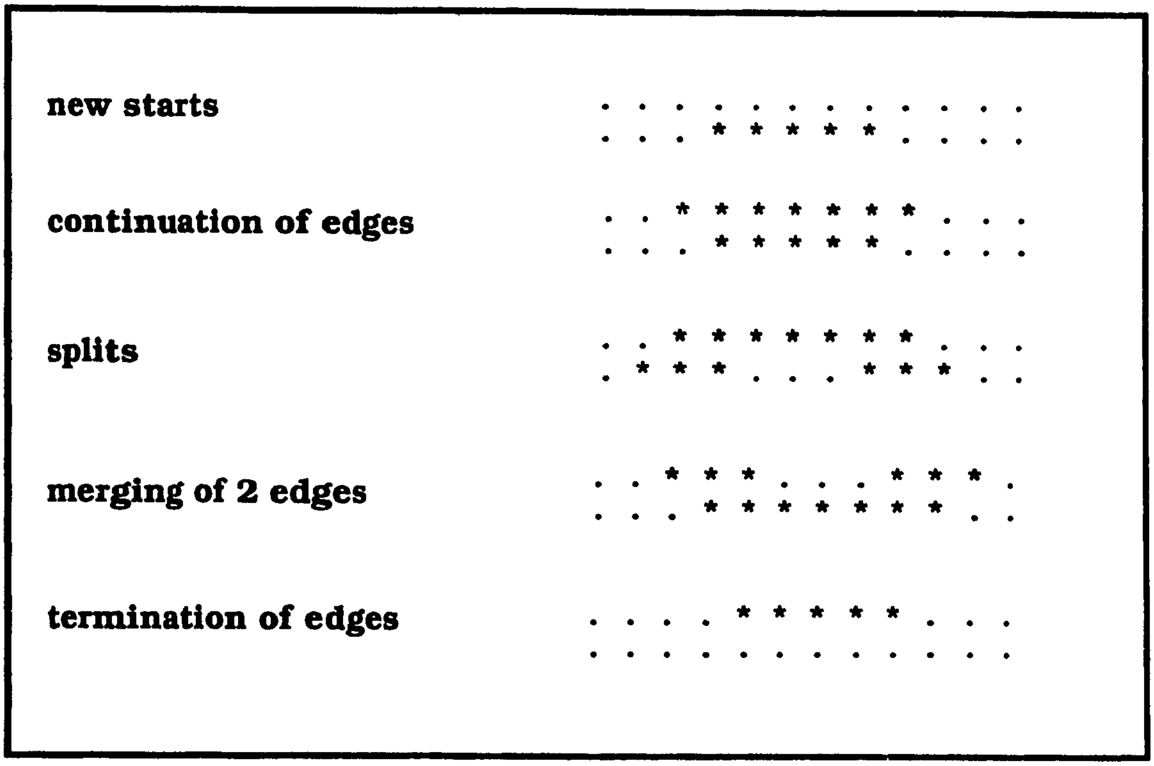

Figure 3.4 The Various States

Figures 3.5 and 3.6 show an example of the output of this program. Sequencing of edges is done alphabetically. The enumeration of edges starts from the letter A. During the horizontal scan, a pair of edges is detected with their meeting point in the middle of the first component on the first row. The left edge is of type 1 and is denoted by the letter A. It joins the right edge of type 2 identified by the letter B producing relation R_1. The detection of new body regions occurs again on rows 18 and 22, generating edges labeled C, D and E, F.

Information such as length of edges, top and bottom rows, left and right columns, i.e. the borders of our bounding box are presented above the image in each scan. The edge table seen in these figures indicates the relation type between edges, as was described in our shape topology Figure 3.2. We can observe the symmetry above and below the diagonal.

Defining our coordinate system as having its origin at the bottom left side of the image, we observe that in a horizontal scan, vertical edges are monotonically decreasing along the y axis. Similarly, horizontal edges monotonically decrease along the x axis of a vertical scan.

EDGE	TYPE	LENGTH	LEFT	TOP	RIGHT	BOTTOM
A	1	45	18	1	31	24
B	2	28	26	1	34	24
C	1	12	29	18	40	24
D	2	36	7	18	41	34
E	1	18	1	22	8	34
F	2	9	9	22	17	24
G	3	11	3	24	8	32
H	4	18	6	24	15	32

```
            1         2         3         4
   12345678901234567890123456789012345678901

 1 ....................AAAAABBBBB...........
 2 .................AAA**********B..........
 3 .................A*************B.........
 4 .................AAAAAAAAAAAA***B........
 5 .............................A**B........
 6 ..............................A*B........
 7 ..............................A**B.......
 8 ..............................A**B.......
 9 ..............................A**B.......
10 ..............................A**B.......
11 .............................A**B........
12 .............................A**B........
13 .............................A**B........
14 ............................A**B.........
15 ............................A**B.........
16 ...........................A**B..........
17 ...........................A**B..........
18 ..........................A**B........CD
19 .........................A***B......CCDD
20 .........................A**B......CCDD..
21 ........................A***B....CC*D....
22 .......EF.............AA***B....C**D.....
23 .....EE**FFF.........A****B..CCC*DD......
24 ...EE*GGHH**FFFFFAAAA******BC**DD........
25 ..E**G....HHHH***************DD..........
26 ..E*G.........H*********DDDDD............
27 .E*G..........H******DDD.................
28 .E*G..........H****DD....................
29 .EG.........HH****D......................
30 E*G.......HH****DD.......................
31 E*G...HHHH****DD.........................
32 .E*GGH*******D...........................
33 .E*******DDDD............................
34 ..EEEEDDD................................
```

EDGE TABLE:

	A	B	C	D	E	F	G	H
A	0	1	0	0	0	0	0	0
B	1	0	4	0	0	0	0	0
C	0	4	0	1	0	0	0	0
D	0	0	1	0	2	0	0	0
E	0	0	0	2	0	1	0	0
F	4	0	0	0	1	0	0	0
G	0	0	0	0	0	0	0	11
H	0	0	0	0	0	0	11	0

Figure 3.5 Digit 2, Pattern 109, Horizontal Scanning (Vertical Edges)

EDGE	TYPE	LENGTH	LEFT	TOP	RIGHT	BOTTOM
A	1	15	27	18	41	24
B	2	42	1	19	41	34
C	1	21	18	1	34	8
D	2	15	27	9	34	23
E	3	16	18	4	31	8
F	4	40	1	9	31	30
G	3	16	3	24	15	30
H	4	13	3	28	15	32

```
            1         2         3         4
   12345678901234567890123456789012345678901

 1 ....................CCCCCCCCCC...........
 2 .................CCC**********C..........
 3 .................C*************C.........
 4 .................EEEEEEEEEEEE***C........
 5 .............................E**C........
 6 ..............................E*C........
 7 ..............................E**C.......
 8 ..............................E**C.......
 9 ..............................F**D.......
10 ..............................F**D.......
11 .............................F**D........
12 .............................F**D........
13 .............................F**D........
14 ............................F**D.........
15 ............................F**D.........
16 ...........................F**D..........
17 ...........................F**D..........
18 ......................... F**D.........AA
19 .........................F***D.......AABB
20 .........................F**D......AABB..
21 ........................F***D....AA*B....
22 .......FF.............FF***D....A**B.....
23 .....FF**FFF.........F****D..AAA*BB......
24 ...FF*GGGG**FFFFFFFFF******AA**BB........
25 ..F**G....GGGG***************BB..........
26 ..F*G...... ..G*********BBBBB............
27 .F*G..........G******BBB.................
28 .F*G..........H****BB....................
29 .FG.........HH****B......................
30 F*G.......HH****BB.......................
31 B*H...HHHH****BB.........................
32 .B*HHH*******B...........................
33 .B*******BBBB............................
34 ..BBBBBBB................................
```

EDGE TABLE:

	A	B	C	D	E	F	G	H
A	0	1	0	4	0	0	0	0
B	1	0	0	0	0	9	0	0
C	0	0	0	1	3	0	0	0
D	4	0	1	0	0	0	0	0
E	0	0	3	0	0	7	0	0
F	0	9	0	0	7	0	0	0
G	0	0	0	0	0	0	0	11
H	0	0	0	0	0	0	11	0

Figure 3.6 Digit 2, Pattern 109, Vertical Scanning (Horizontal Edges)

3.4 Contour Extraction from Edge Chains

Referring to the horizontal scan of digit 2, pattern no. 109 (Figure 3.5), we can trace the outer contour "outside 1" in a counter-clockwise manner by following edge A downward, edge F upward, edge E downward, edge D upward, edge C downward and finally edge B upward. Similarly, the inner contour "inside 2" is followed by edge G downward then edge H upward. The same thing is done with the vertically scanned contour (Figure 3.6), the only exception being that the starting point of edge A is in the rightmost column.

These edge chains along with other pertinent information are illustrated in Figures 3.7 and 3.8. The planar coordinates of the edge junction are established during the counter-clockwise contour extraction(s) in a scan. Where two edges join, we use the convention of recording the starting coordinate of the second edge as the junction coordinate. For example, in Figure 3.5, edge A joins edge F at the coordinate (24,17), the starting coordinate of edge F. Occasionally, edge junctions occur at the same coordinate. This happens when a body region starts with a single pixel component, in which case, we label the common coordinate with the greater of the two edge letters.

CHAIN started with edge A
continued with edge F
continued with edge E
continued with edge D
continued with edge C
ended with edge B

CONTOUR	EDGE JUNCTION	RELATION	POINT NO.	COORDINATES
outside 1	BA	1	1	(1, 25)
outside 1	AF	4	46	(24, 17)
outside 1	FE	1	55	(22, 8)
outside 1	ED	2	73	(34, 7)
outside 1	DC	1	109	(18, 40)
outside 1	CB	4	121	(24, 28)

CHAIN started with edge G
ended with edge H

CONTOUR	EDGE JUNCTION	RELATION	POINT NO.	COORDINATES
inside 2	HG	11	149	(24, 8)
inside 2	GH	11	160	(32, 6)

Figure 3.7 Digit 2, Pattern 109, Horizontal Scanning

CHAIN started with edge A
continued with edge D
continued with edge C
continued with edge E
continued with edge F
ended with edge B

CONTOUR	EDGE JUNCTION	RELATION	POINT NO.	COORDINATES
outside 1	BA	1	108	(18, 41)
outside 1	AD	4	122	(23, 27)
outside 1	DC	1	137	(8, 34)
outside 1	CE	3	10	(4, 18)
outside 1	EF	7	26	(9, 31)
outside 1	FB	9	66	(31, 1)

CHAIN started with edge G
ended with edge H

CONTOUR	EDGE JUNCTION	RELATION	POINT NO.	COORDINATES
inside 2	HG	11	170	(27, 15)
inside 2	GH	11	157	(31, 3)

Figure 3.8 Digit 2, Pattern 109, Vertical Scanning

CHAPTER 4

FEATURE EXTRACTION

4.1 Introduction

Outer and inner contour processing is explained, followed by the reference point definition. We then offer a simplification technique in dealing with shapely holes and set forth our hole identification procedure. The treatment of coincident relations in the superimposed horizontal and vertical scans is described. With the use of a reference point addressing technique, we then construct our feature strings. Finally, a hole reduction method is offered and justified, which removes spurious small cavities.

4.2 Processing of Outer and Inner Contours

By convention, the point identified as point No. 1 will always be the first point of edge A on the horizontal scan. The last point of the contour is the last point of edge B. This final point can occupy the same position as point No. 1 because a single pixel can belong to two different edges by superimposition.

All points of each outer contour edge are ordered as they are encountered during the extraction of the contour(s) in the horizontal scan. We number the points of the outer contour by proceeding counter-clockwise and sequentially along the edge chains, enumerating them as we go along. In this way, all outer contour points have an identity, their "point number". The point numbers of the edge junctions in the vertical scan are those associated with the corresponding points in the horizontal scan.

The first point extracted from an inner contour when scanning horizontally, is the leading point of the left edge for the first detected body region split. Referring to Figure 4.1 a, the boldfaced G at coordinate (24,8) identifies such a point. The numbering is as explained in the discussion of outer contours.

4.3 Selection of Reference Points

Edge junctions are the selected reference points where relations will be located. Each junction point is by convention the first point of the second edge obtained during the counter-clockwise extraction process along the edge chains. These points are identified with boldfaced letters as illustrated in Figure 4.1.

Each reference point in a horizontal scan (Figure 4.2 a) is denoted first by the letter H, and secondly, by the relation number at this junction. The same procedure is effected for the vertical scan (Figure 4.2 b) denoting its reference points by the letter V. We have associated to these edge junctions their respective point numbers in parentheses in order to present a visual representation of the above procedure.

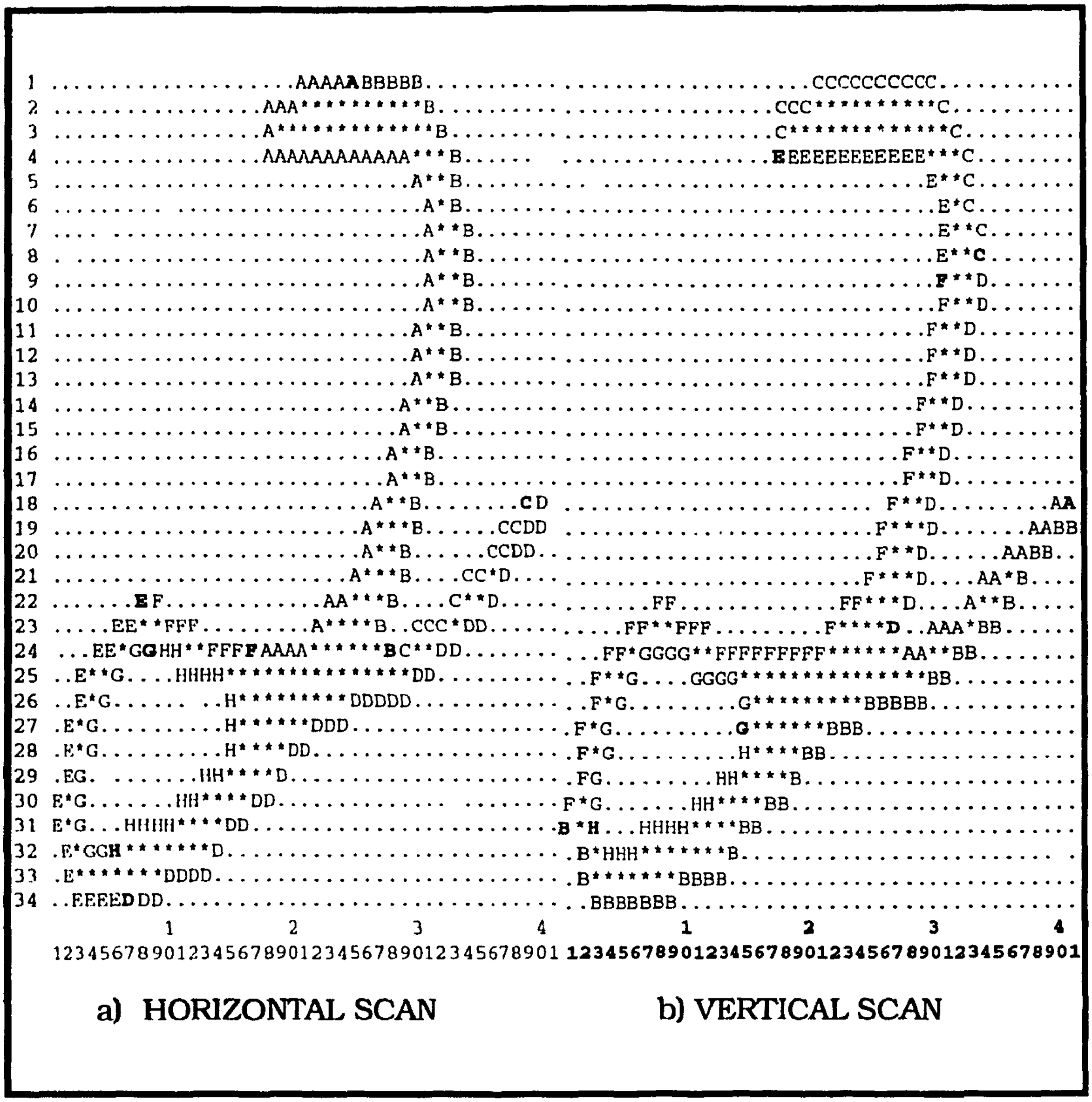

Figure 4.1 Bolded Reference Points of Digit 2 Pattern 109

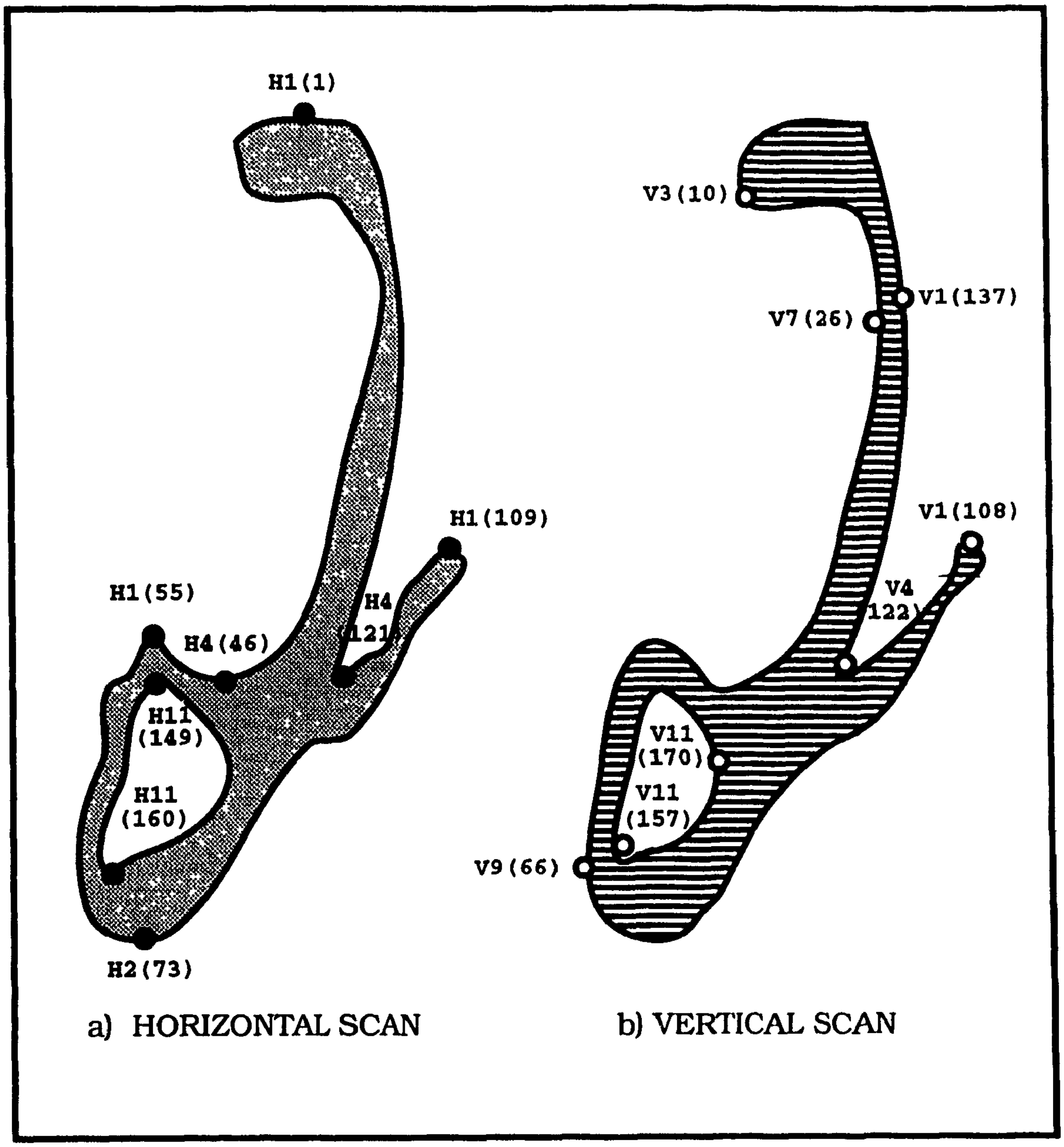

Figure 4.2 Reference Points and Point Number

4.4 Feature String

A feature string is generated by superimposing the horizontal and vertical scans and sequentially recording the combined edge-junction relations. The junction points intertwine or lay one on top of the other. To each edge junction or reference point Ji there corresponds a point number relative to the (x, y) coordinates. These point numbers provide us with a sequential method of extracting the junction points. The image area is divided into quadrants by overlaying a fixed-size grid. The grid quadrants are then numbered to identify them. Each edge-junction relation point Ji is localized in a quadrant whose number will always be associated with this Ji. This quadrant information will be used to discriminate among similar feature strings.

First, the outer contour of the superimposed scans is traced in a counter-clockwise fashion and the reference points are selected in increasing point-number sequence, producing a string of edge-junctions relations. The edge-junction relations of the inner contour of the pattern are then inserted in this outer contour sequence.

The feature-string generation process will be demonstrated through the use of an example. We will use our previous sample of the digit 2, whose superimposed horizontal and vertical scans are illustrated in Figure 4.3. First we trace the outer contour in a counter-clockwise fashion starting at the top of the image to produce an outer contour relation string. For our sample of the digit 2, this would generate the string H1 V3 V7 H4 H1 V9 H2 V1 H1 H4 V4 V1. Now, the inner contour corresponding to the hole must be inserted in this string. The coordinate position of each relation will be used to determine where to insert the inner contour relations in the outer contour string. Each inner contour relation is treated separately. We use the following lexicographic-like rule to insert an inner contour relation. Let (i,j) denote the row and column coordinates of the inner contour relation to be inserted. The outer contour string is searched from left to right until the first relation is encountered with coordinates (r,s) such that $i \leq r$. If $(i < r)$ or $(i = r$ and $j < s)$, the inner contour relation is inserted immediately before this relation. Otherwise, $i = r$ and $j > s$ and the search continues until we locate the first relation with coordinates (u,v) such that $(u = i$ and $j < v)$ or $(u > i)$. The inner contour relation is inserted immediately before this one. In this way, the row coordinate is used as a major index and the column coordinate is used as a minor index to locate an insertion point. Note that it is always possible to find such an insertion point, as the inner contour is always contained entirely within the outer contour. In other words, the row coordinates of all inner contour relations are less than the row coordinate of at least one outer contour relation. Similarly, at least one outer contour relation has a row coordinate which is less than the row coordinates of all inner contour relations. Analogous statements can be made for the column coordinates. Thus, each inner contour relation is uniquely positioned within the outer contour by this rule. A little thought reveals that the positioning of the inner contour relations within the outer contour relation string, according to this rule, actually localizes the inner contour relations near those of the outer contour which envelope the inner contour in the original image. Thus, this is more than just some arbitrary insertion rule. The inner contour relations are, in a sense, surrounded by the outer contour relations in the resultant string, mimicing the way in which the outer contour surrounds the inner one.

Returning to our example, the relations of the inner contour are H11, V11, H11, V11, with their respective coordinates being (24,8), (31,3), (32,6), (27,15). After applying the insertion rule for each of these relations to our outer contour relation string H1 V3 V7 H4 H1 V9 H2 V1 H1 H4 V4 V1, with the respective relation coordinates (1,25), (4,18), (9,31), (24,17), (22,8), (31,1), (34,7), (8,34), (18,40), (24,28), (23,27), (18,41), we obtain the final feature string H1 V3 V7 H11 H4 H1 V11 V9 V11 H11 H2 V1 H1 H4 V4 V1 which has as it's respective coordinates (1,25), (4,18), (9,31), (24,8), (24,17), (22,8), (27,15), (31,1), (31,3), (32,6), (34,7), (8,34), (18,40), (24,28), (23,27), (18,41).

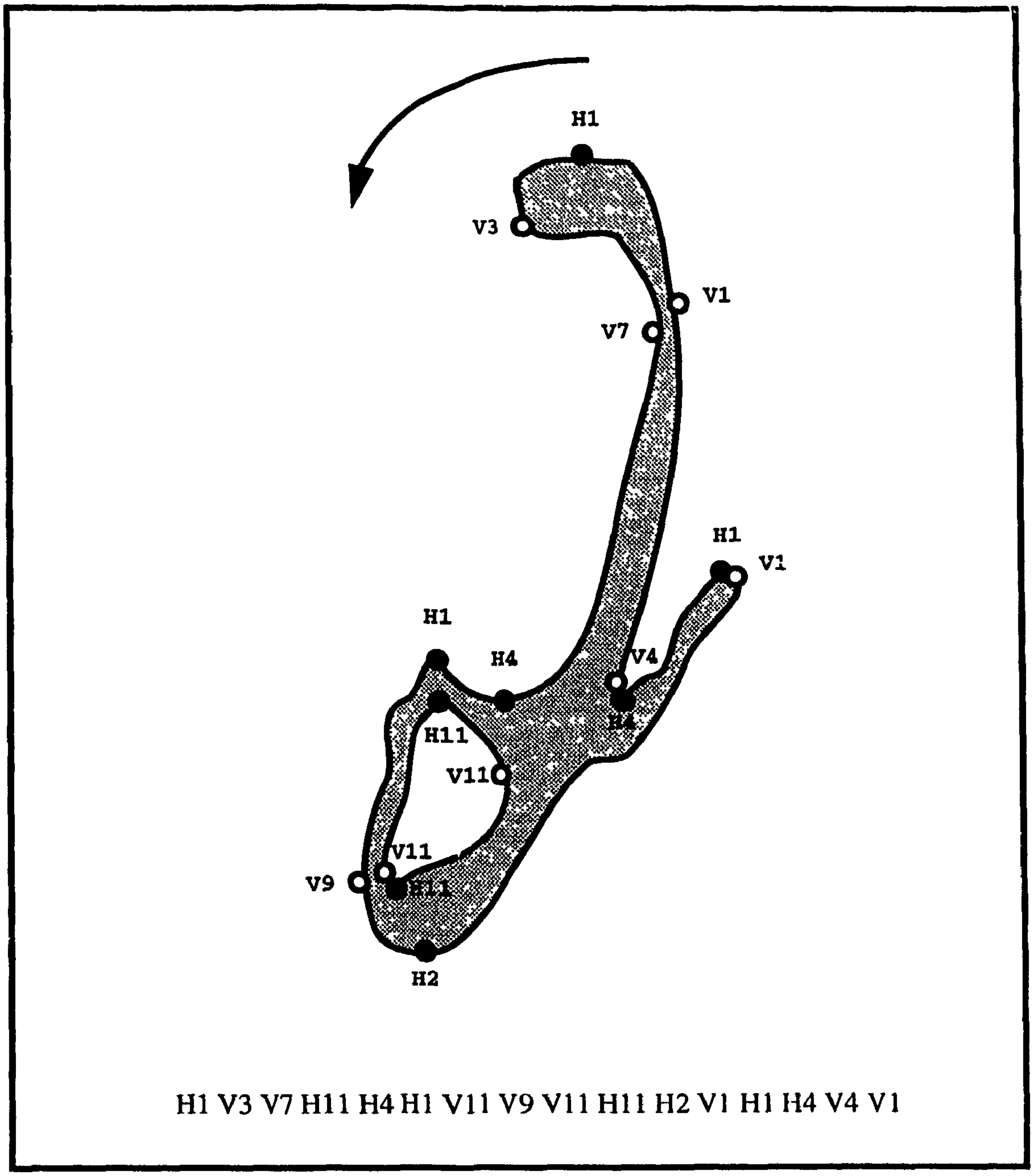

Figure 4.3 Superimposed Scans and Counter-Clockwise Extraction of Reference Points

It is possible for different digits to have the same shape string as shown in Figure 4.4. The classes in which the same shape string occurs can be distinguished on the basis of statistical frequencies, as will be elaborated on in Chapter 5. However, we can incorporate other information to distinguish feature strings and we will do so by localizing the individual relations of all feature strings in regions of the image.

Digit 0 and Digit 6

H1 V2 H2 V1 H1 H4 V4 V1

H12 H11 V11 V2 V11 H11 H12 V1 V4 V1

Digit 1 and Digit 7

H12 V3 V7 V9 H12 V1

H12 V3 V7 V9 H12 V1 V4 V1

Figure 4.4 Equivalent Shape Strings in our Data Sets

In order to incorporate such spatial-locality information for each of the relations in a feature string, we partition the rectangular area of the image into $m \times n$ quadrants by overlaying an $m \times n$ grid. The quadrants of this grid are then numbered from 1 to $m \times n$, starting in the upper-left quadrant, proceeding across rows and then from row to row. An example of a 4×3 grid with quadrant numbers is illustrated in Figure 4.5.

1	2	3
4	5	6
7	8	9
10	11	12

Figure 4.5 Grid with Quadrant Numbers

Each relation in a feature string occurs in one of the quadrants. We will simply record the corresponding quadrant number immediately after each relation to obtain the final string. For example, in Figure 4.6, a 4×3 grid is used to localize the relations for our sample of digit 2. Using this grid results in the final feature string

H1 **2** V3 **2** V7 **3** H11 **7** H4 **8** H1 **7** V11 **8** V9 **10** V11 **10** H11 **10** H2 **10** V1 **6** H1 **6** H4 **8** V4 **8** V1 **3**

Figure 4.7 illustrates the use of a 3×3 grid for the same digit sample and yields the completed feature string

H1 **2** V3 **2** V7 **3** H11 **4** H4 **5** H1 **4** V11 **8** V9 **7** V11 **7** H11 **7** H2 **7** V1 **6** H1 **6** H4 **5** V4 **5** V1 **3**

In Chapter 5, we examine the performance for various grid partitionings to determine a satisfactory choice for m and n.

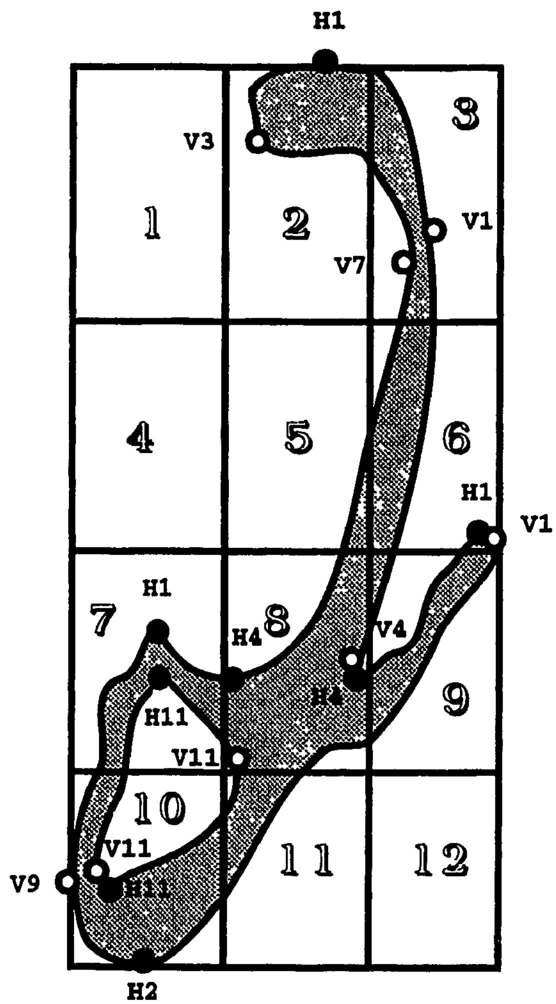

H1 **2** V3 **2** V7 **3** H11 **7** H4 **8** H1 **7** V11 **8** V9 **10** V11 **10** H11 **10** H2 **10** V1 **6** H1 **6** H4 **8** V4 **8** V1 **3**

Figure 4.6 Reference Points Localized in a 4x3 Quadrant Configuration and the Generated Feature String

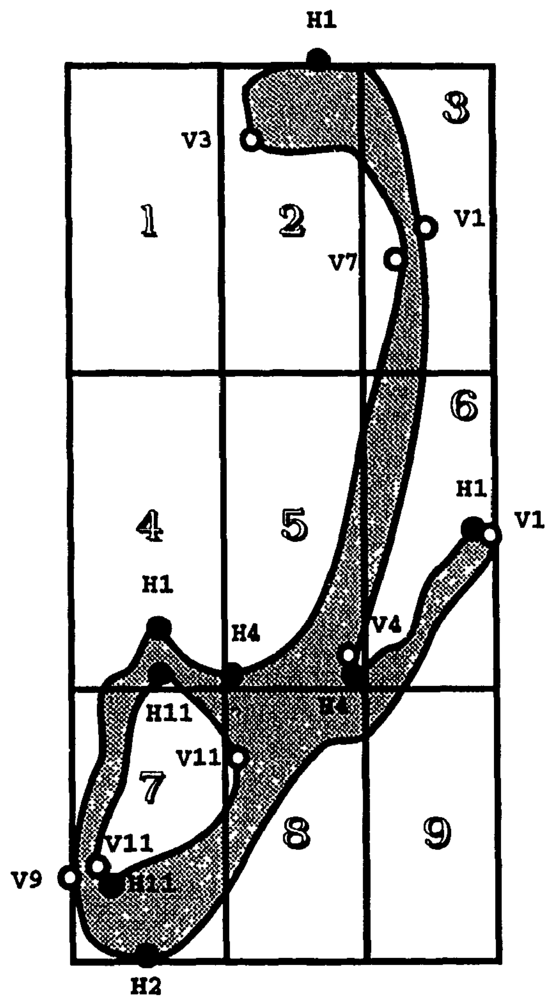

H1 2 V3 2 V7 3 H11 4 H4 5 H1 4 V11 8 V9 7 V11 7 H11 7 H2 7 V1 6
H1 6 H4 5 V4 5 V1 3

Figure 4.7 Reference Points Localized in a 3x3 Quadrant Configuration and the Generated Feature String

The ordering of the component relations, together with the quadrant information within the feature string is of major importance because we can reconstruct a shape resembling the original image from the string when it is encoded in this fashion.

4.5 Superimposed Edge Points

Coincident relations or those which occur at the same (x,y) coordinates in the superimposed horizontal and vertical scans will be referred to as superimposed edge points. Referring to Figures 4.8 and 4.9, the boldfaced B at coordinate (25,2) identifies such a point. Superimposed edge points present a slight problem when generating a feature string since the ordering of relations in a string is based on their coordinates, as described in Section 4.4.

Since the relations encountered are recorded sequentially, an occurrence of superimposed edge points HR_i and VR_j could be encoded as either $HR_i\,VR_j$ or $VR_j\,HR_i$. Whenever this happens, we will generate two feature strings, one encoded as ...$HR_i\,VR_j$... and the other as ...$VR_j\,HR_i$.... Thus, the occurrence of n such reference point pairs will generate 2^n possible strings.

EDGE	TYPE	LENGTH	LEFT	TOP	RIGHT	BOTTOM
A	1	24	2	2	14	25
B	2	24	2	2	14	25

```
             1
    12345678901234

 1  ..............
 2  .............B
 3  ............AB
 4  ...........A*B
 5  ...........AB.
 6  ..........A*B.
 7  ..........AB..
 8  .........A*B..
 9  ........A*B...
10  .......A*B....
11  .......A*B....
12  ......A*B.....
13  ......A*B.....
14  .....A*B......
15  .....A*B......
16  ....A*B.......
17  ....A*B.......
18  ...A*B........
19  ...AB.........
20  ..A*B.........
21  ..AB..........
22  ..AB..........
23  .AB...........
24  .AB...........
25  .B............
```

CHAIN started with edge A
ended with edge B

CONTOUR	EDGE JUNCTION	RELATION	POINT NO.	COORDINATES
outside 1	BA	12	1	(2, 14)
outside 1	AB	12	24	(25, 2)

Figure 4.8 Digit 1, Pattern 111, Training A, Horizontal Scanning

EDGE	TYPE	LENGTH	LEFT	TOP	RIGHT	BOTTOM
A	1	24	2	2	14	24
B	2	22	2	4	14	25

```
             1
    12345678901234
 1  ..............
 2  .............A
 3  ............AA
 4  ...........A*B
 5  ...........AB.
 6  ..........A*B.
 7  ..........AB..
 8  .........A*B..
 9  ........A*B...
10  .......A*B....
11  .......A*B....
12  ......A*B.....
13  ......A*B.....
14  .....A*B......
15  .....A*B......
16  ....A*B.......
17  ....A*B.......
18  ...A*B........
19  ...AB.........
20  ..A*B.........
21  ..AB..........
22  ..AB..........
23  .AB...........
24  .AB...........
25  .B............
```

CHAIN started with edge A
ended with edge B

CONTOUR	EDGE JUNCTION	RELATION	POINT NO.	COORDINATES
outside 1	BA	12	46	(3, 14)
outside 1	AB	12	24	(25, 2)

Figure 4.9 Digit 1, Pattern 111, Training A, Vertical Scanning

As a result, there may be more than one feature string generated per sample, and, hence, the total number of feature strings for a class may exceed the number of samples in the original set. We will refer to the set of feature strings generated for each original set as the extended set. In the case of digit 1, we started with 400 samples which in turn generated 416 different shape string feature strings. The following table (Table 4.1) indicates the number of feature strings which were generated by our training sets for each class.

Digit	Initial Number of Samples	Number of Generated Shape Strings S_i
0	400	405
1	400	416
2	400	422
3	400	408
4	400	458
5	400	419
6	400	421
7	400	430
8	400	423
9	400	426

Table 4.1 Extended Sample Set Sizes

4.6 Treatment of Holes

From our original premise that all characters are connected, we can assume that our patterns display one outer contour, possibly containing one or more inner contours. It is also reasonable to assume that due to the characteristics of the tip of a writing instrument, inner and outer contours would typically be largely collinear in the sense that the inner contours would follow the shape of the surrounding portions of the outer contour. Deviations from this property could be attributed to noise introduced due to ink flow, paper quality, etc., or simply due to an individual's writing style.

Inner contours always identify holes in an image and, in the context of our methodology, the fact that a hole is present is much more significant than the detailed description of the contour itself. The size and location of a hole is also relevant information and this is taken into consideration through the construction of the feature string.

For the reasons cited above, we will refine all inner contours by cropping excessive detail from them and redefining the shape strings describing holes with the relations H11 and V11 used to describe well-formed holes. Exactly how this is accomplished will be discussed next.

Among all relations describing an inner contour, we select only four of them to describe the cropped hole. Since we are interested in the size (horizontal and vertical widths), we choose the horizontal relation with a minimum x coordinate to locate the upper-most extremity of the hole. If there is more than one such reference point, we select the one with a minimum y coordinate. This will always be an H7 type of relation due to the scanning process. Similarly, the scanning process always defines a V7 type of relation for the right-most extremity. This relation is one with a maximum y coordinate and if it is not unique, we choose the one with a minimum x coordinate. In general, the lower-most and left-most relations may not be of type H8 and V8, respectively. In any case, we select a horizontal reference point with a maximum x coordinate. If there is more than one, we choose the one with a maximum y coordinate to define the lower-most extremity of the hole. Regardless of the type of this relation, we associate the relation type H8 with this point. In an analogous fashion, we pick a vertical reference point with minimum y coordinate and if it is not unique, the one with a maximum x coordinate is used. We associate the relation type V8 with this reference point. The pairs H7 H8 and V7 V8 are then relabeled as H11 H11 and V11 V11 to identify them as hole relations, distinguishing them from H7, H8, V7 and V8 type relations which occur elsewhere, i.e. not part of a hole. By a well-formed hole, we mean one which is defined by the shape relation $H11 = H7 \wedge H8$ and $V11 = V7 \wedge V8$.

Referring to the inside contour of Figure 4.10, we notice that in this horizontal scan, the curvature of the hole is described by eight relations: H7 (6, 14), H10 (10,10), H7 (7, 9), H5 (21,8), H1 (19,10), H6 (20,12), H7 (6, 19), H10 (8,16). The composition of that same hole, when scanned vertically in Figure 4.11, is not as elaborate: V11 (17,3) , V11 (8,21). In the horizontal inner contour, we shall retain only two of these eight reference points: H7 (6, 14), H5 (21,8) and relabel our relation string with H11 (6,14) H11 (21,8). The resultant shape string is H12 (1,14) V3 (2,9) V7 (3,12) H11 (6,14) V11 (8,21) V9 (17,1) V11 (17,3) H11 (21,8) H12 (23,9) V1 (9,22).

Subsequent holes in a same image are processed in an equivalent manner. They will, however, be identified by "H(11x*hole number*) H(11x*hole number*)" and "V(11x*hole number*) V(11x*hole number*)". Hence a second hole will be denoted by "H22 H22" and "V22 V22", and so on.

EDGE	TYPE	LENGTH	LEFT	TOP	RIGHT	BOTTOM
A	1	35	1	1	14	23
B	2	30	9	1	22	23
C	3	5	11	6	14	10
D	4	3	15	6	16	8
E	3	3	17	6	19	8
F	4	16	12	6	21	20
G	3	16	3	7	8	21
H	4	4	9	7	10	10
I	1	3	8	19	9	21
J	2	2	9	19	11	20

```
            1         2
   1234567890123456789012
 1 .............AB.......
 2 ........AAAAA**BBB....
 3 ...........A*****B....
 4 .........AA*******BB..
 5 .......AA***********B.
 6 ......A******CD***EFB.
 7 .....A**H***C..D*E..FB
 8 ....A**G.H*C...DE...FB
 9 ...A**G..HC.........FB
10 ..A**G...HC.........FB
11 .A**G..............F*B
12 .A*G...............FB.
13 A**G..............F*B.
14 A*G...............FB..
15 A*G..............F*B..
16 A*G.............F*B...
17 A*G............F*B....
18 A*G...........FBB.....
19 A**G....IJ...FB.......
20 A***GG..I*JFFB........
21 .A****GI****BB........
22 ..AAA*****BB..........
23 .....AAABB............
```

CHAIN started with edge A
ended with edge B

CONTOUR	EDGE JUNCTION	RELATION	POINT NO.	COORDINATES
outside 1	BA	12	1	(1, 14)
outside 1	AB	12	36	(23, 9)

CHAIN started with edge C
continued with edge H
continued with edge G
continued with edge I
continued with edge J
continued with edge F
continued with edge E
ended with edge D

CONTOUR	EDGE JUNCTION	RELATION	POINT NO.	COORDINATES
inside 2	DC	7	66	(6, 14)
inside 2	CH	10	71	(10, 10)
inside 2	HG	7	74	(7, 9)
inside 2	GI	5	90	(21, 8)
inside 2	IJ	1	93	(19, 10)
inside 2	JF	6	95	(20, 12)
inside 2	FE	7	111	(6, 19)
inside 2	ED	10	114	(8, 16)

Figure 4.10 Digit 0 with a Detailed Inner Contour, Horizontal Scan

EDGE	TYPE	LENGTH	LEFT	TOP	RIGHT	BOTTOM
A	1	18	9	1	22	9
B	2	29	1	10	22	23
C	3	27	3	6	21	16
D	4	24	3	9	21	21
E	3	4	9	2	12	3
F	4	16	1	3	12	16

```
            1         2
   1234567890123456789012
 1 .............AA.......
 2 ........EEEAA**AAA....
 3 ...........F*****A....
 4 .........FF*******AA..
 5 .......FF***********A.
 6 ......F******CC***CCA.
 7 .....F**C***C..C*C..CA
 8 ....F**C.C*C...CC...CA
 9 ...F**C..CC.........DA
10 ..F**C...CC.........DB
11 .F**C..............D*B
12 .F*C...............DB.
13 F**C..............D*B.
14 F*C...............DB..
15 F*C..............D*B..
16 F*C.............D*B...
17 B*D............D*B....
18 B*D...........DBB.....
19 B**D....DD...DB.......
20 B***DD..D*DDDB........
21 .B****DD****BB........
22 ..BBB*****BB..........
23 .....BBBBB............
```

CHAIN started with edge A
continued with edge E
continued with edge F
ended with edge B

CONTOUR	EDGE JUNCTION	RELATION	POINT NO.	COORDINATES
outside 1	BA	1	54	(9, 22)
outside 1	AE	3	6	(2, 9)
outside 1	EF	7	9	(3, 12)
outside 1	FB	9	25	(17, 1)

CHAIN started with edge C
ended with edge D

CONTOUR	EDGE JUNCTION	RELATION	POINT NO.	COORDINATES
inside 2	DC	11	107	(8, 21)
inside 2	CD	11	84	(17, 3)

Figure 4.11 Digit 0 with a Detailed Inner Contour, Vertical Scan

CHAPTER 5

CLASSIFICATION ALGORITHM

5.1 Introduction

This chapter describes, in detail, the classification algorithm and its underlying data structure. The collections of feature strings described in Chapter 4 are, most naturally, represented by a *forest* or *collection of trees*. A dynamically-allocated multiway-tree data structure called a *trie* is selected for this purpose. A single trie is created for each class. The feature strings of the training sets define paths in these tries, whose nodes correspond to individual shape relations and have associated attributes and parameters. Some basic properties of tries and some relationships among their node parameters are discussed. A measure is then introduced, to quantitatively distinguish between feature strings. The decision-making process which applies this measure in a search to locate a "most-likely" class for a given test string is presented.

5.2 A Simple Representation, a Trie

A trie is an n-ary digital search tree which can be used to efficiently discriminate names, words or, more generally, strings formed from an n-letter alphabet [ENCY93]. The word is trie taken from the middle letters of the word "retrieval", but pronounced "try". Given a collection of strings, we use the ordering of letters in each string to create the trie representing the collection. If the alphabet contains 24 letters, each node in the tree could be up to a 24-way branch, one for each possible letter. The advantage of a digital search tree is that in many circumstances the multiway branch required at every node of the tree will require little or no more time than a binary decision.

Strings are selected arbitrarily from the given collection and inserted in the trie. The first string creates a single path whose nodes starting from the root and ending at a leaf, follow the order of letters in the string. Subsequent strings are inserted by following the path corresponding to a maximum-length prefix of the string to be inserted to the node associated with the last letter of this prefix. At this point, the string differs from all strings currently contained in the trie and so, a branch is created at this node where the remaining letters will be inserted in a new path according to their order. Multiple instances of a particular string generate only one path, since a string is a maximum-length prefix of itself. The nodes at which strings terminate will be referred to as *terminal nodes.* Clearly, all leaf nodes are terminal nodes but a terminal node is not necessarily a leaf, as some strings may be substrings of others. We will clarify the notion of a trie by way of an example.

In Figure 5.1, we have built a trie, inserting sequentially the five following words: "THE TREE TRIE SEARCH SEA". Next to each node, we have placed a one or a summation of ones indicating the number of times the node was traversed when creating the trie. We refer to this number as the *passage count.* Terminal vertices are shown as shaded nodes. This particular tree is composed of 5 strings.

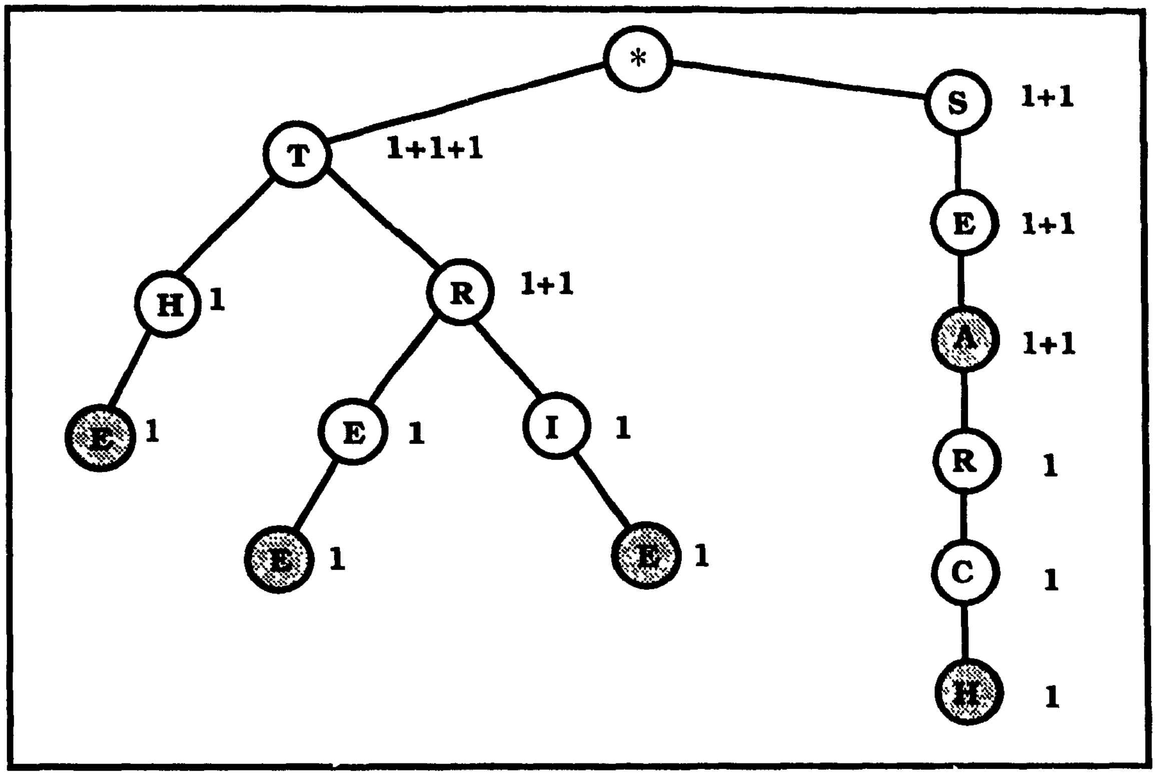

Figure 5.1 A Trie

In our case, we will use the feature strings from both training sets to implement a trie for each class. There are 10 of these structures as we have 10 digits (Appendix C). At each node, we shall keep track of the passage count, and compute the average quadrant where the associated relation was found. We shall also maintain the feature string count at each terminal, which will be referred to as the *terminal count*. In our tables, Pass and Term denote the passage count and the terminal count, respectively.

Table 5.1 gives the feature strings generated from our database for the digit 1, whose trie is illustrated in Figure 5.2.

j	Term	Pass	Step 0	Step 1	Step 2	Step 3	Step 4	Step 5	Step 6	Step 7
1	363	363	H12	V12	H12	V12				
2	9	9	H12	V12	V12	H12				
3	10	11	H12	V2	H12	V1	V4	V1		
4	1	1	H12	V2	H12	V1	V4	V1	V4	V1
5	11	12	H12	V3	V7	V9	H12	V1		
6	1	1	H12	V3	V7	V9	H12	V1	V4	V1
7	6	6	H12	H12	V12	V12				
8	1	1	H1	V3	H3	H7	V7	H9	V9	V1
9	1	1	H1	V3	H3	H7	V7	V9	H9	V1
10	2	3	H1	V12	H3	H7	H9	V12		
11	1	1	H1	V12	H3	H7	H9	V12	H1	H4
12	1	1	H1	H4	H1	V12	H2	V12		
13	9	9	V12	H12	V12	H12				
Extended sample set size : 416										

Table 5.1 Feature Strings for Digit 1

Training strings are extracted from the trie in preorder and sequentially assigned an integer j. Those which are proper substrings of others tend to bunch together in our listing, e.g., strings 3, 5, 10 are substrings of 4, 6, 11, respectively. The first string in a *bunch* is a shortest prefix of its subsequent strings, if any, and each string is, in turn, a proper substring of the following strings.

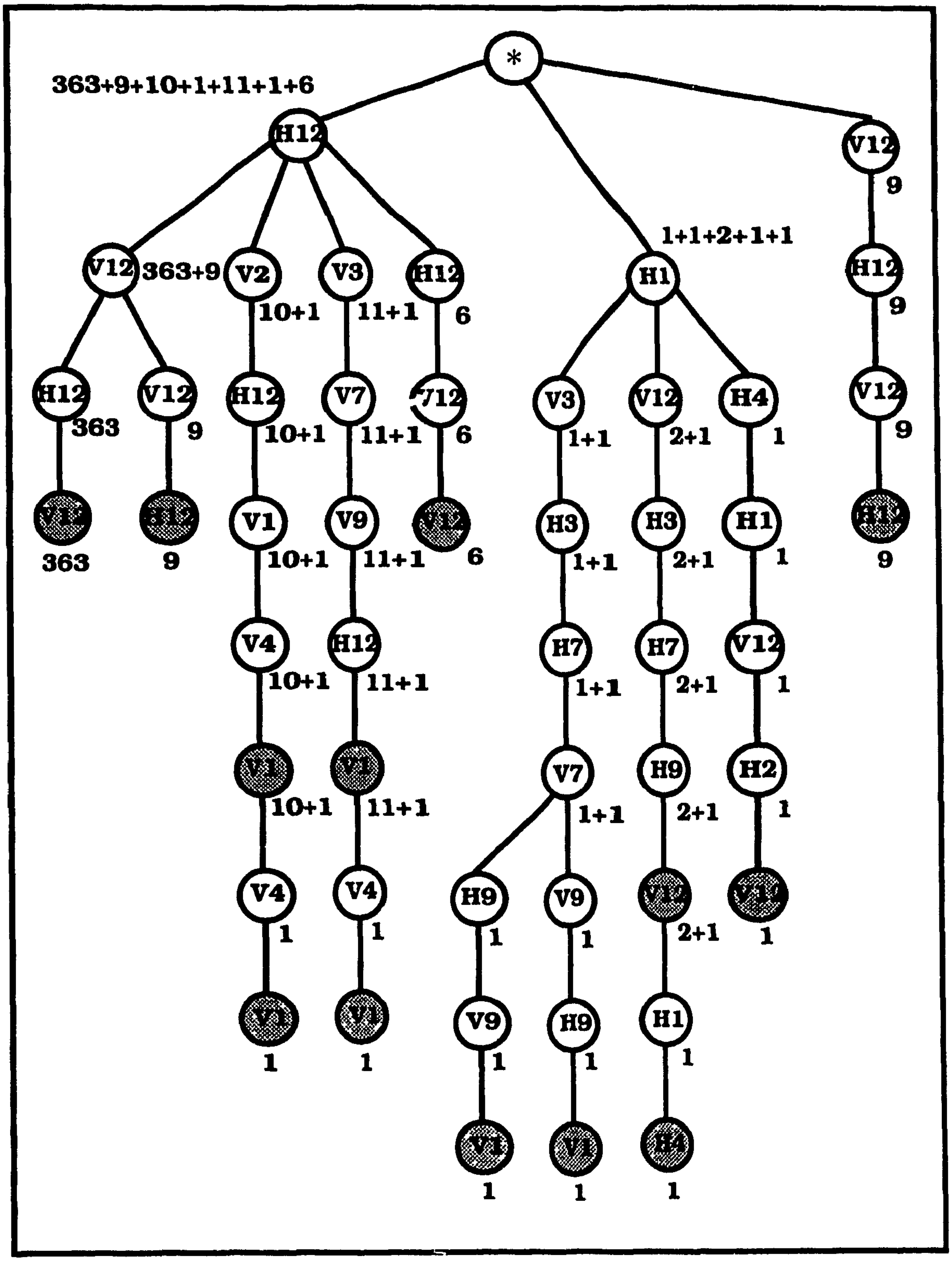

Figure 5.2 Trie Representation of Digit 1

These bunches are part of larger *clumps* since, in general, a training string is a prefix of all strings which terminate in the subtree rooted at its terminal node. We can identify these clumps in the preorder listing of the feature strings using the numbers Term and Pass. The passage count of a terminal node gives the total number of occurrences of all training strings which terminate in the subtree rooted at this node, including those terminating at the root. The number of occurrences of the training string terminating at the root is exactly the terminal count. Thus the quantity (Pass - Term) gives the total number of occurrences of training strings which terminate within the subtree, not including the root. This property is, clearly, recursively true.

To formalize this notion, let n denote the number of distinct feature strings in a clump. Further, let $Pass_j$ and $Term_j$ denote the passage and terminal counts, respectively, for the jth string in the clump, $j = 1, ..., n$. From the above discussion, the passage and terminal counts satisfy the following properties:

$$Pass_j = Term_j + Rem_j, \; j = 1, ..., n,$$

where $Rem_j \geq 0$ is the remaining number of occurrences of training strings terminating within the proper subtree, i.e. not including the root. We have

$$Pass_1 = \sum_{j=1}^{n} Term_j \quad \text{and} \quad Rem_1 = \sum_{j=2}^{n} Term_j .$$

The first training string identifies the number $Pass_1$ of occurrences of feature strings in the clump. Excluding the $Term_1$ occurrences of the first string, there are $Rem_1 = Pass_1 - Term_1$ occurrences of feature strings remaining in the clump. If $Rem_1 > 0$, then n is at least 2. Since strings are listed in preorder, the next string in the list is part of the clump and there are $\mathrm{Term}_2 > 0$ occurrences of it and $\mathrm{Rem}_1 - \mathrm{Term}_2 = \mathrm{Pass}_1 - (\mathrm{Term}_1 + \mathrm{Term}_2)$ remaining. If this number is not zero, then the next string is included. After including j strings, there are

$$\mathrm{Pass}_1 - \sum_{i=1}^{j} \mathrm{Term}_i$$

occurrences of strings left in the clump. The nth string is included as soon as the above quantity reaches 0. The next string in a listing is the first in the new clump. A clump corresponds to the set of training strings terminating in the subtree rooted at the first terminal node in a path from the root of the trie. Our example for digit one has ten clumps (Figure 5.2).

It will be convenient to extend the definitions of passage and terminal counts to all nodes in each trie T_c for class c. In order to do so, let us number all nodes in T_c in preorder with the indices 0, 1,..., $|T_c|$-1. Figure 5.3 depicts the preorder numbering for the root of a trie and its children, assuming the root has b subtrees containing n_1, n_2, ..., n_b nodes, respectively.

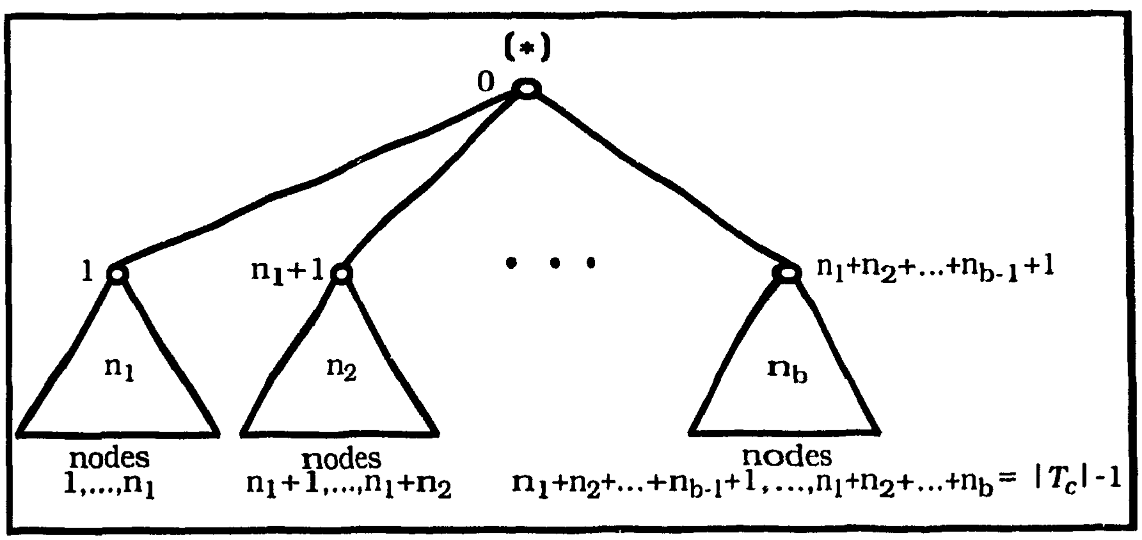

Figure 5.3 Preorder Numbering for a Trie

In general, let node i branch into b_i subtrees and let s_i and t_i denote the passage and terminal counts, respectively, for nodes $i = 0, 1, \ldots, |T_c| - 1$. Since training strings only terminate at terminals, then we define $t_i = 0$ when node i is a nonterminal and $t_i = Term_j$ when node i is the jth terminal node. Figure 5.4 illustrates the passage count relation for a general node in the trie T_c. The passage count s_i is given by

$$s_i = t_i + \sum_{k=1}^{b_i} s_{r_k}$$

where r_k, $k = 1, \ldots, b_i$, are the indices of the root nodes of the b_i subtrees of node i. Note that $s_i = t_i$ when node i is a leaf of T_c.

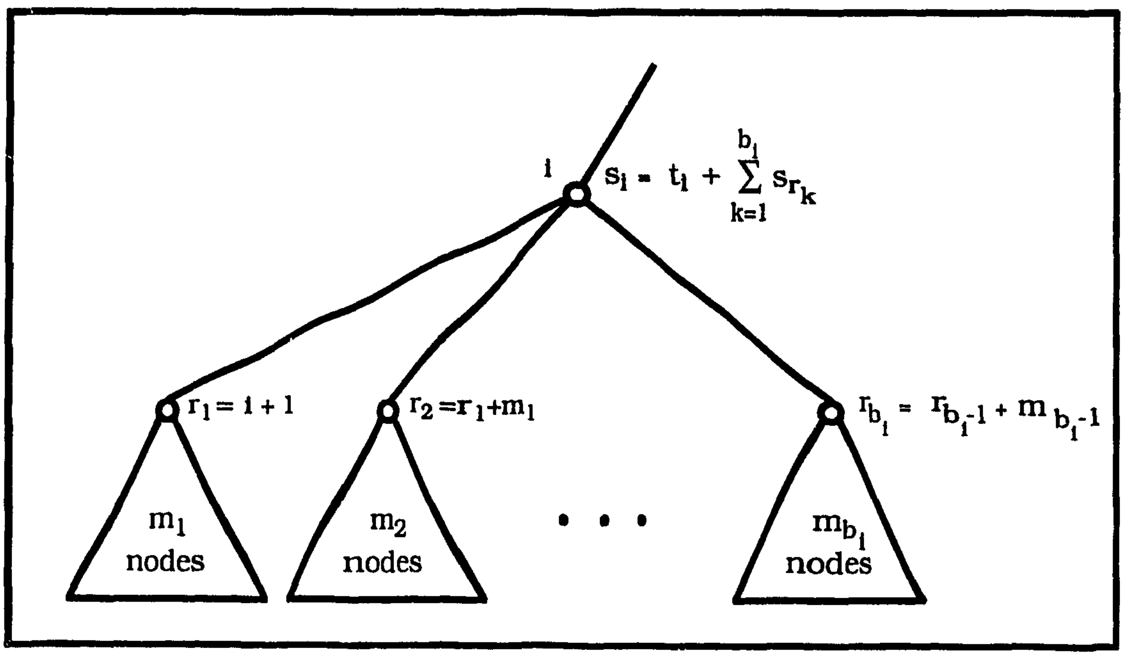

Figure 5.4 Passage Count Relation for a General Trie Node

Solving this last expression recursively gives s_i explicitly in terms of the terminal counts t_j contained in the subtree rooted at i, as

$$s_i = t_i + \sum_{k=1}^{b_i} \sum_{j=r_k}^{r_k+m_k} t_j = t_i + \sum_{j=i+1}^{i+1+m_1+\ldots+m_{b_i}} t_j = \sum_{j=i}^{i+1+m_1+\ldots+m_{b_i}} t_j$$

Thus, in general, the passage count of a node is simply the sum of the terminal counts of all nodes contained in the subtree rooted at the node. For the root of the trie T_c, i = 0 and we obtain the important relation

$$s_0 = \sum_{j=0}^{1+n_1+\ldots+n_{b_0}} t_j = \sum_{j=0}^{|T_c|-1} t_j = \mathrm{Ext}(T_c)$$

where $\mathrm{Ext}(T_c)$ is the extended sample set size for class c. We will use these quantities and relationships to introduce probabilistic measures in the next section.

5.3 Probability Distribution of the Classes

The finite resolution of the digitization process implies that all feature strings are finite in length, as we can have at most one feature per image coordinate. Since there are only 24 possible feature relations, the universal trie $\mathscr{T}_c$ representing the sample space of all possible class c feature strings is finitely branching and, therefore, finite.

Clearly, classification is trivial if the sample spaces are disjoint. In general, $\mathscr{T}_c \cap \mathscr{T}_d \neq \phi$, $c \neq d$. Theoretically, we will assume the worst case scenario where $\mathscr{T}_c = \mathscr{T}_d$, $c \neq d$, i.e., the sample spaces of all classes are the same. Allowing for arbitrary noise in a received feature string, we can assume further that each universal trie $\mathcal{T}_c$ is the complete 24-way tree corresponding to the set of all possible strings composed of the 24 "letters", up to some maximum length. For notation simplicity, let us number the nodes in each universal trie so that node k refers to the same node in every tree and let us further assume that $\mathcal{T}_c$ is preorder numbered.

Let F_c denote an arbitrary feature string from class c. Each F_c is a member of the universal trie $\mathcal{T}_c$ and terminates at some node k in $\mathcal{T}_c$. Let $\mathcal{T}_{ck}$ denote the subtree of $\mathcal{T}_c$ rooted at node k. Note that $\mathcal{T}_{ck} = \mathcal{T}_{dk}$, $c \neq d$ since $\mathcal{T}_c = \mathcal{T}_d$ and the tries are numbered in one-to-one correspondence. We use the notations $F_x = \mathcal{T}_{ck}$ and $F_x \in \mathcal{T}_{ck}$ to mean that a feature string F_x from an unknown class x terminates at node k of $\mathcal{T}_c$ and at some node within the subtree $\mathcal{T}_{ck}$, respectively. Associated with each universal trie $\mathcal{T}_c$, are the probability distribution $P(F_x = \mathcal{T}_{ck})$ of feature strings and the accumulated distribution $P(F_x \in \mathcal{T}_{ck})$ of feature strings with a prefix terminating at node k. The accumulated distribution is related to the feature string distribution by

$$P(F_x \in \mathcal{T}_{ck}) = \sum_{j \in \mathcal{T}_{ck}} P(F_x = \mathcal{T}_{cj})$$

$$= \sum_{j=k}^{k+|\mathcal{T}_{ck}|-1} P(F_x = \mathcal{T}_{cj})$$

The last expression follows from the preorder numbering of $\mathcal{T}_c$. For every prefix of an incoming feature string F_x, we define the likelihood of class c as the conditional probability $P(x = c \mid F_x \in \mathcal{T}_{ck})$. Applying Bayes' rule [FRWA80], this conditional probability can be computed as follows.

$$P(x = c \mid F_x \in \mathscr{T}_{ck}) = \frac{P(F_x \in \mathscr{T}_{ck}, x = c)}{P(F_x \in \mathscr{T}_{ck})}$$

$$= \frac{P(F_x \in \mathscr{T}_{ck} \mid x = c)\, P(x = c)}{\sum_{d=0}^{9} P(F_x \in \mathscr{T}_{ck} \mid x = d)\, P(x = d)}$$

Assuming the classes are equally likely, $P(x = c) = 1/10$ and the above conditional probability reduces to

$$P(x = c \mid F_x \in \mathscr{T}_{ck}) = \frac{P(F_x \in \mathscr{T}_{ck} \mid x = c)}{\sum_{d=0}^{9} P(F_x \in \mathscr{T}_{ck} \mid x = d)}$$

If the distributions of feature strings were known for each class, we could use the above equation to implement a maximum-likelihood classifier for our decision making process. At best, we can either assume the forms of the distributions or try to estimate them. Since our tries are built from training strings which are supposedly representative of the universe of possible feature strings, we shall use the latter approach. Figure 5.5 depicts a portion of the probability distributions for two classes $\mathscr{T}_c$ and $\mathscr{T}_d$. A maximum-likelihood decision process could simply associate the incoming feature string F_x with the class c having the highest probability of occurrence of F_x. For instance, F_x shown in Figure 5.5 is more likely to be from class c than from class d. This is also true for any prefix of a feature string. If the distributions of $\mathscr{T}_c$ and $\mathscr{T}_d$ are largely disjoint, then classification by way of maximum likelihood will work well statistically.

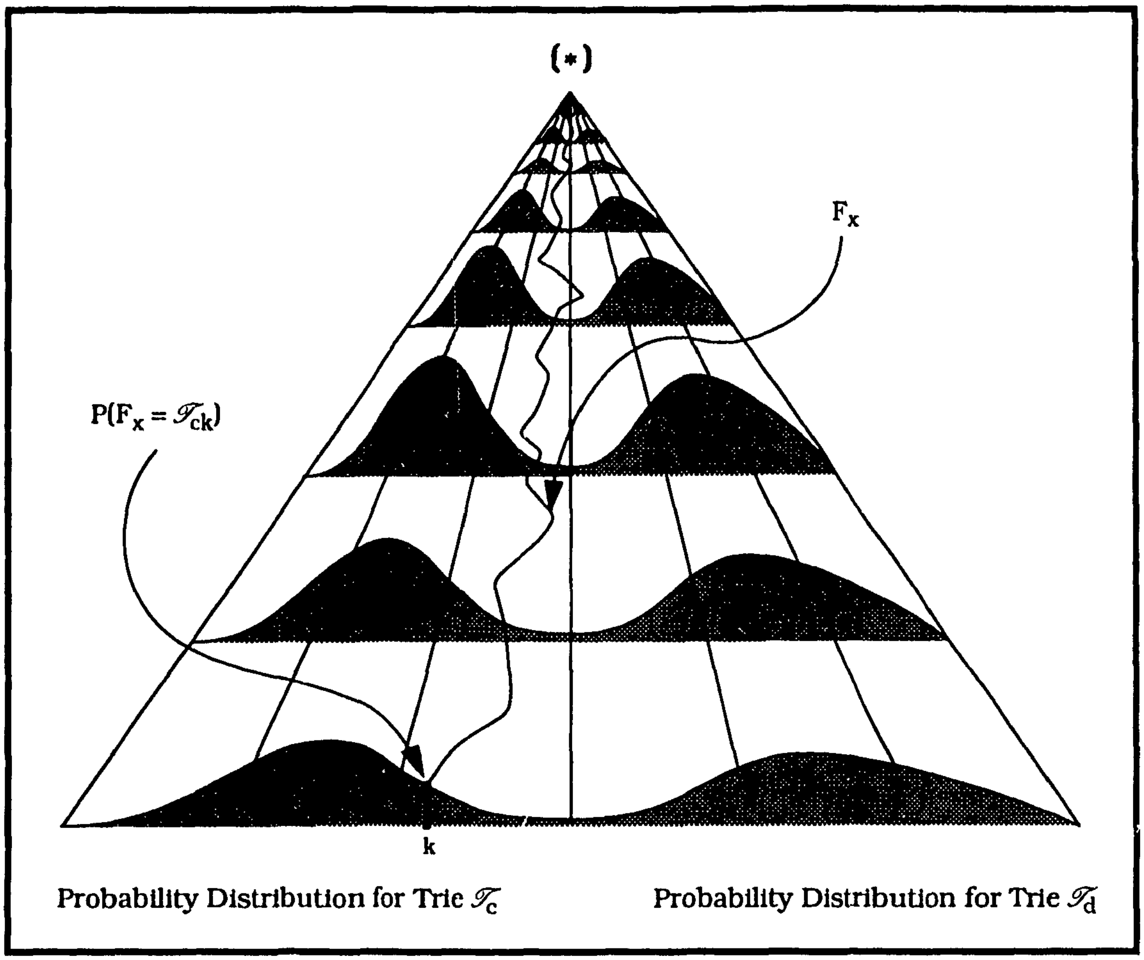

Figure 5.5 Portion of the Intersection of the Distributions of $\mathscr{T}_c$ and $\mathscr{T}_d$

Unfortunately, the distributions of the sample spaces are unknown. All that can be estimated are the frequencies of strings in the training sets. Figure 5.6 depicts the learning process through training. The trie represents the most probable feature strings or the mass of the sample space for class c. The striped regions correspond to known strings or strings in the training sets. The dark regions represents "the Land of the missing strings". They are probable strings which have not previously occurred in the training sets but would eventually become known through continued training. In other words, as learning continues, these unknown strings would get inserted in the trie T_c and therefore the striped regions would grow into the dark regions to include the entire mass of the distribution.

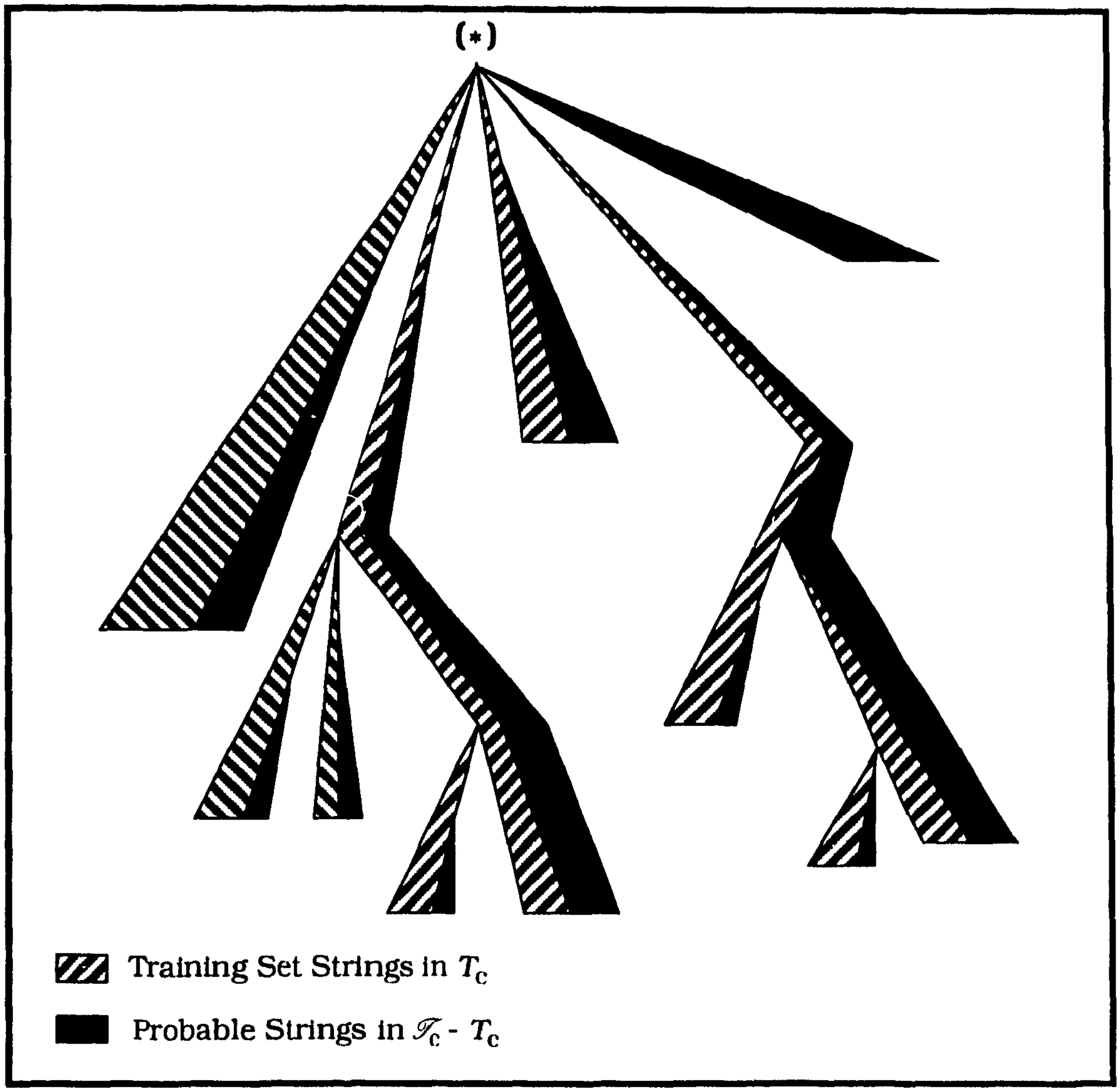

Figure 5.6 Learning the Distribution of $\mathscr{T}_c$ through Training

An incoming feature string F_x is either entirely or partially contained in T_c. In the former case, we can use our passage and terminal counts to estimate its relative frequency in $\mathscr{T}_c$. In the latter case, there is a prefix (possibly null) of F_X contained in T_C, the successor relation of which causes a *miss*. At this point, the incoming string diverges from the set of known strings. If we consider this missing relation as erroneous, we can examine the *suffix* or the remaining sequence of relations of F_X in the known subtrie rooted at the node corresponding to the relation just prior to where the miss occurred. The suffix of F_X can be treated as the prefix of a new sequence entering this subtrie. Consequently, any incoming string can be compared to every known string allowing for any number of misses. Any relations remaining in F_X when a leaf of T_C is encountered in a path are considered to be additional misses for that path. Among all such known strings, there is a subset which most closely matches the incoming string on the basis of the number of matching relations or, equivalently, on the number of misses. The passage and terminal counts of each of these closest strings in T_C will be used to estimate the probability of the incoming string in the trie $\mathcal{T}_C$.

Under this matching process, each event $F_x \in \mathcal{T}_{ck}$ maps to the set of strings

$$\{F_c^i \in T_{ck_i}\}_{i = 1, \ldots, u}$$

in T_C with a minimum number of differing relations. The relative frequency of the ith event in this set is estimated by

$$w_{k_i} = \frac{s_{k_i}}{\mathrm{Ext}(T_c)}$$

where s_{k_i} is the passage count of the node k_i in T_C. We will use these numbers in our decision process to determine the likelihood of each event in this set.

5.4 Goodness of Fit Measure

In order to define a goodness of fit measure $E_c(F_x)$, we will make use of the estimate of the relative frequency discussed in Section 5.3, as well as a quadrant distance measure, and an attribute of the way in which F_x terminates in our decision process.

Each feature string F_x has an associated quadrant string Q_x localizing each shape relation of F_x in some grid quadrant of the image. Let $Q_x(\ell)$ denote the quadrant associated with the ℓth shape relation in F_x and let $Q_c^i(\ell)$ be the averaged quadrant for the ℓth shape relation in a string $F_c^i \in T_c$ against which F_x is compared. We measure *quadrant distances* as

$$D_c^i(\ell) = \left|Q_x(\ell) - Q_c^i(\ell)\right|, \ell = 1, \ldots, \text{length}(Q_c^i(\ell))$$

on a per relation basis. The distance between strings F_x and F_c^i is taken to be

$$D_c^i(F_x) = \sum_{\ell=1}^{\text{length}(F_c^i)} \ln(D_c^i(\ell) + 1)$$

which was empirically determined. The Naperian logarithm function was preferred over the use of the simpler distance measure

$$\sum_{\ell=1}^{\text{length}(F_c^i)} D_c^i(\ell)$$

as it increased recognition.

The last relation in a feature string belonging to the test set may not have been a terminal node in the trie representation which evolved from our training samples. To account for this attribute of termination, we will introduce a term bias $B_c^i(F_x)$ to adjust the relative frequency measure $W_c^i(F_x)$ for strings F_x terminating at nonterminals in T_c. The term bias was empirically set at the value 1 if the node is a terminal vertex or a leaf and at the value 2 for a non-terminal node.

Then we define the goodness of fit between the incoming string F_x and the string F_c^i in T_c to which it is compared as

$$E_c^i(F_x) = \frac{W_c^i(F_x)}{B_c^i(F_x)\,(1 + D_c^i(Q_x))}$$

or expanded as

$$E_c(F_x) = \frac{W_c^i(F_x)}{B_c^i(F_x) \bullet [1 + \ln(D_c^i(1) + 1) + \ldots + \ln(D_c^i(\text{length}(F_c^i)) + 1)]}$$

Thus the best fit is given by

$$E_c(F_x) = \max_{i=1,\ldots,u}\{E_c^i(F_x)\}$$

where the maximum is taken over the set of strings $\{F_c^i\}$ which have a minimum number of misses for F_x in T_c.

To determine the most likely class for an incoming string F_x, we match F_x in each of the ten tries and select those classes $\{c_1, \ldots, c_u\}$ in which F_x experienced a minimum number of misses. Among these classes, we choose the one which maximizes $E_c(F_x)$ as the recognized digit class d, i.e.,

$$E_d(F_x) = \max_{i=1,\ldots,u}\{E_{c_i}(F_x)\}$$

5.5 Decision Making Process

The method implemented is called the Perfect Match. We generate a feature string for an unknown sample and attempt to match this unknown string in each of our ten tries. We select the *best* matching sequence of nodes in each trie, which is the optimal choice per trie. We then pick the best of these ten possibilities and accept the corresponding digit as the recognized class.

The matching is performed by searching the tries in a preorder fashion. We compare the incoming relation of our unknown string to the relation at each node. When a match occurs, we proceed down a branch and try matching our next incoming relation at the next level in our tree. However, if a match does not occur, we treat mismatched relations, the relation node in the tree and the incoming relation, as *wildcards*. Allowing for a maximum of three misses, we jump forward in our tree and in the incoming string and try to match the next relation at the subsequent level. When descending along a path, we stop if a third miss occurs, or either a leaf node of the trie or the final relation of the incoming string is encountered. Then we climb back up to the previous node on this path and continue our matching process in the remaining subtries rooted at this node in the usual preorder fashion.

In order to compute a best match, let us introduce the following two measures. Let M_{ck} denote the minimum number of misses that occur in the subtrie T_{ck} during this traversal. Also, let m_{ck} be the binary variable which indicates whether or not a miss occurs at node k, i.e., $m_{ck} = 1$ if a miss occurs at node k and $m_{ck} = 0$, otherwise. Let d_{ck} denote the quadrant distance measure for relations compared at node k. $d_{ck} = D^i_c(\ell)$ when F_x visits node k at the ℓ th relation. Further, let D_{ck} be a variable used to accumulate the distance measure for the best path in T_{ck}.

Figure 5.7 illustrates the variables used by a node k in this computation. As we traverse the trie during the matching process, we compute the quantities M_{ck} , D_{ck}, W_{ck} and B_{ck} recursively at each node k as follows.

$$M_{ck} = m_{ck} + \min_{j \in \{r_1, \ldots, r_{b_k}\}} \{M_{cj}\}$$

where r_j, j = 1, ..., b_k are the node numbers of the children of node k. We choose the child v of node k satisfying

$$\frac{W_{cv}/B_{cv}}{D_{cv} + \ln(d_{ck}+1)} = \max_{j \in \{r_{i_1}, \ldots, r_{i_u}\}} \left\{ \frac{W_{cj}/B_{cj}}{D_{cj} + \ln(d_{ck}+1)} \right\}$$

where i_1, ..., i_u are the children of node k where the minimum number of misses occur. Then

$$D_{ck} = D_{cv} + \ln(d_{ck} + 1)$$

$$W_{ck} = W_{cv}$$

$$B_{ck} = B_{cv}$$

where

$$D_{cn_j} = \ln(d_{cn_j} + 1)$$

$$W_{cn_j} = w_{n_j}$$

$$B_{cn_j} = b_{n_j}$$

at the node $n_j \in T_{cj}$ at which F_x terminates and w_{n_j} and b_{n_j} are the relative frequency and the terminal bias associated with node n_j respectively.

When the computation terminates, M_{c0} is the minimum number of misses in T_c and

$$E_c(F_x) = \frac{W_{c0}}{B_{c0}D_{c0}}$$

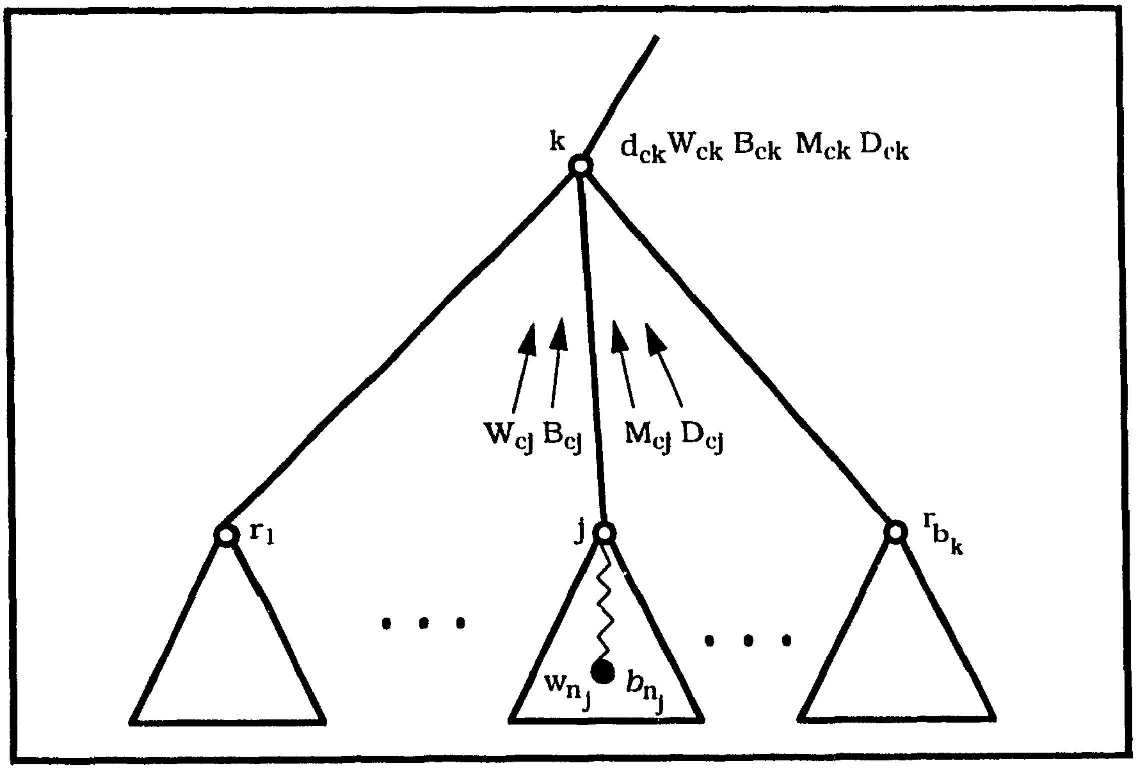

Figure 5.7 Variables Used by the Decision Making Process

CHAPTER 6

PRELIMINARY STATISTICAL INFORMATION

6.1 Introduction

In this chapter, we present, observe and analyze the behavior of the variables used to construct our feature strings. These parameters provide us with significant characteristics, thus justifying their application in the string differentiating process.

These statistical variables are used for their discerning capabilities as the ordered relations in a feature string are not unique. The statistical approach provide us with a good analytical means to examine the database. All statistical computations are done with the number of samples in the extended sample sets.

6.2 Hole Statistics

Table 6.1 contains the average hole count and its rounded value for each digit in our training sets. It can be seen that the digit 8 has on the average more than one but less than two holes and that all other digits have less than one hole on the average. These figures are intuitively reasonable based on observations of well-formed digits and hence digit samples with more than two holes are statistically rare. Based on this fact and that insertion of multiple holes in an outer contour string complicates the structure of the resultant string, as described in Chapter 4, we, decided to used the rounded average hole count as an upper limit on the number of holes included in a feature string for each class. The selected holes, if any, are the larger ones.

DIGIT	AVERAGE HOLE COUNT	ROUNDING OFF THE HOLE COUNT AVERAGES
0	0.86	1
1	0.00	0
2	0.55	1
3	0.10	0
4	0.01	0
5	0.06	0
6	0.89	1
7	0.01	0
8	1.50	2
9	0.65	1

Table 6.1 Average Hole Count per Digit

6.3 Relation Counts and Relative Frequencies

As a point of interest, we have computed the counts of each relation per digit in Tables 6.2 and 6.3. This permits us to observe which relations characterize the planar shapes of these images. Note that H11 and V11 give the total hole counts in Tables 6.2, 6.3, 6.4 and 6.5.

DIGIT	EXT.	H COUNTS											
		H1	H2	H3	H4	H5	H6	H7	H8	H9	H10	H11	H12
0	405	125	60	14	47	7	8	22	0	14	1	687	674
1	416	7	1	4	2	0	0	4	0	5	0	0	814
2	422	549	69	346	138	1	76	440	0	276	93	434	138
3	408	610	271	210	137	0	152	261	0	58	51	0	158
4	458	911	293	145	481	0	0	158	0	149	11	0	8
5	419	755	299	140	316	1	76	143	1	66	1	0	110
6	421	771	369	24	368	14	13	40	1	27	1	728	74
7	430	394	12	322	74	0	1	332	0	334	8	0	167
8	423	421	187	42	164	34	17	76	0	67	0	1220	398
9	426	434	64	229	82	61	2	300	0	307	8	524	227

Table 6.2 Counts of Horizontal Relations

DIGIT	EXT.	V COUNTS											
		V1	V2	V3	V4	V5	V6	V7	V8	V9	V10	V11	V12
0	405	152	62	50	33	6	32	56	0	25	0	686	646
1	416	38	11	13	13	0	0	13	0	14	0	0	782
2	422	804	17	399	364	7	9	441	0	397	35	434	2
3	408	750	24	404	317	3	22	817	0	385	410	0	0
4	458	1083	45	380	633	0	3	390	0	386	8	0	26
5	419	878	35	406	428	0	32	422	0	377	16	0	8
6	421	884	397	48	427	7	38	58	1	19	2	728	16
7	430	475	4	407	47	3	0	421	0	423	9	0	10
8	423	728	93	278	332	6	28	310	0	261	26	1220	128

DIGIT	EXT.	V COUNTS											
		V1	V2	V3	V4	V5	V6	V7	V8	V9	V10	V11	V12
9	426	598	16	378	164	16	3	412	0	406	16	524	22

Table 6.3 Count of Vertical Relations

We divide the counts of relations in Tables 6.2 and 6.3 by the extended set sizes. These numbers give the average number of occurrences of each relation per string in the database and are seen in Tables 6.4 and 6.5. These values are rounded to two decimals of precision.

DIGIT	H COUNTS/EXTENDED NO. OF SAMPLES											
	H1	H2	H3	H4	H5	H6	H7	H8	H9	H10	H11	H12
0	0.31	0.15	0.03	0.12	0.02	0.02	0.05	0	0.03	0.00	1.70	1.66
1	0.02	0.00	0.01	0.00	0	0	0.01	0	0.01	0	0	1.96
2	1.30	0.16	0.82	0.33	0.00	0.18	1.04	0	0.65	0.22	1.03	0.33
3	1.50	0.66	0.51	0.34	0	0.37	0.64	0	0.14	0.12	0	0.39
4	1.99	0.64	0.32	1.05	0	0	0.35	0	0.33	0.02	0	0.02
5	1.80	0.71	0.33	0.75	0.00	0.18	0.34	0.00	0.16	0.00	0	0.26
6	1.83	0.88	0.06	0.87	0.03	0.03	0.10	0.00	0.06	0.00	1.73	0.18
7	0.92	0.03	0.75	0.17	0	0.00	0.77	0	0.78	0.02	0	0.39
8	1.00	0.44	0.10	0.39	0.08	0.04	0.18	0	0.16	0	2.88	0.94
9	1.02	0.15	0.54	0.19	0.14	0.00	0.70	0	0.72	0.02	1.23	0.53

Table 6.4 Average Numbers of Horizontal Relations per String

DIGIT	V COUNTS/EXTENDED NO. OF SAMPLES											
	V1	V2	V3	V4	V5	V6	V7	V8	V9	V10	V11	V12
0	0.38	0.15	0.12	0.08	0.01	0.08	0.14	0	0.06	0	1.69	1.60
1	0.09	0.03	0.03	0.03	0	0	0.03	0	0.03	0	0	1.88
2	1.91	0.04	0.95	0.86	0.02	0.02	1.05	0	0.94	0.08	1.03	0.00
3	1.84	0.06	0.99	0.78	0.01	0.05	2.00	0	0.94	1.00	0	0
4	2.36	0.10	0.83	1.38	0	0.01	0.85	0	0.84	0.02	0	0.06
5	2.10	0.08	0.97	1.02	0	0.08	1.01	0	0.90	0.04	0	0.02
6	2.10	0.94	0.11	1.01	0.02	0.09	0.14	0.00	0.05	0.00	1.73	0.04
7	1.10	0.01	0.95	0.11	0.01	0	0.98	0	0.98	0.02	0	0.02
8	1.72	0.22	0.66	0.78	0.01	0.07	0.73	0	0.62	0.06	2.88	0.30
9	1.40	0.04	0.89	0.38	0.04	0.01	0.97	0	0.95	0.04	1.23	0.05

Table 6.5 Average Numbers of Vertical Relations per String

Table 6.6, contains some statistics on the number of relations comprising a typical string. Tables 6.7 and 6.8 gives the relative frequencies of each of the horizontal and vertical relations for strings in each class.

Digit	Average Number of H's	Average Number of V's	Average Length of a Feature String	% of H's	% of V's
0	4.10	4.32	8.41	49	51
1	2.01	2.13	4.14	49	51
2	6.07	6.89	12.96	47	53
3	4.68	7.68	12.35	38	62
4	4.71	6.45	11.16	42	58
5	4.55	6.21	10.76	42	58
6	5.77	6.24	12.01	48	52
7	3.82	4.18	8.00	48	52
8	6.21	8.06	14.27	44	56
9	6.00	5.25	11.25	53	47

Table 6.6 Statistics on the Number of Relations in a String

DIGIT	RELATIVE FREQUENCIES OF THE H RELATIONS											
	H1	H2	H3	H4	H5	H6	H7	H8	H9	H10	H11	H12
0	.15	.07	.02	.06	.01	.01	.03	0	.02	.00	.83	.81
1	.01	.00	.00	.00	0	0	.00	0	.01	0	0	.96
2	.61	.08	.39	.15	.00	.08	.49	0	.31	.10	.48	.15
3	.57	.25	.20	.13	0	.14	.24	0	.05	.05	0	.15
4	.85	.27	.13	.45	0	0	.15	0	.14	.01	0	.01
5	.76	.30	.14	.32	.00	.08	.14	.00	.07	.00	0	.11
6	.88	.42	.03	.42	.02	.01	.05	.00	.03	.00	.83	.08
7	.44	.01	.36	.08	0	.00	.37	0	.37	.01	0	.19
8	.47	.21	.05	.18	.04	.02	.08	0	.07	0	1.36	.44

DIGIT	RELATIVE FREQUENCIES OF THE H RELATIONS											
	H1	H2	H3	H4	H5	H6	H7	H8	H9	H10	H11	H12
9	.54	.08	.28	.10	.08	.00	.38	0	.38	.01	.65	.28

Table 6.7 Relative Frequencies of the Horizontal Relations

DIGIT	RELATIVE FREQUENCIES OF THE V RELATIONS											
	V1	V2	V3	V4	V5	V6	V7	V8	V9	V10	V11	V12
0	.19	.08	.06	.04	.01	.04	.07	0	.03	0	.86	.81
1	.05	.01	.02	.02	0	0	.02	0	.02	0	0	.96
2	1.01	.02	.50	.46	.01	.01	.55	0	.50	.04	.55	.00
3	1.14	.04	.61	.48	.00	.03	1.24	0	.59	.62	0	0
4	1.37	.06	.48	.80	0	.00	.49	0	.49	.01	0	.03
5	1.11	.04	.51	.54	0	.04	.53	0	.48	.02	0	.01
6	1.09	.49	.06	.53	.01	.05	.07	.00	.02	.00	.90	.02
7	.59	.00	.50	.06	.00	0	.52	0	.52	.01	0	.01
8	.90	.11	.34	.41	.01	.03	.38	0	.32	.03	1.51	.16
9	.66	.02	.42	.18	.02	.00	.45	0	.45	.02	.59	.02

Table 6.8 Relative Frequencies of the Vertical Relations

The relative frequencies given in Tables 6.7 and 6.8 are plotted in the following 10 histograms. Sorting the relative frequencies in decreasing order, we obtain Table 6.9. Relations with the same relative frequency are clustered into subsets.

DIGIT	SEQUENTIAL SETS
0	{V11} {H11} {H12 V12} {V1} {H1} {V2} {H2 V7} {H4 V3} {V4 V6} {H7 V9} {H3 H9} {H5 H6 V5}
1	{H12 V12} {V1} {V3 V4 V7 V9} {H1 V2}
2	{V1} {H1} {V7 V11} {V3 V9} {H7} {H11} {V4} {H3} {H9} {H4 H12} {H10} {H2 H6} {V10} {V2} {V5 V6}
3	{V1} {V7} {V10} {V3} {V9} {H1} {V4} {H2} {H7} {H3} {H12} {H6} {H4} {H9 H10} {V2} {V6}
4	{V1} {H1} {V4} {V7 V9} {V3} {H4} {H2} {H7} {H9} {H3} {V2} {V12} {H10 H12 V10}
5	{V1} {H1} {V4} {V7} {V3} {V9} {H4} {H2} {H3 H7} {H12} {H6} {H9} {V2 V6} {V10} {V12}
6	{V1} {V11} {H1} {H11} {V4} {V2} {H2 H4} {H12} {V7} {V3} {H7 V6} {H3 H9} {H5 V9 V12} {H6 V5}
7	{V1} {V7 V9} {V3} {H1} {H7 H9} {H3} {H12} {H4} {V4} {H2 H10 V10 V12}
8	{V11} {H11} {V1} {H1} {H12} {V4} {V7} {V3} {V9} {H2} {H4} {V12} {V2} {H7} {H9} {H3} {H5} {H6 V6 V10} {V5}
9	{V1} {H11} {V11} {H1} {V7 V9} {V3} {H7} {H3 H12} {V4} {H4} {H2 H5} {V2 V5 V10 V12} {H10}

Table 6.9 Decreasing Sequence of Sets

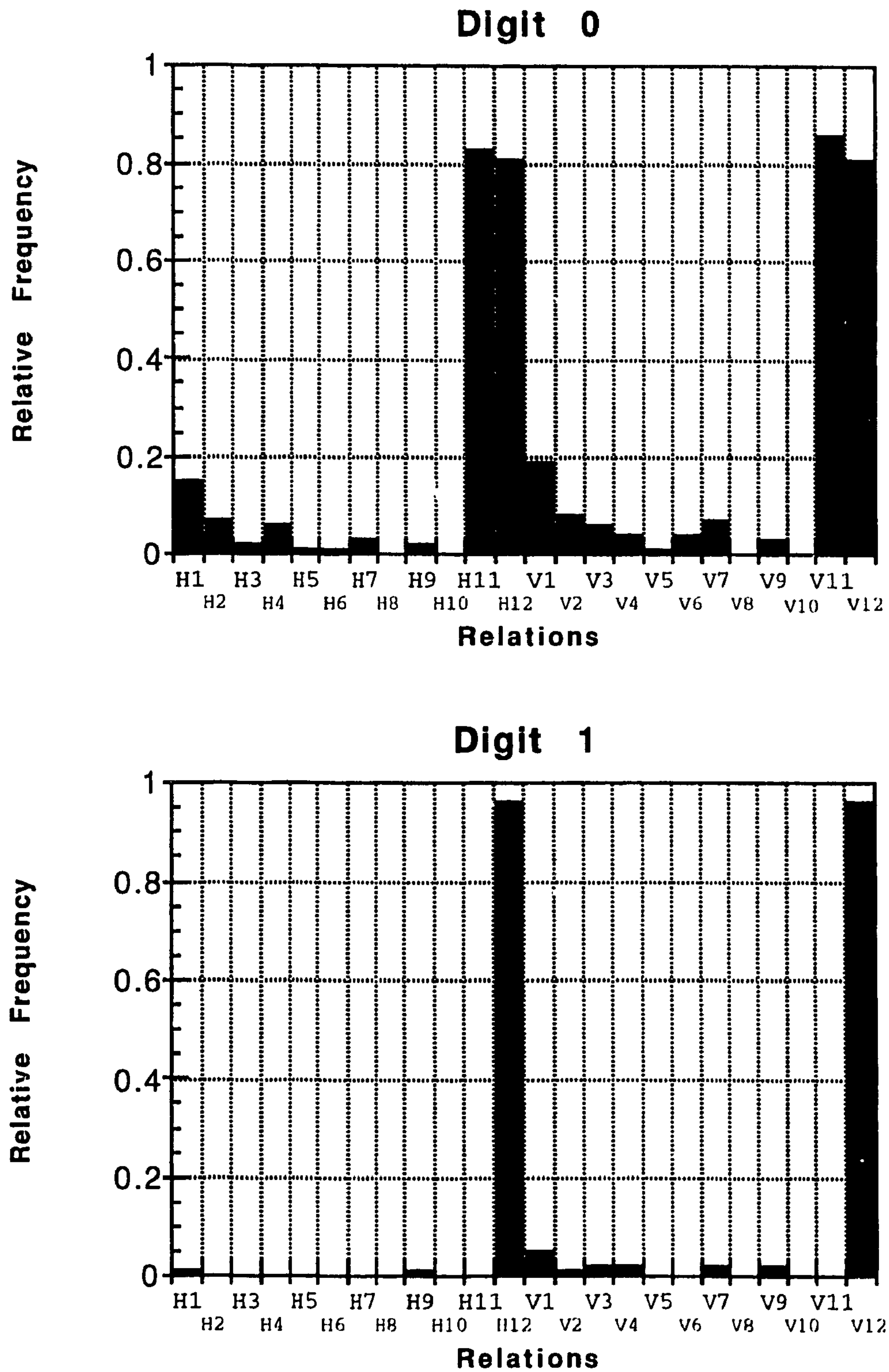

Figure 6.1 Relation Histograms for Digits 0 and 1

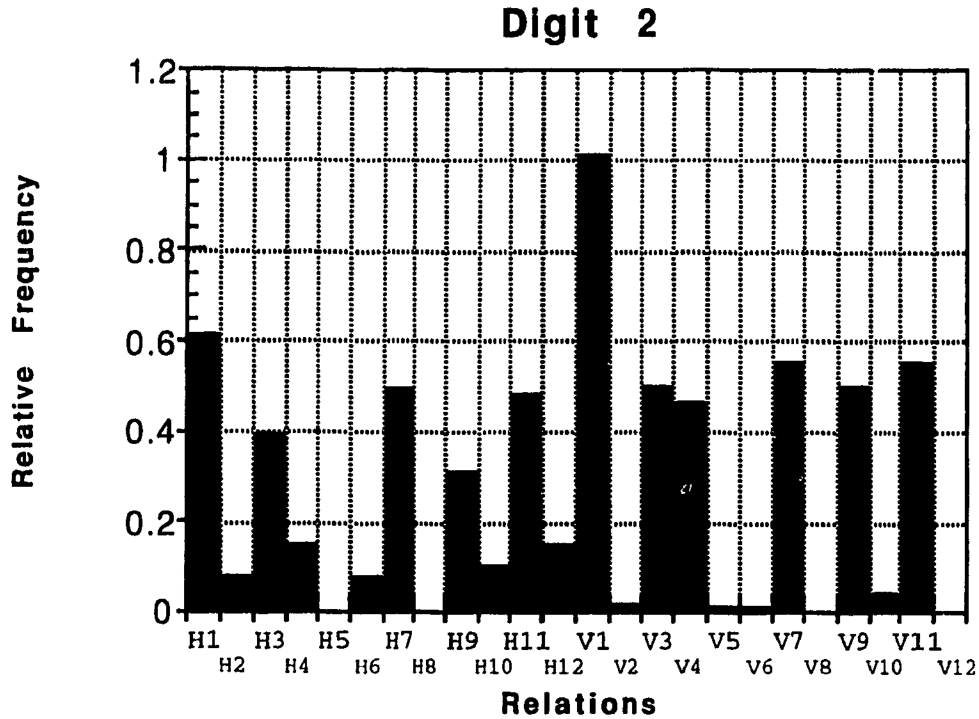

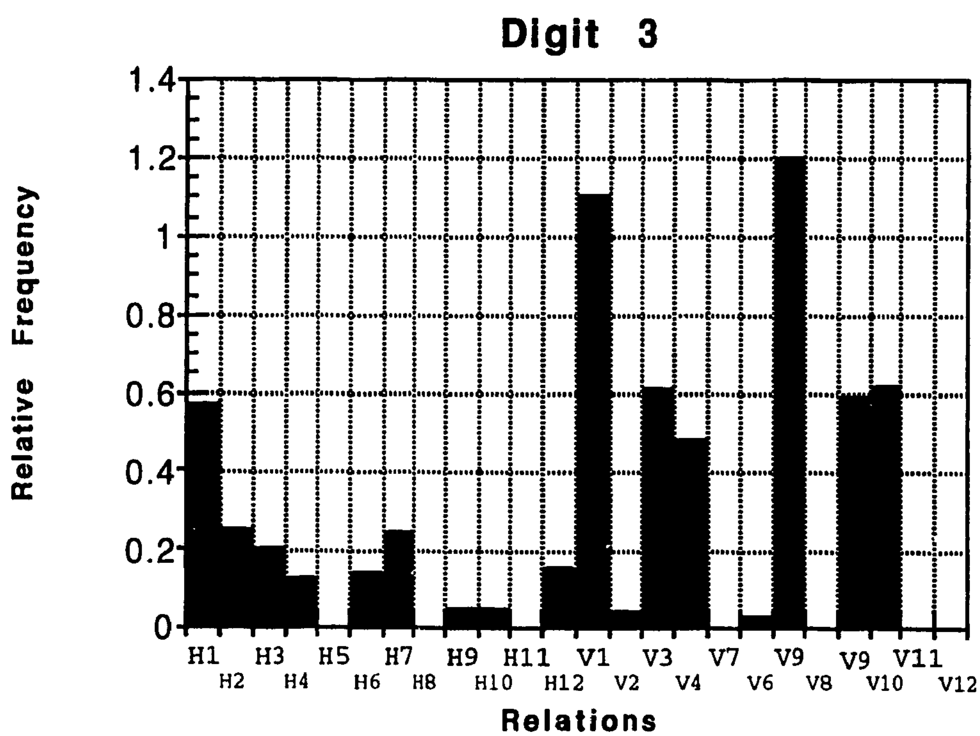

Figure 6.2 Relation Histograms for Digits 2 and 3

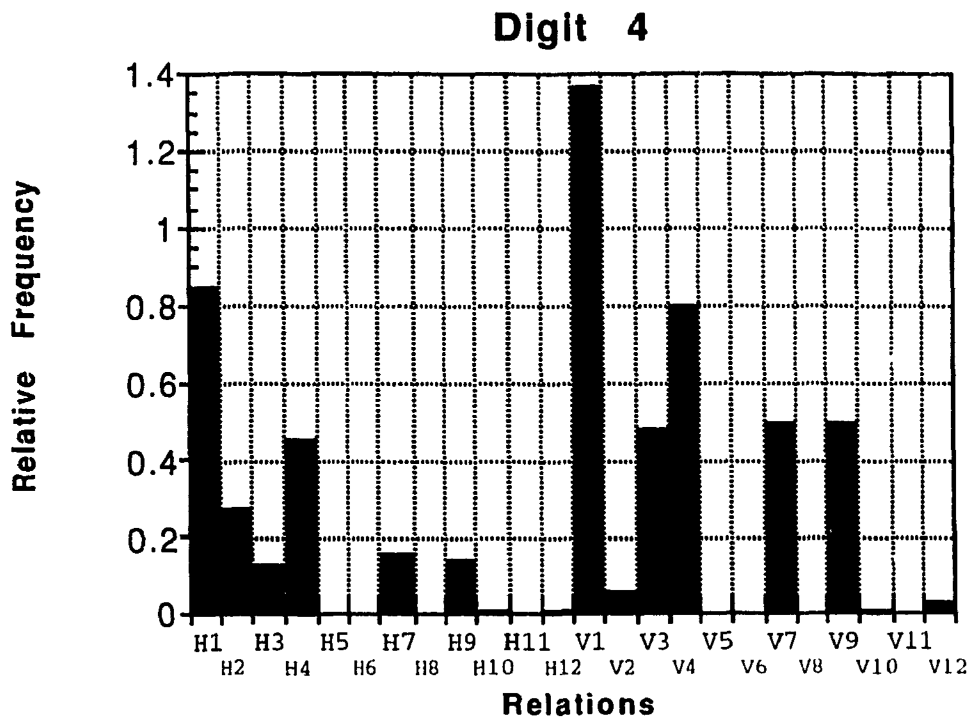

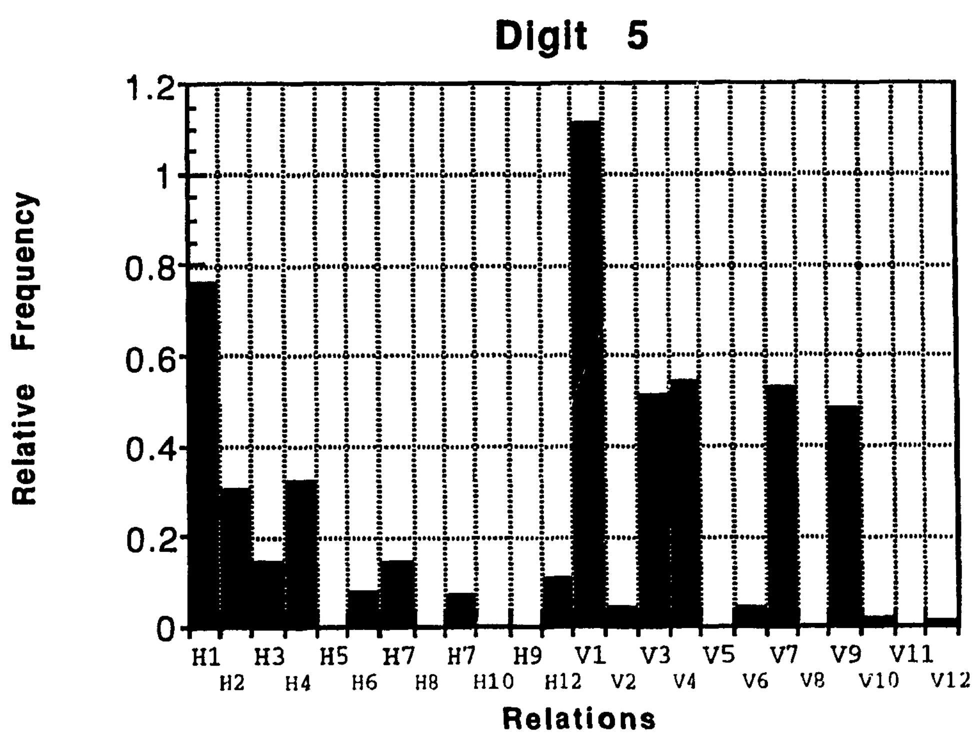

Figure 6.3 Relation Histograms for Digits 4 and 5

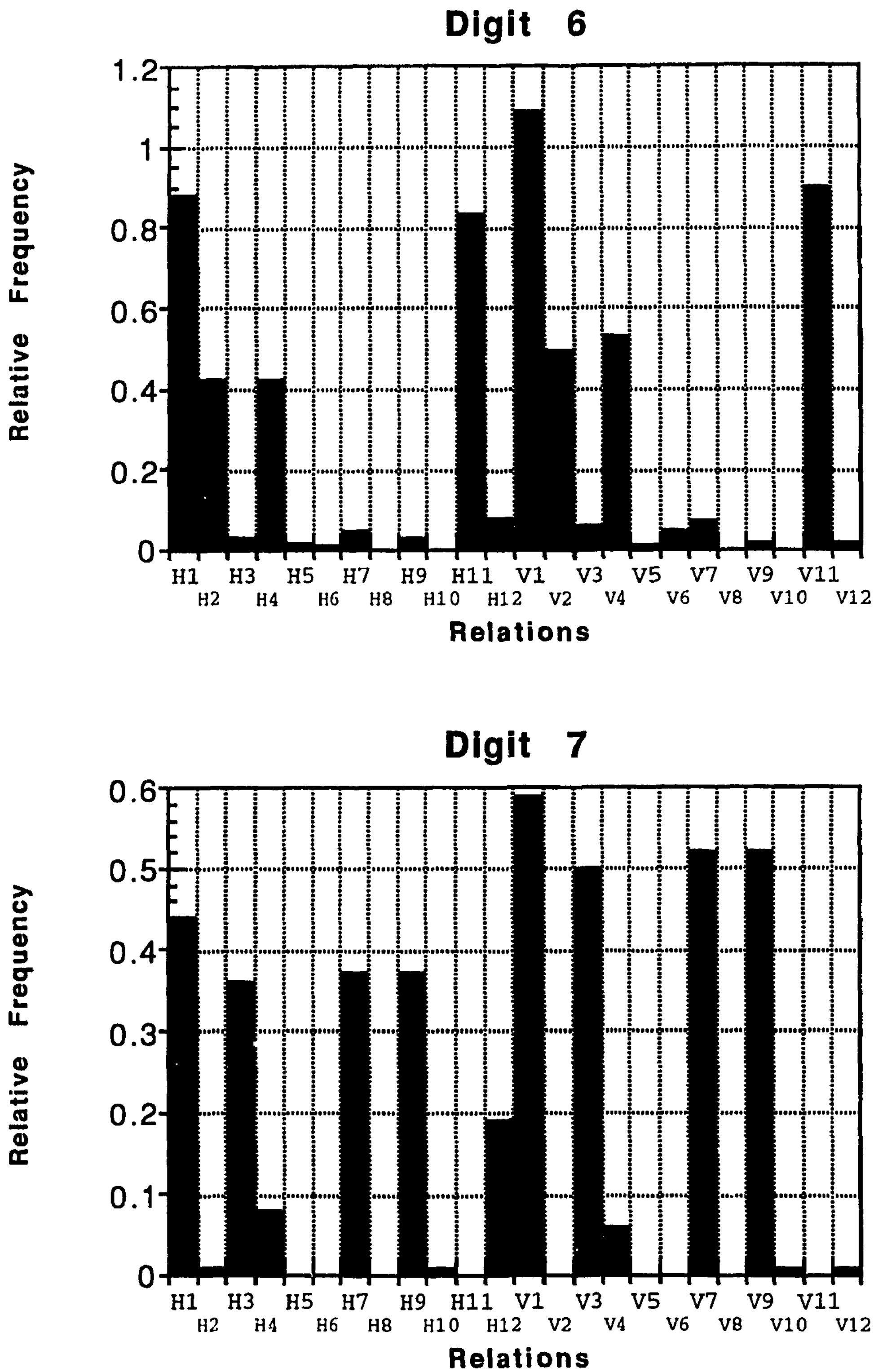

Figure 6.4 Relation Histograms for Digits 6 and 7

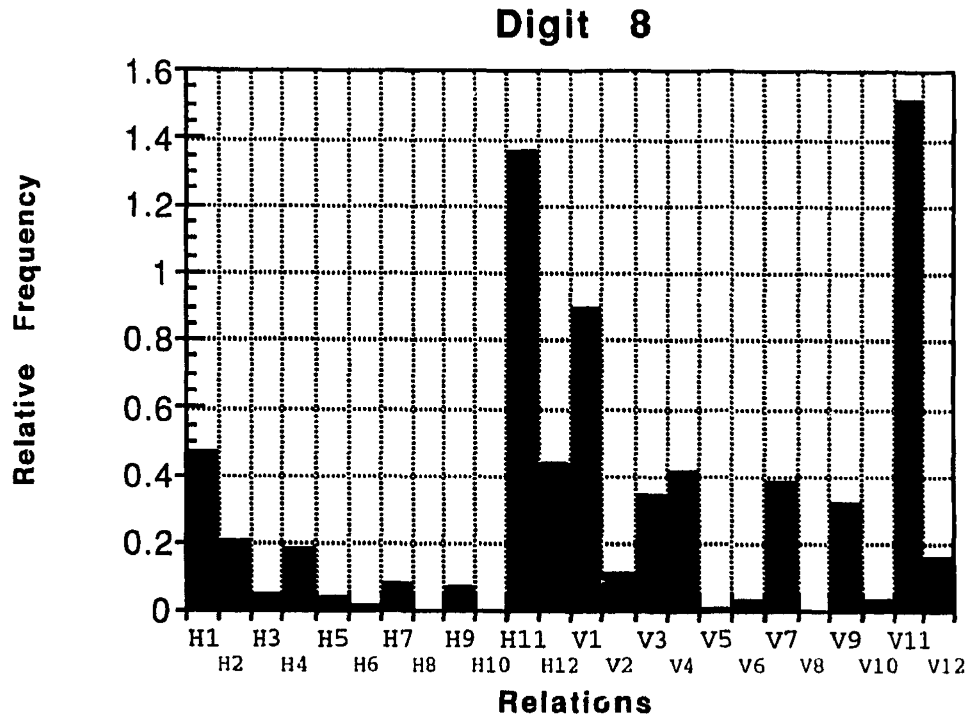

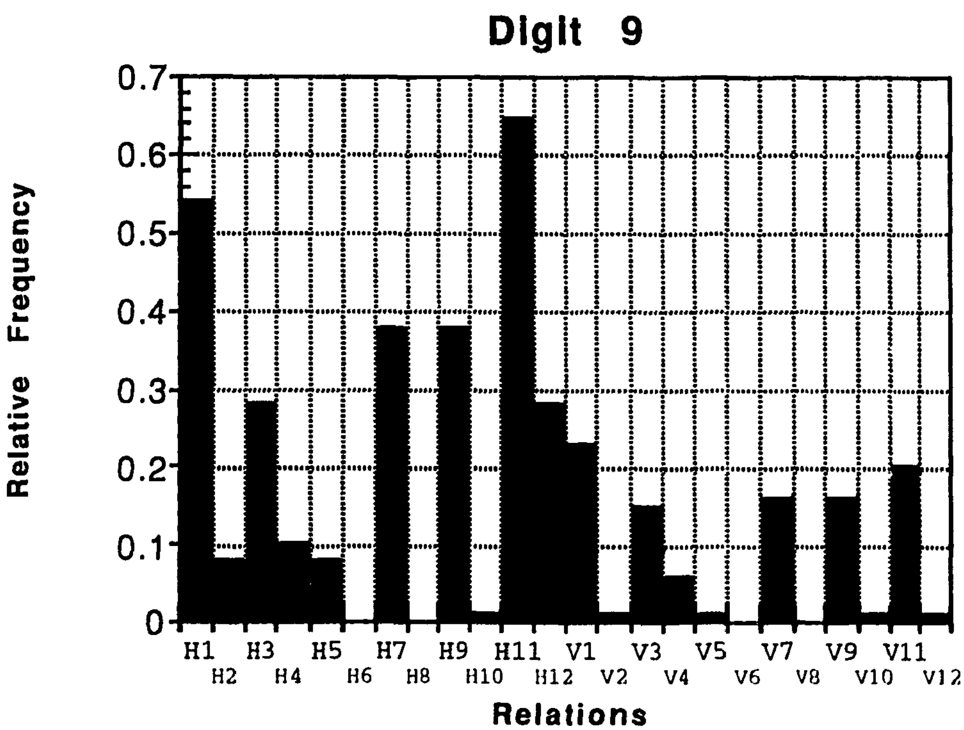

Figure 6.5 Relation Histograms for Digit 8 and 9

6.4 Quadrant Parameters

Another statistical parameter found at each node once the tree is built is the average quadrant. The average quadrant evaluated at each node is a real number to which we have truncated all but one decimal digit.

Table 6.10 contains the counts of all relations present in each quadrant Q_t for each digit in a 4x3 grid and Table 6.11 contains the counts for a 3x3 partitioning. Both tables include a total over the quadrants for all digits and the number of reference points per digit occupies the last column. We obtained a grand total of 44,584 reference points over 4000 samples.

Digit	Q1	Q2	Q3	Q4	Q5	Q6	Q7	Q8	Q9	Q10	Q11	Q12	Total per Digit
0	50	462	533	51	65	556	563	95	93	557	375	7	3407
1	25	26	791	4	7	5	21	9	2	780	24	27	1721
2	389	605	492	184	277	244	509	589	332	1050	305	493	5469
3	380	592	846	187	435	266	329	216	577	671	431	110	5040
4	335	426	830	668	420	219	529	574	173	495	375	66	5110
5	102	309	764	480	349	70	523	400	329	811	333	40	4510
6	90	243	531	55	53	302	604	535	858	846	784	154	5055
7	480	353	1208	356	23	84	20	10	12	624	238	35	3443
8	249	575	1121	347	738	144	413	688	91	1219	347	104	6036
9	88	411	1199	912	558	374	183	160	26	669	164	49	4793
Total per Quadrant	2188	4002	8315	3244	2925	2264	3694	3276	2493	7722	3376	1085	44,584

Table 6.10 Relation Count per Quadrant for each Digit in a 4x3 Grid

Digit	Q1	Q2	Q3	Q4	Q5	Q6	Q7	Q8	Q9	Total per Digit
0	55	502	735	263	39	437	903	456	17	3407
1	25	30	793	10	9	4	795	27	28	1721
2	481	733	622	298	422	268	1353	621	571	5469
3	406	671	948	312	516	490	849	487	361	5040
4	452	476	852	1005	873	345	570	446	91	5110
5	220	429	778	637	506	283	1059	456	142	4510
6	99	255	565	290	305	887	1206	1055	393	5055
7	668	371	1267	187	13	31	625	240	41	3443
8	421	702	1218	385	1071	86	1422	575	156	6036
9	272	510	1400	900	614	194	680	169	54	4793
Total per Quadrant	3099	4679	9178	4287	4368	3025	9462	4532	1954	44,584

Table 6.11 Relation Count per Quadrant for each Digit in a 3x3 Grid

The following 11 figures are constructed from the data presented in Tables 6.10 and 6.11 and provide a visual representation of the distribution of features over the grid quadrants for each digit. We have inserted the relation count in each quadrant for the respective digit classes in the top arrays, shading has been performed in the middle ones (the darker nuances representing the higher counts) and the percentages of features occurring in each quadrant are shown in the bottom ones. Note that the shading of the 3x3 grid is totally independent of the shading of the 4x3, but depends on the relative magnitudes of the feature distribution.

55	502	735
263	39	437
903	456	17

50	462	533
51	65	556
563	95	93
557	375	7

2%	15%	22%
8%	1%	13%
27%	13%	0%

1%	14%	16%
1%	2%	16%
17%	3%	3%
16%	11%	0%

Figure 6.6 Quadrant Averages and Shading for Digit 0

25	30	793
10	9	4
795	27	28

25	26	791
4	7	5
21	9	2
780	24	27

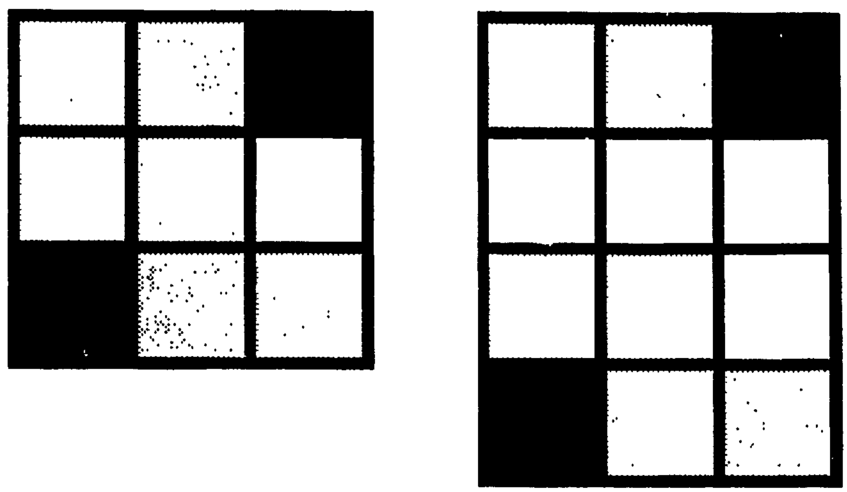

1%	2%	46%
1%	1%	0%
46%	2%	2%

1%	2%	46%
0%	0%	0%
1%	1%	0%
45%	1%	2%

Figure 6.7 Quadrant Averages and Shading for Digit 1

481	733	622
298	422	268
1353	621	671

389	605	492
184	277	244
509	589	332
1050	305	493

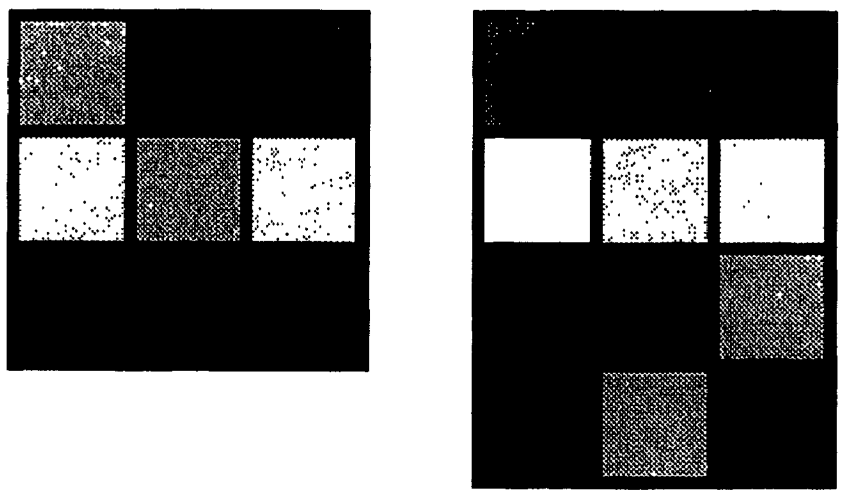

9%	13%	11%
5%	8%	5%
25%	11%	12%

7%	11%	9%
3%	5%	4%
9%	11%	6%
19%	6%	9%

Figure 6.8 Quadrant Averages and Shading for Digit 2

406	671	948
312	516	490
849	487	361

380	592	846
187	435	266
329	216	577
671	431	110

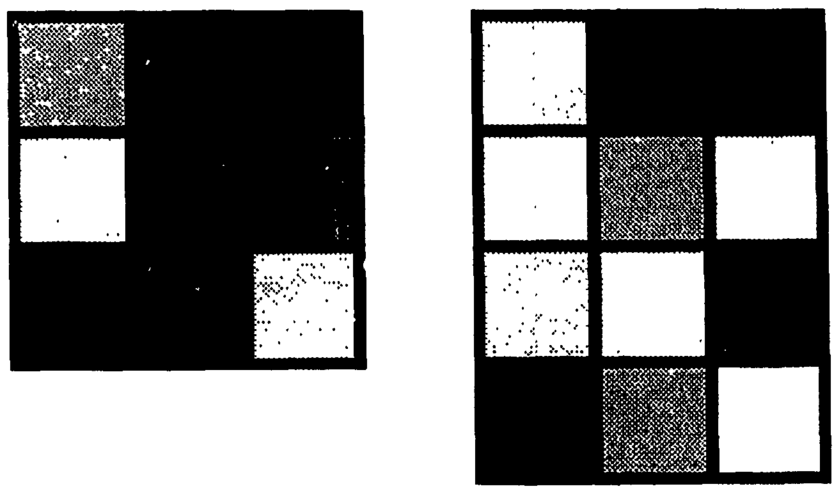

8%	13%	19%
6%	10%	10%
17%	10%	7%

8%	12%	17%
4%	9%	5%
7%	4%	11%
13%	9%	2%

Figure 6.9 Quadrant Averages and Shading for Digit 3

452	476	852
1005	873	345
570	446	91

335	426	830
668	420	219
529	574	173
495	375	66

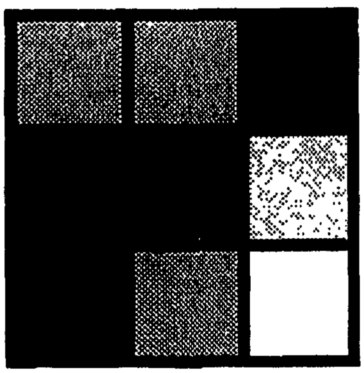

9%	9%	17%
20%	17%	7%
11%	9%	2%

7%	8%	16%
13%	8%	4%
10%	11%	3%
10%	7%	1%

Figure 6.10 Quadrant Averages and Shading for Digit 4

220	429	778
637	506	283
1059	456	142

102	309	764
480	349	70
523	400	329
811	333	40

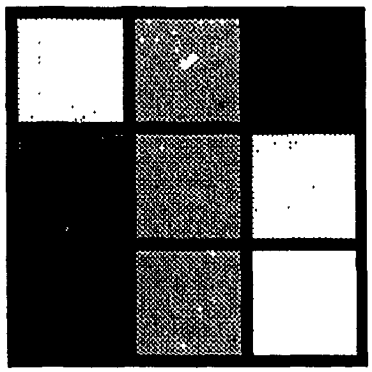

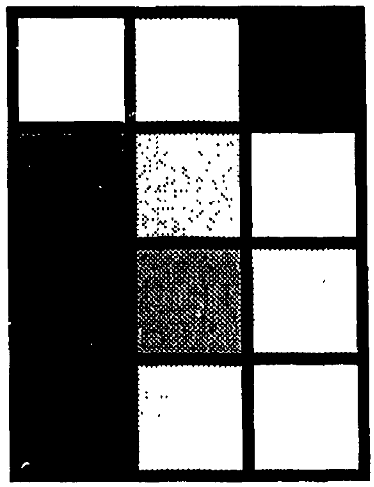

5%	10%	17%
14%	11%	6%
23%	10%	3%

2%	7%	17%
11%	8%	2%
12%	9%	7%
18%	7%	1%

Figure 6.11 Quadrant Averages and Shading for Digit 5

99	255	565
290	305	887
1206	1055	393

90	243	531
55	53	302
604	535	858
846	784	154

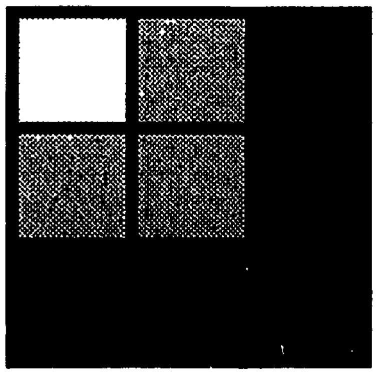

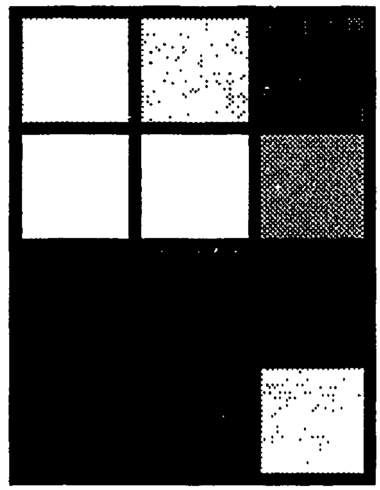

2%	5%	11%
6%	6%	18%
24%	21%	8%

2%	5%	11%
1%	1%	6%
12%	11%	17%
17%	16%	3%

Figure 6.12 Quadrant Averages and Shading for Digit 6

668	371	1267
187	13	31
625	240	41

480	353	1208
356	23	84
20	10	12
624	238	35

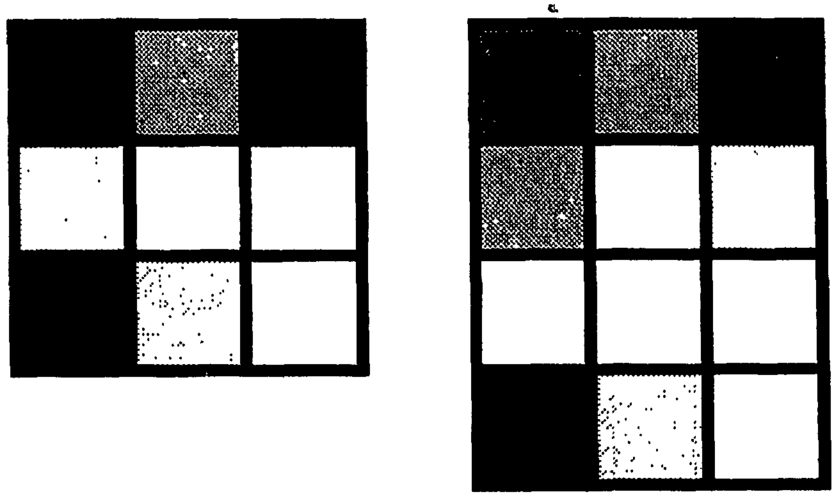

19%	11%	37%
5%	0%	1%
18%	7%	1%

14%	10%	35%
10%	1%	2%
1%	0%	0%
18%	7%	1%

Figure 6.13 Quadrant Averages and Shading for Digit 7

421	702	1218
385	1071	86
1422	575	156

249	575	1121
347	738	144
413	688	91
1219	347	104

7%	12%	20%
6%	18%	1%
24%	10%	3%

4%	10%	19%
6%	12%	2%
7%	11%	2%
20%	6%	2%

Figure 6.14 Quadrant Averages and Shading for Digit 8

272	510	1400
900	614	194
680	169	54

88	411	1199
912	558	374
183	160	26
669	164	49

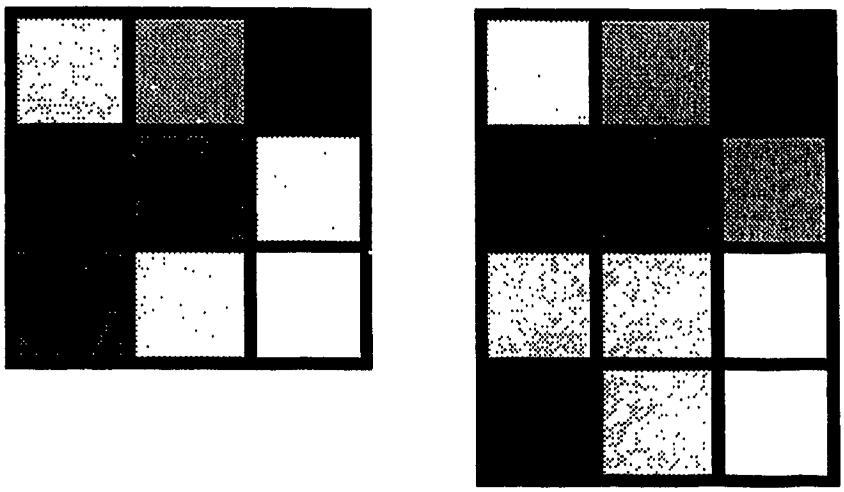

6%	11%	29%
19%	13%	4%
14%	4%	1%

2%	9%	25%
19%	12%	8%
4%	3%	1%
14%	3%	1%

Figure 6.15 Quadrant Averages and Shading for Digit 9

3099	4679	9178
4287	4368	3025
9462	4532	1954

2188	4002	8315
3244	2925	2266
3694	3276	2493
7722	3376	1085

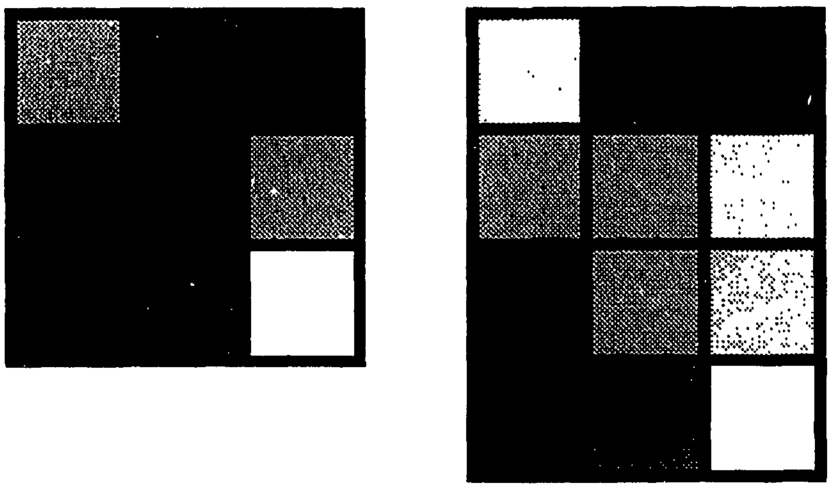

7%	10%	21%
10%	10%	7%
21%	10%	4%

5%	9%	19%
7%	7%	5%
8%	7%	6%
17%	8%	2%

Figure 6.16 Quadrant Averages and Shading over all Sample Data : "The Slant Phenomenon "

It's interesting the things we notice by stretching an image. For example, we observed in the behavioral pattern of digit 4, that the peak distribution of reference points changed regions. In digit 0, the variation occurred mostly in the top right and bottom left sides where the weight distributed evenly. For digit 1, we noticed that the previously middle area expanded leaving the top and bottom areas unchanged. The interesting point with digit 2, is that by tracing sequentially quadrants 1, 2, 3, 8, 10, 7, 12, we observe that we had many samples with a bottom loop. Digit 3 seems to materialize by following the sequence 2, 3, 5, 9, 11 and 10. For digit 5, the points remained dense in quadrant 3 and in the left side below the first quadrant. The weight in digit 6 concentrated itself in the bottom-half area. The characteristic of digit 7 emerging from this expansion was the hook traced from quadrant 4 to 1 and the concentration of features in the bottom-left grid quadrant. The elongation of digit 8 provided us with a better representation of the dense areas. This was a well distributed metamorphosis from our previous representation. Digit 9 seems to have benefited from weight redistribution. As for our global portrait, it seems to infer that digits are typically slanted from left to right.

6.6 Statistical Parameters of the Tries

Table 6.12 gives us a number of statistics relating to the tries generated from the database of training strings for each digit class. Ext is the number of samples in the extended set for each class, max[$Term_j$] gives the number of occurrences of the most frequent string. The next column gives this number relative to the size of the extended set which is an estimate of the mode of the distribution of feature strings for the class.

Node count gives the total number of nodes in T_c. The number of terminals is the number of distinct feature strings in a training set. The number of first level subtrees is given by b_0 and the number of terminal nodes in each of these subtrees is listed in the last column.

Digit	Ext	max[Term$_j$]	max[Term$_j$] / Ext	Node Count	Number of Terminals	Number of Leaves	b_0	Number of Subtree Terminals
0	405	160	0.395	297	43	43	2	15,28
1	416	363	0.873	51	13	10	3	7,5,1
2	422	43	0.102	1026	167	132	2	14,153
3	408	66	0.162	376	66	45	2	6,60
4	458	50	0.109	697	135	101	3	119,14,2
5	419	157	0.375	451	76	65	3	66,4,6
6	421	110	0.261	677	93	83	3	76,8,9
7	430	218	0.507	226	40	32	3	4,34,2
8	423	28	0.066	1747	211	193	4	139,68,3,1
9	426	63	0.148	571	94	81	3	78,14,2

Table 6.12 Tabulated Trie Outlook

It is interesting to compare the number of leaves to the number of terminal vertices. In Table 6.13, we observe that none of the feature strings belonging to the class of digit 0 properly contained another. Digit 9 also exhibited a few feature strings which were proper substrings of others. The remaining digits have a significant percentage of feature strings which are proper substrings of others.

Digit	Number of Nonleaf Terminals	% of Nonleaf Terminals
0	0	0
1	3	23
2	35	21
3	21	32
4	34	25
5	11	14
6	10	11
7	8	20
8	18	9
9	13	14

Table 6.13 Number and Percentage of Nonleaf Terminals

CHAPTER 7

EXPERIMENTAL RESULTS

7.1 Introduction

In this chapter of our work, we present and discuss the experimental results and observations on the performance of our recognition method. We shall explain why our method is nearing the stage of completion, but is not quite there yet. In our results, no samples have been rejected. Not knowing the mechanics of the probabilistic process, it makes it rather difficult to find appropriate confidence levels per numeral in order to establish uncertainty in the decision process.

7.2 Experimental Results

The data used for our recognition scheme was originally collected from the dead letter envelopes by the U.S. Postal Services at different American locations and served to create the first U.S. zipcode database of the Concordia University OCR research team. The OCR research team of Concordia University prepared three standard sets of 2000 digits, each incorporating 200 samples for each numeral or class. Two sets, Training Set A (Tr_A) and Training Set B (Tr_B) are used for training while one is used as the testing set. These are the sets used for the experimental results presented here.

Before introducing the results, let us present thew reliability rate formula. Expressed as a percentage, the reliability is given by

$$\text{reliability} = \frac{\text{recognition} \times 100}{\text{recognition} + \text{substitution}}$$

where the recognition rate is the percentage of all patterns correctly recognized and the substitution rate is the percentage of all patterns that were misclassified.

In general, it is customary to reject some test patterns and attempt to classify only selected ones. However, we decided to classify all test patterns in our experiments because it was not apparent how to obtain a rejection threshold for feature strings generated from test patterns.

The best results were obtained by encoding feature strings using a 4x3 quadrant grid. The results for Training Set A and B and the Testing Set are presented in Tables 7.1, 7.2 and 7.3. These tables give the recognition, substitution and reliability rates for each of the 10 digit classes of 200 samples each and the average rates over all classes. A confusion table is also shown which portrays the number of correctly recognized patterns along the main diagonal and the number of patterns of class c which were misclassified as class d for $c \neq d$.

DIGIT	RECOGNITION	SUSTITUTION	REJECTION	RELIABILITY	TESTING
0	92.500	7.500	0.000	92.500	200
1	97.000	3.000	0.000	97.000	200
2	89.000	11.000	0.000	89.000	200
3	98.500	1.500	0.000	98.500	200
4	95.500	4.500	0.000	95.500	200
5	91.500	8.500	0.000	91.500	200
6	99.500	0.500	0.000	99.500	200
7	91.500	8.500	0.000	91.500	200
8	92.000	8.000	0.000	92.000	200
9	91.000	9.000	0.000	91.000	200
	93.800	6.200	0.000	93.800	2000

CONFUSION TABLE

IN \ OUT	0	1	2	3	4	5	6	7	8	9
0	185	0	4	0	2	0	9	0	0	0
1	0	194	0	0	0	1	0	5	0	0
2	0	0	178	5	5	7	0	3	0	2
3	0	0	0	197	0	2	0	1	0	0
4	1	0	0	0	191	3	0	4	0	1
5	0	0	2	4	5	183	0	0	0	6
6	0	0	0	0	0	0	199	0	1	0
7	0	2	7	3	5	0	0	183	0	0
8	0	0	2	0	0	0	13	0	184	1
9	2	0	0	0	15	1	0	0	0	182

Table 7.1 Results for Training Set A in a **4x3** Quadrant Frame

DIGIT	RECOGNITION	SUSTITUTION	REJECTION	RELIABILITY	TESTING
0	95.500	4.500	0.000	95.500	200
1	96.000	4.000	0.000	96.000	200
2	92.500	7.500	0.000	92.500	200
3	98.500	1.500	0.000	98.500	200
4	95.000	5.000	0.000	95.000	200
5	93.500	6.500	0.000	93.500	200
6	99.000	1.000	0.000	99.000	200
7	86.500	13.500	0.000	86.500	200
8	93.500	6.500	0.000	93.500	200
9	87.500	12.500	0.000	87.500	200
	93.750	6.250	0.000	93.750	2000

CONFUSION TABLE

IN \ OUT	0	1	2	3	4	5	6	7	8	9
0	191	0	0	0	6	0	3	0	0	0
1	0	192	0	0	0	1	0	7	0	0
2	1	0	185	3	1	8	0	2	0	0
3	0	0	0	197	0	3	0	0	0	0
4	0	0	0	0	190	1	5	2	0	1
5	0	0	1	2	6	187	0	0	0	4
6	0	1	0	0	0	0	198	0	1	0
7	0	0	12	3	10	1	0	173	0	1
8	0	0	1	0	0	0	11	0	187	1
9	1	0	0	0	21	0	2	1	0	175

Table 7.2 Results for Training Set B in a **4x3** Quadrant Frame

We observe the closeness in overall recognition rates for both training sets, Tr_A: 93.8% and Tr_B: 93.75%. However, very strong variations occur within the digit rates. The rates for a zero and a two have increased in Tr_B by 3% and 3.5%, respectively over those for Tr_A. On the other hand, the recognition rates for a seven and a nine have decreased by 5% and 3.5%, respectively. The other numerals are more or less stable.

DIGIT	RECOGNITION	SUSTITUTION	REJECTION	RELIABILITY	TESTING
0	83.500	16.500	0.000	83.500	200
1	96.000	4.000	0.000	96.000	200
2	86.500	13.500	0.000	86.500	200
3	96.000	4.000	0.000	96.000	200
4	87.500	12.500	0.000	87.500	200
5	91.000	9.000	0.000	91.000	200
6	93.500	6.500	0.000	93.500	200
7	86.000	14.000	0.000	86.000	200
8	76.500	23.500	0.000	76.500	200
9	85.000	15.000	0.000	85.000	200
	88.150	11.850	0.000	88.150	2000

CONFUSION TABLE

IN \ OUT	0	1	2	3	4	5	6	7	8	9
0	167	0	9	0	2	3	13	0	2	4
1	0	192	0	0	1	1	0	6	0	0
2	1	0	173	8	3	9	1	4	1	0
3	0	0	5	192	0	1	0	0	1	1
4	0	0	1	0	175	7	1	9	0	7
5	0	0	3	10	1	182	0	0	2	2
6	1	0	1	0	2	0	187	0	7	2
7	0	0	10	5	9	4	0	172	0	0
8	0	0	4	0	2	2	33	0	153	6
9	10	0	1	0	11	2	2	0	4	170

Table 7.3 Results for the Testing Set in a **4x3** Quadrant Frame

Looking at the Testing Set results, it is obvious that there were quite a few new incoming strings which were assigned improper weights because of the lack of balance and completeness of our sample database.

Tables 7.4, 7.5 and 7.6 present the performance results for feature strings encoded in a 3x3 quadrant grid.

DIGIT	RECOGNITION	SUSTITUTION	REJECTION	RELIABILITY	TESTING
0	89.500	10.500	0.000	89.500	200
1	97.000	3.000	0.000	97.000	200
2	80.500	19.500	0.000	80.500	200
3	98.000	2.000	0.000	98.000	200
4	96.000	4.000	0.000	96.000	200
5	88.500	11.500	0.000	88.500	200
6	99.000	1.000	0.000	99.000	200
7	89.000	11.000	0.000	89.000	200
8	91.500	8.500	0.000	91.500	200
9	84.000	16.000	0.000	84.000	200
	91.300	8.700	0.000	91.300	2000

CONFUSION TABLE

IN \ OUT	0	1	2	3	4	5	6	7	8	9
0	179	0	5	0	2	0	13	0	0	1
1	0	194	0	0	1	0	0	5	0	0
2	0	0	161	6	15	11	0	3	0	4
3	0	0	1	196	0	2	0	1	0	0
4	1	0	0	0	192	3	0	4	0	0
5	0	0	8	4	6	177	0	0	0	5
6	0	0	0	0	0	0	198	0	2	0
7	1	2	6	3	8	1	0	178	0	1
8	0	0	2	0	0	0	14	0	183	1
9	3	0	0	0	27	1	1	0	0	168

Table 7.4 Results for Training Set A in a **3x3** Quadrant Frame

DIGIT	RECOGNITION	SUSTITUTION	REJECTION	RELIABILITY	TESTING
0	95.500	4.500	0.000	95.500	200
1	96.000	4.000	0.000	96.000	200
2	88.500	11.500	0.000	88.500	200
3	98.000	2.000	0.000	98.000	200
4	95.000	5.000	0.000	95.000	200
5	90.500	9.500	0.000	90.500	200
6	97.500	2.500	0.000	97.500	200
7	83.000	17.000	0.000	83.000	200
8	93.000	7.000	0.000	93.000	200
9	85.500	14.500	0.000	85.500	200
	92.250	7.750	0.000	92.250	2000

CONFUSION TABLE

IN \ OUT	0	1	2	3	4	5	6	7	8	9
0	191	0	0	0	6	0	3	0	0	0
1	0	192	0	0	0	1	0	7	0	0
2	2	0	177	4	7	8	0	2	0	0
3	0	0	1	196	0	3	0	0	0	0
4	0	1	0	0	190	1	5	2	0	1
5	0	0	6	3	9	181	0	0	0	1
6	0	1	0	0	0	0	195	0	4	0
7	0	0	11	3	16	2	0	166	0	2
8	1	0	1	0	0	0	11	0	186	1
9	1	0	0	0	24	0	2	1	1	171

Table 7.5 Results for Training Set B in a **3x3** Quadrant Frame

We can observe a greater difference in recognition rates between the two training sets, Tr_A: 91.3% and Tr_B: 92.25%. The vicissitudes are quite salient within certain digits. The rate for a zero in Tr_B has augmented by 6%, that of a two by 8.5%, but recognition for the seven has again diminished, this time by 6%. Except for the nine, which had previously presented a more pronounced instability, the digits which are mostly affected are the same.

DIGIT	RECOGNITION	SUSTITUTION	REJECTION	RELIABILITY	TESTING
0	82.000	18.000	0.000	82.000	200
1	96.000	4.000	0.000	96.000	200
2	80.500	19.500	0.000	80.500	200
3	96.500	3.500	0.000	96.500	200
4	89.000	11.000	0.000	89.000	200
5	87.500	12.500	0.000	87.500	200
6	93.000	7.000	0.000	93.000	200
7	84.500	15.500	0.000	84.500	200
8	76.500	23.500	0.000	76.500	200
9	79.000	21.000	0.000	79.000	200
	86.450	13.550	0.000	86.450	2000

CONFUSION TABLE

IN \ OUT	0	1	2	3	4	5	6	7	8	9
0	164	0	9	0	2	4	14	0	3	4
1	0	192	0	0	2	0	0	6	0	0
2	1	0	161	8	12	9	1	4	1	3
3	0	0	4	193	0	1	0	0	1	1
4	1	1	1	0	178	6	1	8	0	4
5	0	0	10	10	1	175	0	0	2	2
6	1	0	1	0	2	0	186	0	8	2
7	0	1	13	5	10	1	0	169	0	1
8	0	0	4	0	2	2	33	0	153	6
9	10	0	1	0	21	2	3	1	4	158

Table 7.6 Results for the Testing Set in a **3x3** Quadrant Frame

Averaging out the results of Tr_A and Tr_B for both grid types, and subtracting from these values the outcomes of the respective testing set strings, we obtain a drop in recognition of 5.625% for the 4x3 partitioning and 5.325% for the 3x3 subdivisions. Expressed as a percentage drop, the degradation in recognition when moving from the training sets to the testing sets is approximately the same (6%) in both cases.

The numbers of correctly classified patterns and the number of substitutions taken from the confusion tables for each of the sets are organized for comparison in Tables 7.7, 7.8, 7.9 and 7.10 and plotted in Figures 7.1 and 7.2.

Digit	Training Set A	Training Set B	Testing Set	Total per Digit
0	185	191	167	543
1	194	192	192	578
2	178	185	173	536
3	197	197	192	586
4	191	190	175	556
5	183	187	182	552
6	199	198	187	584
7	183	173	172	528
8	184	187	153	524
9	182	175	170	527
Total per Set	1876	1875	1763	5514

Table 7.7 Total Number of Matches Per Digit per Set for 4x3 Quadrants

Digit	Training Set A	Training Set B	Testing Set	Total per Digit
0	179	191	164	534
1	194	192	192	578
2	161	177	161	499
3	196	196	193	585
4	192	190	178	560
5	177	181	175	533
6	198	195	186	579
7	178	166	169	513
8	183	186	153	522
9	168	171	158	497
Total per Set	1826	1845	1729	5400

Table 7.8 Total Number of Matches Per Digit per Set for 3x3 Quadrants

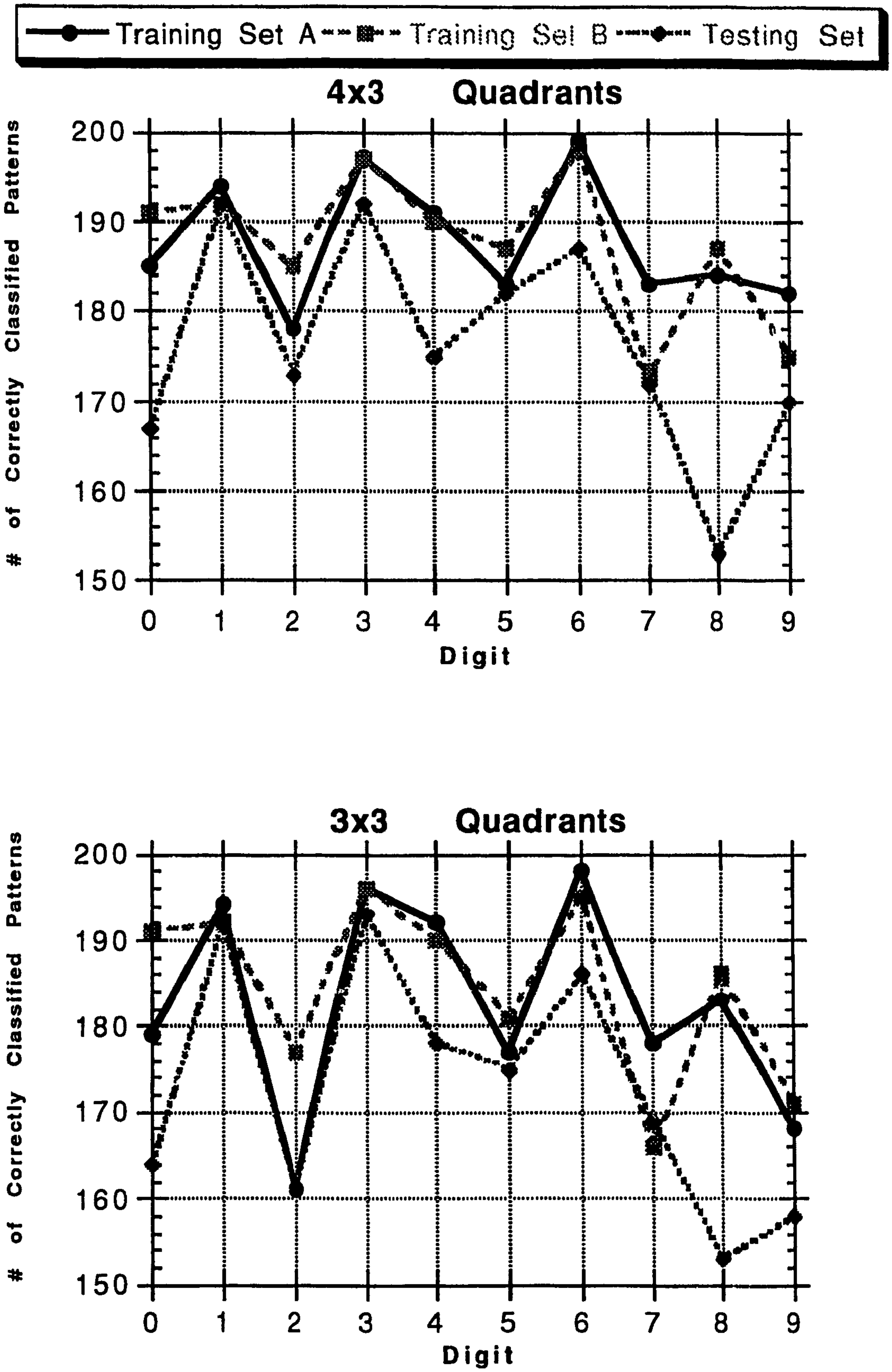

Figure 7.1 Recognition Graphs

Digit	Training Set A	Training Set B	Testing Set	Total per Digit
0	15	9	33	57
1	6	8	8	22
2	22	15	27	64
3	3	3	8	14
4	9	10	25	44
5	17	13	18	48
6	1	2	13	16
7	17	27	28	72
8	16	13	47	76
9	18	25	30	73
Total per Set	124	125	237	486

Table 7.9 Total Number of Errors Per Digit per Set for 4x3 Quadrants

Digit	Training Set A	Training Set B	Testing Set	Total per Digit
0	21	9	36	66
1	6	8	8	22
2	39	23	39	101
3	4	4	7	15
4	8	10	22	40
5	23	19	25	67
6	2	5	14	21
7	22	34	31	87
8	17	14	47	78
9	32	29	42	103
Total per Set	174	155	271	600

Table 7.10 Total Number of Errors Per Digit per Set for 3x3 Quadrants

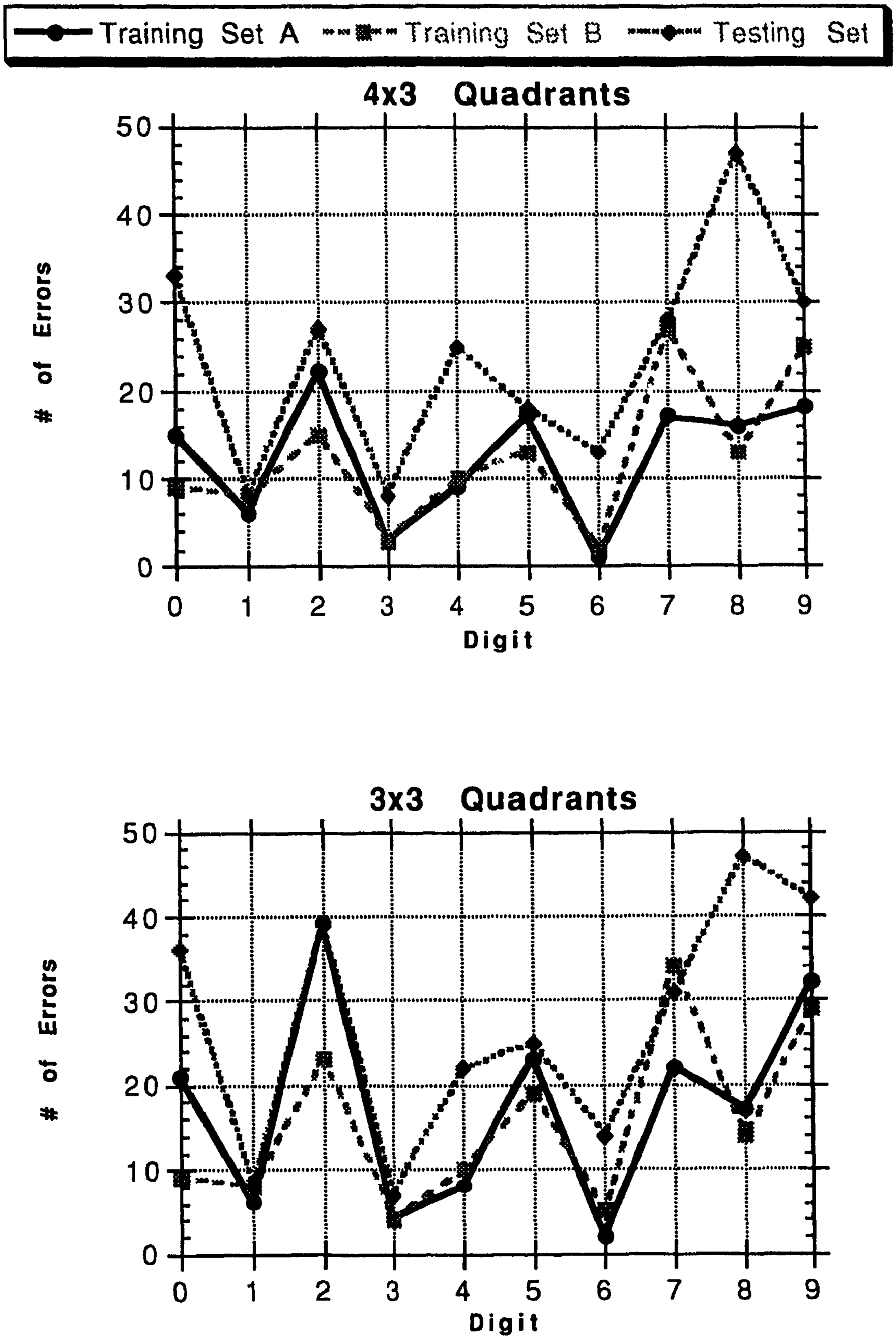

Figure 7.2 Substitution Graphs

7.3 Analysis of Errors

In order to analyze the discrepancies in errors, we need to normalize our results. We simply add the total number of errors per set per grid, and use this value as our normalizing factor. The results are presented in Table 7.11.

Digit	Errors in 4x3 Frame %	Errors in 3x3 Frame %	Difference (4x3) - (3x3) %
0	5	6	-1
1	2	2	0
2	6	9	-3
3	1	1	0
4	4	4	0
5	4	6	-2
6	1	2	-1
7	7	8	-1
8	7	7	0
9	7	9	-2
Total	45	55	-10

Table 7.11 Error Analysis (Normalization to 486+600=1086)

We observe a 10% decrease in errors with the use of the 4x3 grid. The numerals benefiting most by the stretch were the 2, 5 and 9. In the following confusion plots, Figures 7.3 to 7.12, we can see how the errors were redistributed among the digits.

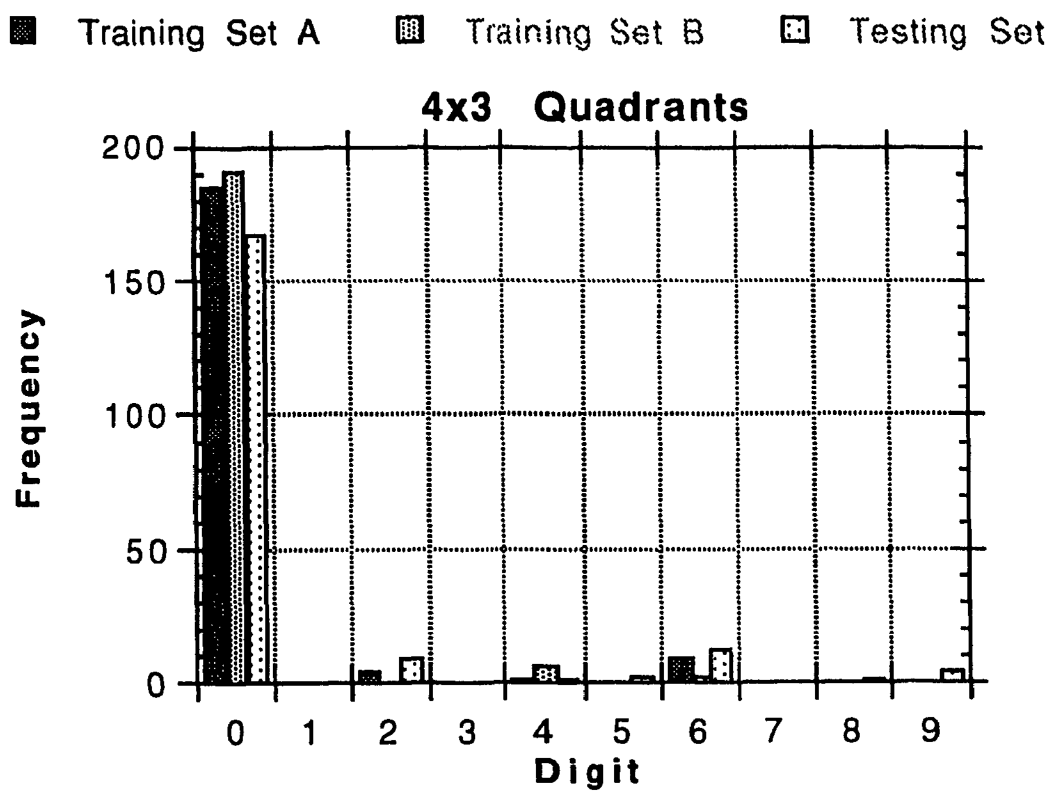

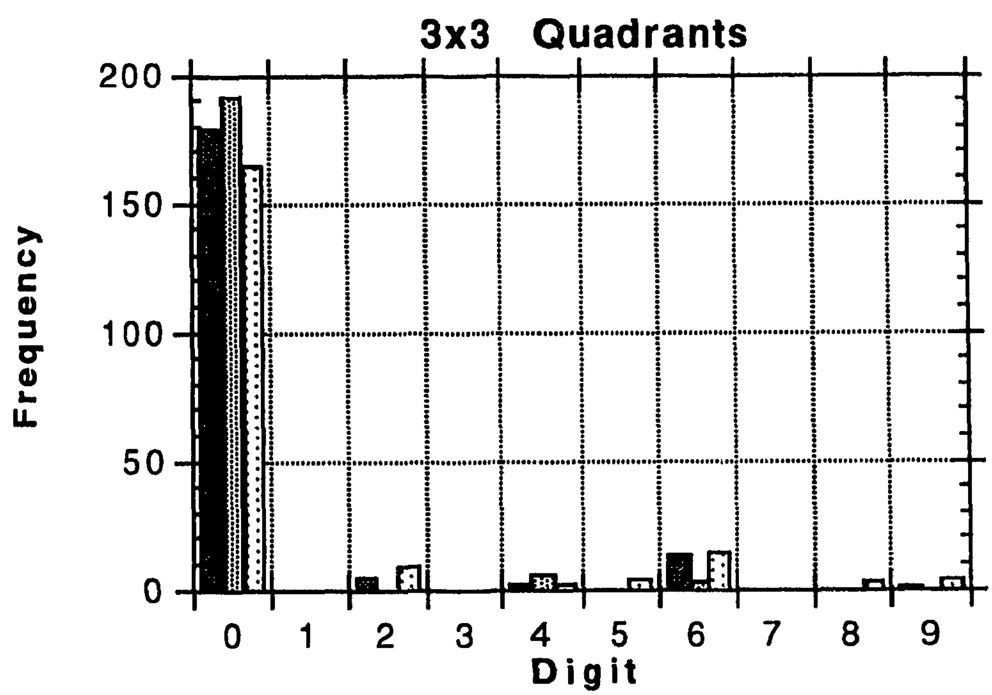

Figure 7.3 Confusion Plots for Samples of Digit 0

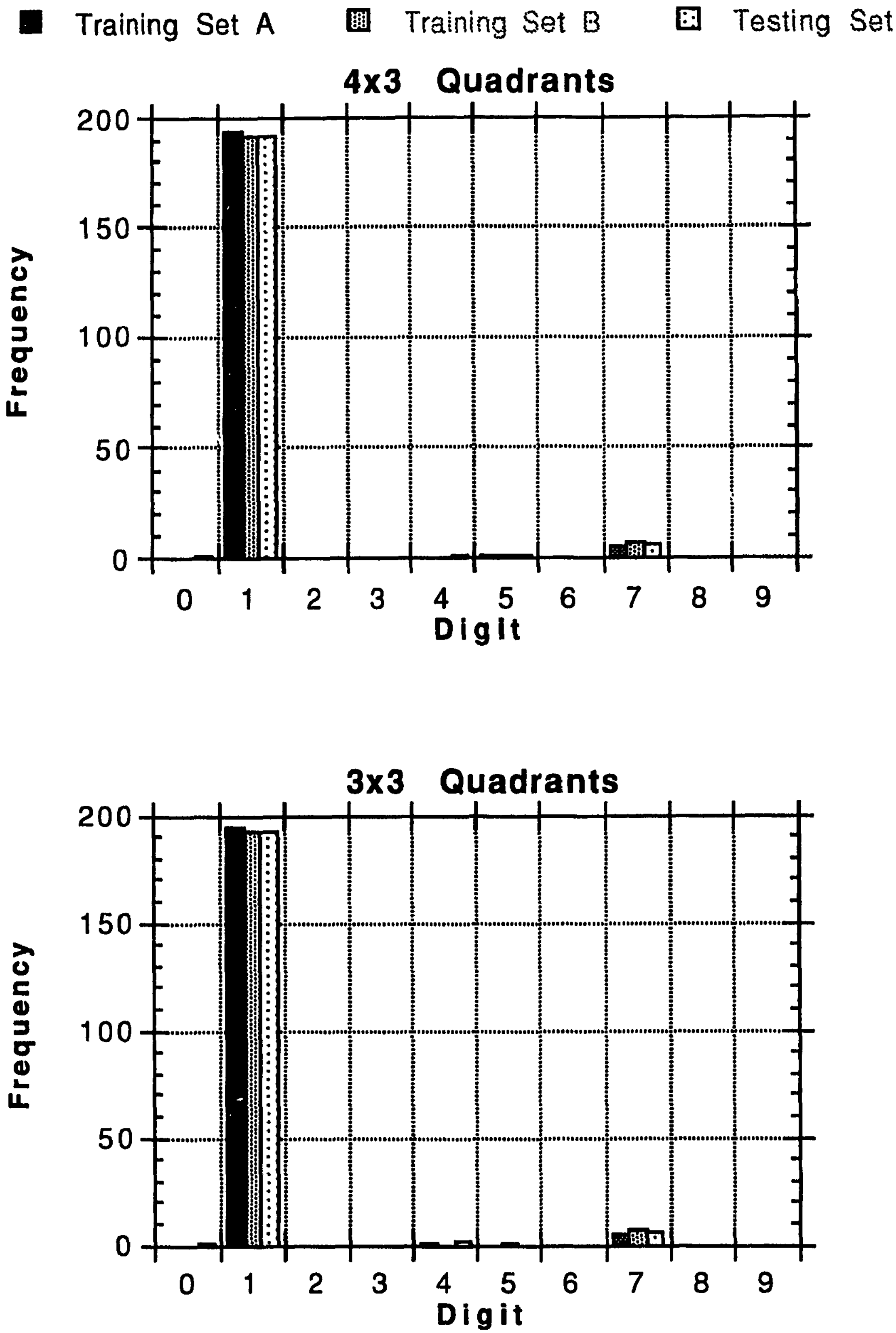

Figure 7.4 Confusion Plots for Samples of Digit 1

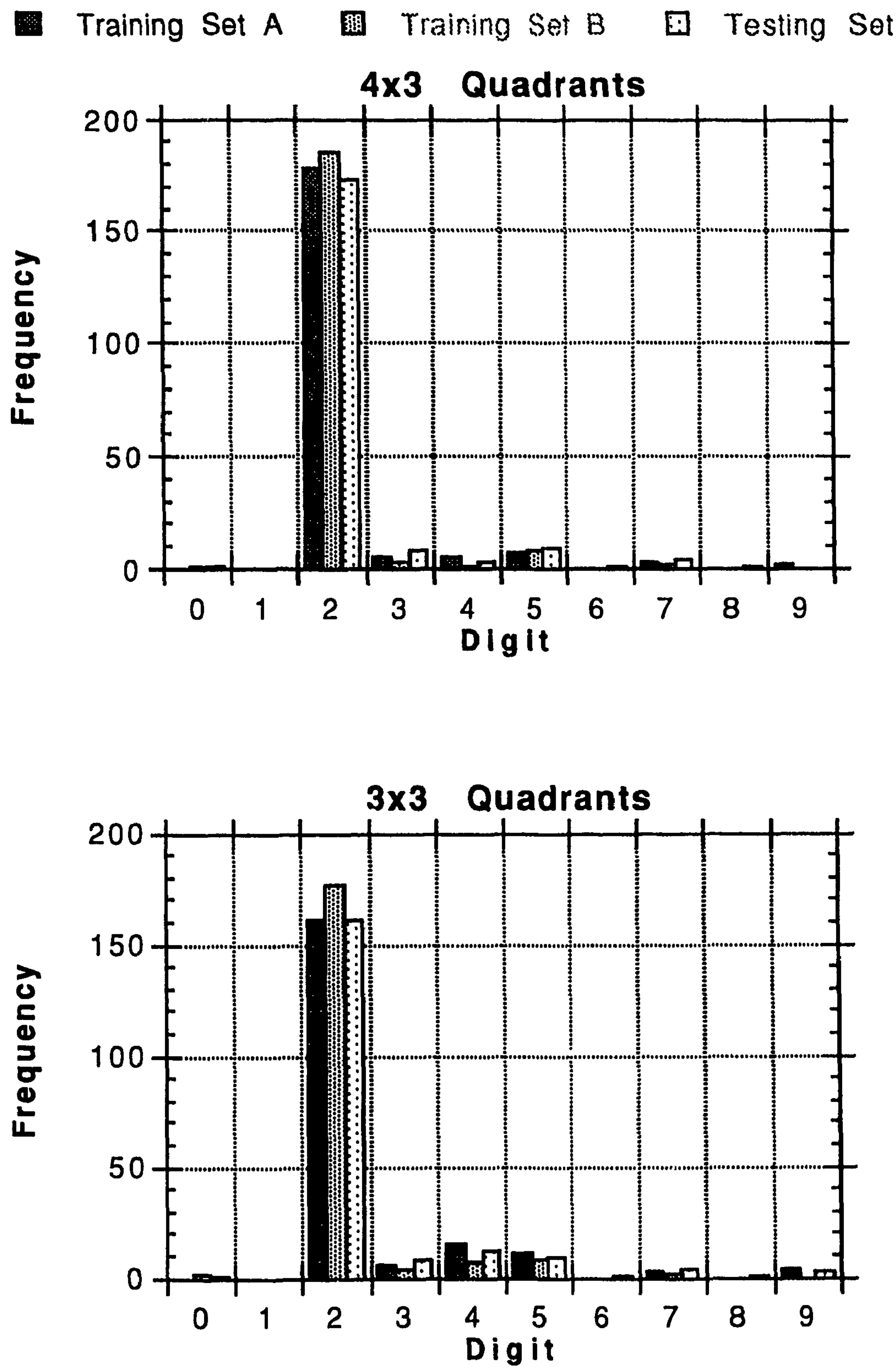

Figure 7.5 Confusion Plots for Samples of Digit 2

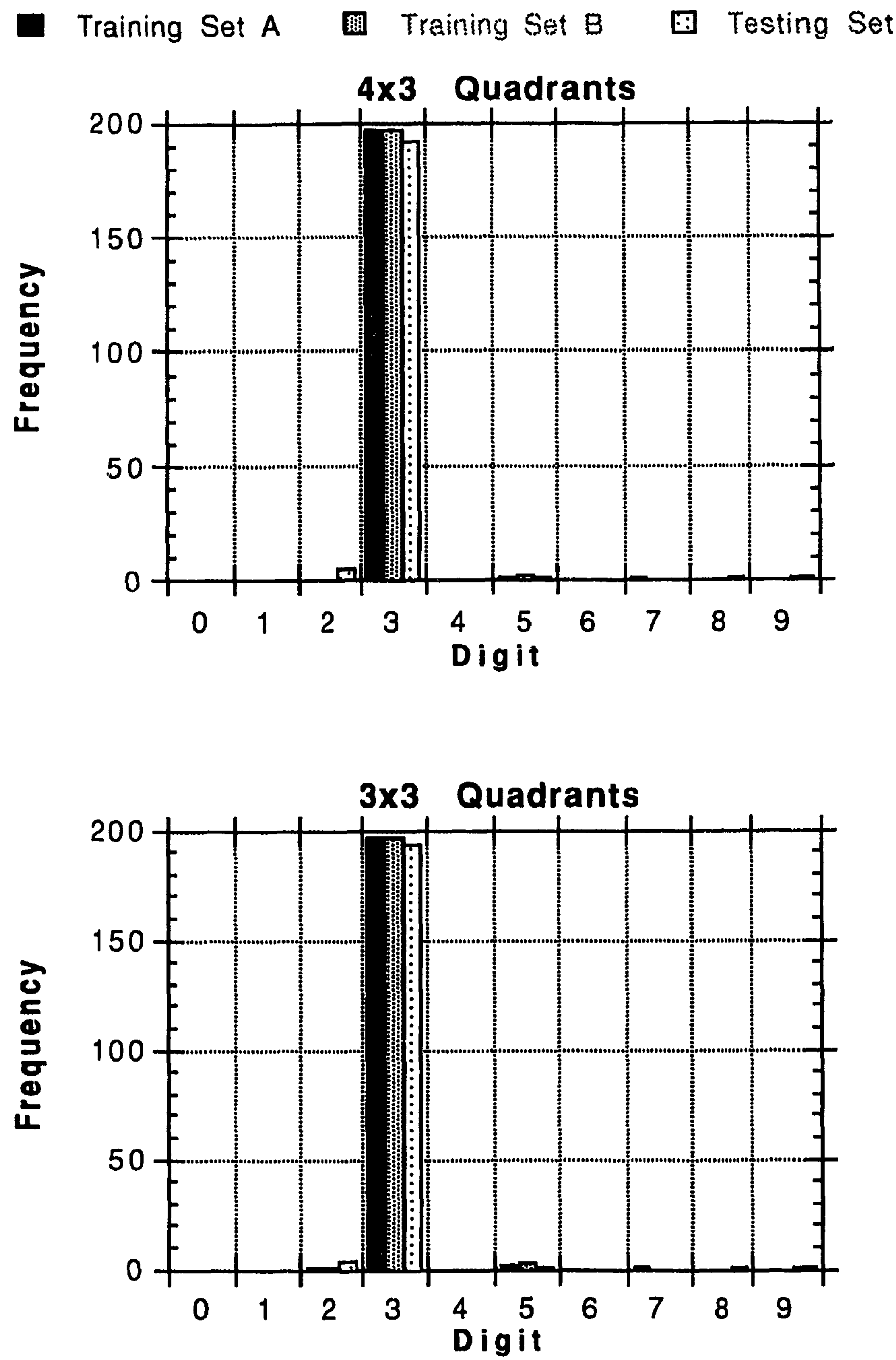

Figure 7.6 Confusion Plots for Samples of Digit 3

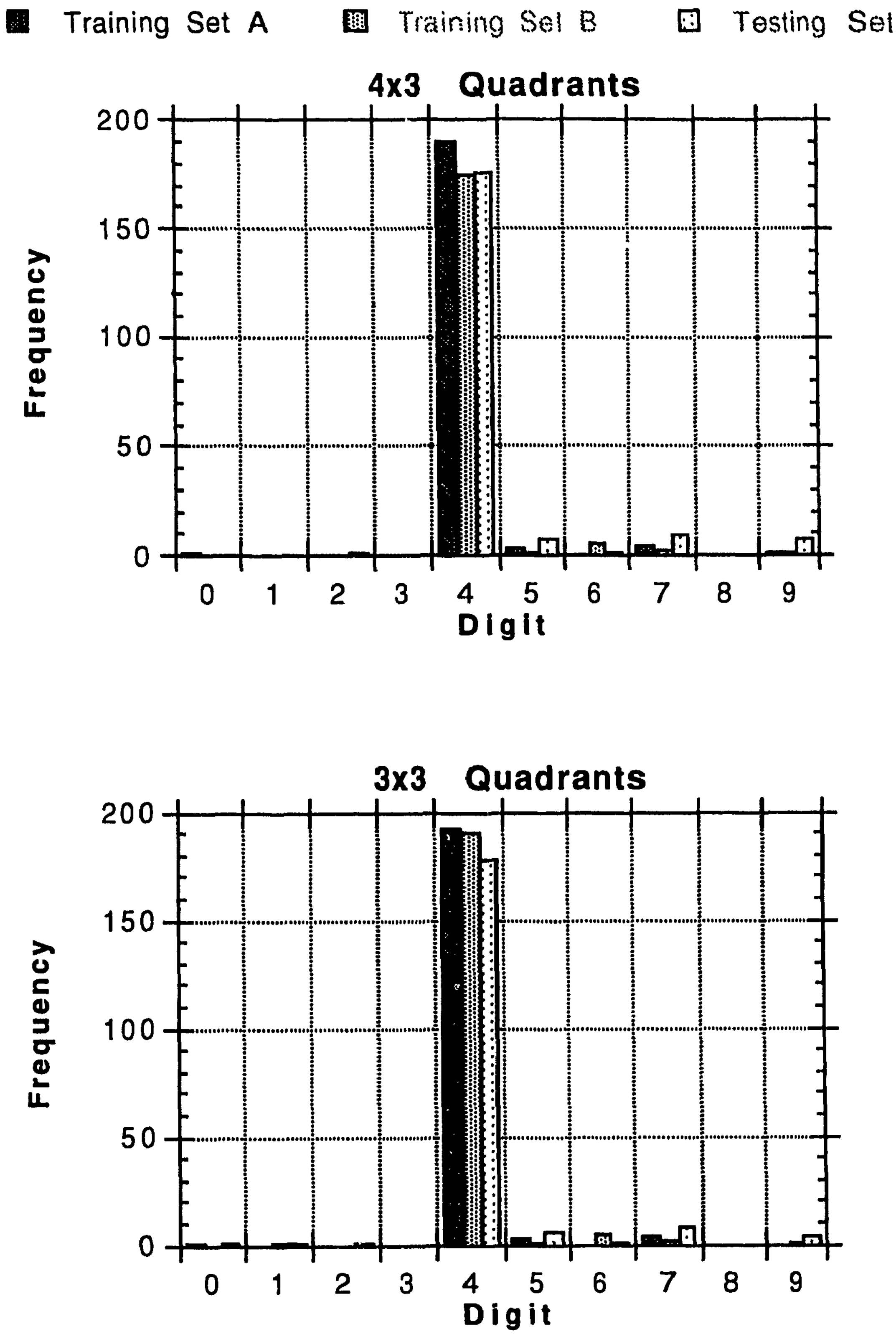

Figure 7.7 Confusion Plots for Samples of Digit 4

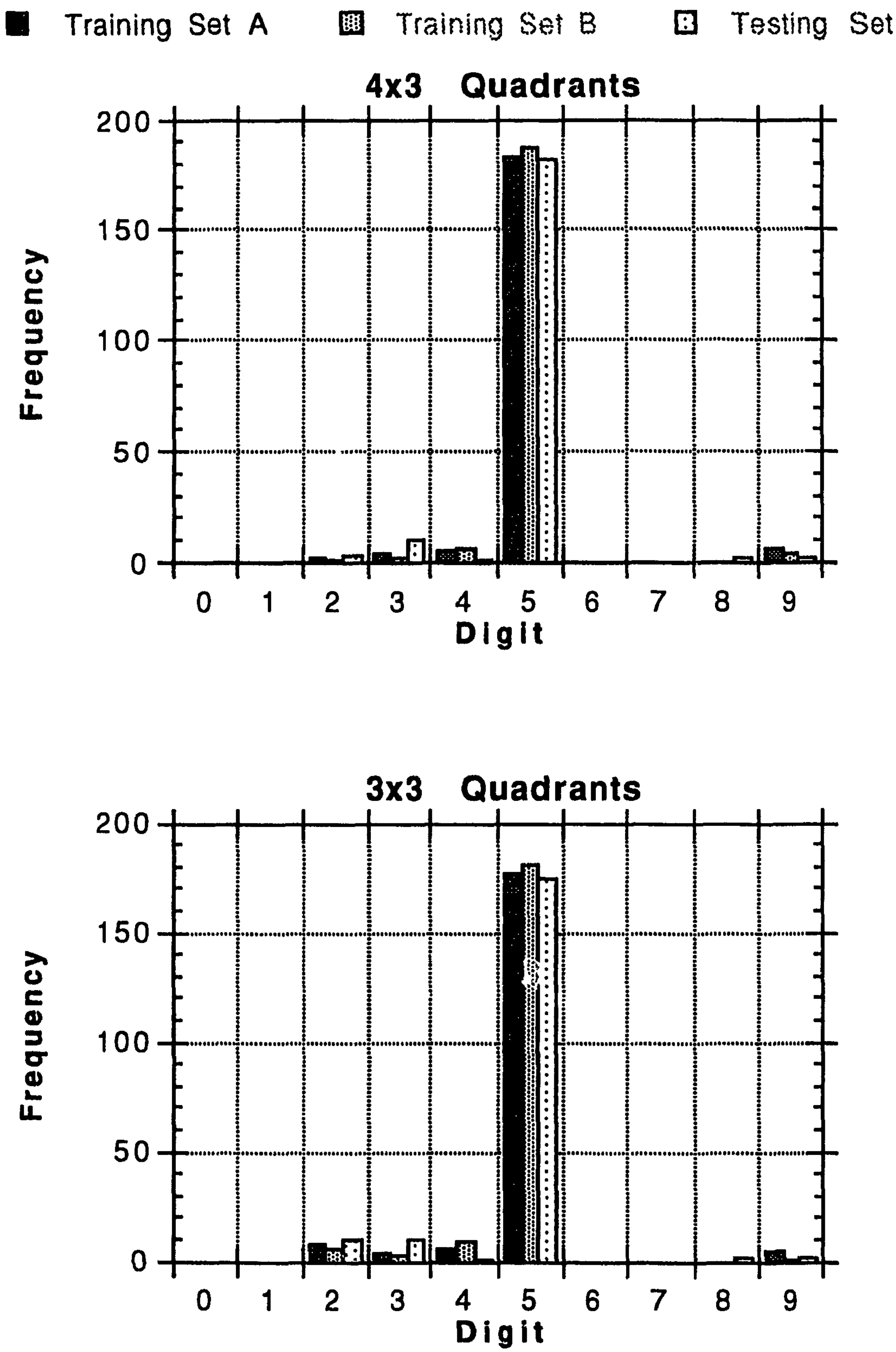

Figure 7.8 Confusion Plots for Samples of Digit 5

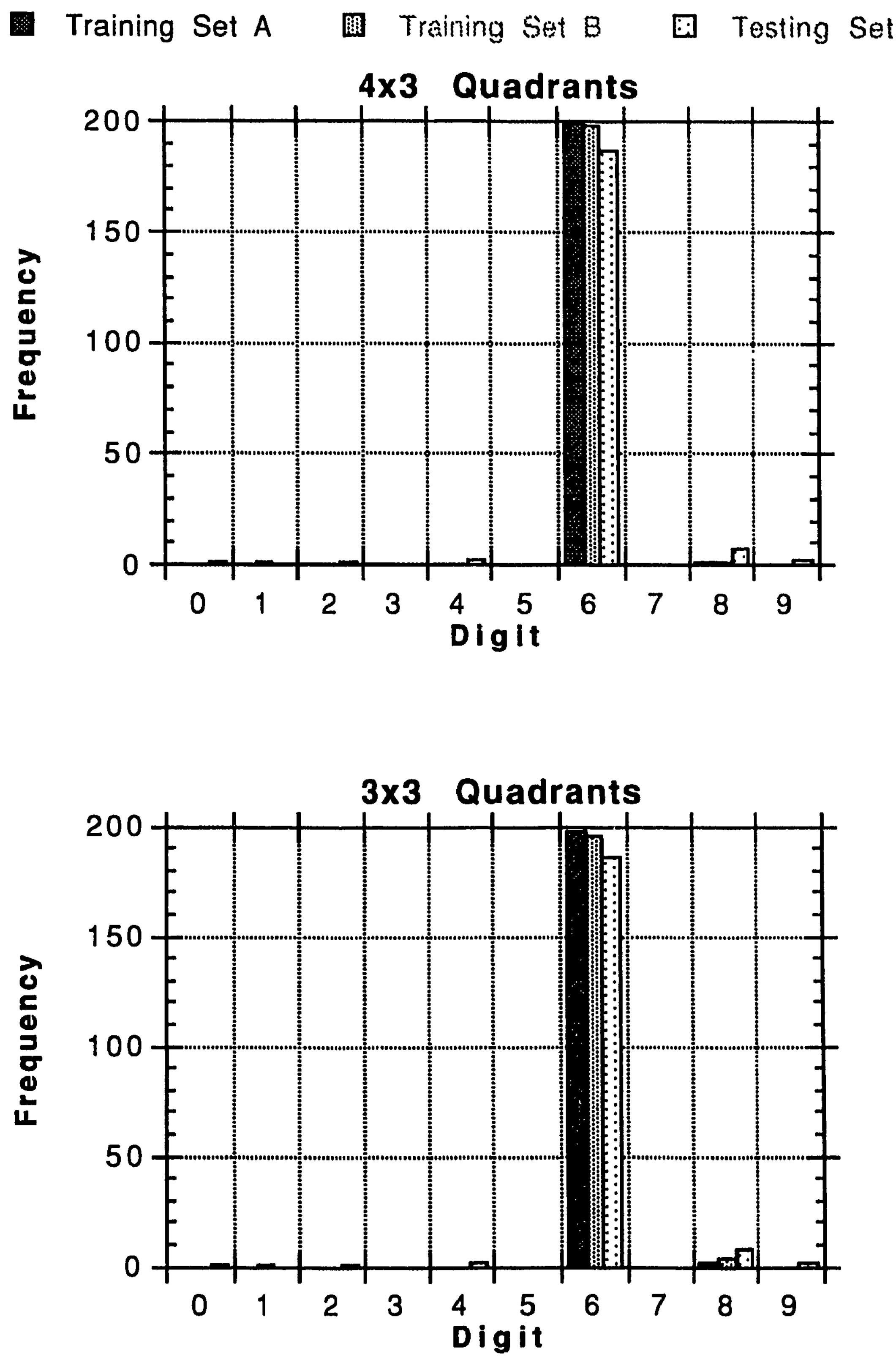

Figure 7.9 Confusion Plots for Samples of Digit 6

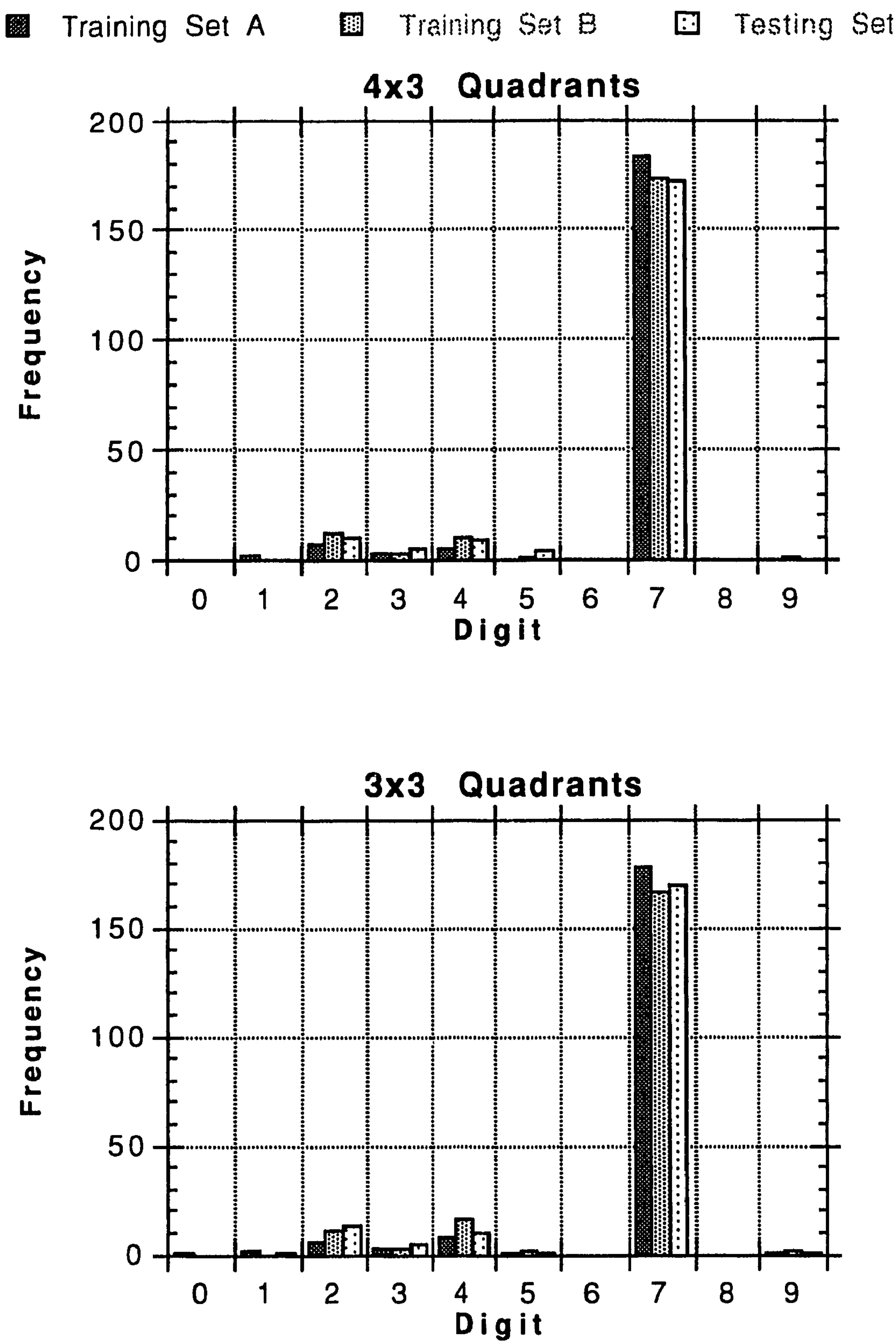

Figure 7.10 Confusion Plots for Samples of Digit 7

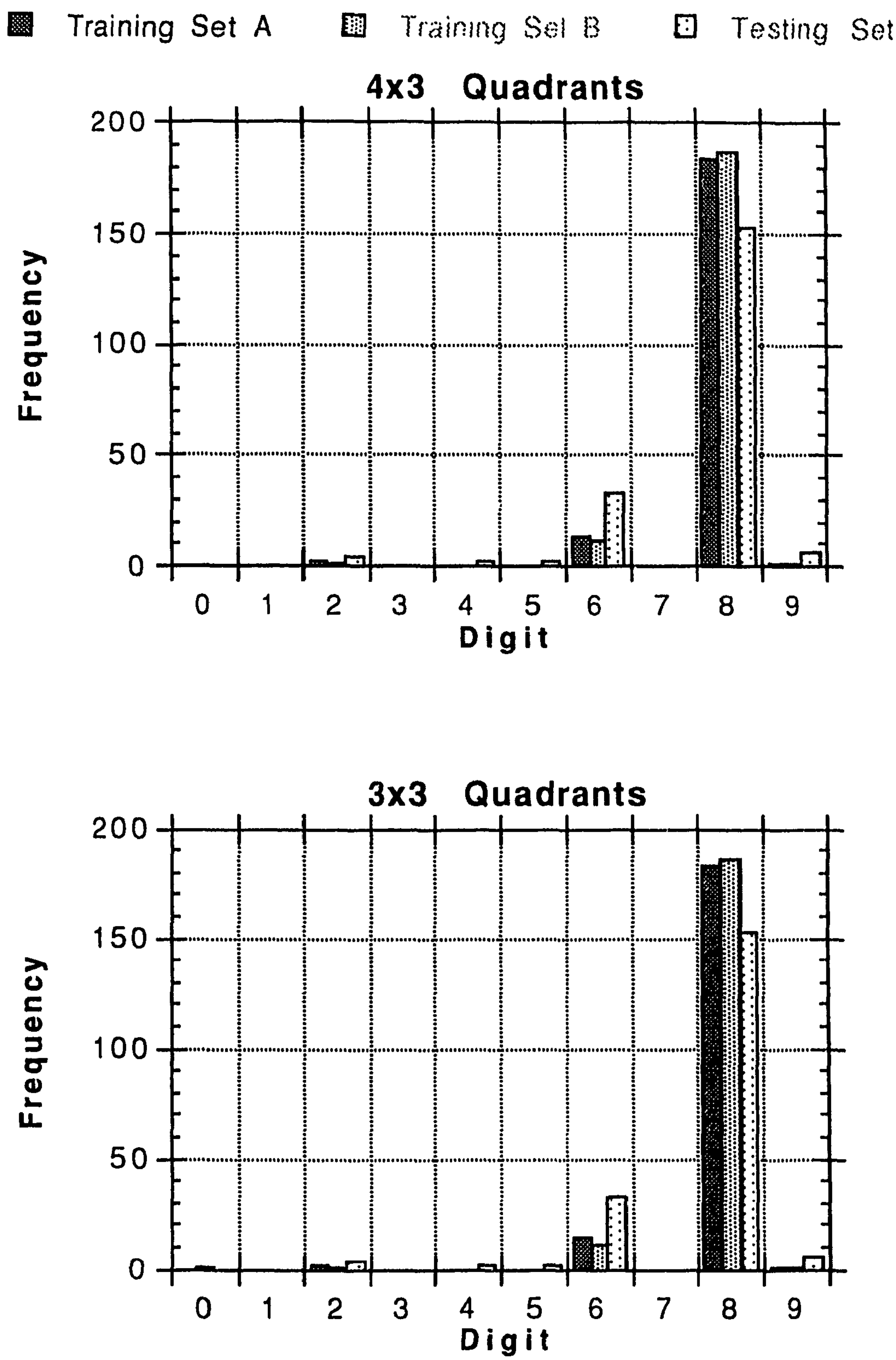

Figure 7.11 Confusion Plots for Samples of Digit 8

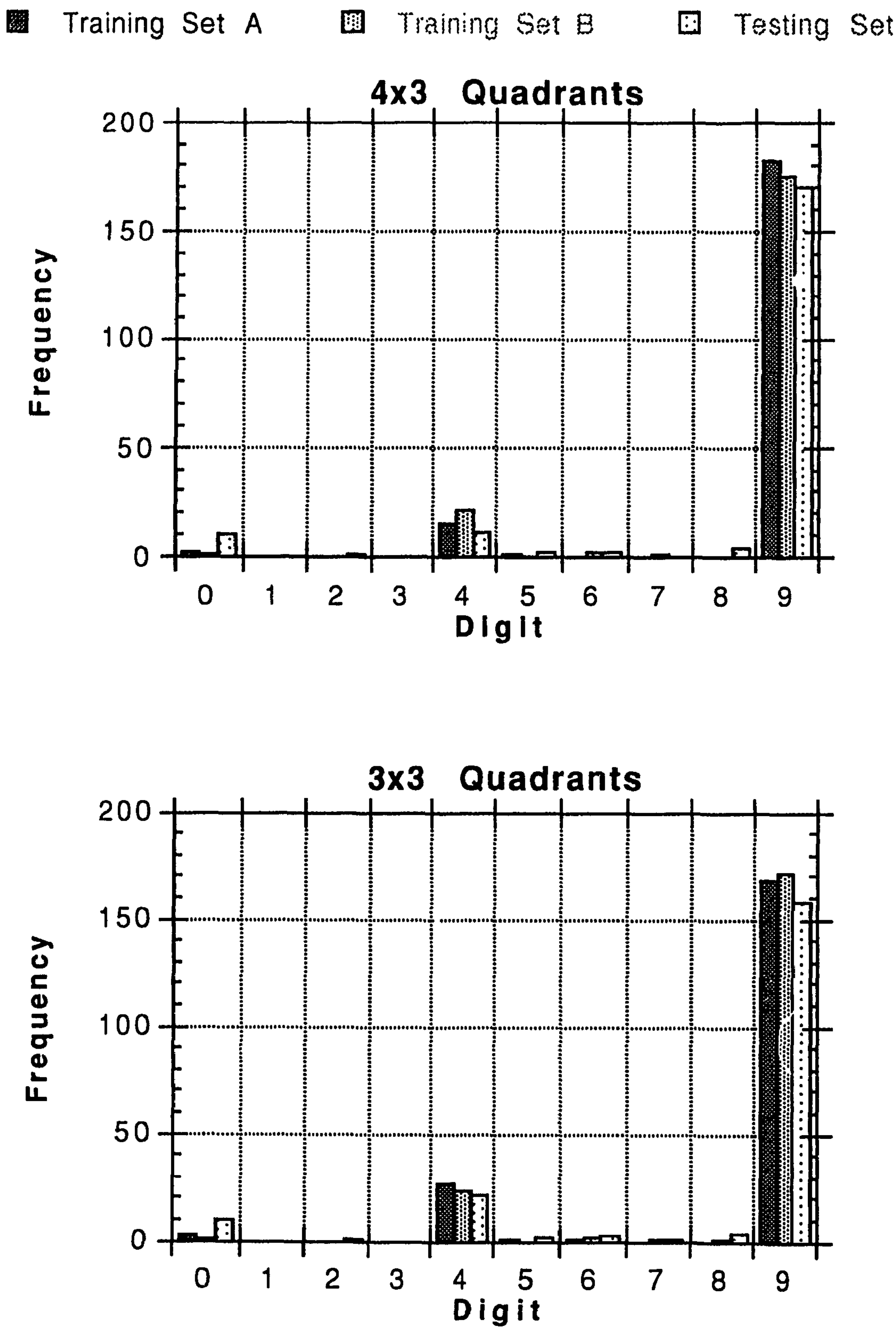

Figure 7.12 Confusion Plots for Samples of Digit 9

7.4 Sensitivity of Recognition

We were able to empirically determine the values of the hole count and grid size parameters by varying their quantities and observing the effects on the recognition rates.

We have compared the recognition results of digits with an unaltered hole count (86.90%) to those with a limited number of inner contours (88.15%), as seen in Figure 7.13 and have noticed that in this recognition scheme, "hole dropping" was beneficial. This small increase in recognition was constant overall the digits with the exception of digit 2 whose recognition rate decreased by 0.5%.

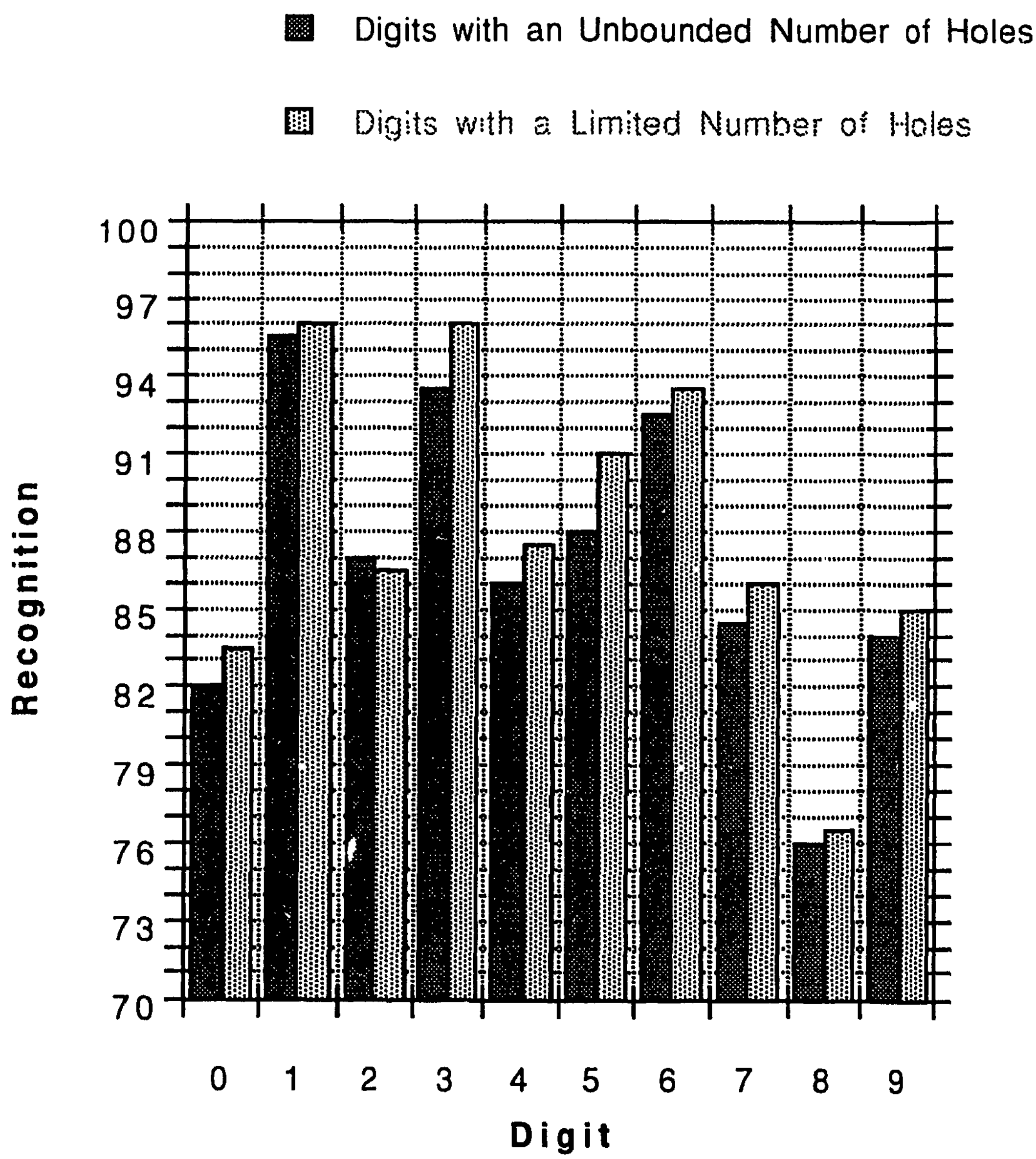

Figure 7.13 Recognition Rates of Digits with all Inner Contours versus those with a Limited Number of Inner Contours

Different partitions [SUGL92] lead to different recognition results. Figure 7.14 is a plot of the recognition rates for various grid sizes. From this figure, we can observe that an mxn rectangular grid, where m > n, induced better classification rates. The peak in this graph, occurred for a 4x3 quadrant grid.

The shortest occurring string has 4 relations (Digits 1 and 7) while the longest string has 24 relations (Digit 8) as given in Table 7.12. The average length of a feature string is 10.53 relations, as was seen in Table 6.5. Since a typical string yields on the average 11 relations, a 4x3 partitioning would tend to localize a shape in a quadrant for uniformly distributed features.

DIGIT	MINIMUM STRING LENGTH	MAXIMUM STRING LENGTH
0	8	14
1	4	8
2	6	22
3	6	22
4	6	18
5	6	18
6	6	22
7	4	16
8	10	24
9	8	20

Table 7.12 Minimum and Maximum String Lengths

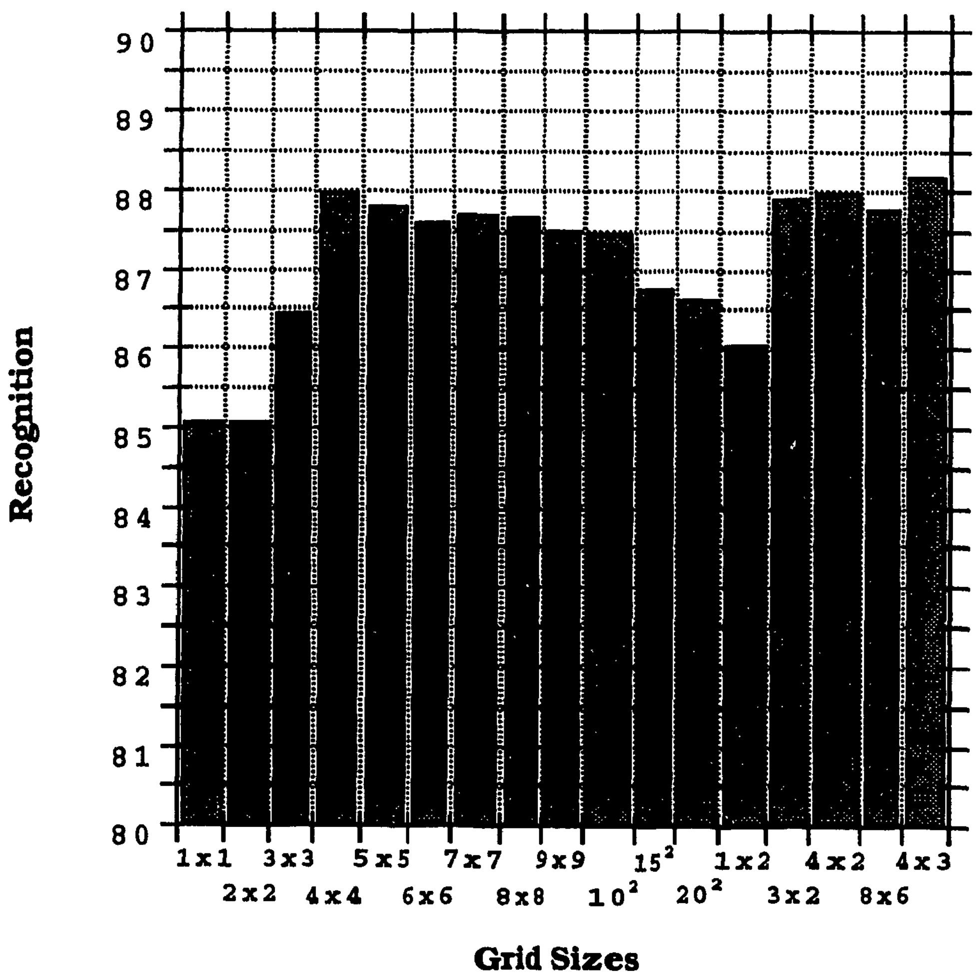

Figure 7.14 Recognition Rates in Various Grids

As we have observed in Chapter 5, the relations are not distributed uniformly. Some quadrants may be empty while others can localize 1, 2 or 3 relations. Referring to Figures 4.6 and 4.7, we notice that the height extension has increased the number of empty quadrants from 2 to 6 with our sample of digit 2 whose feature string had 16 relations. In this 4x3 grid, we locate the empty quadrants numbered 1, 4, 5, 9, 11 and 12. The same sample in the 3x3 grid has two empty quadrants, 1 and 9. This supports our observation of the nonuniform distribution of features which was seen in Section 6.4, more specifically in Figure 6.8 for digit 2. Therefore, decreasing the areas would leave many empty quadrants as there would be more partitions than features. Instinctively, the probability of a feature being contained in a quadrant is more likely than the possibility of a feature being contained in a pixel. Too many partitions would imply not many features per quadrant. This can be justified intuitively as follows.

Assuming digit features are uniformly distributed over a bounding box, a uniform grid with 4x3 quadrants yield an average of approximately one feature per quadrant. A finer grid would result in many empty quadrants and would not improve the resolution capabilities as we saw in Figure 7.14. Perhaps a different type of uniform grid [TSUK92], [HYTS93], one with slanted regions (direction elements) could offer better recognition capabilities. If the method were applied to the recognition of objects with lesser or greater detail than the digits, a different (coarser of finer) partitioning may be appropriate. It would be interesting to study the relationship between optimal granularity of the partitioning and the level of detail present in this object set. Since the difference in recognition rates when passing from a 1x1 (85.05%) to a 4x3 grid (88.15%), is of only 3.1%, for objects with nonuniformly distributed features, a nonuniform (nonlinear) grid partitioning may yield better results than a uniform one for the complexity of the digits.

Examining the average height over width ratio for each digit, as seen in Table 7.13, we observe an average value of 1.27 indicating that the images are rather rectangular in perspective. Approximating this average with our grid size, dividing 4 by 3, we obtain 1.33, which is close to our average ratio. Hence, since we are working with a uniform grid, we select the 4x3 partitioning.

DIGIT	AVERAGE HEIGHT/WIDTH RATIO
0	1.12
1	1.70
2	0.99
3	1.22
4	1.17
5	1.02
6	1.38
7	1.32
8	1.35
9	1.46
AVERAGE	1.27

Table 7.13 Height/Width Ratio

Figure 7.15 depicts each digit's outcome in the various grids. Digit 1 is totally unaffected by these variations while digit 2 experienced quite a variety of effects in which our selected grid size offered the best results.

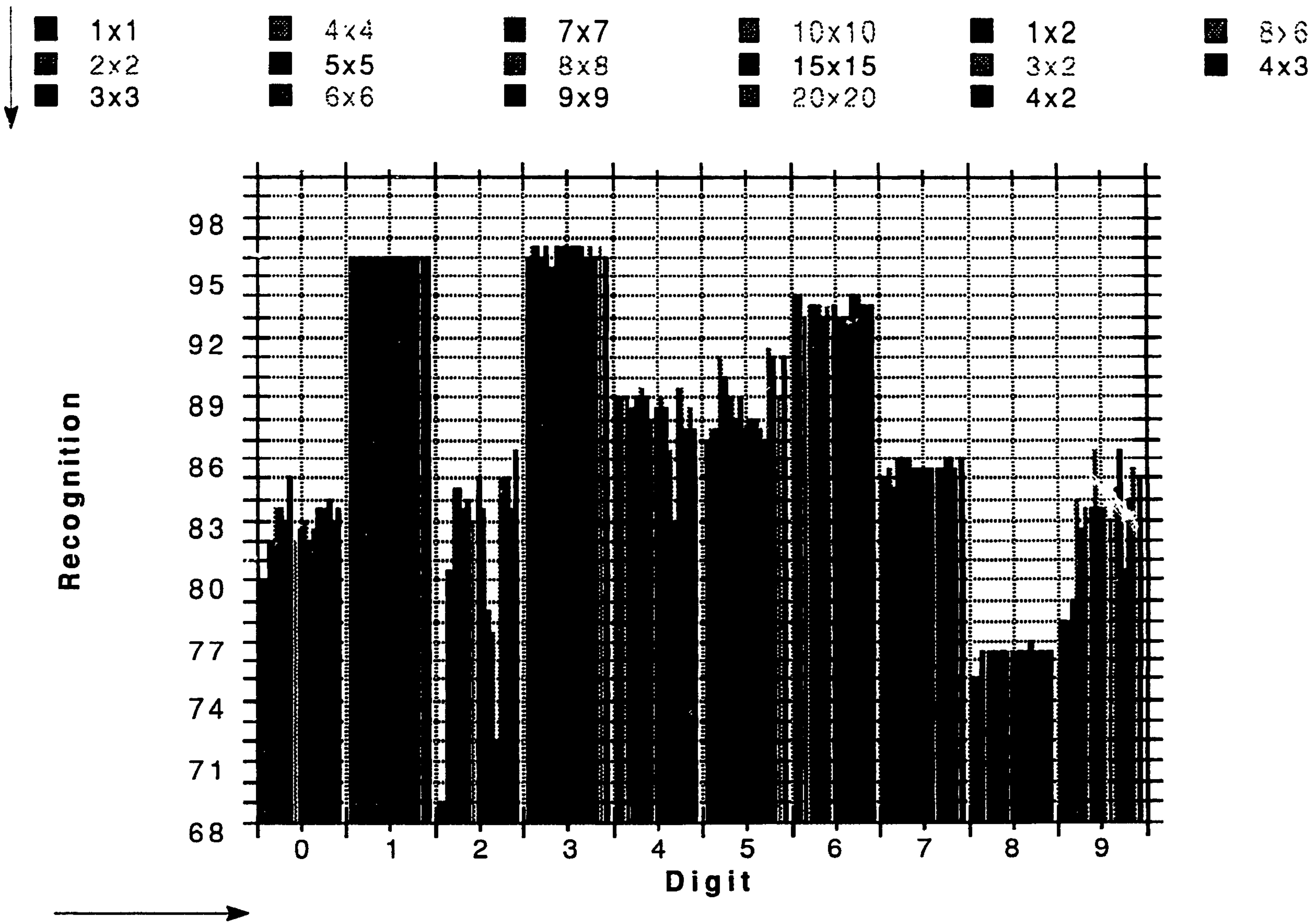

Figure 7.15 Digit Recognition Rates in Various Grids

7.5 Observation of a Sample

Let us observe the behavior of a sample. We chose from the Training Set B of digit 5, pattern 178. We selected this sample because of its appearance and its performance in the 4x3 and 3x3 grids. We can refer to Figures 7.16 and 7.17 for the information used to generate the feature strings. A number is given for each class, which is associated to the best outcome in the corresponding trie. This value is computed by adding the goodness of fit measure to the total number of misses. Note that the minimum number of misses is represented by the lowest integer part. For samples with the same lowest value, we select the greater fractional part which corresponds to the maximization of $E_c(F_x)$.

EDGE	TYPE	LENGTH	LEFT	TOP	RIGHT	BOTTOM
A	1	31	2	2	27	21
B	2	62	9	2	28	34
C	3	14	4	17	17	21
D	4	43	6	17	25	34
E	3	14	10	27	16	31
F	4	13	17	27	23	31

```
             1         2
    12345678901234567890123456789
  1 .............................
  2 .........................AAB.
  3 ........................A**B.
  4 .......................A**B..
  5 .....................AA**B...
  6 ..................AAA***B....
  7 ...........AAAAAAA****BB.....
  8 ...........A**BBBBBBBB.......
  9 ..........A**B...............
 10 .........A***B...............
 11 ........A***B................
 12 .......A***B.................
 13 ......A***B..................
 14 .....A***BB..................
 15 ....A***B....................
 16 ...A*****BBBBBBBBBBBBBB......
 17 ..A***********CCCDDD***B.....
 18 .A*********CCC......D***B....
 19 .A******CCC..........DD**B...
 20 .A***CCC...............D*B...
 21 .AACC..................D**B..
 22 ........................D*B..
 23 ........................D**B.
 24 ........................D**B.
 25 ......DDDDDDDDDDDDDDDDDD***B.
 26 ......D********************B.
 27 .....D****EEEEEEFFFFFF****B..
 28 .....D***E............F***B..
 29 .....D***E...........F****B..
 30 ......D***EEEE...FFFF****B...
 31 .....DD*******EEF******BB....
 32 ........DD************B......
 33 ..........D*******BBBB.......
 34 ..........DDDDBBBB...........
```

CONTOUR	EDGE JUNCTION	RELATION	POINT NO.	COORDINATES
outside 1	BA	1	1	(2, 27)
outside 1	AC	3	32	(21, 4)
outside 1	CD	7	46	(17, 18)
outside 1	DB	9	89	(34, 15)

CONTOUR	EDGE JUNCTION	RELATION	POINT NO.	COORDINATES
inside 2	FE	11	151	(27, 16)
inside 2	EF	11	165	(31, 17)

Figure 7.16 Digit 5, Pattern 178 from Tr_B, Horizontal Scanning

EDGE	TYPE	LENGTH	LEFT	TOP	RIGHT	BOTTOM
A	1	29	2	2	28	19
B	2	22	9	3	28	15
C	1	23	9	15	28	24
D	2	28	6	25	28	34
E	3	27	2	17	25	23
F	4	22	6	24	25	28
G	3	14	10	27	23	28
H	4	14	10	28	23	31

```
             1         2
    12345678901234567890123456789

 1  .............................
 2  .........................AAA.
 3  ........................A**B.
 4  .......................A**B..
 5  .....................AA**B...
 6  ..................AAA***B....
 7  ...........AAAAAAA****BB.....
 8  ...........A**BBBBBBBB.......
 9  ..........A**B...............
10  .........A***B...............
11  ........A***B................
12  .......A***B.................
13  .. ...A***B..................
14  .....A***BB..................
15  ....A***C....................
16  ...A*****CCCCCCCCCCCCCC......
17  ..A***********EEEEEE***C.....
18  .A*********EEE......E***C....
19  .A******EEE..........EE**C...
20  .E***EEE...............E*C...
21  .EEEE..................E**C..
22  ........................E*C..
23  ........................E**C.
24  ........................F**C.
25  ......FFFFFFFFFFFFFFFFFF***D.
26  ......F********************D.
27  .....F****GGGGGGGGGGGG****D..
28  .....F***G...........H***D..
29  .....D***H...........H****D..
30  ......D***HHHH...HHHH****D...
31  ......DD******HHH******DD....
32  ........DD************D......
33  ..........D*******DDDD.......
34  ..........DDDDDDDD...........
```

CONTOUR	EDGE JUNCTION	RELATION	POINT NO.	COORDINATES
outside 1	BA	1	150	(2, 28)
outside 1	AE	3	29	(20, 2)
outside 1	EF	7	56	(24, 25)
outside 1	FD	9	78	(29, 6)
outside 1	DC	1	106	(24, 28)
outside 1	CB	4	128	(15, 9)

CONTOUR	EDGE JUNCTION	RELATION	POINT NO.	COORDINATES
inside 2	HG	11	171	(28, 23)
inside 2	GH	11	158	(29, 10)

Figure 7.17 Digit 5, Pattern 178 from Tr_B, Vertical Scanning

Let us first build the string without any quadrant coefficients. We would obtain `H1 V3 H3 H11 V11 V11 H11 H7 V7 V9 H9 V1 V4 V1` were we to include the hole but since **digit 5** is processed with no holes, we generate `H1 V3 H3 H7 V7 V9 H9 V1 V4 V1.`

In a **4x3** quadrant grid, **sample 178** looks as follows:

`3 H1 7 V3 7 H3 5 H7 9 V7 10 V9 11 H9 9 V1 4 V4 3 V1`

There are 14 occurrences of this string and the passage count though the node associated to `3 V1` is also 14. The extended sample set size of this object class is 419.

The **averaged** feature string produced is:

`2.7 H1 4.1 V3 5.4 H3 5.0 H7 8.1 V7 10.1 V9 10.5 H9 8.0 V1 4.5 V4 3.0 V1`

Evaluating the best matches of our string in each trie, we obtained the numbers listed in Table 7.14. Please note that the averaged quadrant coefficients have a possible 0.05 error due to the spatial constraints of our outputs.

Tree	Best Matches
0	4.00039
1	2.00018
2	0.00512
3	4.00428

Tree	Best Matches
4	0.00096
5	0.00559
6	6.00039
7	0.00299
8	4.00008
9	0.00058

Table 7.14 Best Matches Generated by our String in a 4x3 Grid

Our string was properly classified as a 5. Interesting to note that next in line was the 2. We had observed in Chapter 6, that most of the samples of digit 2 had a bottom loop. Looking at the bottom half of our sample of digit 5, we notice the presence of such a loop which explains the correlation between these numbers.

In a **3x3** quadrant grid, **sample 178** looks as follows:

```
3 H1 4 V3 4 H3 5 H7 6 V7 7 V9 8 H9 6 V1 4 V4 3 V1
```

The **averaged** feature string produced was:

```
2.6 H1 3.2 V3 4.0 H3 4.4 H7 6.0 V7 7.0 V9 7.4 H9 6.2 V1 3.1 V4
3.0 V1
```

Evaluating the best matches of our string in each trie, we obtained the results presented in Table 7.15.

Tree	Best Matches
0	4.00038
1	2.00017
2	0.00442
3	4.00424
4	0.00072
5	0.00304
6	6.00035
7	0.00266
8	4.00007
9	0.00053

Table 7.15 Best Matches Generated by our String in a 3x3 Grid

Our string is misclassified as a 2 in the 3x3 grid. The 4x3 partitioning produced the desired result. Searching for the closest matching string of our sample of digit 5 in the scope of feature strings of digit 2, we find that the best match corresponds to a string having 26 occurrences and a passage count of 27 though its terminal node. The extended sample set size of this object class is 422.

In the **4x3** quadrant grid, the **averaged** feature string produced was:

2.0 H1 2.2 V3 2.9 H3 2.2 H7 4.0 V7 9.6 V9 9.1 H9 9.5 V1 8.6 V4 4.1 V1

In the **3x3** quadrant grid, the **averaged** string was:

1.9 H1 1.6 V3 2.0 H3 2.2 H7 3.1 V7 6.9 V9 6.5 H9 7.6 V1 7.1 V4 3.5 V1

7.6 Goodness of Fit of the Samples in Appendix A

The samples in Appendix A are representative of our training sets and were selected as an exemplification of the diversity of patterns in the database. The following results are the numbers corresponding to the best matches of the feature strings produced by these samples, which are generated by their passage through each of the 10 tries in a 4x3 quadrant grid environment.

Samples of Zero

Tree	Tr_B (126)	Tr_A (126)	Tr_B (156)	Tr_A (102)	Tr_B (139)	Tr_A (57)
0	**0.04787**	0.00222	**0.01210**	**0.08076**	**0.00506**	**0.00138**
1	7.12874	6.00019	7.13191	6.12827	8.00021	9.00026
2	2.00037	3.00009	0.00059	3.00039	5.00116	4.00018
3	6.02202	5.00017	6.02671	6.02366	4.00049	5.00010
4	7.00046	0.00101	7.00051	7.00054	5.00019	6.00006
5	6.00014	5.00035	6.00015	6.00017	0.00267	4.00019
6	2.00099	**0.00384**	2.00075	2.00129	5.00036	8.00006
7	7.00130	4.00018	7.00152	6.00069	6.00008	3.00035
8	2.00020	3.00019	2.00266	3.00568	0.00013	2.00016
9	0.00027	2.00039	3.00062	0.00046	3.00009	3.00009

Tree	Tr_B (5)	Tr_A (24)	Tr_B (89)	Tr_A (48)	Tr_B (194)	Tr_B (103)
0	**0.00109**	**0.04012**	**0.00169**	**0.05276**	**0.00507**	**0.00999**
1	9.00030	7.12597	10.00026	7.11944	8.00021	7.14882
2	6.00015	2.00029	4.00013	2.00035	5.00121	0.00041
3	6.00009	6.02650	4.00074	6.03375	4.00043	6.02276
4	6.00054	7.00035	6.00019	7.00035	5.00019	7.00056
5	6.00046	6.00012	4.00012	6.00016	0.00298	6.00021
6	2.00284	2.00094	9.00044	2.00109	5.00039	2.00077
7	7.00687	7.00134	10.00040	7.00129	6.00008	7.00118
8	2.00136	2.00023	5.00010	2.00023	0.00011	2.00239
9	4.00062	0.00042	6.00011	0.00032	3.00009	3.00056

Tree	Tr_B (145)	Tr_B (97)	Tr_B (169)	Tr_B (96)	Tr_B (199)	Tr_B (121)
0	**0.05711**	**0.05686**	**0.04554**	**0.06274**	0.00320	**0.08561**
1	7.13845	7.12775	7.14146	6.11178	6.00029	6.12775
2	2.00035	2.00030	2.00032	3.00039	4.00061	3.00029
3	2.02062	6.02492	6.01920	6.03206	3.00010	6.02594
4	7.00045	7.00039	7.00052	7.00045	**0.00552**	7.00036
5	6.00014	6.00015	6.00013	6.00014	4.00021	6.00014
6	2.00115	2.00106	2.00108	2.00113	3.00021	2.00122
7	7.00120	7.00127	7.00124	6.00077	3.00031	6.00091
8	2.00013	2.00021	2.00014	3.00646	3.00065	3.00612
9	0.00023	0.00028	0.00023	0.00055	3.00023	0.00055

Samples of One

Tree	Tr_A (89)	Tr_B (33)	Tr_A (167)	Tr_B (194)	Tr_A (144)	Tr_B (10)
0	2.02841	2.02878	2.02841	2.02841	2.02841	3.00092
1	**0.41722**	**0.35023**	**0.41722**	**0.41722**	**0.41722**	**0.00093**
2	3.00665	3.00713	3.00665	3.00665	3.00665	3.01577
3	3.01331	3.01473	3.01331	3.01331	3.01331	3.02394
4	3.00074	3.00067	3.00074	3.00074	3.00074	0.00026
5	3.00983	3.00946	3.00983	3.00983	3.00983	3.00845
6	2.00019	2.00018	2.00019	2.00019	2.00019	4.00056
7	0.00076	0.00084	0.00076	0.00076	0.00076	0.00073
8	3.01198	3.01207	3.01198	3.01198	3.01198	4.00016
9	2.00037	2.00037	2.00037	2.0037	2.00037	2.00056

Tree	Tr_B (55)	Tr_B (105)	Tr_B (9)	Tr_B (28)	Tr_A (4)	Tr_B (124)
0	2.02841	2.02841	2.02841	2.02841	2.02841	2.00212
1	**0.41722**	**0.41722**	**0.41722**	**0.41722**	**0.41722**	**0.00577**
2	3.00665	3.00665	3.00665	3.00665	3.00665	3.01052
3	3.01331	3.01331	3.01331	3.01331	3.01331	3.01472
4	3.00074	3.00074	3.00074	3.00074	3.00074	3.00130
5	3.00983	3.00983	3.00983	3.00983	3.00983	3.02182
6	2.00019	2.00019	2.00019	2.00019	2.00019	3.00027
7	0.00076	0.00076	0.00076	0.00076	0.00076	2.00079
8	3.01198	3.01198	3.01198	3.01198	3.01198	2.00018
9	2.00037	2.00037	2.00037	2.00037	2.00037	3.01310

Tree	Tr_A (175)	Tr_A (10)	Tr_B (150)	Tr_A (154)	Tr_B (38)	Tr_A (69)
0	2.02841	2.02841	2.02841	2.02841	2.02841	2.02804
1	**0.41722**	**0.41722**	**0.41722**	**0.41722**	**0.41722**	**0.14026**
2	3.00665	3.00665	3.00665	3.00665	3.00665	3.00806
3	3.01331	3.01331	3.01331	3.01331	3.01331	3.01215
4	3.00074	3.00074	3.00074	3.00074	3.00074	3.00079
5	3.00983	3.00983	3.00983	3.00983	3.00983	3.01066
6	2.00019	2.00019	2.00019	2.00019	2.00019	2.00017
7	0.00076	0.00076	0.00076	0.00076	0.00076	0.00073
8	3.01198	3.01198	3.01198	3.01198	3.01198	3.01298
9	2.00037	2.00037	2.00037	2.00037	2.00037	2.00029

Samples of Two

Tree	Tr_A (101)	Tr_B (92)	Tr_B (124)	Tr_B (185)	Tr_B (15)	Tr_B (164)
0	13.00018	6.00063	7.00024	11.00020	8.00071	16.00066
1	15.00025	6.00020	9.00023	14.00019	11.00023	17.00029
2	**0.00020**	**0.00021**	**0.00044**	**0.00097**	**0.00043**	**0.00030**
3	11.00012	5.00017	7.00627	10.00023	0.00035	14.00025
4	13.00011	0.00007	7.00011	11.00011	7.00010	15.00009
5	11.00017	2.00015	7.00007	10.00029	2.00018	14.00013
6	13.00012	8.00007	9.00008	10.00070	9.00025	16.00013
7	14.00013	2.00200	9.00216	13.00140	8.00047	16.00166
8	11.00010	7.00006	5.00010	8.00016	8.00016	14.00014
9	14.00275	1.00016	8.00278	10.00022	9.00278	15.00024

Tree	Tr_A (4)	Tr_B (136)	Tr_B (197)	Tr_A (6)	Tr_A (52)	Tr_B (59)
0	13.00076	12.00088	12.00017	0.00032	4.00062	4.00043
1	13.00035	12.00020	13.00020	8.00017	4.00022	2.00021
2	**0.00139**	**0.00043**	**0.00099**	**0.00638**	**0.00351**	**0.00711**
3	9.00015	10.00008	7.00018	5.02352	5.01627	4.00646
4	12.00020	11.00018	8.00018	0.00573	0.00288	0.00081
5	10.00012	9.00010	8.00024	0.00018	0.00113	0.00350
6	12.00012	13.00011	11.00012	3.00015	8.00011	6.00049
7	13.00232	12.00227	11.00027	2.00153	0.00229	0.00479
8	5.00013	7.00012	11.00005	2.00017	5.00007	4.00009
9	10.00022	9.00019	12.00005	0.00501	0.00323	0.00069

Tree	Tr_A (102)	Tr_B (132)	Tr_B (14)	Tr_B (128)	Tr_B (133)	Tr_A (24)
0	11.00050	10.00069	8.00069	**0.00817**	8.00066	4.00013
1	19.00036	11.00019	9.00022	7.15080	9.00017	10.00019
2	**0.00099**	**0.00028**	**0.00082**	0.00037	**0.00034**	0.00035
3	16.00014	7.00017	5.00020	6.01914	5.00020	**0.00143**
4	15.00111	8.00020	7.00073	0.00073	6.00014	6.00020
5	16.00021	6.00015	4.00014	6.00014	5.00036	0.00026
6	13.00023	9.00016	9.00015	2.00107	3.00009	7.00009
7	17.00044	7.00042	5.00043	7.00050	7.00045	10.00031
8	11.00015	8.00015	8.00009	2.00213	8.00012	2.00013
9	11.00011	8.00027	7.00050	3.00051	7.00013	8.00031

Samples of Three

Tree	Tr_B (17)	Tr_B (63)	Tr_A (136)	Tr_A (70)	Tr_B (29)	Tr_B (154)
0	6.00329	4.00289	5.00010	5.00045	4.00028	6.00295
1	9.00019	7.00019	8.00022	6.00027	4.00028	9.00018
2	3.00009	2.00012	2.00012	0.00028	0.00068	3.00010
3	**0.02343**	**0.04104**	**0.00078**	**0.03548**	**0.03518**	**0.02795**
4	4.00013	4.00011	4.00020	6.00037	4.00038	4.00010
5	0.00063	0.00045	0.00029	0.00033	0.00016	0.00054
6	5.00008	4.00011	4.00010	5.00266	5.00098	5.00009
7	6.00036	4.00037	4.00008	6.00116	4.00140	6.00044
8	5.00012	4.00014	0.00014	5.00023	4.00027	5.00011
9	7.00509	5.00457	4.00010	6.00020	4.00024	7.00451

Tree	Tr_A (157)	Tr_B (156)	Tr_B (108)	Tr_A (12)	Tr_A (15)	Tr_A (43)
0	6.00287	5.00041	6.00070	7.00006	12.00068	2.00011
1	9.00019	6.00023	9.00021	10.00017	13.00022	5.00023
2	3.00009	0.00032	0.00010	4.00044	6.00017	0.00030
3	**0.02291**	**0.01929**	**0.02063**	**0.00100**	**0.00032**	0.00065
4	4.00009	6.00034	6.00010	5.00010	11.00009	4.00092
5	0.00047	0.00021	0.00026	4.00009	9.00021	**0.00566**
6	5.00010	5.00216	9.00013	6.00010	14.00016	5.00017
7	6.00042	6.00136	6.00047	2.00040	11.00037	0.00045
8	5.00011	5.00020	8.00008	4.00022	10.00034	3.00034
9	7.00421	6.00021	7.00274	6.00008	7.00029	0.00029

Tree	Tr_A (10)	Tr_A (26)	Tr_A (28)	Tr_A (88)	Tr_A (96)	Tr_A (192)
0	5.00007	12.00070	14.00060	9.00013	6.00356	6.00086
1	10.00019	13.00021	15.00021	13.00019	9.00018	9.00025
2	5.00015	5.00017	7.00015	6.00019	3.00012	0.00010
3	**0.00332**	**0.00081**	**0.00017**	**0.00062**	**0.01651**	**0.01904**
4	6.00014	8.00018	10.00021	8.00011	4.00016	6.00010
5	0.00012	11.00015	13.00018	8.00036	0.00042	0.00017
6	6.00014	12.00016	14.00020	7.00018	5.00009	9.00011
7	5.00037	8.00014	10.00012	12.00048	6.00038	6.00049
8	0.00023	8.00028	10.00024	6.00016	5.00011	8.00008
9	6.00016	11.00009	12.00009	8.00015	7.00485	7.00281

Samples of Four

Tree	Tr_A (11)	Tr_A (20)	Tr_A (149)	Tr_B (192)	Tr_A (56)	Tr_B (144)
0	8.00168	8.00185	10.00134	5.00166	7.00190	8.00056
1	9.00024	9.00029	9.00031	8.00027	10.00026	8.00020
2	5.00023	3.00025	5.00037	5.00018	6.00009	2.00016
3	6.00007	5.00008	5.00006	3.00009	5.00009	5.00012
4	**0.00039**	**0.00038**	**0.00130**	**0.03012**	**0.01370**	**0.00018**
5	2.00050	4.00054	0.00026	5.00055	7.00029	4.00019
6	7.00116	5.00690	7.00064	4.00144	4.00163	8.00012
7	4.00101	4.00099	2.00276	4.00030	0.00045	4.00186
8	9.00008	9.00010	9.00008	3.00023	2.00018	9.00010
9	9.00013	9.00015	9.00014	4.00019	0.00021	3.00007

Tree	Tr_B (118)	Tr_B (162)	Tr_B (45)	Tr_B (75)	Tr_A (199)	Tr_A (36)
0	10.00160	0.00020	2.00147	0.00021	4.00058	4.00058
1	8.00040	8.00024	4.00100	8.00026	4.00019	4.00021
2	5.00372	0.00420	3.00013	0.00470	0.00206	0.00208
3	8.00006	5.01529	4.01665	5.01661	5.01060	5.01075
4	**0.00028**	**0.01201**	**0.00196**	**0.01552**	**0.00351**	**0.00460**
5	5.00093	0.00027	3.00057	0.00031	0.00098	0.00119
6	4.00019	3.00008	4.00074	3.00009	8.00006	8.00007
7	7.00005	2.00235	4.00064	2.00282	0.00199	0.00220
8	9.00006	2.00024	3.00012	2.00026	5.00006	5.00006
9	9.00018	0.00941	3.00059	0.00896	0.00286	0.00348

Tree	Tr_B (31)	Tr_A (1)	Tr_A (7)	Tr_A (94)	Tr_A (105)	Tr_A (126)
0	11.00185	9.00179	4.00056	5.00197	9.00190	4.00091
1	14.00035	12.00027	4.00019	8.00025	12.00027	0.00039
2	8.00054	6.00015	0.00223	5.00017	6.00007	4.00287
3	9.00012	5.00013	5.01128	3.00009	7.00013	3.00015
4	**0.00023**	**0.00349**	**0.00456**	**0.03209**	**0.00072**	**0.00323**
5	8.00032	9.00109	0.00137	5.00058	7.00011	0.00161
6	8.00017	4.00035	8.00007	4.00159	7.00013	4.00036
7	4.00010	6.00012	0.00209	4.00028	8.00016	3.00266
8	4.00010	6.00019	5.00007	3.00022	8.00019	3.00020
9	4.00015	8.00015	0.00362	4.00016	9.00023	4.00014

Samples of Five

Tree	Tr_B (33)	Tr_A (156)	Tr_B (144)	Tr_A (117)	Tr_B (192)	Tr_A (95)
0	5.00009	5.00008	5.00009	5.00009	10.00150	5.00013
1	6.00017	6.00016	6.00017	6.00017	9.00023	9.00021
2	0.00114	0.00118	0.00144	0.00114	4.00033	0.00016
3	2.00021	2.00021	2.00026	2.00021	6.00008	2.00014
4	0.00017	0.00014	0.00018	0.00017	4.00042	6.00108
5	**0.05890**	**0.04169**	**0.07080**	**0.05890**	**0.00270**	**0.00044**
6	5.00039	5.00038	5.00044	5.00039	7.00019	7.00021
7	5.00006	5.00006	5.00007	5.00006	7.00116	4.00023
8	4.00007	4.00007	4.00008	4.00007	9.00008	6.00006
9	5.00007	5.00007	5.00008	5.00007	9.00014	3.00021

Tree	Tr_A (190)	Tr_A (96)	Tr_A (11)	Tr_A (22)	Tr_A (10)	Tr_A (129)
0	5.00020	5.00009	5.00010	10.00135	9.00015	10.00048
1	0.00029	6.00016	6.00021	9.00023	10.00018	11.00019
2	0.01171	0.00122	0.00134	4.00038	4.00123	4.00015
3	0.00036	2.00022	2.00029	6.00010	6.00023	4.00078
4	0.00064	0.00017	0.00017	4.00040	4.00016	6.00024
5	**0.02536**	**0.06875**	**0.04713**	**0.00197**	**0.00057**	**0.00051**
6	6.00108	5.00040	5.00043	7.00016	5.00052	10.00023
7	0.00135	5.00007	5.00007	7.00107	9.00012	9.00038
8	5.00029	4.00007	4.00008	9.00008	4.00011	10.00005
9	0.00041	5.00008	5.00010	9.00017	9.00013	8.00052

Tree	Tr_B (68)	Tr_B (99)	Tr_B (72)	Tr_B (42)	Tr_A (75)	Tr_B (159)
0	5.00010	5.00010	9.00151	4.00013	11.00023	5.00010
1	6.00018	6.00017	9.00026	9.00018	14.00028	6.00017
2	0.00125	0.00110	7.00166	0.00013	3.00006	0.00118
3	2.00023	2.00021	6.00007	4.00017	5.00019	2.00022
4	0.00016	0.00016	4.00020	4.00099	9.00020	0.00016
5	**0.08448**	**0.07204**	**0.00097**	**0.00242**	**0.00038**	**0.08715**
6	5.00042	5.00040	8.00013	5.00015	11.00050	5.00041
7	5.00007	5.00007	5.00116	4.00019	7.00022	5.00007
8	4.00008	4.00007	9.00006	6.00006	6.00032	4.00007
9	5.00008	5.00008	7.00015	2.00020	7.00020	5.00008

Samples of Six

Tree	Tr_B (97)	Tr_A (100)	Tr_B (104)	Tr_B (50)	Tr_B (124)	Tr_B (181)
0	5.00058	0.00023	0.00224	0.00229	2.00209	0.00277
1	6.00017	8.00023	6.00019	6.00019	6.12356	6.00021
2	7.00012	4.00007	3.00009	3.00009	4.00022	3.00009
3	5.00023	5.01287	5.00017	5.00017	6.01834	5.00017
4	4.00027	8.00047	0.00112	0.00114	7.00036	0.00146
5	5.00079	5.00023	5.00040	5.00039	6.00011	5.00040
6	**0.01130**	**0.00402**	**0.00471**	**0.00475**	**0.00118**	**0.00562**
7	6.00166	8.00108	4.00016	4.00016	6.00099	4.00017
8	2.00009	0.00017	3.00015	3.00015	2.00029	3.00019
9	6.00295	0.00015	2.00040	2.00040	3.00019	2.00040

Tree	Tr_B (103)	Tr_B (169)	Tr_B (56)	Tr_B (43)	Tr_A (16)	Tr_B (11)
0	0.00185	2.00118	8.00049	7.00015	3.00023	5.00055
1	8.00034	10.00023	12.00016	15.00029	7.00021	10.00017
2	5.00007	7.00006	10.00005	8.00004	5.00021	9.00012
3	6.00006	8.00005	10.00094	11.00010	5.01247	5.00021
4	0.00017	2.00013	7.00012	10.00014	8.00053	5.00027
5	6.00033	6.00067	10.00084	10.00026	5.00023	5.00074
6	**0.00280**	**0.00076**	**0.00096**	**0.00018**	**0.00315**	**0.03840**
7	5.00031	7.00028	11.00135	13.00028	8.00110	6.00165
8	5.00010	6.00016	4.00033	9.00015	0.00048	0.00109
9	4.00031	6.00012	7.00011	8.00010	3.00016	5.00015

Tree	Tr_B (107)	Tr_A (144)	Tr_B (78)	Tr_A (34)	Tr_A (96)	Tr_A (70)
0	4.00156	5.00084	9.00045	5.00068	5.00080	17.00017
1	10.00016	10.00019	12.00015	10.00019	10.00021	16.00028
2	7.00006	9.00013	7.00005	7.00012	9.00013	17.00011
3	9.00006	5.00018	10.00082	5.00020	5.00016	19.00011
4	4.00093	5.00028	6.00072	4.00036	5.00028	12.00014
5	6.00118	5.00073	5.00011	5.00079	5.00084	15.00011
6	**0.00046**	**0.01926**	**0.00153**	**0.00714**	**0.01809**	**0.00062**
7	8.00016	6.00213	8.00033	6.00179	6.00207	19.00027
8	6.00016	0.00167	5.00010	2.00009	0.00193	17.00015
9	6.00014	5.00014	7.00011	6.00404	5.00013	14.00037

Samples of Seven

Tree	Tr_B (34)	Tr_A (153)	Tr_A (34)	Tr_B (2)	Tr_B (5)	Tr_B (24)
0	3.00033	2.00070	2.00077	2.00073	2.00067	7.00149
1	0.00760	0.00026	0.00023	0.00023	0.00028	10.00023
2	0.01619	0.01541	0.01453	0.01296	0.01453	6.00017
3	0.00111	3.01280	3.01441	3.01359	3.01265	5.00010
4	0.00140	0.00434	0.00364	0.00323	0.00449	**0.01095**
5	0.00921	0.00315	0.00254	0.00234	0.00328	7.00027
6	4.00033	5.00054	5.00042	5.00041	5.00054	4.00119
7	**0.04804**	**0.12613**	**0.11991**	**0.09997**	**0.12462**	0.00037
8	3.00074	2.00013	2.00013	2.00013	2.00013	2.00019
9	0.00041	0.00899	0.00721	0.00650	0.00936	0.00024

Tree	Tr_A (18)	Tr_B (97)	Tr_B (179)	Tr_B (81)	Tr_B (141)	Tr_A (190)
0	2.00078	2.00067	2.00086	3.00031	2.00086	2.00067
1	0.00021	0.00028	0.00023	0.00872	2.00023	0.00028
2	0.01477	0.01453	0.01690	0.01701	0.01690	0.01453
3	3.01375	3.01265	3.01549	0.00126	3.01549	3.01265
4	0.00325	4.00449	0.00366	0.00143	3.00366	4.00449
5	0.00227	0.00328	0.00241	0.00941	0.00241	0.00328
6	5.00040	5.00054	5.00042	4.00033	5.00042	5.00054
7	**0.10608**	**0.12462**	**0.13220**	**0.05367**	**0.13220**	**0.12462**
8	2.00013	2.00013	2.00015	3.00079	2.00015	2.00013
9	0.00636	0.00936	0.00708	0.00046	0.00708	0.00936

Tree	Tr_A (147)	Tr_A (2)	Tr_A (125)	Tr_B (54)	Tr_A (89)	Tr_B (197)
0	5.00008	8.00132	2.00081	2.00075	2.00064	2.00067
1	4.00020	7.00024	0.00022	0.00023	0.00027	0.00028
2	0.00009	5.00036	0.01481	0.01380	0.01296	0.01453
3	5.00070	3.00011	3.01454	3.01384	3.01201	3.01265
4	0.00067	0.00241	0.00325	0.00343	0.00389	0.00449
5	2.00303	0.00012	0.00224	0.00249	0.00297	0.00328
6	6.00033	5.00008	5.00041	5.00042	5.00052	5.00054
7	**0.00085**	**0.00588**	**0.10817**	**0.10844**	**0.10323**	**0.12462**
8	6.00007	7.00010	2.00014	2.00013	2.00012	2.00013
9	0.00035	8.00018	0.00640	0.00683	0.00821	0.00936

Samples of Eight

Tree	Tr_A (195)	Tr_B (13)	Tr_B (28)	Tr_B (2)	Tr_A (86)	Tr_B (32)
0	11.03377	2.00056	2.00022	13.00285	10.00075	14.00062
1	15.13234	9.00022	10.00021	15.00017	14.00025	17.00025
2	11.00016	0.00046	4.00010	10.00066	11.00009	6.00012
3	14.00015	5.00044	5.00045	13.00021	9.00004	13.00068
4	15.00036	9.00041	7.00020	13.00029	12.00027	9.00020
5	15.00023	7.00017	6.00264	11.00013	12.00085	10.00012
6	11.00127	9.00143	4.00013	7.00079	5.00015	10.00101
7	15.00102	9.00120	6.00021	14.00034	10.00010	13.00017
8	**0.00303**	**0.00051**	**0.00064**	**0.00021**	**0.00026**	**0.00012**
9	8.00023	9.00025	6.00018	14.00484	6.00021	11.00018

Tree	Tr_B (35)	Tr_A (196)	Tr_B (19)	Tr_A (33)	Tr_A (171)	Tr_A (6)
0	7.00040	12.00058	9.00158	7.00078	11.00283	8.00286
1	13.14896	15.00029	12.00032	12.00019	14.00019	14.00025
2	7.00021	8.00005	6.00007	7.00005	7.00018	8.00014
3	12.00021	12.00016	5.00014	9.00018	7.00015	8.00013
4	13.00036	10.00006	5.00040	8.00012	5.00015	12.00015
5	13.00025	11.00014	9.00089	9.00115	7.00015	7.00020
6	9.00136	10.00478	8.00031	0.00018	9.00016	10.00012
7	13.00089	13.00010	6.00012	10.00203	12.00033	12.00014
8	**0.00073**	**0.00043**	**0.00035**	**0.00113**	**0.00123**	**0.00027**
9	6.00022	9.00013	7.00017	6.00024	11.00029	8.00014

Tree	Tr_A (139)	Tr_B (178)	Tr_A (95)	Tr_B (26)	Tr_A (3)	Tr_A (62)
0	8.00077	2.00047	9.00287	8.00077	10.00014	11.00016
1	10.00017	9.00027	11.00017	10.00018	12.00017	13.00033
2	8.00011	**0.00056**	3.00009	8.00011	10.00005	5.00011
3	8.00008	5.00043	7.00041	8.00009	10.00010	5.00014
4	8.00736	9.00037	5.00011	8.00677	10.00018	12.00018
5	5.00577	7.00024	5.00016	5.00769	5.00026	8.00012
6	3.00030	9.00186	4.00075	3.00024	0.00046	12.00011
7	8.00032	9.00125	10.00039	8.00034	11.00033	11.00021
8	**0.00052**	0.00048	**0.00435**	**0.00061**	**0.00070**	**0.00022**
9	4.00855	9.00020	9.00031	4.00816	9.00015	10.00019

Samples of Nine

Tree	Tr_B (15)	Tr_B (185)	Tr_B (25)	Tr_B (7)	Tr_B (144)	Tr_B (14)
0	4.00025	10.00058	8.00055	5.00018	8.00060	7.00054
1	9.11390	13.00029	11.00023	9.00026	11.00025	10.00024
2	0.00031	6.00011	5.00009	5.00028	2.00011	8.00009
3	5.00010	5.00017	5.00012	6.00009	5.00008	5.00043
4	9.00031	5.00424	5.01319	6.00021	4.01077	7.00057
5	8.00018	8.00094	7.00039	7.00051	8.00257	5.00098
6	4.00066	6.00012	6.00007	3.00006	5.00018	5.00007
7	9.00093	5.00015	5.00040	7.00043	4.00045	9.00290
8	3.00047	6.00014	5.00023	5.00020	0.00018	4.00019
9	**0.00108**	**0.00170**	**0.01950**	**0.00054**	**0.00750**	**0.00064**

Tree	Tr_B (60)	Tr_A (199)	Tr_B (53)	Tr_A (196)	Tr_B (84)	Tr_B (48)
0	4.00022	0.00020	0.00022	8.00050	6.00032	0.00022
1	10.00022	9.14896	8.00021	11.00023	11.13944	8.00021
2	4.00440	0.00017	0.00450	8.00017	6.00022	0.00455
3	5.00006	5.00011	5.01580	6.00016	9.00019	5.01626
4	4.00013	9.00037	**0.01191**	5.00145	11.00038	**0.01119**
5	4.00077	8.00019	0.00084	6.00077	11.00023	0.00037
6	3.00007	4.00144	3.00009	4.00012	7.00128	3.00009
7	5.00214	9.00100	2.00206	6.00026	11.00114	2.00201
8	0.00022	3.00134	2.00024	5.00009	4.00404	2.00024
9	**0.00591**	**0.02064**	0.01103	**0.00146**	**0.00054**	0.00901

Tree	Tr_B (30)	Tr_A (118)	Tr_A (162)	Tr_B (81)	Tr_B (36)	Tr_B (199)
0	4.00017	4.00009	2.00019	11.00015	12.00060	9.00062
1	10.00021	8.00024	9.12477	10.00019	12.00019	8.00020
2	4.00350	4.00059	2.00014	7.00014	7.00014	7.00016
3	6.00006	4.00112	5.00011	10.00013	12.00015	5.00005
4	4.00010	0.00028	9.00033	7.00118	7.00013	6.00019
5	4.00023	0.00143	8.00017	8.00391	8.00019	7 00023
6	3.00006	5.00009	4.00131	13.00070	15.00019	12.00013
7	5.00174	5.00234	9.00101	7.00052	8.00173	7.00232
8	0.00017	5.00025	0.00043	11.00004	12.00008	8.00005
9	**0.00355**	**0.00361**	**0.02689**	**0.00031**	**0.00013**	**0.00070**

In the 0 samples, pattern 126 from Tr_A was recognized as a 6 with the second choice being a 0. To the human eye, it is a conceivable selection. The samples of digit 1 were properly recognized. We notice the repetition of feature strings through the duplication of columns. As for the 2's, pattern 128 from Tr_B was recognized as a 0, which is again an understandable decision. Pattern 24 of Tr_A presented some complicating features, and was misclassified as a 3 with the second option being a 2. One of the samples of digit 3, pattern 43 of Tr_A was read as a 5 with the next choice being a 3. In this case, we can refer to the samples of numeral 5, which were all recognized properly, and look at patterns 33 and 72 from Tr_B. These models could have easily been representative of digit 3 and exhibit a degree of similarity with our misinterpreted sample. The 4's, 5's and 6's have been interpreted properly. A sample of digit 7, pattern 24 of

Tr_B was classified as a 4, with the second and third options being respectively a 7 and a 9. The open loop at the top is the reason for this decision. It is surprising to the eye that Tr_B(13) from the samples of numeral 8, was interpreted correctly. Pattern 178 from Tr_B was however characterized as a 2. Referring to the sample, we can understand this confusion. In the case of digit 9, both patterns 53 and 48 from Tr_B were construed as 4's. However, in the case of pattern 53, it was a close call between a 4 and a 9. It is logical to infer that the loop being more open in the latter case was the cause of the greater discrepancy in these numbers.

Our method is totally dependent on the sample data and the quantity of similar models which in turn provide us with the weights. If the database is unbalanced, as is the case here, it is not surprising to have a display of such results. An experiment has been conducted on this database using 360 of the most confusing numerals and some numerals have been reclassified [LESN90]. This is the third modification to the database which originated during Ahmed's work. The original database included some touching characters, as can be seen in A.3. The last sample of the two's, Tr_A Pattern 24, contains a segmentation error. The digit 1 is touching the numeral 2. The second version of the database was obtained once all such segmentation errors were located and removed. Also eliminated were characters displaying a minimum 90-degree rotation. In our work, we used the original database, which contained all these factors. Quite a few recognition techniques have been applied to these modified data sets and can be found in several publications [FRAN92], [SNLM92], [GHFP90], [MASU90], [SNML90], [LESU89], [LASU88], [NASU88].

7.7 Comparison to other Recognition Schemes

Table 7.16 presents a compilation of the best results found in literature for the computer recognition of unconstrained handwritten numerals, which was reported in [SNLM92].

METHODS	RECOG-NI-TION	SUBSTI-TUTION	REJEC-TION	RELIA-BILITY	TRAINING	TESTING	DPI
Ahmed et Suen (1987)	87.85	4.90	7.25	94.72	5000	3540	166
Beun (1973)	90.87	2.92	6.21	96.89	15000	10000	
Cohen,Hull, Srihari (1991)	95.54	1.99	2.47	97.96		2711	300
	97.10	0.96	1.94	99.02		1762	300
Duerr, Haettich, Tropf, Winkler (1980)	99.5	0.50	0.00	99.50	5000	5000	
Gader, Hepp, Forester, Peurach, Mitchell (1990)	96.35	1.00	2.65	98.97		6000	166
	98.20	0.77	1.03	99.23		2219	300
Krzyzak, Dai, Suen (1990)	86.40	1.00	12.60	98.85	4000	2000	166
	94.85	5.15	0	94.85	4000	2000	166
Kuan et Srihari (1988)	93.30	2.50	4.20	97.39	1820	7100	300
Le Cun, Boser et al (1990)	90.00	1.00	9.00	98.90	7291	2007	300

METHODS	RECOG-NITION	SUBSTI-TUTION	REJEC-TION	RELIA-BILITY	TRAINING	TESTING	DPI
	92.00	2.00	6.00	97.80	7291	2007	300
Mitchell et Gillies (1989)	87.95	1.04	11.01	93.83		2103	
Stringa (1989)	92.60	4.60	2.80	95.30	19377	19394	
Suen,Nadal, Mai,Lam, Legault (1990)	93.05	0.00	6.95	100.00	4000	2000	166
Nadal et Suen (1988)	86.05	2.25	11.70	97.45	4000	2000	166
Lam et Suen (1988)	93.10	2.95	3.95	96.98	4000	2000	166
Mai et Suen (1990)	92.95	2.15	4.90	97.74	4000	2000	166
Legault et Suen (1989)	93.90	1.60	4.50	98.32	4000	2000	166

Table 7.16 Comparison Table

The following statement has been made in [SNLM92]:

> "In Ahmed et Suen (1987), the data used form a subset of the CENPARMI database. The test set used was not balanced and the reported recognition and substitution rates are respectively 89.55% and 3.34%. With the information given in a performance matrix, we were able to normalize those rates to 87.85% and 4.90% to better compare them with others appearing in this study."

Unfortunately, we did not have the opportunity to use the performance matrix, so our results are not normalized to those in this study. We were, however, using the unbalanced database in question.

Any statistical approach is predicated on the assumption that training data are truly representative of data that would be encountered in a real application. A balanced database is one containing samples which should exhibit the various problematic characteristics that one would expect in practice [FEHU93]. This is a very difficult objective to achieve.

According to Director Sargur Srihari of the Postal Service-funded Center of Excellence for Document Analysis and Recognition (Cedar) at the State University of New York at Buffalo, on a Sun Microsystems, Inc. SPARCstation, the software deciphers addresses and ZIP codes 40% of the time and recognizes the five-digit ZIP code alone, enough to get the mail to the right post office 75% of the time [ANTH93].

CHAPTER 8

DISTRIBUTED PROCESSING

8.1 Introduction

A distributed processing approach has been adopted because class recognition can be naturally accomplished in parallel. Each training set is used as input to the C program called ***strings*** which, as output, produces the feature strings for each extended class. These data strings are directed to "tree modules" where they are used to construct each trie. The resulting forest of tries represents the knowledge base.

The recursive structure of the tries allow for an efficient parallel matching process as all the subtries of any node can be searched independently and in parallel. Each of these subtries, in turn, may be broken into smaller subtrees and searched in parallel. Consequently, a high degree of parallelism may be achieved by simply spawning processes to conduct the searches within the subtries as they are encountered in the matching process.

Without having access to a distributed computing platform, we will describe a multitasking implementation of the recognition system which simulates its operation on a parallel architecture. We restrict the number of concurrent tasks to the 10 at the top level. It is left for future research to distribute the tasks over multiple processors.

8.2 Implementation

The implementation was done on a Sun SPARC Server 4/690 Multi-Processor running UNIX SunOS 4.1.3. The software is written in C and in C++ which, with its object-oriented style, permits large portions of programs to be re-used. This produces an environment to develop the model that helps keep debugging problems to a minimum by the re-use of previously created data objects and allows the researcher to concentrate on developing the model as opposed to software development issues. Furthermore, the object-oriented style provides a basis for extension of the model to a parallel computing environment. This is accomplished by making use of the UNIX™ operating system and its inter-process/inter-machine communications.

In the C++ implementation of this model, it was possible to easily manipulate the image data at the bit level so there was no need to use large unpacked data structures that store only a single pixel per byte. This amounts to an 8 to 1 reduction in the amount of storage required. Also, the complexity of the software is reduced by the amalgamation of the routines for horizontal and vertical scans into a single routine. C++ is used to develop a tree classifier at the upper levels of the model. The distributed processing architecture block diagram is depicted in Figure 8.1.

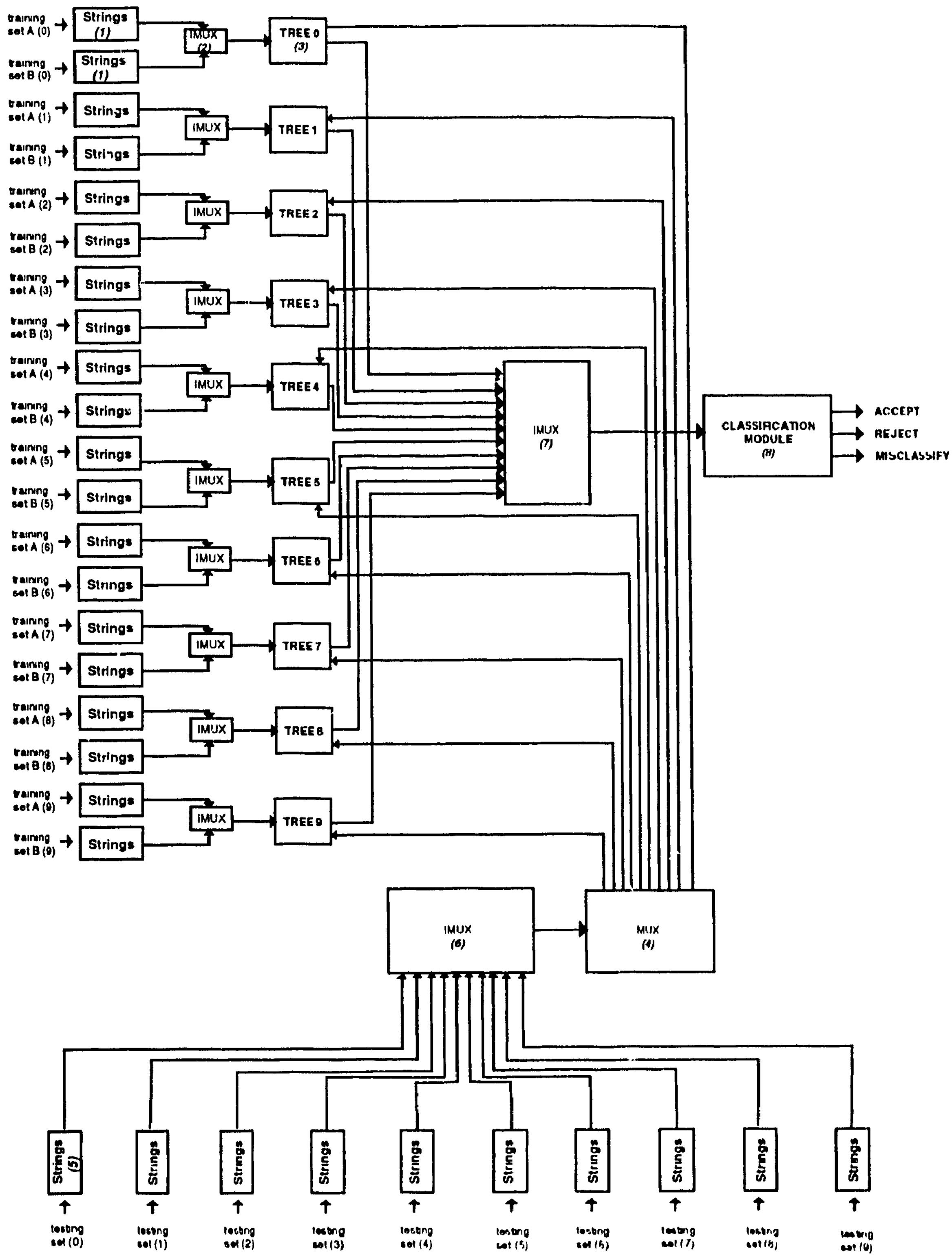

Figure 8.1 Distributed Processing Architecture

There are two training sets of 200 samples per class. Each training set is processed by ***strings(1)*** to produce the shape relation feature string. The resulting strings from the training sets of a class are combined by the data concentrator process, ***imux(2)***, which are then passed as the training input to the ***tree(3)*** process. Once all the training strings have been processed by ***tree***, it switches to the recognition mode reading the data stream from the data broadcast module, ***mux(4)***. The data broadcast by this ***mux*** module originates from the strings produced by ***strings(5)*** operating on the testing data sets which have been concentrated into a single data stream by ***imux(6)*** . The classification results from the ***tree*** modules are concentrated by ***imux(7)*** to provide the input data stream to the ***classification module(8)***. This module is responsible for making the final classification or rejection of the test samples.

CHAPTER 9

CONCLUSION AND FUTURE DEVELOPMENTS

9.1 Introduction

We conclude this thesis by summarizing the methodology presented, discussing our experience with it, and outlining a possible direction for future research within the framework of our approach. The concept of *descriptive* feature strings is introduced as an extension of the feature string representation model described in the thesis. Descriptive feature strings exploit a certain clustering phenomenon, characteristic of tries, in order to effectively compress the trie representations and to permit an enhancement of the basic methodology. A "Sliding Window Technique" is then suggested to construct a canonical tree of descriptive feature strings. This canonical representation could be used as the basis of an improved recognition scheme and warrants further research.

9.2 Summary and Contributions

This thesis describes a method for machine recognition of alphanumeric patterns. Our work has focused on the problem of recognizing the digits { 0, 1, 2, 3, 4, 5, 6, 7, 8, 9 } but the methodology is directly applicable to other sets of pattern classes of this type. Incorporating minor modifications, the scheme can be adapted for recognition of more general sets of planar shapes.

Digitized images are first preprocessed using an edge smoothing algorithm. Small random cavities which result from edge smoothing are removed through a subsequent filtering process. The filtered images then undergo horizontal and vertical scanning to identify contour edges of the corresponding shapes. Scanning yields different edge types which interconnect with each other in various topological ways to produce shape relations [AHME86]. Each junction of edges uniquely defines a shape relation.

Chains of connected edges form the inner and outer contours of each shape. During a contour extraction process, the relations associated with the edge junctions are determined. It is assumed for simplicity that the shapes are connected. Shapes are thus composed of a single outer contour containing one or more inner contours(holes). Inner contours are refined by removing excessive detail from them and recording their descriptions with fewer, more meaningful relations. As small superfluous holes seem to have little relevance for classification of the digits with our scheme, we decided to retain a maximum of two holes per shape. Larger holes were kept in favour of smaller holes which were simply discarded.

Superimposing the horizontal and vertical scans and following the outer contour in a counter clockwise fashion, the shape relations for all contours are sequentially encoded into a feature string which serves as a representation of the original image. Each relation in a feature string is further attributed with spacial information in the form of a quadrant number, localizing the relation in a rectangular grid partitioning the image area.

Feature strings are generated for all shape samples in the training sets and used to construct a trie of strings for each class. These tries provide a partial view of the space of all possible feature strings for shapes of these classes and represent a knowledge base for our classification algorithm. Statistical properties of the feature strings and their component relations are computed during the training process and recorded in each trie.

The classification algorithm implements its decision making process by matching a test feature string, generated from an image to be classified, against those in each trie, computing a "best fit" in each and selecting the best-fitting trie as the recognized class. The goodness of fit measure used for classification is a composite one which combines a "Hamming-like" metric for mismatched relations with a likelihood approximation, based on the statistical frequencies determined during training, and a quadrant distance measure. The actual form of the goodness of fit measure was determined through inspired empiricism and, as is, seems to produce good results. However, the classification algorithm is quite general and can easily incorporate other measures with little or minor modification.

Preliminary statistical information concerning the properties of feature strings, their relations and the resultant tries are gathered and presented in the form of tables and histograms. Observation of these statistics tends to support our view that the shape-relation-based representation of dig ts captures sufficient information for the purpose of classification.

Extensive experimentation with the method was conducted and showed results. It was possible to achieve substantial recognition rates with relativity small training sets. Our experience with this recognition scheme also clearly demonstrated that the feature-based description alone accounted for 85.05% recognition. Localization of features in grid quadrants improved recognition by an additional 3.1%. Rejection of samples was not considered in this work.

Finally, an implementation of our recognition system suitable for distribution over a parallel computing platform is described. In this implementation, each trie can be assigned to an independent processor whose task is to match a test string in its trie. Classification then proceeds in parallel with a central classification module collecting the results from each processor to determine the unknown class of the test string. A multitasking simulation of this distributed recognition system was actually used to run all training and testing experiments in the thesis.

The templates used for preprocessing, given in Chapter 2, were borrowed from [NALS90]. The characterization of edge relations obtained during contour extraction, as described in Chapter 3, was taken from [AHME86]. The essential contributions of this thesis begin in Chapter 4. The idea and method of encoding shape relations into feature strings during the feature extraction phase is new. The refinement procedure for inner contours and the manner in which certain holes are discarded are also contributions. We selected tries as a natural underlying representation for a knowledge base composed of feature strings. A major contribution of this thesis is the classification algorithm, together with its goodness of fit measure, described in Chapter 5. All of the experimental results contained in Chapters 6 and 7 are also new. The distributed processing architecture of Chapter 8 is a minor contribution which could be developed further into a full-blown parallel recognition scheme. The notion of descriptive shape strings and the Sliding Window technique outlined in this chapter is a final contribution for future research.

9.3 Discussion

The recognition scheme developed in this thesis is easy to implement and provides good results with a simple representation of patterns in terms of strings of shape relations extracted from contours. As mentioned above, this elementary topological description of patterns provided 85% recognition with no rejection. Incorporation of geometric information which positions shape relations in grid quadrants improved recognition, but only marginally, by an additional 3%. Perhaps, other geometric attributes such as measurements of curvature associated with each relation would provide more substantial increases in recognition. However, this aspect was not explored in this thesis. Also, as seen in Chapter 6, features are not uniformly distributed in the image plane and, therefore, it may be more appropriate to employ nonuniform grids or even more general tessellations of the image area. This being said, our scheme seems promising as a recognition methodology for alphanumeric characters, with a great deal of flexibility for implementation. The method is easily extensible to other planar shape recognition problems in a straight forward manner.

A closer examination of the properties of feature strings under transformations of the image would reveal certain structural invariances. For instance, rotations and flips of a shape yield feature strings which are related to one and other under isomorphic mappings. Simple scaling of the image together with the grid will not change the resulting feature string. On the other hand, a feature string will tend to remain unchanged up to certain thresholds when stretching in one scanning dimension only. At these stretching thresholds, certain permutations and/or losses of relations occur, yielding new feature strings. Some nonlinear transformations such as twisting and other types of distortion may also exhibit similar structural invariances. It would be interesting to study the effect of such transformations on the generated feature strings.

In general, the research in pattern recognition reveals the need for larger training sets than those currently used in many experimental studies [MASU90] and there is a growing trend to self-learning approaches [LESU93]. Our classification scheme is naturally suited for adaptive recognition as feature strings are stored in the knowledge base. It would be a simple matter to allow the classification algorithm to learn the class distributions by inserting foreign strings into the database as they arise, in much the same way a spell checker can incorporate new words into its dictionary. To avoid exponential storage growth, a filtering mechanism can be employed to provide selective learning by accepting only "strange" feature strings to be added to the database. This *strangeness* of a string could be based on the minimum number of misses that occur during classification but should also not bias the database over a period of time, so as to maintain a balanced database throughout the life cycle of the recognition process. This sort of adaptation assumes an interactive environment in which learning may take place automatically.

Possible extensions and improvements to the basic methodology are numerous. For instance, feature strings can be encoded in different ways, possibly allowing for "tighter" classification. It would be interesting to observe the effect of other methods of insertion of inner contour relations in feature strings on the overall recognition rate. Other measures of goodness of fit could be examined easily in the classification algorithm. These factors are, obviously, closely coupled and would probably require iterative experimentation to determine better ones.

There is a growing trend to viewing the pattern recognition problem in a manner analogous to that of the detection and estimation of signals embedded in noise. The approach used in this thesis supports this model to a certain extent, by addressing the noise removal problem in our treatment of holes.

In the remainder of this chapter, we outline an extension of our basic classification method which provides a much reduced representation of the underlying knowledge base and is proposed as an avenue of possible future research based on the feature string representation model.

9.4 Descriptive Shape Strings

The preorder listing of the feature strings has enabled us to identify a clump as a prefix sequence of shape patterns. This sequence of nodes or concatenation of shape patterns can be looked upon as a syllable, in this case, the first syllable. Words are composed of many syllables as paths are built from many smaller sequences of strings called *substrings*.

Examining our feature strings, we notice recurring sequences of shapes or substrings within the strings. These substructures of our planar shapes could possibly be identified as the canonical forms of the different classes. These core features are what we call *descriptive shape strings*. They are embedded in intermittent sequences of shapes that could possibly be considered as noise.

Descriptive shape strings can be extracted from our tree classification technique simply by locating the most frequent shapes corresponding to the predominant relations or sequences of relations. We will propose a method to identify these substrings and will call this feature selection process, our "Sliding Window" technique. This technique could be developed in order to collocate the misclassified feature strings in their proper classes, but basically, it should be developed to reduce the trie representation of classes to a unique decision tree model for all classes. To this new knowledge base, could be apply an altered recognition algorithm. Since random noise is incorporated in our feature strings, we would have to ignore these shapes by simply jumping over the related nodes. A proper search procedure should be implemented which could effectively travel the paths of this decision tree.

9.5 The "Sliding Window" Technique

The "Sliding Window" Technique is suggested as a method used to recover the pattern attributes characteristic of each class. This technique, once developed, would identify the core substrings of a set of planar shapes. The basic idea underlying this method is to select the recurring substrings by first, considering the most frequent feature strings as very representative and then, trying to match to these strings the other less frequent ones. Conceptually, substrings in different feature strings could intersect, by shifting the feature strings left and right, trying to optimize the contents of the intersections as we perform the comparisons. The degree of similarity of the strings is increased when the positions or *step positions* of the relations within the compared strings, is close or identical.

One of the first things to do is to compute the frequency count of the individual shape feature k for string j of digit i, n_{ijk}, for each string in the class. The most deterministic of these values belong to the feature strings with the highest frequency rates. One factor must, however, not be omitted, equivalent relations may occur in many different feature strings, but may be present in different step positions. This would implies that there should be a trade-off between the frequency counts and the closeness of their positions. Locating this threshold is of prime importance. One suggestion that should be of value in making the assessment as to a degree of correlation between feature string a and feature string b, is to first compute a distance measure

$$\sum_{k=1}^{24} |n_{iak} - n_{ibk}|$$

for each string pair. A low value of this measure is indicative to a certain degree of the resemblance of two strings. An optimal subgroup of this set should be selected in order to favor the most comparable strings.

The next move would be to develop a weighing factor, which holds as its measures the quadrant locations and step positions of the relations in the feature strings selected from the optimal subgroup. Perhaps one possible direction worth exploring in weight attribution would be to multiply the step position p_{ijkm} in the feature string by its quadrant coefficient q_{ijkm}, to sum up these values over m occurrences, and then multiply each sum by W_{ik} the relative frequency of each relation; the latter values extracted from Tables 6.6 and 6.7. The summation of these results over all relations,

$$\sum_{k=1}^{24} W_{ik} \left| \sum_{m=1}^{n_{ijk}} p_{ijkm} q_{ijkm} \right|$$

provide us with significant values for each string, to be used in establishing the degree of correlation between pairs from the proper subgroups. A handful of strings can then be selected from each subgroup, and should be used as the subset from which the canonical forms will be extracted. Once the core features are known, it will be possible to identify the noise inducing relations which should correspond to node jumps or *look-aheads* in the search algorithm.

The canonical tree model in Figure 9.1 was developed to illustrate the goal to be attained. The samples used in this representation were those with a feature string frequency greater or equal to 10 as summarized in Table 9.1. They total 2734 of the 4228 samples in the extended sets representing 64.66% of the data and are contained in 29 canonical feature strings. Note that these new strings are representative of **at least** 65% of our sample population.

Digit i	S_i	Count	# of clus-ters	Cluster Sizes	%
0	405	323	4	160, 124, 24,15	79.75
1	416	384	3	363, 11, 10	92.31
2	422	148	7	43, 26, 22, 20, 13, 13, 11	35.07
3	408	301	9	66, 64, 58, 31, 22, 18, 16, 15, 11	73.77
4	458	253	9	50, 44, 36, 32, 26, 25, 18, 12, 10	56.10
5	419	283	6	157, 51, 30, 16, 15, 14	67.54
6	421	246	6	110, 35, 33, 31, 23, 14	58.43
7	430	367	7	218, 76, 19, 15, 14, 13, 12	85.36
8	423	131	9	28, 23, 14, 13, 11, 11, 11, 10, 10	30.97
9	426	298	10	63, 57, 33, 31, 29, 22, 19, 18, 16, 10	69.95

Table 9.1 Clusters of Size ≥ 10

When we eventually refer to cluster numbers (their identity) in Table 9.2, we assign the value 1 to the cluster with the highest occurrence, the value 2 for the second greatest count and so on. The notation for the canonical tree of Figure 9.1 is the following:

◆◆	no other relations
✷	jump a number of nodes
	relation permutation

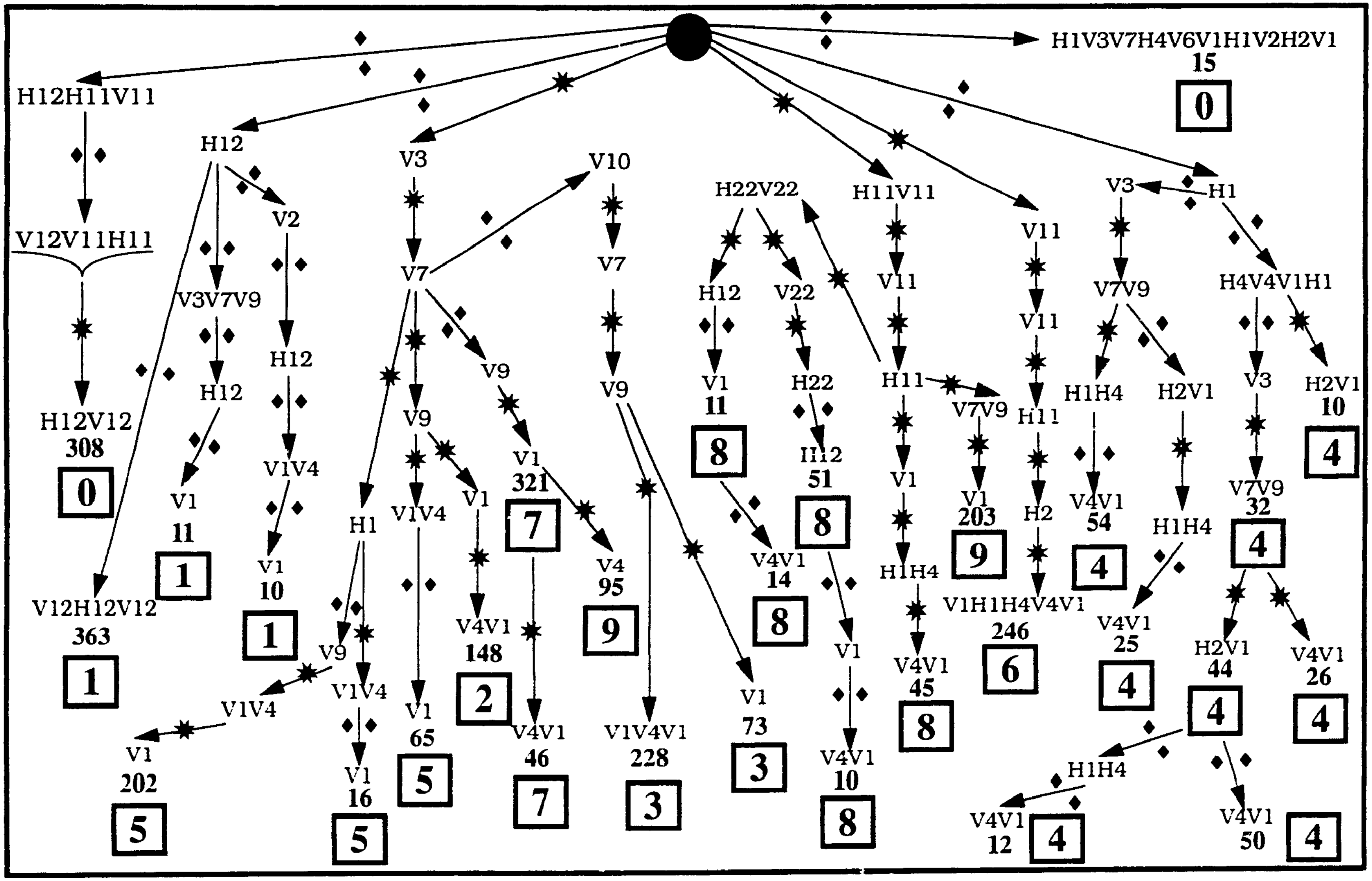

Figure 9.1 Canonical Tree Model

Certain seeming redundant subbranches are present in this model. To illustrate this statement, follow the ...V3 ...V7 V9 ... V1(321) branching describing digit 7 which has a ... V4V1(46) extension for the same digit. Perhaps this extending string of two relations is of importance, perhaps not. Only further research will express the degree of significance of these apparently non meaningful substrings. We have decided to preserve these relations here in order to extract their relative frequencies for each class (Table 9.6 and 9.7) and compare the histograms generated by these values to those developed in Chapter 6. Tables 9.6 and 9.7 were derived with the help of Tables 9.3, 9.4 and 9.5.

Digit i	**Count**	**Clus-ter #s**	**Canonical Feature string**	**Count per string**
0	323	1,2,3	♦ H12 H11 V11 ♦ {V12 V11 H11} ✷ H12 V12	308
		4	♦ H1 V3 V7 H4 V6 V1 H1 V2 H2 V1	15
1	384	1	♦ H12 ♦ V12 H12 V12	363
		2	♦ H12 ♦ V3 V7 V9 ♦ H12 ♦ V1	11
		3	♦ H12 ♦ V2 ♦ H12 ♦ V1V4 ♦ V1	10
2	148	all	✷ V3 ✷ V7 ✷ V9 ✷ V1 ✷ V4V1	148
3	301	1,2,3, 5,6	✷ V3 ✷ V7 ♦ V10 ✷ V7 ✷ V9 ✷ V1 V4 V1	228
		4,7,8, 9	✷ V3 ✷ V7 ♦ V10 ✷ V7 ✷ V9 ✷ V1	73
4	253	4	♦ H1♦ H4 V4 V1 H1 ♦ V3 ✷ V7 V9	32
		2	♦ H1♦ H4 V4 V1 H1 ♦ V3 ✷ V7 V9 ✷ H2 V1	44
		8	♦ H1♦ H4 V4 V1 H1 ♦ V3 ✷ V7 V9 ✷ H2 V1 ♦ H1 H4 ♦ V4 V1	12
		1	♦ H1♦ H4 V4 V1 H1 ♦ V3 ✷ V7 V9 ✷ H2 V1 ♦ V4 V1	50

Digit i	Count	Clus-ter #s	Canonical Feature string	Count per string
		5	♦ H1 ♦ H4 V4 V1 H1 ♦ V3 ✷ V7 V9 ✷ V4 V1	26
		9	♦ H1 ♦ H4 V4 V1 H1 ✷ H2 V1	10
		3,7	♦ H1 ♦ V3 ✷ V7 V9 ✷ H1 H4 ♦ V4 V1	54
		6	♦ H1 ♦ V3 ✷ V7 V9 ♦ H2 V1 ✷ H1 H4 ♦ V4 V1	25
5	283	1,3,5	✷ V3 ✷ V7 ✷ H1 ♦ V9 ✷ V1 V4 ✷ V1	202
		4	✷ V3 ✷ V7 ✷ H1 ✷ V1 V4 ♦ V1	16
		2,6	✷ V3 ✷ V7 ✷ V9 ✷ V1 V4 ♦ V1	65
6	246	all	✷ V11 ✷ V11 ✷ H11 ✷ H2 ✷ V1 H1 H4 V4 V1	246
7	367	1,2,4,7	✷ V3 ✷ V7 ♦ V9 ✷ V1	321
		3,5,6	✷ V3 ✷ V7 ♦ V9 ✷ V1 ✷ V4 V1	46
8	131	5	✷ H11 V11 ✷ V11 ✷ H11 ✷ H22 V22 ✷ H12 ♦ V1	11
		3	✷ H11 V11 ✷ V11 ✷ H11 ✷ H22 V22 ✷ H12 ♦ V1 ♦ V4 V1	14
		1,2	✷ H11 V11 ✷ V11 ✷ H11 ✷ H22 V22 ✷ V22 ✷ H22 ♦ H12	51
		8	✷ H11 V11 ✷ V11 ✷ H11 ✷ H22 V22 ✷ V22 ✷ H22 ♦ H12 ♦ V1 ♦ V4V1	10
		4,6,7,9	✷ H11 V11 ✷ V11 ✷ H11 ✷ V1 ✷ H1 H4 ✷ V4 V1	45
9	298	5,7,8,9	✷ V3 ✷ V7 ♦ V9 ✷ V1 ✷ V4	95
		1,2,3,4,6	✷ H11 V11 ✷ V11 ✷ H11 ✷ V7 V9 ✷ V1	203

Table 9.2 Canonical Feature Vectors

DIGIT	COUNT	H COUNTS											
		H1	H2	H3	H4	H5	H6	H7	H8	H9	H10	H11	H12
0	323	30	15		15							616	616
1	384												768
2	148												
3	301												
4	253	518	141		265								
5	283	218											
6	246	246	246		246							246	
7	367												
8	131	45			45							409	86
9	298											406	

Table 9.3 Counts of Horizontal Relations in the Clusters

DIGIT	COUNT	V COUNTS											
		V1	V2	V3	V4	V5	V6	V7	V8	V9	V10	V11	V12
0	323	30	15	15			15	15				616	616
1	384	31	10	11	10			11		11			726
2	148	296		148	148			148		148			
3	301	529		301	228			602		301	301		
4	253	482		243	341			243		243			
5	283	566		283	283			283		267			
6	246	492			246							492	
7	367	224		367	46			367		367			
8	131	149			69							409	
9	298	298		95	95			298		298		406	

Table 9.4 Counts of Vertical Relations in the Clusters

Digit	Average Number of H's in a Cluster	Average Number of V's in a Cluster	Average Length of a Feature String in a Cluster	% of H's	% of V's
0	4.00	4.09	8.09	49	51
1	2.00	2.11	4.11	49	51
2	0	6.00	6.00	0	100
3	0	7.51	7.51	0	100
4	3.65	6.13	9.78	37	63
5	.77	5.94	6.71	11	89
6	4.00	5.00	9.00	44	56
7	0	3.74	3.74	0	100
8	4.47	4.79	9.26	48	52
9	1.36	5.00	6.36	21	79

Table 9.5 Statistics of the Number of Relations in a String in a Cluster

DIGIT	COUNT	RELATIVE FREQUENCIES OF THE H RELATIONS											
		H1	H2	H3	H4	H5	H6	H7	H8	H9	H10	H11	H12
0	323	.05	.02		.02							.93	.93
1	384												1.17
2	148												
3	301												
4	253	.76	.21		.39								
5	283	.08											
6	246	.44	.44		.44							.44	

DIGIT	COUNT	RELATIVE FREQUENCIES OF THE H RELATIONS											
		H1	H2	H3	H4	H5	H6	H7	H8	H9	H10	H11	H12
7	367												
8	131	.16			.16							1.50	.31
9	298											.29	

Table 9.6 Relative Frequencies of Horizontal Relations in the Clusters

DIGIT	COUNT	RELATIVE FREQUENCIES OF THE V RELATIONS											
		V1	V2	V3	V4	V5	V6	V7	V8	V9	V10	V11	V12
0	323	.05	.02	.02			.02	.02				.97	.97
1	384	.04	.01	.01	.01			.01		.01			.96
2	148	2.00		1.00	1.00			1.00		1.00			
3	301	1.76		1.00	.76			2.00		1.00	1.00		
4	253	1.20		.60	.85			.60		.60			
5	283	1.78		.89	.89			.89		.84			
6	246	1.12			.56							1.12	
7	367	.61		1.00	.12			1.00		1.00			
8	131	.59			.27							1.62	
9	298	.79		.25	.25			.79		.79		1.08	

Table 9.7 Relative Frequencies of Vertical Relations in the Clusters

The relative frequencies given in Tables 9.6 and 9.7 are plotted in the following 10 histograms. Keep in mind the percentage of actual representation defined by these groups, a percentage which was evaluated in Table 9.1. Listing the digits in a decreasing order of descriptive representation, we capture the ensuing arrangement: 1, 7, 0, 3, 9, 5, 6, 4, 2 with digit 8 being the less representative of all. Sorting the relative frequencies in decreasing order, we obtain Table 9.8. Table 9.9 represents the decreasing sequence of original sets.

DIGIT	SEQUENTIAL SETS	DESCRIPTIVE ORDER AND %
0	{V11 V12} {H11 H12} {H1 V1} {H2 H4 V2 V3 V6 V7}	3 (79.75%)
1	{H12} {V12} {V1} {V2 V3 V4 V7 V9}	1 (92.31%)
2	{V1} {V3 V4 V7 V9}	9 (35.07%)
3	{V7} {V1} {V3 V9 V10} {V4}	4 (73.77%)
4	{V1} {V4} {H1} {V3 V7 V9} {H4} {H2}	8 (56.10%)
5	{V1} {V3 V4 V7} {V9} {H1}	6 (67.54%)
6	{V1 V11} {V4} {H1 H2 H4 H11}	7 (58.43%)
7	{V3 V7 V9} {V1} {V4}	2 (85.36%)
8	{V11} {H11} {V1} {H12} {V4} {H1 H4}	10 (30.97%)
9	{V11} {V1 V7 V9} {H11} {V3 V4}	5 (69.95%)

Table 9.8 Decreasing Sequence of Selected Canonical Sets

DIGIT	ORIGINAL SEQUENTIAL SETS	DESCRIPTIVE ORDER AND % OF CLUSTERS
0	{V11} {H11} {H12 V12} {V1} {H1} {V2} {H2 V7} {H4 V3} {V4 V6} {H7 V9} {H3 H9} {H5 H6 V5}	3 (79.75%)
1	{H12 V12} {V1} {V3 V4 V7 V9} {H1 V2}	1 (92.31%)
2	{V1} {H1} {V7 V11} {V3 V9} {H7} {H11} {V4} {H3} {H9} {H4 H12} {H10} {H2 H6} {V10} {V2} {V5 V6}	9 (35.07%)
3	{V1} {V7} {V10} {V3} {V9} {H1} {V4} {H2} {H7} {H3} {H12} {H6} {H4} {H9 H10} {V2} {V6}	4 (73.77%)
4	{V1} {H1} {V4} {V7 V9} {V3} {H4} {H2} {H7} {H9} {H3} {V2} {V12} {H10 H12 V10}	8 (56.10%)
5	{V1} {H1} {V4} {V7} {V3} {V9} {H4} {H2} {H3 H7} {H12} {H6} {H9} {V2 V6} {V10} {V12}	6 (67.54%)
6	{V1} {V11} {H1} {H11} {V4} {V2} {H2 H4} {H12} {V7} {V3} {H7 V6} {H3 H9} {H5 V9 V12} {H6 V5}	7 (58.43%)
7	{V1} {V7 V9} {V3} {H1} {H7 H9} {H3} {H12} {H4} {V4} {H2 H10 V10 V12}	2 (85.36%)
8	{V11} {H11} {V1} {H1} {H12} {V4} {V7} {V3} {V9} {H2} {H4} {V12} {V2} {H7} {H9} {H3} {H5} {H6 V6 V10} {V5}	10 (30.97%)
9	{V1} {H11} {V11} {H1} {V7 V9} {V3} {H7} {H3 H12} {V4} {H4} {H2 H5} {V2 V5 V10 V12} {H10}	5 (69.95%)

Table 9.9 Decreasing Sequence of Original Sets

Note that strings having a lesser occurrence than 10 may also be represented in these subgroups. This method has not been implemented in our research. The information has been selected and analyzed manually.

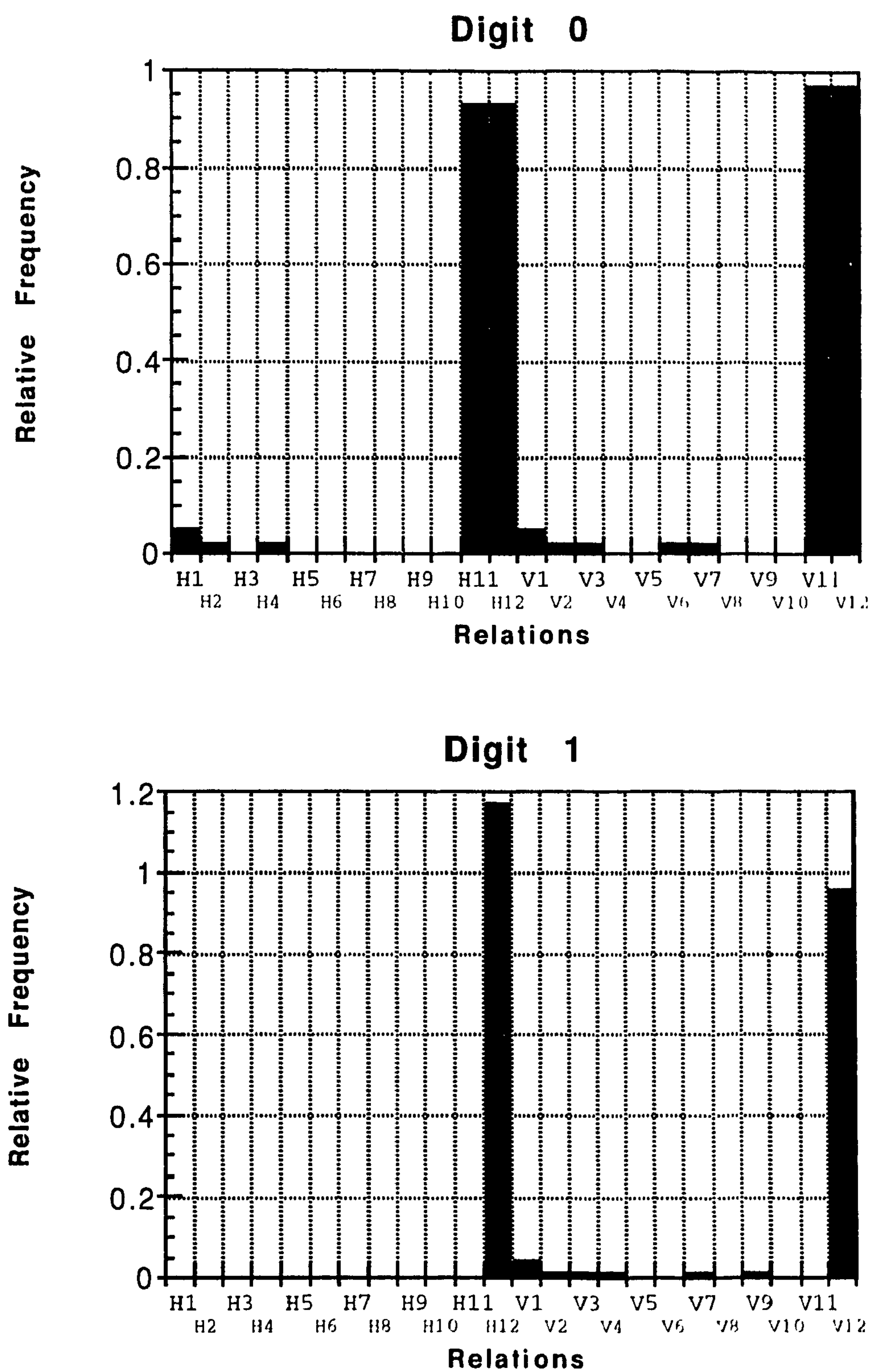

Figure 9.2 Relation Histograms in Clusters for Digits 0 and 1

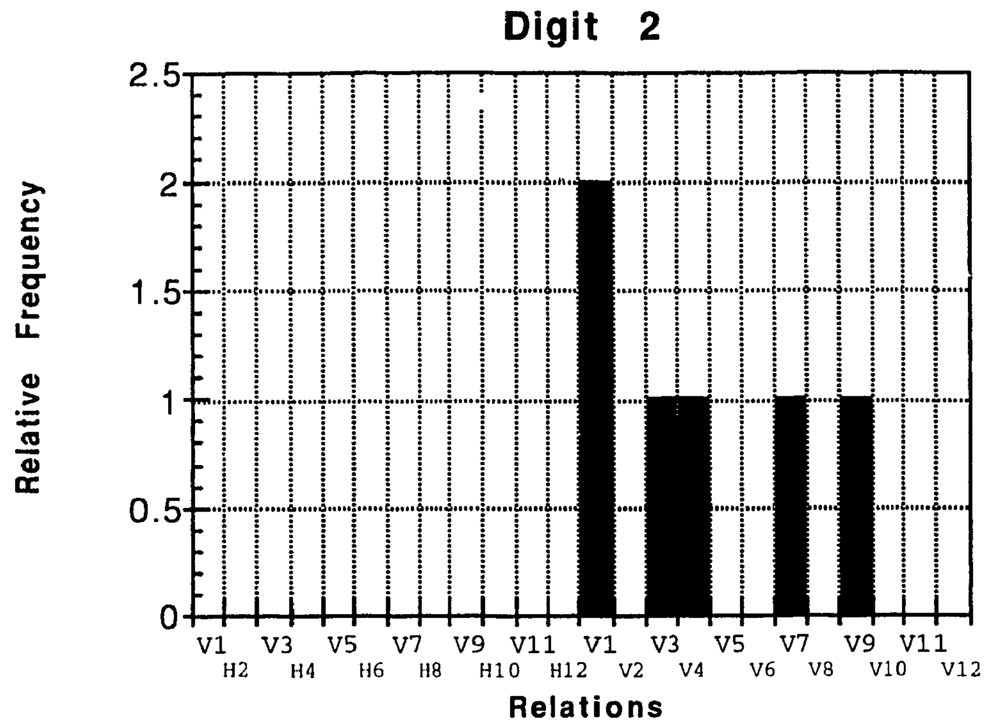

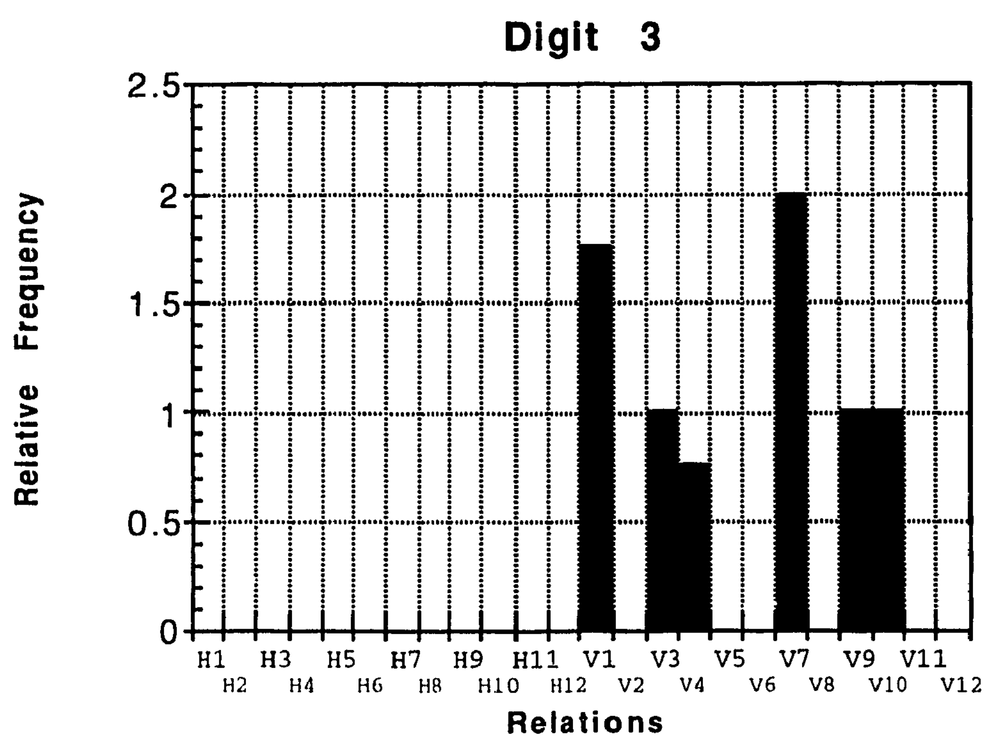

Figure 9.3 Relation Histograms in Clusters for Digits 2 and 3

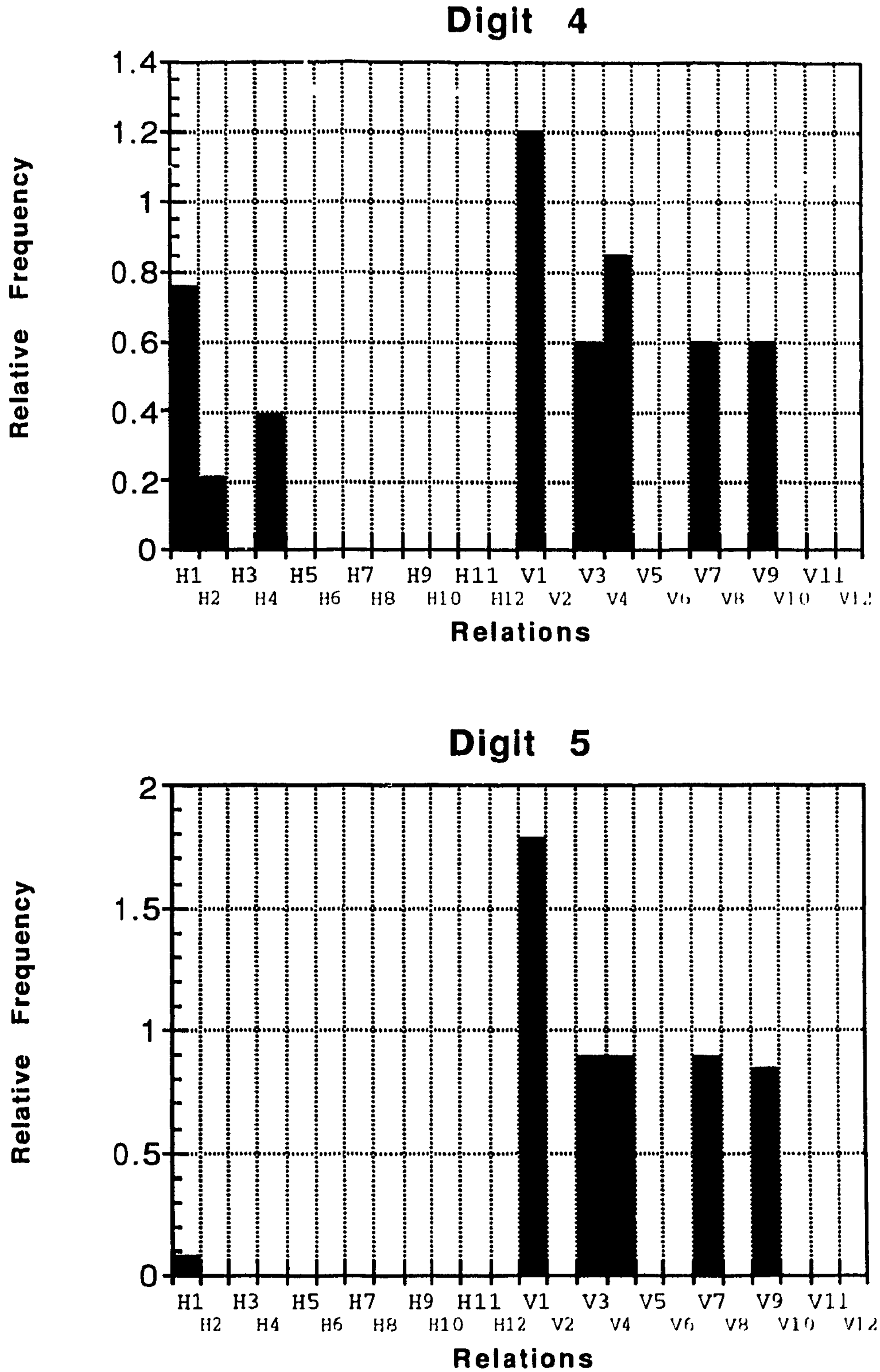

Figure 9.4 Relation Histograms in Clusters for Digits 4 and 5

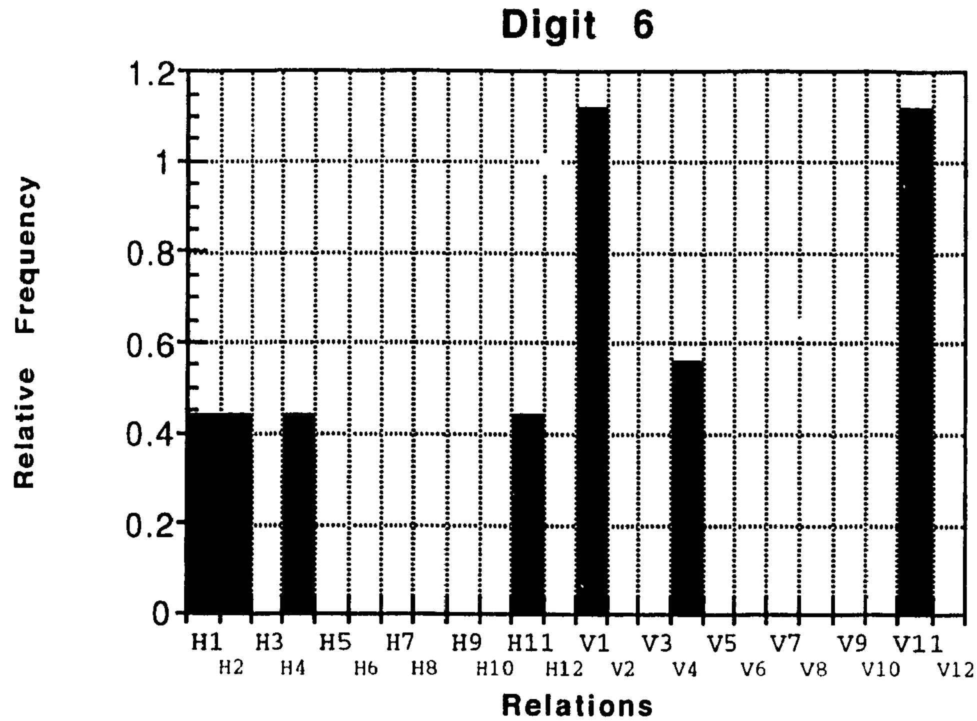

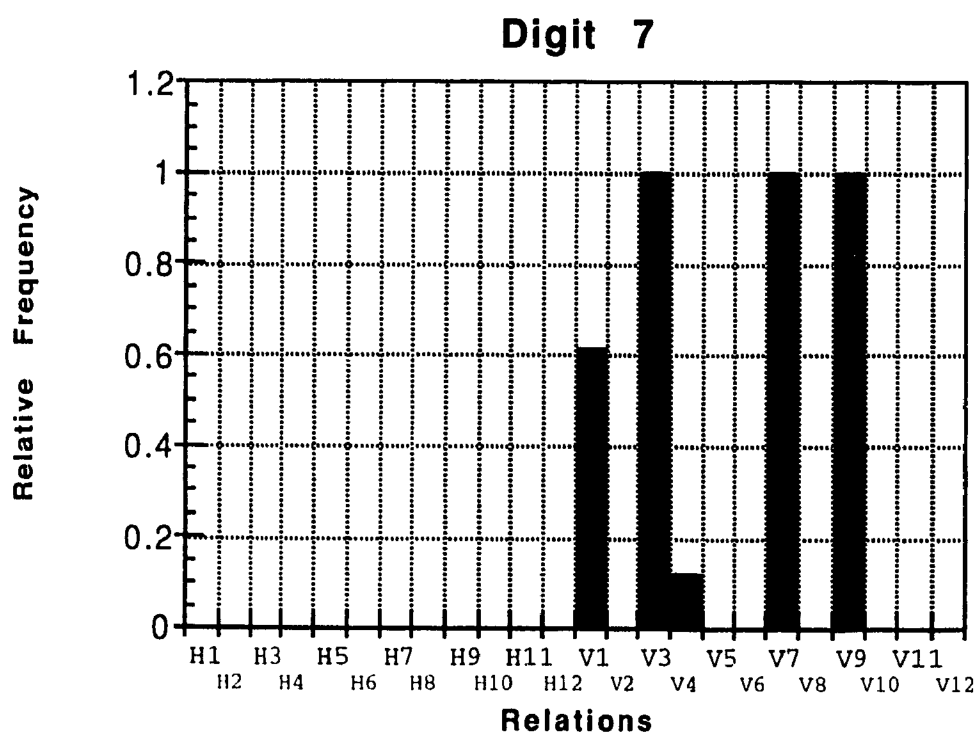

Figure 9.5 Relation Histograms in Clusters for Digits 6 and 7

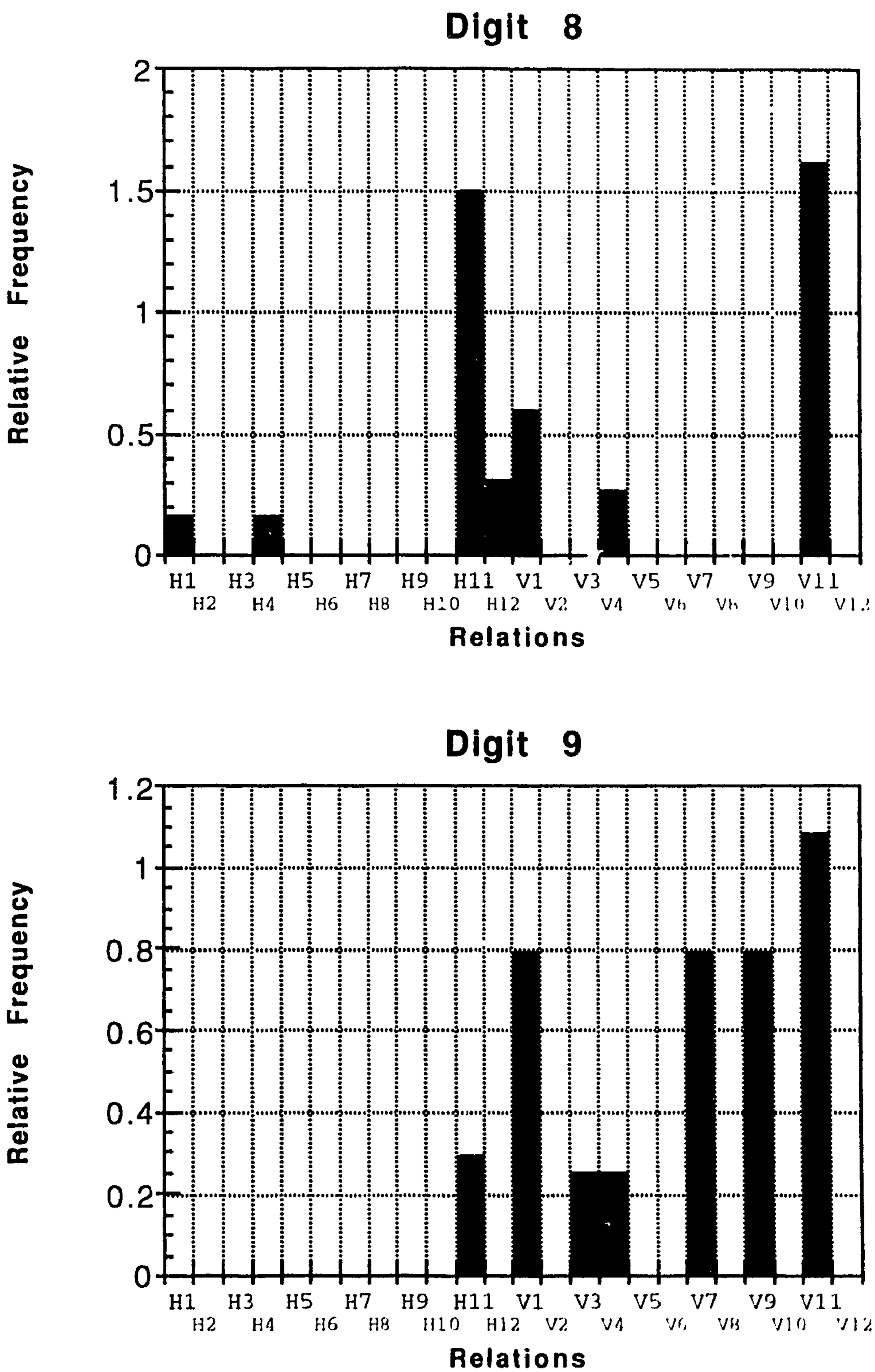

Figure 9.6 Relation Histograms in Clusters for Digits 8 and 9

Comparing these 10 histograms with the ones from Section 6.3, we can observe that digit 0 has retained its peaks and most of the occurring relations in this group representing 80% of these sample numerals. Digit 1 had the same good fortune. Not a very big surprise since this group comprised 92% of the model patterns. Digit 2, with its 35% representation has lost its horizontal delegates, events occurring in several non-repetitive strings. Extracting the canonical forms will actuate a clustering of these types of feature strings. The decreasing sequence of canonical shapes conforms in majority with the original sequence. The performance of digit 3 harmonizes well with that of numeral 2 although the sample canonical set contained more than twice the number of patterns of digit 2, 74%. The 56% representation of digit 4 patterns well the behavior exhibited in Figure 6.3. In the case of the 5, the 68% representation mirrors the behavior of digits 2 and 3 with the particularity that it retained certain H1 relations. Digit 6, with its 59% subset, reflects the behavior presented in Figure 6.4. It is interesting to note that with 85% of the original feature strings used to develop the canonical ones, the horizontal relations for Digit 7 seem unimportant. Digit 8, with a rather small subset, 31%, maintained its peaks. This digit had the lowest recognition rate. Digit 9, with its 70% representation, also shows us that several relations appeared within strings of few occurrences, rendering all but one horizontal relation, inexistent.

These observations concur well with the statistics gathered in Chapter 6. A reduced representation of the feature string model does seem to be a path well worth following.

9.6 Conclusion

Our method is obviously totally dependent on the sample data, and we have apparently succeeded in supporting the conclusion reported in [SNLM92]: "The test set was not balanced". Nevertheless, the refined objective which emerged through the analysis process of the resulting statistical information was that to truly exploit this approach, the ensuing route to proceed in is definitely the one discerning the pristine substructures of the various planar classes. This type of technique would deal appropriately with spurious detail in the image, random noise and would not allocate much importance to the presence of correlation in the errors.

Unfortunately, research is not like dynamic programming, whereas the later is a mathematical technique dealing with the optimization of multistage processes. The basic concept of this perspective is contained within the "principle of optimality". The optimal set of decisions in a multistage decision process, has the property that whatever the initial stage, state and decisions are, the remaining decisions constitute an optimal sequence of decisions for the remaining problem. The stage and state resulting from the first decision (or occurring naturally) are considered as initial conditions. Unfortunately, in research, you cannot evaluate the shortest route to a modifiable destination!

As a result of the inordinate amount of time and effort it took to reach our natural conclusion, the exciting follow-up to this work will hopefully be done in another research. Now, had I done a Ph. D. ...

"No single model exists for all pattern recognition problems and no single technique is applicable to all problems. Rather what we have in pattern recognition is a bag of tools and a bag of problems." [KANA93]

REFERENCES

[AHME86] Ahmed P., Computer Recognition of Totally Unconstrained Handwritten ZIP Codes, Ph.D. Thesis, Dept. of Computer Science, Concordia University, Montréal, July 1986, pp. 45-50.

[AHSU87] Ahmed P., Suen C. Y., "Computer Recognition of Totally Unconstrained Handwritten Zip Codes", International Journal of Pattern Recognition and Artificial Intelligence, Volume 1, Number 1, 1987, pp. 1-15.

[ANTH93] Anthes G. H., "Translation, please?", Computerworld, October 1993, p.26.

[BERT82] Berthod M., "On-line Analysis of Cursive Writing", Computer Analysis and Perception: Visual Signs, Volume 1, CRC Press, 1982, pp. 55-81.

[CHEN73] Chen C. H., Statistical Pattern Recognition, Hayden Book Company, New York, 1973.

[CHER88] Cheriet M., Optimisation et Mise en Oeuvre d'un Système d'Interrogation en Vue de la Reconnaissance de Caractères Imprimés Multipolices, Thèse de Doctorat, Université Paris VI, LAFORIA (Laboratoire Formes et Intelligence Artificielle), 9 mai 1988.

[DEKI86] Devijver P. A., Kittler J., Pattern Recognition Theory and Applications, Springer-Verlag, Berlin, 1986.

[DEKI82] Devijver P. A., Kittler J., Pattern Recognition: A Statistical Approach, Prentice-Hall, Englewood Cliffs, New Jersey, 1982.

[ENCY93] Encyclopedia of Computer Science, Third Edition, A Van Nostrand Reinhold Book, IEEE Press, 1993.

[FEHU93] Fenrich R., Hull J. J., "Concerns in Creation of Image Databases", Pre-Proceedings IWFHR III, Third International Workshop on Frontiers in Handwriting Recognition, May 1993, pp. 112-121.

[FRAN92] Franke J., "Experiments on the CENPARMI Data Set with Different Structured Classifiers, Proceedings of the 5th Advanced Technology Conference of the USPS, Washington, 1992, A167-A181.

[FREE62] Freeman H., "On the Digital-Computer Classification of Geometric Line Patterns", Proceedings National Electron. Conference, 18, 1962, pp. 312-324.

[FRWA80] Freund J. E., Walpole R.E., Mathematical Statistics, Third Edition, Prentice-Hall, Englewood Cliffs, New Jersey, 1980.

[FUKS82] Fu K. S., Syntactic Pattern Recognition and Applications, Prentice-Hall, Englewood Cliffs, New Jersey, 1982.

[FUKS74] Fu K. S., Syntactic Methods in Pattern Recognition, Academic Press, New York, 1974.

[FUKU72] Fukunaga K., Introduction to Statistical Pattern Recognition, Academic Press, New York, 1972.

[GHFP90] Gader P. D., Hepp D., Forester B., Peurach T., Mitchell B. T., "Pipelined Systems for Recognition of Handwritten Digits in USPS Zip Codes", Proceedings U. S. Postal Services Advanced Technology Conference, 1990, pp. 539-548.

[HYTS93] Hamanaka M., Yamada K., Tsukumo J.,"On-Line Japanese Character Recognition Experiments by an Off-Line Method Based on Normalization-cooperated Feature Extraction", Proceedings of the Second International Conference on Document Analysis and Recognition, Japan, October 1993, pp. 204-207.

[KANA93] Kanal L. N., 11th International Conference on Pattern Recognition August 31 - September 3, 1992, "On Pattern, Categories, and Alternate Realities", Pattern Recognition Letters, International Association for Pattern Recognition, IAPR-92 Conference Special, Volume 14, Number 3, 1993, pp. 241-248.

[KANA74] Kanal L. N., "Patterns in Pattern Recognition: 1968-1974", IEEE Transactions on Information Theory, Volume IT-20, Number 6, November 1974, pp. 697-722.

[KANA72] Kanal L. N., "Interactive Pattern Analysis and Classification Systems -- A Survey and Commentary", Proceedings of the IEEE, Volume 60, Number 10, 1972, pp. 1200-1215.

[LASU88] Lam L., Suen C. Y., "Structural Classification and Relaxation Matching of Totally Unconstrained Handwritten Zip-Code Numbers", Pattern Recognition, Volume 21, Number 1, 1988, pp. 19-31.

[LESN90] Legault R., Suen C. Y., Nadal C., "Classification of Confusing Handwritten Numerals by Human Subjects", Proceedings of the International Workshop on Frontiers in Handwriting Recognition, Concordia University, Montréal, April 1990, pp. 181-193.

[LESR93] Lee D.-S., Srihari S. N., "Handprinted Digit Recognition: A Comparison of Algorithms", Pre-Proceedings IWFHR III, Third International Workshop on Frontiers in Handwriting Recognition, 1993, pp. 153-174.

[LESU93] Legault R., Suen C. Y., "Refining Curvature Feature Extraction to Improve Handwriting Recognition", Pre-Proceedings IWFHR III, Third International Workshop on Frontiers in Handwriting Recognition, May 1993, pp. 31-40.

[LESU89] Legault R., Suen C. Y., "A Contour-Based Recognition System for Totally Unconstrained Handwritten Numerals", Technical Report, CENPARMI (Center for Pattern Recognition and Machine Intelligence), Department of Computer Science, Concordia University, Montréal, 1989, pp. 18-27.

[MASU90] Mai T. A., Suen C. Y., "A Generalized Knowledge-Based System for the Recognition of Unconstrained Handwritten Numerals", IEEE Transactions on Systems, Man, and Cybernetics, Volume 20, Number 4, July/August 1990, pp. 835-848.

[MOSY92] Mori S., Suen C. Y., Yamamoto K., "Historical Review of OCR Research and Development", Proceedings of the IEEE, Volume 80, Number 7, 1992, pp. 1029-1058.

[NALS90] Nadal C., Legault R., Suen C. Y., "Complementary Algorithms for the Recognition of Totally Unconstrained Handwritten Numerals", Proceedings of the 10th International Conference on Pattern Recognition, IEEE Computer Society Press, Volume 1, New Jersey, 1990, pp. 443-449.

[NASU88] Nadal C., Suen C. Y., Recognition of Totally Unconstrained Handwritten Digit by Decomposition and Vectorization, Technical Report, Concordia University, Montréal, 1988.

[PAVL77] Pavlidis T., Structural Pattern Recognition, Springer Verlag, New York, 1977.

[PAVL76] Pavlidis T., "Syntactic Feature Extraction for Shape Recognition", Proceedings 3rd International Joint Conference on Pattern Recognition, 1976, pp. 95-99.

[SIMO89] Simon J. C. (Editor), From Pixels to Features, North-Holland Publishing Company, Amsterdam, Netherland, 1989.

[SNLM92] Suen C. Y., Nadal C., Legault R., Mai T. A., Lam L., "Computer Recognition of Unconstrained Handwritten Numerals", Special Issue on Optical Character Recognition, Proceedings of the IEEE, Volume 80, Number 7, July 1992, pp. 1162-1180.

[SNML90] Suen C. Y., Nadal C., Mai T. A., Legault R., Lam L., "Recognition of Totally Unconstrained Handwritten Numerals Based on the Concept of Multiple Experts, Proceedings of the International Workshop on Frontiers in Handwriting Recognition, Concordia University, Montréal, April 1990, pp. 131-143.

[STAN80] Standish T. A., Data Structure Techniques, Addison Wesley, Reading, MA, 1980.

[SUEN82] Suen C. Y., "Distinctive Features in Automatic Recognition of Handprinted Characters", Signal Processing, Volume 4, North-Holland, Amsterdam, 1982, pp. 193-207.

[SULG92] Suen C. Y., Guo J., Li Z. C., "Analysis and Recognition of Alphanumeric Handprints by Parts", Proceedings of the 11th International Association for Pattern Recognition (IAPR), IEEE Computer Society Press, Volume II, The Netherlands, 1992, pp. 338-341.

[TASW90] Tappert C. C., Suen C. Y., Wakahara T., "The State of the Art in On-Line Handwriting Recognition", IEEE Transactions on Pattern Analysis and Machine Intelligence, Volume 12, Number 8, August 1990, pp. 787-808.

[TSUK92] Tsukumo J., "Handprinted Kanji Character Recognition based on Flexible Template Matching", Proceedings of the 11th International Association for Pattern Recognition (IAPR), IEEE Computer Society Press, Volume II, 1992, pp. 483-486.

[YHGR81] Yhap E. F., Greanias E. C., "An On-Line Chinese Character Recognition System", IBM Journal of Research and Development, Volume 25, 1981, pp. 187-195.

[YOCA74] Young T. Y., Calvert T. W., Classification, Estimation and Pattern Recognition, American Elsevier, New York, 1974.

APPENDIX A

SAMPLES FROM THE DATA SET

A.1 Samples of Zero

 Tr_B **Pattern 126**	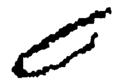 Tr_A **Pattern 126**	 Tr_B **Pattern 156**
 Tr_A **Pattern 102**	 Tr_B **Pattern 139**	 Tr_A **Pattern 57**
 Tr_B **Pattern 5**	 Tr_A **Pattern 24**	 Tr_B **Pattern 89**
 Tr_A **Pattern 48**	 Tr_B **Pattern 194**	 Tr_B **Pattern 103**
 Tr_B **Pattern 145**	 Tr_B **Pattern 97**	 Tr_B **Pattern 169**
 Tr_B **Pattern 96**	 Tr_B **Pattern 199**	 Tr_B **Pattern 21**

A.2 Samples of One

 **Tr_A Pattern 89**	 **Tr_B Pattern 33**	 **Tr_A Pattern 167**
 **Tr_B Pattern 194**	 **Tr_A Pattern 144**	 **Tr_B Pattern 10**
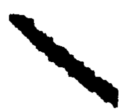 **Tr_B Pattern 55**	 **Tr_B Pattern 105**	 **Tr_B Pattern 9**
 **Tr_B Pattern 28**	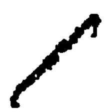 **Tr_A Pattern 4**	 **Tr_B Pattern 124**
 **Tr_A Pattern 175**	 **Tr_A Pattern 10**	 **Tr_B Pattern 150**
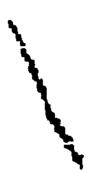 **Tr_A Pattern 154**	 **Tr_B Pattern 38**	 **Tr_A Pattern 69**

A.3	Samples of Two	
 Tr_A Pattern 101	 Tr_B Pattern 92	 Tr_B Pattern 124
 Tr_B Pattern 185	 Tr_B Pattern 15	 Tr_B Pattern 164
 Tr_A Pattern 4	 Tr_B Pattern 136	 Tr_B Pattern 197
 Tr_A Pattern 6	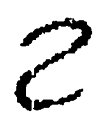 Tr_A Pattern 52	 Tr_B Pattern 59
 Tr_A Pattern 102	 Tr_B Pattern 132	 Tr_B Pattern 14
 Tr_B Pattern 128	 Tr_B Pattern 133	 Tr_A Pattern 24

A.4 **Samples of Three**

 Tr_B Pattern 17	 Tr_B Pattern 63	 Tr_A Pattern 136
 Tr_A Pattern 70	 Tr_B Pattern 29	 Tr_B Pattern 154
 Tr_A Pattern 157	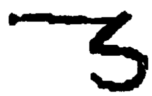 Tr_B Pattern 156	 Tr_B Pattern 108
 Tr_A Pattern 12	 Tr_A Pattern 15	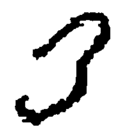 Tr_A Pattern 43
 Tr_A Pattern 10	 Tr_A Pattern 26	 Tr_A Pattern 28
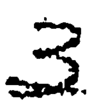 Tr_A Pattern 88	 Tr_A Pattern 96	 Tr_A Pattern 192

A.5	Samples of Four	
 Tr_A Pattern 11	 Tr_A Pattern 20	 Tr_A Pattern 149
 Tr_B Pattern 192	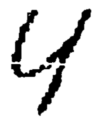 Tr_A Pattern 56	 Tr_B Pattern 144
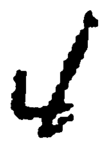 Tr_B Pattern 118	 Tr_B Pattern 162	 Tr_B Pattern 45
 Tr_B Pattern 75	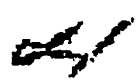 Tr_A Pattern 199	 Tr_A Pattern 36
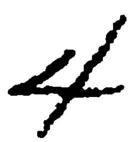 Tr_B Pattern 31	 Tr_A Pattern 1	 Tr_A Pattern 7
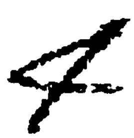 Tr_A Pattern 94	 Tr_A Pattern 105	 Tr_A Pattern 126

A.6	**Samples of Five**	
 **Tr_B Pattern 33**	 **Tr_A Pattern 156**	 **Tr_B Pattern 144**
 **Tr_A Pattern 117**	 **Tr_B Pattern 192**	 **Tr_A Pattern 95**
 **Tr_A Pattern 190**	 **Tr_A Pattern 96**	 **Tr_A Pattern 11**
 **Tr_A Pattern 22**	 **Tr_A Pattern 10**	 **Tr_A Pattern 129**
 **Tr_B Pattern 68**	 **Tr_B Pattern 99**	 **Tr_B Pattern 72**
 **Tr_B Pattern 42**	 **Tr_A Pattern 75**	 **Tr_B Pattern 159**

A.7 **Samples of Six**

 Tr_B Pattern 97	 Tr_A Pattern 100	 Tr_B Pattern 104
 Tr_B Pattern 50	 Tr_B Pattern 124	 Tr_B Pattern 181
 Tr_B Pattern 103	 Tr_B Pattern 169	 Tr_B Pattern 56
 Tr_B Pattern 43	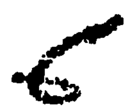 Tr_A Pattern 16	 Tr_B Pattern 11
 Tr_B Pattern 107	 Tr_A Pattern 144	 Tr_B Pattern 78
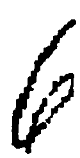 Tr_A Pattern 34	 Tr_A Pattern 96	 Tr_A Pattern 70

A.8 Samples of Seven

 Tr_B Pattern 34	 Tr_A Pattern 153	 Tr_B Pattern 113
 Tr_B Pattern 2	 Tr_B Pattern 5	 Tr_A Pattern 113
 Tr_A Pattern 18	 Tr_B Pattern 97	 Tr_B Pattern 179
 Tr_B Pattern 81	 Tr_B Pattern 141	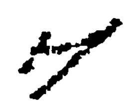 Tr_A Pattern 190
 Tr_A Pattern 147	 Tr_A Pattern 2	 Tr_A Pattern 125
 Tr_B Pattern 54	 Tr_A Pattern 89	 Tr_B Pattern 197

A.9	**Samples of Eight**	
 **Tr_A Pattern 195**	 **Tr_B Pattern 13**	 **Tr_B Pattern 28**
 **Tr_B Pattern 2**	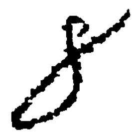 **Tr_A Pattern 86**	 **Tr_B Pattern 32**
 **Tr_B Pattern 35**	 **Tr_A Pattern 196**	 **Tr_B Pattern 19**
 **Tr_A Pattern 33**	 **Tr_A Pattern 171**	 **Tr_A Pattern 6**
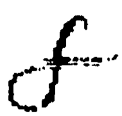 **Tr_A Pattern 139**	 **Tr_B Pattern 178**	 **Tr_A Pattern 95**
 **Tr_B Pattern 26**	 **Tr_A Pattern 3**	 **Tr_A Pattern 62**

A.10 **Samples of Nine**

 **Tr_B Pattern 15**	 **Tr_B Pattern 185**	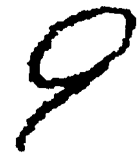 **Tr_B Pattern 25**
 **Tr_B Pattern 7**	 **Tr_B Pattern 144**	 **Tr_B Pattern 14**
 **Tr_B Pattern 60**	 **Tr_A Pattern 199**	 **Tr_B Pattern 53**
 **Tr_A Pattern 196**	 **Tr_B Pattern 84**	 **Tr_B Pattern 48**
 **Tr_B Pattern 30**	 **Tr_A Pattern 118**	 **Tr_A Pattern 162**
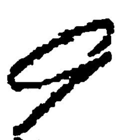 **Tr_B Pattern 81**	 **Tr_B Pattern 36**	 **Tr_B Pattern 199**

APPENDIX B

FEATURE VECTORS

B.1 Feature Strings for Digit 0

j	Term/Ext	Pass/Ext	H/W	Hole	Term	Pass	Feature String													
1	0.3062	0.3062	1.11	1	124	124	2.5 h12	2.9 h11	5.8 v11	7.4 v11	8.3 v12	9.7 h11	10.5 h12	4.9 v12						
2	0.0593	0.0593	1.09	1	24	24	2.5 h12	2.9 h11	5.8 v11	7.4 v11	9.0 h11	9.4 v12	10.0 h12	4.3 v12						
3	0.0050	0.0050	1.04	1	2	2	2.5 h12	2.9 h11	[illegible]3 v11	7.4 v11	8.5 v3	9.0 h11	10.0 v7	10.0 v9	10.5 h12	9.0 v1	7.5 v4	6.0 v1		
4	0.0025	0.0025	0.87	1	1	1	2.5 h12	2.9 h11	5.8 v11	7.4 v11	7.0 v2	11.0 h11	11.0 h12	6.0 v1	3.0 v4	3.0 v1				
5	0.3951	0.3951	1.12	1	160	160	2.5 h12	2.9 h11	5.8 v11	7.7 v12	7.9 v11	10.1 h11	10.6 h12	5.8 v12						
6	0.0124	0.0124	1.23	1	5	5	2.5 h12	2.9 h11	5.8 v11	7.6 v2	7.6 v11	9.6 h11	10.6 h12	6.6 v1	2.8 v4	2.8 v1				
7	0.0223	0.0223	1.33	1	9	9	2.5 h12	2.9 h11	4.4 v12	5.4 v11	7.6 v11	10.7 h11	11.0 h12	8.0 v12						
8	0.0025	0.0025	0.95	1	1	1	2.5 h12	2.9 h11	1.4 v3	2.5 v7	6.0 v11	7.0 v11	7.0 v9	11.0 h11	11.0 h12	6.0 v1				
9	0.0025	0.0025	1.21	1	1	1	2.5 h12	2.9 h11	1.4 v3	2.5 v7	6.0 v11	7.0 v9	7.0 v11	11.0 h11	11.0 h12	6.0 v1				
10	0.0025	0.0025	0.76	1	1	1	2.5 h12	2.9 h11	1.4 v3	3.0 v11	5.0 v7	7.0 v11	7.0 v9	10.0 h11	10.0 h12	3.0 v1				
11	0.0025	0.0025	1.34	1	1	1	2.5 h12	1.8 v3	2.3 v7	3.3 h11	7.0 v9	7.0 v11	9.0 v11	11.0 h11	11.0 h12	9.0 v1				
12	0.0050	0.0050	0.96	1	2	2	2.5 h12	1.8 v3	2.3 v7	3.3 h11	6.0 v11	7.0 v9	8.5 v11	10.5 h11	10.5 h12	6.0 v1				
13	0.0050	0.0050	1.47	1	2	2	2.5 h12	1.8 v3	2.3 v7	3.3 h11	6.0 v11	8.5 v11	8.5 v9	10.0 h11	10.0 h12	6.0 v1				
14	0.0075	0.0075	1.39	1	3	3	2.5 h12	1.8 v3	2.5 h11	2.0 v7	5.3 v11	7.0 v11	9.0 v9	10.4 h11	10.4 h12	6.0 v1				
15	0.0025	0.0025	1.18	1	1	1	2.5 h12	1.8 v3	2.5 h11	2.0 v7	5.3 v11	7.0 v9	7.0 v11	10.0 h11	10.0 h12	6.0 v1				
16	0.0075	0.0075	0.91	1	3	3	2.3 h1	2.7 h11	6.8 v11	5.2 v11	6.8 v12	9.4 h11	10.4 h2	5.0 v12	3.0 h1	2.0 h4				
17	0.0025	0.0025	0.60	1	1	1	2.3 h1	2.7 h11	6.8 v11	5.2 v11	6.8 v12	3.5 h3	2.0 h7	5.5 h11	5.5 h9	6.0 v12				
18	0.0025	0.0025	0.60	1	1	1	2.3 h1	2.7 h11	6.8 v11	5.2 v11	7.0 h3	7.0 v12	4.0 h7	11.0 h11	11.0 h9	6.0 v12				
19	0.0025	0.0025	1.81	1	1	1	2.3 h1	2.7 h11	3.0 h4	2.0 h1	6.0 v11	7.0 v12	7.0 v11	11.0 h11	11.0 h2	6.0 v12				
20	0.0173	0.0173	1.35	0	7	7	2.3 h1	7.2 v2	9.3 h2	6.6 v1	4.3 h1	2.9 v3	7.5 v7	10.6 h4	7.0 v6	2.3 v1				
21	0.0025	0.0025	1.24	0	1	1	2.3 h1	7.2 v2	9.3 h2	6.6 v1	4.3 h1	2.9 v3	7.5 v7	11.0 h5	4.0 v6	1.0 h7	2.0 h9	2.0 v1		
22	0.0025	0.0025	0.89	0	1	1	2.3 h1	7.2 v2	9.3 h2	6.6 v1	4.3 h1	2.9 v3	5.0 h3	2.0 h7	6.0 v7	11.0 h6	7.0 v6	2.0 v1		
23	0.0173	0.0173	1.01	0	7	7	2.3 h1	7.2 v2	9.3 h2	6.6 v1	4.3 h1	7.9 h4	6.5 v4	2.8 v1						
24	0.0025	0.0025	1.05	0	1	1	2.3 h1	7.2 v2	9.3 h2	6.6 v1	4.3 h1	8.7 h5	6.8 v5	2.5 h7	3.0 v7	9.0 h9	9.0 v9	6.0 v1		
25	0.0075	0.0075	1.33	0	3	3	2.3 h1	7.2 v2	9.3 h2	6.6 v1	4.3 h1	8.7 h5	6.8 v5	2.5 h7	3.0 v7	6.5 v9	6.5 h9	4.0 v1		
26	0.0025	0.0025	1.36	0	1	1	2.3 h1	7.2 v2	9.3 h2	6.6 v1	4.3 h1	8.7 h5	6.8 v5	2.5 h7	3.0 h10	3.0 h7	6.0 v7	8.0 v9	9.0 h9	3.0 v1
27	0.0025	0.0025	1.23	0	1	1	2.3 h1	7.2 v2	9.3 h2	6.6 v1	4.3 h1	8.7 h5	7.0 v4	2.0 v1	1.0 v4	1.0 h7	6.0 v1	6.0 h9		
28	0.0025	0.0025	0.79	0	1	1	2.3 h1	7.2 v2	9.3 h2	6.0 h1	6.0 v1	10.0 h4	10.0 v4	3.0 v1						
29	0.0025	0.0025	1.00	0	1	1	2.3 h1	7.2 v2	10.5 h3	11.0 v1	7.0 v5	2.0 h7	6.0 v7	8.0 v9	8.0 h9	6.0 v1				
30	0.0050	0.0050	1.40	0	2	2	2.3 h1	7.2 v2	10.5 h3	11.0 v1	7.0 v4	2.5 h7	9.0 h9	6.0 v1						
31	0.0025	0.0025	1.16	0	1	1	2.3 h1	7.2 v2	10.5 h3	11.0 v1	7.0 v4	7.0 v1	7.0 v5	2.0 h7	6.0 v7	11.0 v9	12.0 h9	6.0 v1		
32	0.0173	0.0173	0.98	0	7	7	2.3 h1	9.6 h4	7.5 v4	3.3 v1	2.0 h1	7.9 v2	10.5 h2	3.9 v1						
33	0.0371	0.0371	1.22	0	15	15	2.3 h1	2.1 v3	5.8 v7	10.0 h4	7.3 v6	3.0 v1	2.7 h1	8.2 v2	10.6 h2	5.3 v1				
34	0.0025	0.0025	1.12	1	1	1	2.3 h1	2.1 v3	5.8 v7	10.0 h4	2.0 h1	6.0 h11	6.0 v11	8.0 v11	8.0 h11	10.0 v9	11.0 h2	6.0 v1		
35	0.0025	0.0025	1.14	0	1	1	2.3 h1	2.1 v3	5.8 v7	11.0 h5	4.0 v6	2.0 h7	5.0 h9	2.0 v1	1.0 h1	7.0 v2	11.0 h2	12.0 v1	11.0 v4	6.0 v1
36	0.0025	0.0025	1.36	0	1	1	2.3 h1	2.1 v3	5.8 v7	8.5 v9	11.0 h2	9.0 v1	6.0 h1	11.0 h4	7.0 v4	3.0 v1				
37	0.0025	0.0025	0.82	0	1	1	2.3 h1	2.1 v3	5.8 v7	8.5 v9	11.0 h2	9.0 v1	12.0 v4	9.0 v1	2.0 h1	2.0 v3	9.0 v7	11.0 h4	4.0 v6	2.0 v1
38	0.0099	0.0099	1.05	0	4	4	2.3 h1	2.1 v3	1.5 h3	2.2 h7	5.0 v7	7.5 h6	5.6 v6	2.0 v1	2.0 h1	5.6 v2	8.2 h2	5.3 v1		
39	0.0025	0.0025	1.38	0	1	1	2.3 h1	2.1 v3	1.5 h3	2.2 h7	5.0 v7	7.5 h6	6.0 h1	10.0 h4	7.0 v6	5.0 v1	5.0 h1	10.0 v2	10.0 h2	6.0 v1
40	0.0025	0.0025	1.43	0	1	1	2.3 h1	0.7 v1	10.0 h2	10.0 v2	3.0 h1	6.0 v1	10.0 h4	4.0 v4						
41	0.0025	0.0025	1.43	0	1	1	2.3 h1	0.7 v1	5.0 v2	5.0 h2	1.5 h1	3.0 v1	5.0 h4	4.0 v4						

Digit 0 (continued)

42	0 0025	0 0025	0 91	0	1	1	2.3 h1	1 0 v9	11 0 h2	9 0 v1	2.0 h1	1 0 v3	1 0 h3	2 0 h7	9 0 v7	11 0 h6		
43	0.0025	0 0025	0 74	0	1	1	2.3 h1	2 0 h3	2.0 v3	3 0 h7	6 0 v7	7 0 h6	7 0 v6	2 0 v1	2.0 h1	7 0 v2	10 0 h2	3 0 v1

Extended sample set size 405

B.2 Feature Strings for Digit 1

j	Term / Ext	Pass / Ext	H / W	Hole	Term	Pass	Feature String							
1	0 8726	0 8726	1 75	0	363	363	2.8 h12	9.4 v12	10 0 h12	3 4 v12				
2	0 0217	0 0217	0 99	0	9	9	2.8 h12	9 4 v12	9.7 v12	9 7 h12				
3	0 0241	0 0265	1.86	0	10	11	2.8 h12	9.5 v2	10 2 h12	9 7 v1	8 4 v4	3 3 v1		
4	0 0025	0 0025	2 27	0	1	1	2.8 h12	9 5 v2	10 2 h12	9 7 v1	8 4 v4	3 3 v1	5 0 v4	3 0 v1
5	0.0265	0.0289	1 58	0	11	12	2.8 h12	3.2 v3	3 6 v7	10 0 v9	10 0 h12	3 7 v1		
6	0 0025	0 0025	2 50	0	1	1	2.8 h12	3 2 v3	3 6 v7	10 0 v9	10 0 h12	3 7 v1	10 0 v4	3 0 v1
7	0 0145	0.0145	1.62	0	6	6	2.8 h12	10 0 h12	10 0 v12	3 0 v12				
8	0 0025	0 0025	0 92	0	1	1	2.2 h1	5 0 v3	5 0 h3	3 0 h7	1 0 v7	3 0 h9	3 0 v9	3 0 v1
9	0 0025	0 0025	0 92	0	1	1	2.2 h1	5 0 v3	5 0 h3	3 0 h7	1.0 v7	1.5 v9	1 5 h9	3 0 v1
10	0.0049	0 0073	1 41	0	2	3	2.2 h1	7 0 v12	10.7 h3	6 7 h7	8 7 h9	6 0 v12		
11	0 0025	0 0025	1 86	0	1	1	2.2 h1	7 0 v12	10 7 h3	6 7 h7	8.7 h9	6 0 v12	6 0 h1	9 0 h4
12	0 0025	0 0025	1 06	0	1	1	2.2 h1	7 0 h4	7 0 h1	10 0 v12	10 0 h2	3 0 v12		
13	0 0217	0 0217	0 99	0	9	9	1 5 v12	1 5 h12	4 9 v12	9 7 h12				

Extended sample set size 416

B.3 Feature Strings for Digit 2

J	Term/Ext	Pass/Ext	H/W	Hole	Term	Pass	Feature String															
1	0 0048	0 1067	0 82	0	2	45	1 7 h12	1 3 v3	4 7 v7	9 6 v9	11 0 h12	11 4 v1										
2	0 1019	0 1019	1 02	0	43	43	1 7 h12	1 3 v3	4 7 v7	9 6 v9	11 0 h12	11 4 v1	8 4 v4	4 0 v1								
3	0 0024	0 0048	1 45	0	1	2	1 7 h12	1 3 v3	4 7 v7	7 0 v10	9 5 v7	10 0 v9	10 0 h12	10 5 v1								
4	0 0024	0 0024	1 82	0	1	1	1 7 h12	1 3 v3	4 7 v7	7 0 v10	9 5 v7	10 0 v9	10 0 h12	10 5 v1	8 0 v4	6 0 v1						
5	0 0166	0 0214	1 14	1	7	9	1 7 h12	1 3 v3	4 7 v7	7 0 h11	8 1 v11	9 0 v9	9 4 v11	9 8 h11	10 3 h12	9 0 v1						
6	0 0048	0 0048	0 84	1	2	2	1 7 h12	1 3 v3	4 7 v7	7 0 h11	8 1 v11	9 0 v9	9 4 v11	9 8 h11	10 3 h12	9 0 v1	8 0 v4	4 5 v1				
7	0 0024	0 0119	0 73	1	1	5	1 7 h12	1 3 v3	4 7 v7	7 0 h11	8 1 v11	9 7 v11	10 0 v9	10 0 h11	10 0 h12	9 0 v1						
8	0 0095	0 0095	0 97	1	4	4	1 7 h12	1 3 v3	4 7 v7	7.0 h11	8 1 v11	9 7 v11	10 0 v9	10 0 h11	10 0 h12	9 0 v1	8 5 v4	5 0 v1				
9	0 0024	0 0024	0 79	1	1	1	1 7 h12	1 3 v3	4 7 v7	7 0 h11	8 1 v11	9 7 v11	10 0 h11	10 0 v9	10 0 h12	9 0 v1	8 0 v4	5 0 v1				
10	0 0048	0 0072	0 92	1	2	3	1 7 h12	1 3 v3	4 7 v7	7 0 h11	7 0 v9	7 0 v11	8 7 v11	10 0 h11	10 4 h12	9 0 v1						
11	0 0024	0 0024	0 88	1	1	1	1 7 h12	1 3 v3	4 7 v7	7 0 h11	7 0 v9	7 0 v11	8 7 v11	10 0 h11	10 4 h12	9 0 v1	8 0 v4	6 0 v1				
12	0 0048	0 0048	1 15	1	2	2	1 7 h12	3 3 h11	1 0 v3	2 0 v11	2 0 v11	2.0 h11	5 0 v7	10 0 v9	11 0 h12	12 0 v1	7 0 v4	2.5 v1				
13	0 0024	0 0024	0 70	1	1	1	1 7 h12	3 3 h11	4 5 v11	5 5 v11	10 0 h11	10 0 v12	10 0 h12	3 0 v12								
14	0 0024	0 0024	0 93	1	1	1	1 7 h12	3 3 h11	4 5 v11	5 5 v11	4 0 v3	4 0 h11	5 0 v7	10 0 v9	10 0 h12	9 0 v1	8 0 v4	2.0 v1				
15	0 0190	0 0214	1 14	1	8	9	2.0 h1	2 2 v3	2 9 h3	2.2 h7	4 0 v7	6 9 h11	7 5 h6	6 0 h1	7 8 v11	8 5 v9	8 6 v11	9 0 h11	9 3 h3	8 2 h7	11 0 h9	11 0 v1
							8 2 v4	5 0 v1														
16	0 0024	0 0024	1 19	1	1	1	2.0 h1	2.2 v3	2 9 h3	2 2 h7	4 0 v7	6 9 h11	7 5 h6	6 0 h1	7 8 v11	8.5 v9	8 6 v11	9 0 h11	9 3 h3	8 2 h7	11 0 h9	11 0 v1
							8 2 v4	5 0 v1	3 0 h1	2 0 h4												
17	0 0024	0 0048	1 16	1	1	2	2 0 h1	2 2 v3	2 9 h3	2 2 h7	4 0 v7	6 9 h11	7 5 h6	6 0 h1	7 8 v11	8 5 v9	8 6 v11	9 0 h11	9 3 h3	8 2 h7	11 0 h9	11 0 v1
							10 5 h1	11 5 h4	9 5 v4	4 5 v1												
18	0 0024	0 0024	1 13	1	1	1	2 0 h1	2 2 v3	2 9 h3	2.2 h7	4 0 v7	6 9 h11	7.5 h6	6 0 h1	7 8 v11	8 5 v9	8 6 v11	9 0 h11	9.3 h3	8 2 h7	11 0 h9	11 0 v1
							10 5 h1	11 5 h4	9 5 v4	4 5 v1	3 0 v4	3 0 v1										
19	0 0024	0 0024	1 12	1	1	1	2.0 h1	2 2 v3	2.9 h3	2 2 h7	4 0 v7	6 9 h11	7 5 h6	6 0 h1	7 8 v11	8 5 v9	8 6 v11	9 0 h11	9 3 h3	8 2 h7	6 0 v1	6 0 h9
							4 5 v4	6 0 v1														
20	0 0048	0 0143	1 10	1	2	6	2 0 h1	2 2 v3	2 9 h3	2 2 h7	4 0 v7	6 9 h11	7 5 h6	6 0 h1	7 8 v11	8 5 v9	8 6 v11	9 0 h11	10 2 h2	10 0 v1		
21	0 0024	0 0048	0 73	1	1	2	2 0 h1	2 2 v3	2 9 h3	2 2 h7	4 0 v7	6 9 h11	7 5 h6	6 0 h1	7 8 v11	8 5 v9	8 6 v11	9 0 h11	10 2 h2	10 0 v1	9 0 h1	10 0 h4
							8 0 v4	4 5 v1														
22	0 0024	0.0024	0 92	1	1	1	2 0 h1	2.2 v3	2 9 h3	2.2 h7	4 0 v7	6 9 h11	7 5 h6	6 0 h1	7.8 v11	8 5 v9	8 6 v11	9 0 h11	10 2 h2	10 0 v1	9 0 h1	10 0 h4
							8 0 v4	4 5 v1	3 0 v4	3 0 v1												
23	0 0048	0.0048	0 87	1	2	2	2 0 h1	2.2 v3	2 9 h3	2 2 h7	4 0 v7	6 9 h11	7 5 h6	6 0 h1	7 8 v11	8 5 v9	8 6 v11	9 0 h11	10 2 h2	10 0 v1	8 5 v4	3 0 v1
24	0 0024	0 0261	0 84	1	1	10	2 0 h1	2 2 v3	2 9 h3	2.2 h7	4 0 v7	6 9 h11	7 5 h6	6.0 h1	7 8 v11	8 0 v11	8 4 v9	8 9 h11	9 0 h3	9 0 h7	10.8 h9	9 9 v1
25	0 0190	0 0190	1 08	1	8	8	2 0 h1	2 2 v3	2 9 h3	2 2 h7	4 0 v7	6 9 h11	7 5 h6	6 0 h1	7 8 v11	8 0 v11	8 4 v9	8 9 h11	9 0 h3	9 0 h7	10 8 h9	9 9 v1
							7 6 v4	3 4 v1														
26	0 0024	0 0024	1 26	1	1	1	2 0 h1	2 2 v3	2 9 h3	2 2 h7	4 0 v7	6 9 h11	7 5 h6	6 0 h1	7 8 v11	8 0 v11	8 4 v9	8 9 h11	9 0 h3	9 0 h7	10 8 h9	9 9 v1
							12 0 h1	12.0 h4	12 0 v4	6 0 v1												
27	0 0024	0 0048	1 13	1	1	2	2 0 h1	2 2 v3	2 9 h3	2 2 h7	4 0 v7	6 9 h11	7 5 h6	6 0 h1	7 8 v11	8 0 v11	8 4 v9	8 9 h11	10 0 h2	9 0 v1		
28	0 0024	0 0024	0 71	1	1	1	2 0 h1	2 2 v3	2 9 h3	2 2 h7	4 0 v7	6 9 h11	7 5 h6	6 0 h1	7 8 v11	8 0 v11	8 4 v9	8 9 h11	10 0 h2	9 0 v1	9 0 v4	6 0 v1
29	0 0024	0 0072	0 86	1	1	3	2.0 h1	2 2 v3	2 9 h3	2.2 h7	4 0 v7	6 9 h11	7 5 h6	6 0 h1	8 2 v9	9 2 v11	9 2 v11	10 2 h11	11 0 h2	11 0 v1		
30	0 0024	0 0024	0 83	1	1	1	2 0 h1	2 2 v3	2.9 h3	2 2 h7	4 0 v7	6 9 h11	7 5 h6	6 0 h1	8 2 v9	9 2 v11	9 2 v11	10 2 h11	11 0 h2	11 0 v1	9 0 h1	11 0 h4
							8 0 v4	3 0 v1														
31	0 0024	0 0024	0 96	1	1	1	2 0 h1	2 2 v3	2.9 h3	2 2 h7	4 0 v7	6 9 h11	7 5 h6	6 0 h1	8 2 v9	9 2 v11	9 2 v11	10 2 h11	11 0 h2	11 0 v1	11 0 v4	6 0 v1
32	0 0024	0 0024	1 16	1	1	1	2 0 h1	2 2 v3	2.9 h3	2.2 h7	4 0 v7	6 9 h11	7.5 h6	6 0 h1	8 2 v9	9 2 v11	9 2 v11	10 2 h11	10 0 h3	9 5 h7	12.0 h9	10 5 v1
							9 0 v4	3 0 v1														

Digit 2 (continued)

33	0 0024	0 0024	1 00	1	1	1	2 0 h1	2 2 v3	2 9 h3	2.2 h7	4 0 v7	6 9 h11	7 5 h6	6 0 h1	8 2 v9	9 2 v11	9 2 v11	10 2 h11	10.0 h3	9 5 h7	12 0 h9	10 5 v1
							9 0 h1	12 0 h4	8 0 v4	3 0 v1												
34	0 0095	0 0522	1 07	1	4	21	2.0 h1	2.2 v3	2 9 h3	2 2 h7	4 0 v7	6 9 h11	7 7 v11	8 6 v11	9 0 v9	9 4 h11	9 7 h10	7 9 h7	11 1 h9	9 9 v1		
35	0 0072	0 0072	0 87	1	3	3	2.0 h1	2 2 v3	2 9 h3	2 2 h7	4 0 v7	6 9 h11	7 7 v11	8 6 v11	9 0 v9	9 4 h11	9 7 h10	7 9 h7	11 1 h9	9 9 v1	9 0 h1	10 7 h4
							8 0 v4	3 4 v1														
36	0 0309	0 0332	1 01	1	13	14	2.0 h1	2 2 v3	2.9 h3	2.2 h7	4 0 v7	6 9 h11	7 7 v11	8 6 v11	9 0 v9	9 4 h11	9 7 h10	7 9 h7	11 1 h9	9 9 v1	8 2 v4	3 2 v1
37	0 0024	0 0024	1 05	1	1	1	2 0 h1	2 2 v3	2 9 h3	2 2 h7	4 0 v7	6 9 h11	7 7 v11	8 6 v11	9 0 v9	9 4 h11	9.7 h10	7 9 h7	11 1 h9	9 9 v1	8 2 v4	3 2 v1
							3 0 h1	2 0 h4														
38	0 0024	0 0024	1 20	1	1	1	2.0 h1	2 2 v3	2 9 h3	2.2 h7	4 0 v7	6 9 h11	7 7 v11	8 6 v11	9 0 v9	9 4 h11	9 7 h10	7 9 h7	4 5 v1	4 5 h9	4 0 v4	3 0 v1
39	0 0048	0 0285	1 08	1	2	11	2 0 h1	2 2 v3	2 9 h3	2 2 h7	4 0 v7	6 9 h11	7 7 v11	8 6 v11	9 0 v9	9 4 h11	8 6 h9	7 8 v1				
40	0 0166	0 0166	0 90	1	7	7	2 0 h1	2 2 v3	2 9 h3	2 2 h7	4 0 v7	6 9 h11	7 7 v11	8 6 v11	9 0 v9	9 4 h11	8 6 h9	7 8 v1	8 0 v4	3 3 v1		
41	0 0048	0 0048	0 96	1	2	2	2 0 h1	2 2 v3	2 9 h3	2 2 h7	4 0 v7	6 9 h11	7 7 v11	8 6 v11	9 0 v9	9 4 h11	8 6 h9	7 8 v1	6 0 h1	6 7 h4	5 4 v4	3 0 v1
42	0 0024	0 0024	0 72	1	1	1	2 0 h1	2 2 v3	2 9 h3	2.2 h7	4 0 v7	6 9 h11	7 7 v11	8 6 v11	9 0 v9	9 4 h11	8 6 h9	9 0 h1	9 0 v1	11 0 h4	8 0 v4	3 0 v1
43	0 0072	0 0403	1 17	1	3	17	2 0 h1	2 2 v3	2 9 h3	2 2 h7	4 0 v7	6 9 h11	7 7 v11	8 6 v11	9 2 h11	9 5 v9	10 0 h10	7 9 h7	11 8 h9	10 9 v1		
44	0 0261	0 0285	0 94	1	11	12	2 0 h1	2 2 v3	2 9 h3	2 2 h7	4 0 v7	6 9 h11	7 7 v11	8 6 v11	9 2 h11	9 5 v9	10 0 h10	7 9 h7	11 8 h9	10 9 v1	7 8 v4	3 4 v1
45	0 0024	0 0024	1 00	1	1	1	2.0 h1	2.2 v3	2 9 h3	2.2 h7	4.0 v7	6 9 h11	7 7 v11	8 6 v11	9 2 h11	9 5 v9	10 0 h10	7 9 h7	11 8 h9	10 9 v1	7 8 v4	3 4 v1
							3 0 h1	2 0 h4														
46	0 0048	0 0048	0 73	1	2	2	2 0 h1	2 2 v3	2 9 h3	2 2 h7	4 0 v7	6 9 h11	7 7 v11	8 6 v11	9 2 h11	9 5 v9	10 0 h10	7 9 h7	11 8 h9	10 9 v1	9 0 h1	11 5 h4
							9 0 v4	3 0 v1														
47	0 0024	0 0024	0 85	1	1	1	2 0 h1	2 2 v3	2 9 h3	2.2 h7	4 0 v7	6 9 h11	7 7 v11	8 6 v11	9 2 h11	9 5 v9	10 0 h10	7 9 h7	5 5 v1	5 5 h9	4 0 v4	3 0 v1
48	0 0024	0 0024	1 50	1	1	1	2 0 h1	2 2 v3	2 9 h3	2.2 h7	4 0 v7	6 9 h11	7 7 v11	8 6 v11	9 2 h11	9 5 v9	10 0 h10	11 0 v1	11 0 v4	11 0 h7	12 0 h9	12 0 v1
							8 0 v4	6 0 v1														
49	0 0024	0 0024	1 11	1	1	1	2 0 h1	2 2 v3	2 9 h3	2 2 h7	4 0 v7	6 9 h11	7 7 v11	8 6 v11	9 2 h11	9 5 v9	10 3 h9	7 5 v1	6 0 v4	3 0 v1		
50	0 0072	0 0072	0 80	1	3	3	2 0 h1	2 2 v3	2 9 h3	2 2 h7	4 0 v7	6 9 h11	7 7 v11	8 6 v11	9 2 h11	9 5 v9	10 3 h9	7 5 v1	8 0 h1	10 0 h4	9 0 v4	3 7 v1
51	0 0024	0 0024	1 00	1	1	1	2 0 h1	2 2 v3	2 9 h3	2 2 h7	4 0 v7	6 9 h11	7 7 v11	8 6 v11	9 2 h11	10 0 v10	10 0 h10	8 0 h7	12 0 v7	11 0 v9	11 0 h9	3 0 v1
52	0 0072	0 0285	1 10	1	3	11	2 0 h1	2 2 v3	2.9 h3	2.2 h7	4 0 v7	6 9 h11	7 7 v11	8 4 v9	8 4 v11	9 0 h11	9 2 h10	7 0 h7	11 0 h9	10 5 v1		
53	0 0190	0 0190	1 07	1	8	8	2 0 h1	2 2 v3	2 9 h3	2 2 h7	4 0 v7	6 9 h11	7 7 v11	8 4 v9	8 4 v11	9 0 h11	9 2 h10	7 0 h7	11 0 h9	10 5 v1	7 8 v4	4 0 v1
54	0 0024	0 0024	1 20	1	1	1	2 0 h1	2 2 v3	2 9 h3	2 2 h7	4 0 v7	6 9 h11	7 7 v11	8 4 v9	8 4 v11	9 0 h11	9 2 h10	7 0 h7	6 0 v1	6 0 h9	4 0 v4	3 0 v1
55	0 0048	0 0119	0 69	1	2	5	2 0 h1	2 2 v3	2 9 h3	2 2 h7	4 0 v7	6 9 h11	7 7 v11	8 4 v9	8 4 v11	9 0 h11	10 2 h9	7 3 v1				
56	0 0048	0 0048	0 67	1	2	2	2 0 h1	2 2 v3	2.9 h3	2 2 h7	4 0 v7	6 9 h11	7 7 v11	8 4 v9	8 4 v11	9 0 h11	10 2 h9	7 3 v1	6 0 h1	7 0 h4		
57	0 0024	0 0024	1 03	1	1	1	2 0 h1	2 2 v3	2 9 h3	2 2 h7	4 0 v7	6 9 h11	7 7 v11	8 4 v9	8 4 v11	9 0 h11	10 2 h9	7 3 v1	6 0 v4	3 0 v1		
58	0 0024	0 0024	0 96	1	1	1	2 0 h1	2 2 v3	2.9 h3	2.2 h7	4 0 v7	6 9 h11	7 7 v11	8 2 h6	7 3 h1	7 0 v9	11 0 v11	10 5 h11	10 0 h3	11 0 h7	12 0 h9	12 0 v1
							8 0 v4	6 0 v1														
59	0 0024	0 0024	1 05	1	1	1	2 0 h1	2 2 v3	2 9 h3	2.2 h7	4 0 v7	6 9 h11	7 7 v11	8 2 h6	7 3 h1	7 0 v9	11 0 v11	10 5 h11	11 0 h2	12 0 v1		
60	0 0048	0 0048	1 05	1	2	2	2 0 h1	2 2 v3	2 9 h3	2 2 h7	4 0 v7	6 9 h11	7 7 v11	8 2 h6	7 3 h1	8 4 v11	10 0 v9	10 4 h11	10 0 h3	11 0 h7	11 5 h9	12 0 v1
							10 0 v4	4 5 v1														
61	0 0024	0 0024	1 04	1	1	1	2 0 h1	2 2 v3	2 9 h3	2 2 h7	4 0 v7	6 9 h11	7 7 v11	8 2 h6	7 3 h1	8 4 v11	10 0 v9	10 4 h11	11 0 v1	11 0 h3	11 0 v4	11 0 h7
							12.0 h9	12 0 v1	12.0 h1	12 0 h4	11 0 v4	6 0 v1										
62	0 0048	0 0048	1 52	1	2	2	2 0 h1	2.2 v3	2 9 h3	2.2 h7	4 0 v7	6 9 h11	8 0 v9	8 0 v11	8 6 v11	8 2 h11	7 0 h10	7 7 h7	8 0 h9	8 0 v1	5 7 v4	6 0 v1
63	0 0024	0 0048	2 00	1	1	2	2 0 h1	2 2 v3	2 9 h3	2.2 h7	4 0 v7	6 9 h11	8 0 v9	8 0 v11	8 6 v11	8 2 h11	10 5 h9	9 0 v1				
64	0 0024	0 0024	0 93	1	1	1	2 0 h1	2 2 v3	2 9 h3	2 2 h7	4 0 v7	6 9 h11	8 0 v9	8 0 v11	8 6 v11	8 2 h11	10 5 h9	9 0 v1	8 0 v4	3 0 v1		
65	0 0072	0 1138	0 93	0	3	44	2 0 h1	2 2 v3	2 9 h3	2 2 h7	4 0 v7	9 6 v9	9 1 h9	9 5 v1								
66	0 0309	0 0332	0 77	0	13	14	2 0 h1	2 2 v3	2 9 h3	2.2 h7	4 0 v7	9 6 v9	9 1 h9	9 5 v1	6 5 h1	7 2 h4	5 4 v4	3 2 v1				
67	0 0024	0 0024	1 03	0	1	1	2 0 h1	2 2 v3	2 9 h3	2.2 h7	4 0 v7	9 6 v9	9 1 h9	9 5 v1	6 5 h1	7 2 h4	5 4 v4	3 2 v1	2 0 h1	2 0 h4		
68	0 0617	0 0640	1 09	0	26	27	2 0 h1	2 2 v3	2 9 h3	2 2 h7	4 0 v7	9 6 v9	9 1 h9	9 5 v1	8 6 v4	4 1 v1						
69	0 0024	0 0024	1 42	0	1	1	2 0 h1	2 2 v3	2 9 h3	2 2 h7	4 0 v7	9 6 v9	9 1 h9	9 5 v1	8 6 v4	4 1 v1	12 0 h1	11 0 h4	10 0 v4	2 0 v1		

Digit 2 (continued)

70	0.0095	0.0095	0.99	0	4	4	2.0 h1	2.2 v3	2.9 h3	2.2 h7	4.0 v7	9.6 v9	9.1 h9	8.3 h1	8.3 v1	8.8 h4	8.3 v4	3.5 v1				
71	0.0024	0.0024	0.95	1	1	1	2.0 h1	2.2 v3	2.9 h3	2.2 h7	4.0 v7	9.6 v9	5.0 h11	5.0 v11	5.0 v11	10.0 h11	3.4 h9	9.0 h1	9.0 v1	5.0 h4	8.0 v4	3.0 v1
72	0.0024	0.0024	0.95	1	1	1	2.0 h1	2.2 v3	2.9 h3	2.2 h7	4.0 v7	9.6 v9	5.0 h11	5.0 v11	5.0 v11	10.0 h11	3.4 h9	4.5 v1	4.5 h1	4.0 h4	4.0 v4	3.0 v1
73	0.0024	0.0024	0.78	0	1	1	2.0 h1	2.2 v3	2.9 h3	2.2 h7	4.0 v7	9.6 v9	10.0 h10	10.0 v1	10.0 v5	8.0 h7	11.0 v7	10.0 v9	11.0 h10	9.0 h7	12.0 h9	12.0 v1
							9.0 v4	3.0 v1														
74	0.0474	0.0474	1.05	0	20	20	2.0 h1	2.2 v3	2.9 h3	2.2 h7	4.0 v7	9.6 v9	10.0 h10	9.3 h7	11.9 h9	10.8 v1	8.0 v4	3.5 v1				
75	0.0048	0.0048	1.06	0	2	2	2.0 h1	2.2 v3	2.9 h3	2.2 h7	4.0 v7	9.5 v9	10.0 h10	9.3 h7	11.9 h9	10.8 v1	10.5 h1	9.5 h4	9.5 v4	3.0 v1		
76	0.0048	0.0072	0.97	0	2	3	2.0 h1	2.2 v3	2.9 h3	2.2 h7	4.0 v7	6.9 v10	7.7 v7	9.6 v9	10.0 h10	9.5 h7	11.8 h9	11.3 v1	8.7 v4	4.7 v1		
77	0.0024	0.0024	1.46	0	1	1	2.0 h1	2.2 v3	2.9 h3	2.2 h7	4.0 v7	6.9 v10	7.7 v7	9.6 v9	10.0 h10	9.5 h7	11.8 h9	11.3 v1	8.7 v4	4.7 v1	2.0 v4	3.0 v1
78	0.0024	0.0024	0.81	0	1	1	2.0 h1	2.2 v3	2.9 h3	2.2 h7	4.0 v7	6.9 v10	7.7 v7	9.6 v9	10.0 h10	9.5 h7	11.8 h9	11.3 v1	9.0 h1	11.0 h4	11.0 v4	3.0 v1
79	0.0024	0.0024	1.20	0	1	1	2.0 h1	2.2 v3	2.9 h3	2.2 h7	4.0 v7	6.9 v10	7.7 v7	9.6 v9	10.7 h9	10.0 v1	12.0 h1	12.0 h4	8.0 v4	6.0 v1		
80	0.0048	0.0048	0.75	0	2	2	2.0 h1	2.2 v3	2.9 h3	2.2 h7	4.0 v7	6.9 v10	7.7 v7	9.6 v9	10.7 h9	10.0 v1	8.5 v4	3.0 v1				
81	0.0024	0.0048	1.35	0	1	2	2.0 h1	2.2 v3	2.9 h3	2.2 h7	4.0 v7	6.9 v10	7.7 v7	9.6 h6	8.5 h1	10.0 v9	10.0 h2	9.0 v1				
82	0.0024	0.0024	0.97	0	1	1	2.0 h1	2.2 v3	2.9 h3	2.2 h7	4.0 v7	6.9 v10	7.7 v7	9.6 h6	8.5 h1	10.0 v9	10.0 h2	9.0 v1	8.0 v4	5.0 v1	2.0 v4	2.0 v1
83	0.0024	0.0024	1.67	0	1	1	2.0 h1	2.2 v3	2.9 h3	2.2 h7	4.0 v7	6.9 v10	7.7 v7	9.6 h6	8.5 h1	10.0 v9	10.0 h3	11.0 h7	12.0 h9	12.0 v1	8.0 v4	6.0 v1
84	0.0024	0.0024	1.12	1	1	1	2.0 h1	2.2 v3	2.9 h3	2.2 h7	4.0 v7	6.9 v10	7.7 v7	9.6 h6	8.5 h1	7.0 h11	8.0 v11	7.0 v9	7.0 v11	10.0 h11	10.0 h3	11.0 h7
							12.0 h9	12.0 v1	8.0 v4	6.0 v1												
85	0.0024	0.0024	0.84	0	1	1	2.0 h1	2.2 v3	2.9 h3	2.2 h7	4.0 v7	6.9 v10	7.7 v7	9.6 h6	10.0 v6	7.0 v1	7.0 h1	10.0 v2	10.0 h2	9.0 v1	8.0 v4	3.0 v1
86	0.0024	0.0024	0.78	1	1	1	2.0 h1	2.2 v3	2.9 h3	2.2 h7	4.0 v7	6.9 v10	7.7 v7	7.0 h11	8.0 v11	10.0 v9	10.0 v11	10.0 h11	10.0 h10	8.0 h7	9.0 h9	9.0 v1
							8.0 v4	2.0 v1														
87	0.0024	0.0024	1.46	0	1	1	2.0 h1	2.2 v3	2.9 h3	2.2 h7	4.0 v7	6.9 v10	8.0 h10	8.0 h7	8.0 v7	10.0 h6	8.5 h1	10.0 v9	10.0 h3	9.0 h7	12.0 h9	12.0 v1
							9.0 v4	6.0 v1														
88	0.0024	0.0024	0.76	0	1	1	2.0 h1	2.2 v3	2.9 h3	2.2 h7	4.0 v7	6.9 v10	8.0 h10	8.0 h7	8.0 v7	10.0 h6	8.5 h1	10.0 v9	10.0 h2	6.0 v1	5.0 v4	3.0 v1
89	0.0024	0.0024	0.92	0	1	1	2.0 h1	2.2 v3	2.9 h3	2.2 h7	4.0 v7	6.9 v10	8.0 h10	8.0 h7	8.0 v7	10.0 v9	10.0 h10	8.0 h7	12.0 h9	12.0 v1	8.0 v4	3.0 v1
90	0.0024	0.0048	0.64	0	1	2	2.0 h1	2.2 v3	2.9 h3	2.2 h7	4.0 v7	7.6 h6	6.0 h1	8.0 v9	11.7 h2	11.0 v1	9.5 v4	4.5 v1				
91	0.0024	0.0024	1.25	0	1	1	2.0 h1	2.2 v3	2.9 h3	2.2 h7	4.0 v7	7.6 h6	6.0 h1	8.0 v9	11.7 h2	11.0 v1	9.5 v4	4.5 v1	3.0 v4	3.0 v1		
92	0.0024	0.0024	0.69	0	1	1	2.0 h1	2.2 v3	2.9 h3	2.2 h7	4.0 v7	7.6 h6	6.0 h1	8.0 v9	11.7 h2	11.0 v1	9.0 h1	11.0 h4	11.0 v4	6.0 v1		
93	0.0024	0.0024	1.22	1	1	1	2.0 h1	2.2 v3	2.9 h3	2.2 h7	4.0 v7	7.6 h6	6.0 h1	7.8 h11	10.0 v9	10.0 v11	10.0 v11	10.0 h11	10.0 h2	12.0 v1	12.0 h1	12.0 h4
							11.0 v4	6.0 v1														
94	0.0024	0.0024	0.85	1	1	1	2.0 h1	2.2 v3	2.9 h3	2.2 h7	4.0 v7	7.6 h6	6.0 h1	7.8 h11	8.0 v11	7.0 v11	10.0 h11	10.0 v9	10.0 h3	8.0 h7	12.0 h9	12.0 v1
							12.0 h1	12.0 h4	8.0 v4	2.0 v1												
95	0.0024	0.0143	0.94	1	1	6	2.0 h1	2.2 v3	2.9 h3	2.2 h7	4.0 v7	7.6 h6	6.0 h1	7.8 h11	8.0 v11	8.5 v9	9.0 v11	10.4 h11	10.2 h3	9.0 h7	12.0 h9	10.5 v1
96	0.0119	0.0119	0.85	1	5	5	2.0 h1	2.2 v3	2.9 h3	2.2 h7	4.0 v7	7.6 h6	6.0 h1	7.8 h11	8.0 v11	8.5 v9	9.0 v11	10.4 h11	10.2 h3	9.0 h7	12.0 h9	10.5 v1
							8.5 v4	3.3 v1														
97	0.0024	0.0024	0.41	0	1	1	2.0 h1	2.2 v3	2.9 h3	2.2 h7	4.0 v7	7.6 h6	6.0 h1	6.3 v10	6.5 v7	8.5 v9	10.0 h3	8.0 h7	11.0 h9	6.0 v1	6.0 h1	11.0 h4
							8.0 v4	5.0 v1	2.0 v4	2.0 v1												
98	0.0024	0.0024	1.13	0	1	1	2.0 h1	2.2 v3	2.9 h3	2.2 h7	4.0 v7	7.6 h6	6.0 h1	6.3 v10	6.5 v7	8.5 v9	11.0 h2	11.0 v1	11.0 v4	3.0 v1		
99	0.0024	0.0024	0.59	0	1	1	2.0 h1	2.2 v3	2.9 h3	2.2 h7	4.0 v7	7.6 h6	6.0 h1	6.3 v10	6.5 v7	9.3 h4	5.2 v6	7.0 h1	7.0 v1	10.0 v2	10.0 h3	8.0 h7
							12.0 h9	12.0 v1	9.0 v4	3.0 v1												
100	0.0048	0.0048	0.66	0	2	2	2.0 h1	2.2 v3	2.9 h3	2.2 h7	4.0 v7	7.6 h6	6.0 h1	6.3 v10	6.5 v7	9.3 h4	5.2 v6	5.6 v1	5.6 h1	6.8 v2	6.7 h3	5.4 h7
							8.0 h9	8.0 v1	6.0 v4	3.0 v1												
101	0.0024	0.0048	0.97	0	1	2	2.0 h1	2.2 v3	2.9 h3	2.2 h7	4.0 v7	7.6 h6	6.0 h1	6.3 v10	6.5 v7	9.3 h4	5.2 v6	5.6 v1	5.6 h1	6.8 v2	11.5 h2	7.5 v1
102	0.0024	0.0024	0.77	0	1	1	2.0 h1	2.2 v3	2.9 h3	2.2 h7	4.0 v7	7.6 h6	6.0 h1	6.3 v10	6.5 v7	9.3 h4	5.2 v6	5.6 v1	5.6 h1	6.8 v2	11.5 h2	7.5 v1
							11.0 v4	6.0 v1														
103	0.0024	0.0024	0.81	0	1	1	2.0 h1	2.2 v3	2.9 h3	2.2 h7	4.0 v7	7.6 h6	6.0 h1	6.3 v10	8.5 h3	7.0 h7	9.5 v7	10.0 v9	12.0 h9	12.0 v1	9.0 v4	3.0 v1

Digit 2 (continued)

104	0 0024	0 0024	1 00	0	1	1	20 h1	22 v3	29 h3	22 h7	40 v7	76 h6	60 h1	63 v10	85 h3	70 h7	95 v7	100 v9	100 h10	110 h7	120 h9	90 v1
							90 h1	110 h4	110 v4	30 v1	30 v4	30 v1										
105	0 0024	0 0024	0 83	0	1	1	20 h1	22 v3	29 h3	22 h7	40 v7	76 h6	34 v6	70 h1	70 v1	100 v2	100 h3	90 h7	120 h9	120 v1	90 v4	30 v1
106	0 0024	0 0024	0 83	0	1	1	20 h1	22 v3	29 h3	22 h7	40 v7	76 h6	34 v6	35 v1	35 h1	50 v2	50 h3	45 h7	60 h9	60 v1	45 v4	30 v1
107	0 0024	0 0024	1 00	1	1	1	20 h1	22 v3	29 h3	22 h7	55 h11	85 v7	80 h6	40 h1	70 v9	70 v11	80 v11	80 h11	110 h3	90 h7	120 h9	12.0 v1
108	0 0024	0 0024	1 14	1	1	1	20 h1	22 v3	29 h3	22 h7	55 h11	85 v7	70 v11	80 h6	40 h1	70 v9	110 v11	110 h11	110 h3	110 h7	12.0 h9	120 v1
							90 v4	60 v1														
109	0 0522	0 0522	0 99	0	22	22	20 h1	22 v3	47 v7	99 v9	90 h2	84 v1	83 h1	90 h4	79 v4	36 v1						
110	0 0048	0 0048	0 94	0	2	2	20 h1	22 v3	47 v7	99 v9	90 h2	90 h1	90 v1	95 h4	70 v4	35 v1						
111	0 0095	0 0237	1 06	0	4	10	20 h1	22 v3	47 v7	99 v9	100 h3	92 h7	120 h9	109 v1								
112	0 0072	0 0072	0 84	0	3	3	20 h1	22 v3	47 v7	99 v9	100 h3	92 h7	120 h9	109 v1	84 h1	110 h4	87 v4	34 v1				
113	0 0072	0 0072	1 08	0	3	3	20 h1	22 v3	47 v7	99 v9	100 h3	92 h7	120 h9	109 v1	80 v4	40 v1						
114	0 0048	0 0048	1 24	0	2	2	20 h1	22 v3	47 v7	59 v10	66 v7	100 v9	100 h3	95 h7	120 h9	120 v1	85 v4	45 v1				
115	0 0024	0 0024	0 80	0	1	1	20 h1	22 v3	47 v7	59 v10	66 v7	100 v9	100 h2	90 v1	90 h1	80 h4	70 v4	20 v1				
116	0 0024	0 0024	0 84	0	1	1	20 h1	22 v3	47 v7	59 v10	66 v7	100 h4	43 v6	70 h1	70 v1	100 v2	100 h2	90 v1	90 v4	30 v1		
117	0 0024	0 0024	0 84	0	1	1	20 h1	22 v3	47 v7	59 v10	66 v7	100 h4	43 v6	40 v1	37 h1	50 v2	50 h2	45 v1	45 v4	30 v1		
118	0 0024	0 0024	1 14	0	1	1	20 h1	22 v3	47 v7	59 v10	66 v7	100 h4	43 v6	40 v1	37 h1	40 v3	70 v7	70 v9	110 h3	90 h7	12.0 h9	12.0 v1
119	0 0024	0 0024	1 03	0	1	1	20 h1	22 v3	47 v7	59 v10	66 v7	100 h4	100 h1	100 v9	100 h3	80 h7	120 h9	120 v1	80 v4	50 v1		
120	0 0048	0 0166	1 36	1	2	7	20 h1	22 v3	47 v7	70 h11	82 v11	87 v11	96 v9	96 h11	100 h3	103 h7	119 h9	112 v1				
121	0 0095	0 0119	0 94	1	4	5	20 h1	22 v3	47 v7	70 h11	82 v11	87 v11	96 v9	96 h11	100 h3	103 h7	119 h9	112 v1	86 v4	65 v1		
122	0 0024	0 0024	0 97	1	1	1	20 h1	22 v3	47 v7	70 h11	82 v11	87 v11	96 v9	96 h11	100 h3	103 h7	119 h9	112 v1	86 v4	65 v1	80 v4	60 v1
123	0 0072	0 0237	0 96	1	3	10	20 h1	22 v3	47 v7	70 h11	82 v11	87 v11	95 h11	100 v9	100 h3	91 h7	116 h9	102 v1				
124	0 0143	0 0143	0 90	1	6	6	20 h1	22 v3	47 v7	70 h11	82 v11	87 v11	95 h11	100 v9	100 h3	91 h7	116 h9	102 v1	84 v4	45 v1		
125	0 0024	0 0024	0 88	1	1	1	20 h1	22 v3	47 v7	70 h11	82 v11	87 v11	95 h11	100 v9	100 h3	91 h7	116 h9	102 v1	90 h1	110 h4	80 v4	30 v1
126	0 0024	0 0024	0 95	1	1	1	20 h1	22 v3	47 v7	70 h11	82 v11	87 v11	80 h4	40 h1	70 v9	110 h11	110 h2	120 v1	120 v4	60 v1		
127	0 0143	0 0261	1 31	1	6	11	20 h1	22 v3	47 v7	70 h11	82 v11	98 v9	98 v11	100 h11	101 h3	92 h7	118 h9	104 v1				
128	0 0095	0 0095	0 96	1	4	4	20 h1	22 v3	47 v7	70 h11	82 v11	98 v9	98 v11	100 h11	101 h3	92 h7	118 h9	104 v1	58 v4	40 v1		
129	0 0024	0 0024	0 59	1	1	1	20 h1	22 v3	47 v7	70 h11	82 v11	98 v9	98 v11	100 h11	101 h3	92 h7	118 h9	104 v1	90 h1	110 h4	80 v4	2.0 v1
130	0 0048	0 0048	0 78	1	2	2	20 h1	22 v3	47 v7	70 h11	82 v11	80 h4	50 h1	70 v9	77 v11	104 h11	100 h3	85 h7	120 h9	120 v1	85 v4	45 v1
131	0 0024	0 0024	0 97	1	1	1	20 h1	22 v3	47 v7	70 h11	82 v11	80 h4	50 h1	70 v9	77 v11	104 h11	120 h2	120 v1	90 v4	90 v1		
132	0 0024	0 0072	1 15	1	1	2	20 h1	22 v3	47 v7	70 h11	76 h4	61 h1	60 v9	60 v11	65 v11	107 h11	53 h2	60 v1				
133	0 0024	0 0024	0 69	1	1	1	20 h1	22 v3	47 v7	70 h11	76 h4	61 h1	60 v9	60 v11	65 v11	107 h11	53 h2	60 v1	30 h1	90 h4		
134	0 0024	0 0024	0 69	1	1	1	20 h1	22 v3	47 v7	70 h11	76 h4	61 h1	60 v9	60 v11	65 v11	107 h11	53 h2	60 h1	60 v1	90 h4		
135	0 0024	0 0024	1 14	1	1	1	20 h1	22 v3	47 v7	70 h11	76 h4	61 h1	60 v9	60 v11	65 v11	107 h11	110 h3	120 h7	120 h9	120 v1		
136	0 0024	0 0024	0 48	1	1	1	20 h1	22 v3	47 v7	70 h11	76 h4	61 h1	84 v11	92 v11	100 h11	100 v9	100 h3	100 h7	110 h9	60 v1	60 h1	110 h4
							70 v4	50 v1														
137	0 0048	0 0048	1 09	1	2	2	20 h1	22 v3	47 v7	70 h11	76 h4	61 h1	84 v11	92 v11	95 v9	95 h11	100 h2	90 v1	85 v4	45 v1		
138	0 0024	0 0024	0 74	1	1	1	20 h1	22 v3	47 v7	70 h11	76 h4	61 h1	84 v11	92 v11	95 v9	95 h11	100 h2	90 v1	90 h1	80 h4	90 v4	60 v1
139	0 0072	0 0072	0 95	1	3	3	20 h1	22 v3	47 v7	70 h11	76 h4	61 h1	84 v11	92 v11	95 v9	95 h11	100 h3	100 h7	12.0 h9	12.0 v1	80 v4	40 v1
140	0 0048	0 0072	0 98	1	2	3	20 h1	22 v3	47 v7	70 h11	76 h4	61 h1	84 v11	92 v9	99 v11	102 h11	107 h3	117 h7	120 h9	100 v1		
141	0 0024	0 0024	1 20	1	1	1	20 h1	22 v3	47 v7	70 h11	76 h4	61 h1	84 v11	92 v9	99 v11	102 h11	107 h3	117 h7	12.0 h9	100 v1	120 h1	12.0 h4
							90 v4	60 v1														
142	0 0072	0 0072	0 83	1	3	3	20 h1	22 v3	47 v7	70 h11	76 h4	61 h1	84 v11	92 v9	99 v11	102 h11	100 h2	98 v1	87 v4	40 v1		
143	0 0024	0 0024	0 83	1	1	1	20 h1	22 v3	47 v7	70 h11	76 h4	61 h1	84 v11	92 v9	99 v11	102 h11	100 h2	98 v1	60 h1	80 h4	80 v4	30 v1
144	0 0024	0 0024	0 72	1	1	1	20 h1	22 v3	47 v7	70 h11	70 v9	70 v11	70 v11	100 h11	100 h3	50 h7	120 h9	120 v1				
145	0 0024	0 0024	0 84	0	1	1	20 h1	22 v3	47 v7	80 h4	59 h1	83 v9	100 h3	80 h7	120 h9	120 v1	90 v4	60 v1				

Digit 2 (continued)

146	0 0143	0 0143	0 96	0	6	6	2 0 h1	2.2 v3	4 7 v7	8 0 h4	5 9 h1	8 3 v9	11 2 h2	11 5 v1	8 7 v4	4 9 v1						
147	0 0024	0 0024	0 67	0	1	1	2.0 h1	2 2 v3	4 7 v7	8 0 h4	5 9 h1	7 5 v10	7 0 h3	4 0 h7	11 0 v7	10 0 h6	10 0 h1	10 0 v9	11 0 h3	12 0 h7	12 0 h9	12 0 v1
							9 0 v4	6 0 v1														
148	0 0024	0 0024	0 82	0	1	1	2 0 h1	2 2 v3	4 7 v7	8 0 h4	5 9 h1	7 5 v10	8 0 v7	10 0 h4	7 0 v6	7 0 v1	7 0 h1	10 0 v2	10 0 h3	11 0 h7	12 0 h9	12 0 v1
							8 0 v4	3 0 v1														
149	0 0024	0 0024	0 79	1	1	1	2 0 h1	2 2 v3	4 7 v7	8 0 h4	5 9 h1	7 0 h11	7 0 v9	7 5 v11	9 0 v11	9 0 h11	10 0 h3	8 0 h7	12 0 h9	12 0 v1		
150	0 0024	0 0024	1 09	1	1	1	2.0 h1	2 2 v3	4 7 v7	8 0 h4	5 9 h1	7 0 h11	7 0 v9	7 5 v11	9 0 v11	9 0 h11	11 0 h2	9 0 v1	9 0 v4	6 0 v1		
151	0 0024	0 0024	0 82	1	1	1	2 0 h1	2.2 v3	4 7 v7	8 0 h4	5 9 h1	7 0 h11	8 0 v11	7 0 v11	7 0 h11	7 0 v9	10 0 h3	8 0 h7	12 0 h9	12 0 v1	9 0 v4	3 0 v1
152	0 0024	0 0024	0 84	1	1	1	2.0 h1	2 2 v3	4 0 h11	7 0 v11	8 0 v7	11 0 h4	4 0 h1	7 0 v9	11 0 v11	11 0 h11	11 0 h2	12.0 v1	12.0 h1	12 0 h4	11 0 v4	9 0 v1
153	0 0024	0 0024	1 78	1	1	1	2 0 h1	1 5 h3	1 5 v3	2 4 h7	4 9 v7	7 2 h11	10 0 v9	10 0 v11	11 0 v11	10 0 h11	11 0 h10	12 0 h7	12.0 h9	12 0 v1	12 0 v4	6 0 v1
154	0 0024	0 0024	0 89	1	1	1	2 0 h1	1 5 h3	1 5 v3	2 4 h7	4 9 v7	7 2 h11	7 5 v11	10 0 v11	10 0 v9	10 0 h11	10 0 h10	11 0 h7	12 0 h9	12 0 v1	8 0 v4	3 0 v1
155	0 0024	0 0024	1 47	1	1	1	2 0 h1	1 5 h3	1 5 v3	2.4 h7	4 9 v7	7 2 h11	7 5 v11	10 0 v9	10 0 v11	10 0 h11	10 0 h10	9 0 h7	12 0 h9	9 0 v1	9 0 v4	6 0 v1
156	0 0024	0 0024	1 24	1	1	1	2 0 h1	1 5 h3	1 5 v3	2.4 h7	4 9 v7	7 2 h11	8 0 h6	6 4 h1	7 7 v11	10 0 v9	10 0 v11	10 0 h11	11 0 h3	12 0 h7	12 0 h9	12.0 v1
							12.0 v4	6 0 v1														
157	0 0024	0 0024	1 05	1	1	1	2 0 h1	1 5 h3	1 5 v3	2.4 h7	4 9 v7	7 2 h11	8 0 h6	6 4 h1	7 7 v11	8 5 v11	10 0 v9	11 0 h11	11 0 h3	12 0 h7	12 0 h9	12.0 v1
							9 0 v4	6 0 v1														
158	0 0024	0 0024	0 75	1	1	1	2 0 h1	1 5 h3	1 5 v3	2.4 h7	4 9 v7	7.2 h11	8 0 h6	6 4 h1	7 7 v11	8 5 v11	10 0 h11	10 0 v9	10 0 h3	11 0 h7	12 0 h9	9 0 h1
							9 0 v1	12.0 h4	8 0 v4	3 0 v1												
159	0 0024	0 0024	1 19	1	1	1	2 0 h1	1 3 v2	1 7 h3	1 9 v1	1.2 v5	1 4 h7	4 0 v7	7 7 h11	8 0 v11	7 0 v9	7 0 v11	10 0 h11	10 0 h10	8 0 h7	12.0 h9	12 0 v1
							8 0 v4	2.0 v1														
160	0 0048	0 0048	1 53	1	2	2	2 0 h1	1 3 v2	1 7 h3	1 9 v1	1 2 v5	1.4 h7	4 0 v7	7.7 h11	8 0 v11	10 0 v11	10 0 h11	10 0 v9	10 0 h9	9 0 v1	9 0 v4	6 0 v1
161	0 0024	0 0024	0 58	0	1	1	2 0 h1	1 3 v2	1.7 h3	1 9 v1	1 2 v5	1 4 h7	4 0 v7	5 0 v9	5 0 h10	4 5 v1	9 0 v4	3 0 h7	9 0 h9	9 0 v1	9 0 h1	7 0 h4
							7 0 v4	5 0 v1														
162	0 0024	0 0024	0 58	0	1	1	2 0 h1	1 3 v2	1 7 h3	1 9 v1	1 2 v5	1.4 h7	4 0 v7	5 0 v9	5.0 h10	4 5 v1	9 0 v4	3 0 h7	4 5 v1	4 5 h9	4 5 h1	3 5 h4
							3 5 v4	5 0 v1														
163	0 0024	0 0024	0 70	1	1	1	2 0 h1	1 3 v2	1 7 h3	1 9 v1	1 2 v5	1.4 h7	4 0 v7	8 0 h6	5 0 h1	8 0 h11	8 0 v11	8 0 v11	7 0 v9	8 0 h11	11 0 h3	11 0 h7
							12 0 h9	12 0 v1	9 0 v4	6 0 v1												
164	0 0024	0 0024	1 04	1	1	1	2.0 h1	1 3 v2	4 0 h2	5 0 v1	2.0 h1	4 0 h5	1 0 v5	2 0 h7	6 0 v7	8 0 h11	9 0 h6	5 0 h1	9 0 v11	7 0 v9	7 0 v11	11 0 h11
							11 0 h3	9 0 h7	12 0 h9	9 0 v1												
165	0 0024	0 0024	1 13	1	1	1	2 0 h1	1 7 h11	2 0 v11	2 0 v11	2.4 h11	4 0 v3	4 0 h3	3 4 h7	4 4 v7	8 5 h6	7 0 h1	10 0 v9	10 0 h3	11 0 h7	12 0 h9	12 0 v1
							8 0 v4	3 0 v1														
166	0 0024	0 0024	0.77	1	1	1	2 0 h1	1 7 h11	2.0 v11	2.0 v11	2.4 h11	4 0 v3	4 0 h3	3 4 h7	4 4 v7	8 5 h6	7 0 h1	10 0 v9	11 0 h2	12 0 v1	9 0 h1	11 0 h4
							10 0 v4	5 0 v1														
167	0 0024	0 0024	1 22	1	1	1	2 0 h1	1 7 h11	2.0 v11	2 0 v11	2.4 h11	4 0 v3	4 0 h3	3 4 h7	4 4 v7	10 C v9	10 0 h10	11 0 h7	12.0 h9	12 0 v1	8 0 v4	6 0 v1

Extended sample set size 422

B.4 Feature Strings for Digit 3

j	Term/Ext	Pass/Ext	H/W	Hole	Term	Pass	Feature String															
1	0 0393	0 1863	1 12	0	16	76	2 0 h12	1 6 v3	3 5 v7	5 1 v10	9 1 v7	10 1 v9	10 5 h12	8 3 v1								
2	0 1422	0 1471	1 27	0	58	60	2 0 h12	1 6 v3	3 5 v7	5 1 v10	9 1 v7	10 1 v9	10 5 h12	8 3 v1	5 6 v4	3 3 v1						
3	0 0050	0 0050	1 26	0	2	2	2 0 h12	1 6 v3	3 5 v7	5 1 v10	9 1 v7	10 1 v9	10 5 h12	8 3 v1	5 6 v4	3 3 v1	1 5 v4	2 5 v1				
4	0 0025	0 0025	1 48	0	1	1	2 0 h12	1 6 v3	3 5 v7	5 1 v10	9 1 v7	8 0 v10	11 0 v7	10 0 v9	11 0 h12	9 0 v1	5 0 v4	3 0 v1				
5	0 0025	0 0050	1 19	0	1	2	2 0 h12	1 6 v3	3 5 v7	10 0 v9	10 0 h12	6 0 v1										
6	0 0025	0 0025	1 30	0	1	1	2 0 h12	1 6 v3	3 5 v7	10 0 v9	10 0 h12	6 0 v1	4 0 v4	3 0 v1								
7	0 0368	0 2108	1 06	0	15	82	2 2 h1	1 7 v3	2 0 h3	2 5 h7	3 2 v7	5 3 v10	8 5 v7	10 0 h6	7 8 h1	8 7 v9	10 2 h2	7 6 v1				
8	0 1569	0 1618	1 29	0	64	66	2 2 h1	1 7 v3	2 0 h3	2 5 h7	3 2 v7	5 3 v10	8 5 v7	10 0 h6	7 8 h1	8 7 v9	10 2 h2	7 6 v1	5 4 v4	3 4 v1		
9	0 0050	0 0050	0 94	0	2	2	2 2 h1	1 7 v3	2 0 h3	2 5 h7	3 2 v7	5 3 v10	8 5 v7	10 0 h6	7 8 h1	8 7 v9	10 2 h2	7 6 v1	5 4 v4	3 4 v1	7 0 v4	3 0 v1
10	0 0025	0 0025	1 27	0	1	1	2 2 h1	1 7 v3	2 0 h3	2 5 h7	3 2 v7	5 3 v10	8 5 v7	10 0 h6	7 8 h1	8 7 v9	10 2 h2	7 6 v1	2 0 h1	1 0 h4	1 0 v4	2 0 v1
11	0 0025	0 0025	1 08	0	1	1	2 2 h1	1 7 v3	2 0 h3	2 5 h7	3 2 v7	5 3 v10	8 5 v7	10 0 h6	7 8 h1	8 7 v9	10 0 h3	11 0 h7	12 0 h9	3 0 v1		
12	0 0025	0 0025	1 11	0	1	1	2 2 h1	1 7 v3	2 0 h3	2 5 h7	3 2 v7	5 3 v10	8 5 v7	10 0 h6	7 8 h1	10 0 v10	11 0 h3	9 0 h7	9 0 v7	10 0 v9	11 0 h9	9 0 v1
							6 0 v4	3 0 v1														
13	0 0123	0 0148	1 26	0	5	6	2 2 h1	1 7 v3	2 0 h3	2 5 h7	3 2 v7	5 3 v10	8 5 v7	10 0 h6	7 8 v6	6 0 v1	6 7 h1	6 4 v2	11 2 h2	10 0 v1	7 0 v4	4 0 v1
14	0 0025	0 0025	1 41	0	1	1	2 2 h1	1 7 v3	2 0 h3	2 5 h7	3 2 v7	5 3 v10	8 5 v7	10 0 h6	7 8 v6	6 0 v1	6 7 h1	6 4 v2	11 2 h2	10 0 v1	7 0 v4	4 0 v1
							6 0 v4	3 0 v1														
15	0 0025	0 0025	1 41	0	1	1	2 2 h1	1 7 v3	2 0 h3	2 5 h7	3 2 v7	5 3 v10	8 5 v7	10 0 h6	7 8 v6	6 0 v1	6 7 h1	6 4 v2	6 0 v1	6 0 h2	5 5 v4	4 5 v1
							3 0 v4	3 0 v1														
16	0 0123	0 0687	1 14	0	5	28	2 2 h1	1 7 v3	2 0 h3	2 5 h7	3 2 v7	5 3 v10	8 5 v7	10 2 v9	10 7 h9	8 1 v1						
17	0 0540	0 0564	1 21	0	22	23	2 2 h1	1 7 v3	2 0 h3	2 5 h7	3 2 v7	5 3 v10	8 5 v7	10 2 v9	10 7 h9	8 1 v1	6 0 v4	3 2 v1				
18	0 0025	0 0025	1 71	0	1	1	2 2 h1	1 7 v3	2 0 h3	2 5 h7	3 2 v7	5 3 v10	8 5 v7	10 2 v9	10 7 h9	8 1 v1	6 0 v4	3 2 v1	3 0 h1	2 0 h4		
19	0 0025	0 0025	2 06	0	1	1	2 2 h1	1 7 v3	2 0 h3	2 5 h7	3 2 v7	5 3 v10	8 5 v7	7 5 v10	9 0 v7	10 0 v9	10 0 h9	9 0 v1	5 0 v4	3 0 v1		
20	0 0025	0 0025	1 42	0	1	1	2 2 h1	1 7 v3	2 0 h3	2 5 h7	3 2 v7	5 3 v10	8 5 v7	7 5 v10	8 0 h10	8 0 h7	9 0 v7	11 0 h6	10 0 h1	10 0 v9	11 0 h2	9 0 v1
							9 0 v4	3 0 v1														
21	0 0074	0 0099	1 06	0	3	4	2 2 h1	1 7 v3	2 0 h3	2 5 h7	3 2 v7	5 3 v10	6 5 h10	6 2 h7	8 9 v7	10 6 h6	10 3 v6	3 3 v1	7 0 h1	8 5 v2	10 8 h2	9 8 v1
							5 8 v4	3 8 v1														
22	0 0025	0 0025	1 57	0	1	1	2 2 h1	1 7 v3	2 0 h3	2 5 h7	3 2 v7	5 3 v10	6 5 h10	6 2 h7	8 9 v7	10 6 h6	10 3 v6	9 3 v1	7 0 h1	8 5 v2	10 8 h2	9 8 v1
							5 8 v4	3 8 v1	2 0 v4	3 0 v1												
23	0 0270	0 0736	1 13	0	11	30	2 2 h1	1 7 v3	2 0 h3	2 5 h7	3 2 v7	5 3 v10	6 5 h10	6 2 h7	8 9 v7	10 5 h6	8 6 h1	9 7 v9	10 6 h2	7 5 v1		
24	0 0442	0 0442	1 27	0	18	18	2 2 h1	1 7 v3	2 0 h3	2 5 h7	3 2 v7	5 3 v10	6 5 h10	6 2 h7	8 9 v7	10 6 h6	8 6 h1	9 7 v9	10 6 h2	7 5 v1	5 8 v4	3 0 v1
25	0 0025	0 0025	0 88	0	1	1	2 2 h1	1 7 v3	2 0 h3	2 5 h7	3 2 v7	5 3 v10	6 5 h10	6 2 h7	8 9 v7	10 5 h6	8 6 h1	9 7 v9	10 6 h2	7 5 v1	2 0 h1	1 0 h4
26	0 0025	0 0025	1 06	0	1	1	2 2 h1	1 7 v3	2 0 h3	2 5 h7	3 2 v7	5 3 v10	6 5 h10	6 2 h7	8 9 v7	10 6 h6	8 6 h1	11 0 v10	11 0 v7	11 0 h4	10 0 v6	7 0 v1
							7 0 h1	10 0 v2	11 0 h2	9 0 v1	6 0 v4	3 0 v1										
27	0 0123	0 0368	1 24	0	5	15	2 2 h1	1 7 v3	2 0 h3	2 5 h7	3 2 v7	5 3 v10	6 5 h10	6 2 h7	8 9 v7	10 2 v9	10 5 h9	8 5 v1				
28	0 0221	0 0246	1 33	0	9	10	2 2 h1	1 7 v3	2 0 h3	2 5 h7	3 2 v7	5 3 v10	6 5 h10	6 2 h7	8 9 v7	10 2 v9	10 5 h9	8 5 v1	5 5 v4	3 4 v1		
29	0 0025	0 0025	1 10	0	1	1	2 2 h1	1 7 v3	2 0 h3	2 5 h7	3 2 v7	5 3 v10	6 5 h10	6 2 h7	8 9 v7	10 2 v9	10 5 h9	8 5 v1	5 5 v4	3 4 v1	5 0 v4	3 0 v1
30	0 0050	0 0074	1 09	0	2	3	2 2 h1	1 7 v3	2 0 h3	2 5 h7	3 2 v7	7 0 h6	5 8 h1	6 0 v9	8 3 h2	5 0 v1						
31	0 0025	0 0025	0 94	0	1	1	2 2 h1	1 7 v3	2 0 h3	2 5 h7	3 2 v7	7 0 h6	5 8 h1	6 0 v9	8 3 h2	5 0 v1	6 0 v4	3 0 v1				
32	0 0025	0 0025	0 98	0	1	1	2 2 h1	1 7 v3	2 0 h3	2 5 h7	3 2 v7	7 0 h6	5 8 h1	5 0 v10	9 0 v7	11 0 h4	7 0 v6	7 0 v1	7 0 h1	7 0 v2	11 0 h2	9 0 v1
							6 0 v4	6 0 v1														
33	0 0760	0 2476	1 09	0	31	101	2 2 h1	1 7 v3	3 7 v7	5 2 v10	9 2 v7	10 6 h4	8 1 h1	9 1 v9	10 8 h2	8 1 v1						
34	0 1618	0 1692	1 28	0	66	69	2 2 h1	1 7 v3	3 7 v7	5 2 v10	9 2 v7	10 6 h4	8 1 h1	9 1 v9	10 8 h2	8 1 v1	5 5 v4	3 4 v1				
35	0 0050	0 0050	1 21	0	2	2	2 2 h1	1 7 v3	3 7 v7	5 2 v10	9 2 v7	10 6 h4	8 1 h1	9 1 v9	10 8 h2	8 1 v1	5 5 v4	3 4 v1	2 0 v4	2 5 v1		
36	0 0025	0 0025	0 59	0	1	1	2 2 h1	1 7 v3	3 7 v7	5 2 v10	9 2 v7	10 6 h4	8 1 h1	9 1 v9	10 8 h2	8 1 v1	5 5 v4	3 4 v1	3 0 h1	3 0 h4		

Digit 3 (continued)

37	0 0025	0 0025	1 24	0	1	1	2 2 h1	1 7 v3	3 7 v7	5 2 v10	9 2 v7	10 6 h4	8 1 h1	9 1 v9	10 8 h2	8 1 v1	6 0 h1	6 0 h4				
38	0 0025	0 0025	1 20	0	1	1	2.2 h1	1 7 v3	3 7 v7	5 2 v10	9 2 v7	10 6 h4	8 1 h1	9 1 v9	11 0 h3	12 0 h7	12 0 h9	12 0 v1	12.0 v4	9 0 v1	6 0 v4	3 0 v1
39	0 0025	0 0025	1 04	0	1	1	2 2 h1	1 7 v3	3 7 v7	5 2 v10	9 2 v7	10 6 h4	8.1 h1	10 0 v10	11 0 v7	10 0 v9	10 0 h2	12.0 v1	12.0 v4	9 0 v1	5 0 v4	3 0 v1
40	0 0050	0 0197	1 15	0	2	8	2 2 h1	1 7 v3	3 7 v7	5 2 v10	9 2 v7	10 6 h4	9 4 v6	7 4 v1	7 3 h1	8 9 v2	10 9 h2	8 7 v1				
41	0 0123	0 0148	1 35	0	5	6	2.2 h1	1 7 v3	3 7 v7	5 2 v10	9 2 v7	10 6 h4	9 4 v6	7 4 v1	7 3 h1	8 9 v2	10 9 h2	8 7 v1	6 4 v4	3 5 v1		
42	0 0025	0 0025	1 49	0	1	1	2 2 h1	1 7 v3	3 7 v7	5 2 v10	9 2 v7	10 6 h4	9 4 v6	7 4 v1	7 3 h1	8 9 v2	10 9 h2	8 7 v1	6 4 v4	3 5 v1	3 0 v4	3 0 v1
43	0 0025	0 0025	0 87	0	1	1	2 2 h1	1 7 v3	3 7 v7	5 2 v10	9 2 v7	10 0 v9	10 0 h3	11 0 h7	12 0 h9	9 0 v1	5 0 v4	3 0 v1				
44	0 0025	0 0025	0 69	0	1	1	2 2 h1	1 7 v3	3 7 v7	5 2 v10	9 2 v7	10 0 v9	12 0 h2	9 0 v1	9 0 h1	9 0 h4	8 0 v4	3 0 v1				
45	0 0025	0 0025	1 19	0	1	1	2 2 h1	1 7 v3	3 7 v7	5 2 v10	9 2 v7	10 0 v10	10 0 h3	8 0 h7	8 0 v7	10 0 v9	10 0 h9	9 0 v1	5 0 v4	3 0 v1		
46	0 0074	0 0295	1 53	0	3	12	2 2 h1	1 7 v3	3 7 v7	5 2 v10	6 0 h3	6 2 h7	8 6 v7	10 7 h6	8 3 h1	9 8 v9	10 9 h2	8 2 v1				
47	0 0221	0 0221	1 24	0	9	9	2 2 h1	1 7 v3	3 7 v7	5 2 v10	6 0 h3	6 2 h7	8 6 v7	10 7 h6	8 3 h1	9 8 v9	10 9 h2	8 2 v1	5 3 v4	2 9 v1		
48	0 0074	0 0172	1 23	0	3	7	2 2 h1	1 7 v3	3 7 v7	5 2 v10	6 0 h3	6 2 h7	8 6 v7	10 3 v9	10 6 h9	8 2 v1						
49	0 0099	0 0099	1 20	0	4	4	2 2 h1	1 7 v3	3 7 v7	5 2 v10	6 0 h3	6 2 h7	8 6 v7	10 3 v9	10 6 h9	8 2 v1	6 5 v4	2 8 v1				
50	0 0025	0 0025	1 21	0	1	1	2 2 h1	1.7 v3	3 7 v7	5 2 v10	6 0 h3	6 2 h7	8 6 v7	7 0 v10	12 0 v7	12 0 h6	8 0 h1	7 0 v9	12 0 h2	12.0 v1	8 0 v4	6 0 v1
51	0 0025	0 0025	0 96	0	1	1	2 2 h1	1 7 v3	3 7 v7	6 8 h4	4 4 h1	7 0 v9	11 0 h2	3 0 v1								
52	0 0050	0 0050	1 09	0	2	2	2 2 h1	1 7 v3	3 7 v7	6 8 h4	4 4 h1	5 2 v10	9 2 v7	10 0 v9	10 0 h2	3 0 v1						
53	0 3025	0 0025	1 23	0	1	1	2 2 h1	1 7 v3	3 7 v7	6 8 h4	4 4 h1	5 2 v10	9 2 v7	10 0 v9	10 0 h3	9 0 h7	9 0 v1	9 0 h9	9 0 v4	3 0 v1		
54	0 0025	0 0050	0 84	0	1	2	2 2 h1	1 7 v3	3 7 v7	6 8 h4	4 4 h1	5 2 v10	9 2 v7	11 0 h4	9 4 h1	8 5 v9	11 0 h2	7 5 v1				
55	0 0025	0 0025	1 44	0	1	1	2.2 h1	1 7 v3	3 7 v7	6 8 h4	4 4 h1	5 2 v10	9 2 v7	11 0 h4	9 4 h1	8 5 v9	11 0 h2	7 5 v1	5 0 v4	2 0 v1		
56	0 0025	0 0025	1 22	0	1	1	2 2 h1	1 7 v3	3 7 v7	6 8 h4	4 4 h1	5 2 v10	9 2 v7	11 0 h4	9 4 h1	10 0 h4	7 0 h1	10 0 v9	11 0 h2	6 0 v1		
57	0 0025	0 0025	0 94	0	1	1	2.2 h1	1 7 v3	3 7 v7	6 8 h4	4 4 h1	5 2 v10	9 2 v7	11 0 h4	7 0 v6	7 0 v1	7 0 h1	7 0 v2	11 0 h2	9 0 v1	6.0 v4	3 0 v1
58	0 0025	0 0123	1 06	0	1	5	2 2 h1	1 7 h3	1 7 v3	2.5 h7	3 4 v7	5 3 v10	9 0 v7	10 5 h6	8 9 h1	9 5 v9	10 6 h2	7 8 v1				
59	0 0099	0 0099	1 22	0	4	4	2 2 h1	1 7 h3	1 7 v3	2 5 h7	3 4 v7	5 3 v10	9 0 v7	10 5 h6	8 9 h1	9 5 v9	10 6 h2	7 8 v1	5 0 v4	3 5 v1		
60	0 0025	0 0025	0 96	0	1	1	2 2 h1	1 7 h3	1 7 v3	2 5 h7	3 4 v7	11 0 h6	7 0 h1	7 0 v9	11 0 h2	3 0 v1						
61	0.0025	0 0025	1 20	0	1	1	2 2 h1	1 7 h4	1.0 v4	1 0 v1	1 0 h1	1 0 v3	5 0 v7	7 0 v10	12 0 v7	11 0 h4	7 0 h1	7 0 v9	12 0 h2	12 0 v1		
62	0 0025	0 0025	1.46	0	1	1	2.2 h1	1 7 h4	1 5 h1	1 0 v3	1 0 h3	2 0 h7	3 0 v7	5 0 v10	9 0 v7	11 0 h6	10 0 h1	10 0 v9	11 0 h2	9 0 v1	6 0 v4	3 0 v1
63	0 0025	0 0025	1 06	0	1	1	2 2 h1	1 7 h4	1 5 h1	1 0 v3	6 0 v7	5 0 v10	5 0 v7	5 0 v10	9 0 v7	11 0 h4	7 0 v6	7 0 v1	7 0 h1	7 0 v2	11 0 h2	9 0 v1
							5 0 v4	6 0 v1	3 0 v4	3 0 v1												
64	0 0025	0 0025	0 97	0	1	1	2 2 h1	0 8 v2	1 5 h3	2.0 v1	1 5 v5	2 5 h7	3 0 v7	4 5 v10	9 0 v7	10 0 v10	11 0 v7	10 0 v9	11 0 h9	3 0 v1		
65	0 0025	0 0025	1 81	0	1	1	2 2 h1	0 8 v2	1 5 h3	2 0 v1	1 5 v5	2.5 h7	3 0 v7	4 5 v10	9 0 v7	11 0 h6	10 0 h1	10 0 v9	11 0 h2	12 0 v1	5 0 v4	3 0 v1
66	0 0025	0 0025	1 81	0	1	1	2.2 h1	0 8 v2	0 5 v1	0 5 h3	0 5 v5	1 0 h7	1 5 v7	2.0 v10	4 5 v7	5 5 h6	5 0 h1	5 0 v9	5 5 h2	6 0 v1	2 5 v4	3 0 v1

Extended sample set size 408

B.5 Feature Strings for Digit 4

J	Term / Ext	Pass / Ext	H / W	Hole	Term	Pass	Feature String															
1	0.0961	0.2577	1.14	0	44	112	2.3 h1	6.0 h4	4.4 v4	2.3 v1	2.0 h1	5.4 v3	7.0 v7	9.7 v9	9.4 h2	5.7 v1						
2	0.0263	0.0306	1.16	0	12	14	2.3 h1	6.0 h4	4.4 v4	2.3 v1	2.0 h1	5.4 v3	7.0 v7	9.7 v9	9.4 h2	5.7 v1	5.9 h1	6.0 h4	5.7 v4	3.5 v1		
3	0.0044	0.0044	1.20	0	2	2	2.3 h1	6.0 h4	4.4 v4	2.3 v1	2.0 h1	5.4 v3	7.0 v7	9.7 v9	9.4 h2	5.7 v1	5.9 h1	6.0 h4	5.7 v4	3.5 v1	5.5 v4	3.0 v1
4	0.1092	0.1201	1.19	0	50	54	2.3 h1	6.0 h4	4.4 v4	2.3 v1	2.0 h1	5.4 v3	7.0 v7	9.7 v9	9.4 h2	5.7 v1	6.7 v4	3.3 v1				
5	0.0066	0.0066	1.13	0	3	3	2.3 h1	6.0 h4	4.4 v4	2.3 v1	2.0 h1	5.4 v3	7.0 v7	9.7 v9	9.4 h2	5.7 v1	6.7 v4	3.3 v1	4.0 v4	3.0 v1		
6	0.0022	0.0022	1.00	0	1	1	2.3 h1	6.0 h4	4.4 v4	2.3 v1	2.0 h1	5.4 v3	7.0 v7	9.7 v9	9.4 h2	5.7 v1	6.7 v4	3.3 v1	6.0 h1	5.0 h4	5.0 v4	3.0 v1
7	0.0044	0.0044	1.22	0	2	2	2.3 h1	6.0 h4	4.4 v4	2.3 v1	2.0 h1	5.4 v3	7.0 v7	9.7 v9	9.4 h2	6.0 h1	6.0 v1	5.0 h4	5.0 v4	3.0 v1		
8	0.0066	0.0066	1.08	0	3	3	2.3 h1	6.0 h4	4.4 v4	2.3 v1	2.0 h1	5.4 v3	7.0 v7	9.7 v9	10.5 h3	8.0 h7	8.7 h9	9.0 v1	7.4 v4	3.0 v1		
9	0.0022	0.0044	1.52	0	1	2	2.3 h1	6.0 h4	4.4 v4	2.3 v1	2.0 h1	5.4 v3	7.0 v7	9.7 v9	10.5 h3	9.5 v1	9.0 v4	5.5 h7	6.0 h9	6.0 v1		
10	0.0022	0.0022	0.75	0	1	1	2.3 h1	6.0 h4	4.4 v4	2.3 v1	2.0 h1	5.4 v3	7.0 v7	9.7 v9	10.5 h3	9.5 v1	9.0 v4	5.5 h7	6.0 h9	6.0 v1	5.0 v4	3.0 v1
11	0.0022	0.0066	1.31	0	1	3	2.3 h1	6.0 h4	4.4 v4	2.3 v1	2.0 h1	5.4 v3	7.0 v7	6.5 v10	8.0 v7	10.0 v9	10.0 h2	6.0 v1				
12	0.0044	0.0044	1.05	0	2	2	2.3 h1	6.0 h4	4.4 v4	2.3 v1	2.0 h1	5.4 v3	7.0 v7	6.5 v10	8.0 v7	10.0 v9	10.0 h2	6.0 v1	5.0 v4	3.0 v1		
13	0.0022	0.0022	1.10	0	1	1	2.3 h1	6.0 h4	4.4 v4	2.3 v1	2.0 h1	5.4 v3	7.0 v7	6.5 v10	7.0 h3	8.0 h7	8.0 v7	10.0 v9	10.0 h9	6.0 v1	6.0 v4	3.0 v1
14	0.0022	0.0022	1.18	0	1	1	2.3 h1	6.0 h4	4.4 v4	2.3 v1	2.0 h1	5.4 v3	7.0 v7	10.0 h2	10.0 v9	6.0 v1	5.0 v4	3.0 v1				
15	0.0699	0.1332	1.20	0	32	59	2.3 h1	6.0 h4	4.4 v4	2.3 v1	2.0 h1	5.4 v3	6.6 h3	6.1 h7	7.3 v7	10.1 v9	10.0 h9	5.1 v1				
16	0.0568	0.0568	1.10	0	26	26	2.3 h1	6.0 h4	4.4 v4	2.3 v1	2.0 h1	5.4 v3	6.6 h3	6.1 h7	7.3 v7	10.1 v9	10.0 h9	5.1 v1	6.3 v4	3.0 v1		
17	0.0022	0.0022	1.11	0	1	1	2.3 h1	6.0 h4	4.4 v4	2.3 v1	2.0 h1	5.4 v3	6.6 h3	6.1 h7	7.3 v7	10.1 v9	10.0 h9	5.1 v1	4.5 h1	4.5 h4	4.0 v4	3.0 v1
18	0.0022	0.0022	1.11	0	1	1	2.3 h1	6.0 h4	4.4 v4	2.3 v1	2.0 h1	5.4 v3	6.6 h3	6.1 h7	7.3 v7	10.1 v9	10.0 h9	9.0 h1	9.0 v1	9.0 h4	8.0 v4	3.0 v1
19	0.0022	0.0066	1.27	0	1	3	2.3 h1	6.0 h4	4.4 v4	2.3 v1	2.0 h1	5.4 v3	6.6 h3	6.1 h7	7.3 v7	10.1 v9	10.2 h10	6.5 h7	8.4 h9	6.7 v1		
20	0.0044	0.0044	0.91	0	2	2	2.3 h1	6.0 h4	4.4 v4	2.3 v1	2.0 h1	5.4 v3	6.6 h3	6.1 h7	7.3 v7	10.1 v9	10.2 h10	6.5 h7	8.4 h9	6.7 v1	5.0 v4	3.0 v1
21	0.0022	0.0022	1.20	0	1	1	2.3 h1	6.0 h4	4.4 v4	2.3 v1	2.0 h1	5.4 v3	6.6 h3	6.1 h7	7.3 v7	10.1 v9	10.2 h10	6.5 h7	6.0 h10	6.0 v1	5.0 v4	3.0 h7
							3.0 h9	3.0 v1														
22	0.0022	0.0022	1.42	0	1	1	2.3 h1	6.0 h4	4.4 v4	2.3 v1	2.0 h1	5.4 v3	6.6 h3	6.1 h7	7.3 v7	10.1 v9	10.2 h10	11.0 v1	11.0 v4	8.0 h7	9.0 h9	9.0 v1
							8.0 v4	3.0 v1														
23	0.0219	0.0372	1.26	0	10	17	2.3 h1	6.0 h4	4.4 v4	2.3 v1	2.0 h1	5.3 v2	10.8 h2	5.5 v1								
24	0.0066	0.0088	1.20	0	3	4	2.3 h1	6.0 h4	4.4 v4	2.3 v1	2.0 h1	5.3 v2	10.8 h2	5.5 v1	7.5 v4	4.3 v1						
25	0.0022	0.0022	1.34	0	1	1	2.3 h1	6.0 h4	4.4 v4	2.3 v1	2.0 h1	5.3 v2	10.8 h2	5.5 v1	7.5 v4	4.3 v1	8.0 v4	3.0 v1				
26	0.0022	0.0066	1.17	0	1	3	2.3 h1	6.0 h4	4.4 v4	2.3 v1	2.0 h1	5.3 v2	10.8 h2	5.5 v1	4.8 h1	9.4 h4						
27	0.0022	0.0044	0.95	0	1	2	2.3 h1	6.0 h4	4.4 v4	2.3 v1	2.0 h1	5.3 v2	10.8 h2	5.5 v1	4.8 h1	9.4 h4	9.5 v4	6.0 v1				
28	0.0022	0.0022	1.57	0	1	1	2.3 h1	6.0 h4	4.4 v4	2.3 v1	2.0 h1	5.3 v2	10.8 h2	5.5 v1	4.8 h1	9.4 h4	9.5 v4	6.0 v1	8.0 v4	3.0 v1		
29	0.0022	0.0022	1.57	0	1	1	2.3 h1	6.0 h4	4.4 v4	2.3 v1	2.0 h1	5.3 v2	10.8 h2	5.5 v1	4.8 h1	5.5 v4	5.5 h4	4.5 v1	4.0 v4	3.0 v1		
30	0.0022	0.0022	0.89	0	1	1	2.3 h1	6.0 h4	4.4 v4	2.3 v1	2.0 h1	5.3 v2	7.0 h3	8.0 h7	11.0 h9	9.0 v1	8.0 v4	3.0 v1				
31	0.0022	0.0022	0.89	0	1	1	2.3 h1	6.0 h4	4.4 v4	2.3 v1	2.0 h1	4.0 h4	4.0 h1	4.0 v3	4.0 h3	5.0 h7	5.0 v7	10.0 v9	10.0 h9	3.0 v1		
32	0.0022	0.0022	1.15	0	1	1	2.3 h1	5.0 h4	4.4 v4	2.3 v1	4.0 v4	2.0 v1	2.0 h1	7.0 v3	7.0 h3	8.0 h7	8.0 v7	11.0 v9	11.0 h9	3.0 v1		
33	0.0022	0.0044	1.34	0	1	2	2.3 h1	6.0 h4	4.4 v4	1.9 h1	1.9 v1	4.8 v3	7.0 h3	6.0 h7	8.0 v7	10.0 v9	11.0 h9	6.0 v1				
34	0.0022	0.0022	0.91	0	1	1	2.3 h1	6.0 h4	4.4 v4	1.9 h1	1.9 v1	4.8 v3	7.0 h3	6.0 h7	8.0 v7	10.0 v9	11.0 h9	6.0 v1	5.0 v4	3.0 v1		
35	0.0066	0.0132	1.09	0	3	6	2.3 h1	6.0 h4	4.4 v4	1.9 h1	1.9 v1	4.8 v3	7.4 v7	10.4 v9	10.4 h2	6.7 v1						
36	0.0044	0.0066	0.95	0	2	3	2.3 h1	6.0 h4	4.4 v4	1.9 h1	1.9 v1	4.8 v3	7.4 v7	10.4 v9	10.4 h2	6.7 v1	10.4 v4	5.0 v1				
37	0.0022	0.0022	1.13	0	1	1	2.3 h1	6.0 h4	4.4 v4	1.9 h1	1.9 v1	4.8 v3	7.4 v7	10.4 v9	10.4 h2	6.7 v1	10.4 v4	5.0 v1	5.0 v4	3.0 v1		
38	0.0066	0.0110	1.62	0	3	5	2.3 h1	6.0 h4	2.0 h1	4.3 v2	11.4 h2	11.0 v1	8.2 v4	6.0 v1								
39	0.0044	0.0044	1.16	0	2	2	2.3 h1	6.0 h4	2.0 h1	4.3 v2	11.4 h2	11.0 v1	8.2 v4	6.0 v1	7.5 v4	3.0 v1						
40	0.0022	0.0022	1.52	0	1	1	2.3 h1	6.0 h4	2.0 h1	4.3 v2	11.4 h2	11.0 v1	11.0 h1	11.0 h4	11.0 v4	12.0 v1	8.0 v4	3.0 v1				
41	0.0022	0.0022	1.00	0	1	1	2.3 h1	6.0 h4	2.0 h1	4.3 v2	7.0 h3	2.8 h7	11.0 h9	10.0 v1	11.0 v4	6.0 v1						
42	0.0022	0.0022	0.91	0	1	1	2.3 h1	6.0 h4	2.0 h1	4.3 v2	7.0 h3	2.8 h7	11.0 h9	10.0 v1	6.0 h1	9.0 h4	8.0 v4	2.0 v1				

Digit 4 (continued)

43	0 0022	0 0022	1 00	0	1	1	2 3 h1	6 0 h4	2.0 h1	4 3 v2	7 0 h3	2 8 h7	5 5 v1	5 5 h9	5 5 v4	6 0 v1						
44	0 0088	0 0241	1 30	0	4	10	2.3 h1	6 0 h4	2.0 h1	4 6 v3	6 7 v7	8 8 v9	8 8 h2	6 0 v1								
45	0 0066	0 0110	1 59	0	3	5	2 3 h1	6 0 h4	2 0 h1	4 6 v3	6 7 v7	8 8 v9	8 8 h2	6 0 v1	7 6 v4	4 3 v1						
46	0 0022	0 0044	2.43	0	1	2	2 3 h1	6 0 h4	2.0 h1	4 6 v3	6 7 v7	8 8 v9	8 8 h2	6 0 v1	7 6 v4	4 3 v1	4 0 v4	3 0 v1				
47	0 0022	0 0022	1 19	0	1	1	2 3 h1	6 0 h4	2 0 h1	4 6 v3	6 7 v7	8 8 v9	8 8 h2	6 0 v1	7 6 v4	4 3 v1	4 0 v4	3 0 v1	3 0 h1	5 0 h4	4 0 v4	2 0 v1
48	0 0022	0 0022	1 53	0	1	1	2 3 h1	6 0 h4	2.0 h1	4 6 v3	6 7 v7	8 8 v9	8 8 h2	6 0 v1	3 0 h1	4 0 h4	4 0 v4	3 0 v1				
49	0 0022	0 0022	1 53	0	1	1	2 3 h1	6 0 h4	2.0 h1	4 6 v3	6 7 v7	8 8 v9	8 8 h2	6 0 h1	6 0 v1	8 0 h4	8 0 v4	3 0 v1				
50	0 0022	0 0022	1 15	0	1	1	2 3 h1	6 0 h4	2 0 h1	4 6 v3	6 7 v7	8 8 v9	6 0 v1	6 0 h2	5 5 v4	3 0 v1						
51	0 0022	0 0022	1 18	0	1	1	2 3 h1	6 0 h4	2 0 h1	4 6 v3	6 7 v7	8 8 v9	10 0 h3	8 0 h7	9 0 h9	9 0 v1	5 0 v4	3 0 v1				
52	0 0088	0 0219	1 18	0	4	10	2 3 h1	6 0 h4	2 0 h1	4 6 v3	5 1 h3	5 4 h7	7 0 v7	10 5 v9	10 9 h9	4 8 v1						
53	0 0110	0 0110	1 10	0	5	5	2 3 h1	6 0 h4	2 0 h1	4 6 v3	5 1 h3	5 4 h7	7 0 v7	10 5 v9	10 9 h9	4 8 v1	5 8 v4	3 0 v1				
54	0 0022	0 0022	0 50	0	1	1	2 3 h1	6 0 h4	2.0 h1	4 6 v3	5 1 h3	5 4 h7	7 0 v7	10 5 v9	10 9 h9	4 8 v1	3 0 h1	8 0 h4	5 0 v4	2 0 v1		
55	0 0022	0 0022	1 00	0	1	1	2 3 h1	6 0 h4	2 0 h1	4 6 v3	5 1 h3	5 4 h7	7 0 h10	5 0 h7	5 0 v7	10 0 v9	10 0 h9	6 0 v1	5 0 v4	3 0 v1		
56	0 0022	0 0066	1 00	0	1	2	2 3 h1	6 0 h4	2 0 h1	4 6 v3	5 1 h3	2 5 v7	2.5 h7	5 3 v9	5 3 h9	3 0 v1						
57	0 0022	0 0022	1 09	0	1	1	2 3 h1	6 0 h4	2 0 h1	4 6 v3	5 1 h3	2 5 v7	2 5 h7	5 3 v9	5 3 h9	3 0 v1	3 0 v4	3 0 v1				
58	0 0132	0 0153	1 45	0	6	7	2 3 h1	6 0 h4	2 0 h1	4 0 v12	11 8 h2	5 6 v12										
59	0 0022	0 0022	1 78	0	1	1	2 3 h1	6 0 h4	2 0 h1	4 0 v12	11 8 h2	5 6 v12	6 0 h1	6 0 h4								
60	0 0022	0 0022	1 49	0	1	1	2 3 h1	6 0 h4	2 0 h1	4 0 h4	4 0 h1	4 0 v2	7 0 h3	4 0 h7	12 0 h10	12 0 v1	8 0 v4	8 0 h7	9 0 h9	9 0 v1		
61	0 0022	0 0022	1 11	0	1	1	2 3 h1	2 0 v1	3 8 v3	3 8 v7	10 4 h2	10 4 v9	3 0 v1	3 u h1	5 0 h4	4 0 v4						
62	0 0044	0 0044	1 49	0	2	2	2 3 h1	2 0 v1	3 8 v3	3 8 v7	10 4 h2	10 4 v9	3 0 h1	3 0 v1	8 0 h4	4 0 v4						
63	0 0066	0 0066	0 94	0	3	3	2 3 h1	2 0 v1	3 8 v3	3 8 v7	7 2 v9	5 4 h2	1 9 v1	1 9 h1	3 3 h4	4 0 v4						
64	0 0044	0 0044	1 12	0	2	2	2 3 h1	2 0 v1	3 8 v3	3 8 v7	7 2 v9	5 4 h2	2 0 h1	2 0 v1	5 0 h4	4 0 v4						
65	0 0022	0 0022	1 50	0	1	1	2 3 h1	2 0 v1	3 8 v3	3 7 h3	3 0 h7	5 4 v7	10 5 v9	5 3 h9	6 0 h1	6 0 v1	6 0 h4	5 0 v4	3 0 v1	3 0 h1	5 0 h4	4 0 v4
66	0 0022	0 0022	1 50	0	1	1	2 3 h1	2 0 v1	3 8 v3	3 7 h3	3 0 h7	5 4 v7	10 5 v9	5 3 h9	4 0 v1	3 0 h1	3 0 h4	2 5 v4	1 5 v1	1 5 h1	2 5 h4	4 0 v4
67	0 0022	0 0022	0 81	0	1	1	2 3 h1	2 0 v1	3 8 v3	3 7 h3	3 u h7	5 4 v7	10 5 v9	5 3 h9	4 0 v1	5 0 v4	3 0 v1	3 0 h1	4 0 h4	4 0 v4		
68	0 0022	0 0066	0 67	0	1	3	2 3 h1	2 0 v1	7 0 h4	3 0 v4	1 5 v1	1 3 h1	4 7 v3	8 0 h3	7 4 h7	7 7 v7	10 0 v9	10 4 h9				
69	0 0044	0 0044	0 89	0	2	2	2 3 h1	2 0 v1	7 0 h4	3 0 v4	1 5 v1	1 3 h1	4 7 v3	8 0 h3	7 4 h7	7 7 v7	10 0 v9	10 4 h9	8 5 v1	6 5 v4		
70	0 0022	0 0022	1 00	0	1	1	2 3 h1	2 0 v1	7 0 h4	3 0 v4	1 5 v1	1 3 h1	4 7 v3	5 3 v7	10 0 h2	10 0 v9	6 0 v1	5 0 v4				
71	0 0110	0 0328	1 13	0	5	12	2 3 h1	2 0 v1	7 0 h4	3 0 v4	1 5 v1	1 3 h1	4 7 v3	5 3 v7	7 8 v9	8 4 h2						
72	0 0088	0 0110	0 94	0	4	5	2 3 h1	2 0 v1	7 0 h4	3 0 v4	1 5 v1	1 3 h1	4 7 v3	5 3 v7	7 8 v9	8 4 h2	6 4 v1	7 0 v4				
73	0 0022	0 0022	1 00	0	1	1	2 3 h1	2 0 v1	7 0 h4	3 0 v4	1 5 v1	1 3 h1	4 7 v3	5 3 v7	7 8 v9	8 4 h2	6 4 v1	7 0 v4	9 0 v1	8 0 v4		
74	0 0022	0 0022	0 91	0	1	1	2 3 h1	2 0 v1	7 0 h4	3 0 v4	1 5 v1	1 3 h1	4 7 v3	5 3 v7	7 8 v9	8 4 h2	6 4 v1	9 0 h1	8 0 h4	8 0 v4		
75	0 0022	0 0022	1 48	0	1	1	2 3 h1	2 0 v1	7 0 h4	3 0 v4	1 5 v1	1 3 h1	4 7 v3	5 3 v7	7 8 v9	8 4 h2	3 0 h1	3 0 v1	4 5 h4	6 0 v4		
76	0 0022	0 0022	0 91	0	1	1	2.3 h1	2 0 v1	7 0 h4	3 0 v4	1 5 v1	1 3 h1	4 7 v3	5 3 v7	4 0 v10	7 0 h3	5 0 h7	5 0 v7	10 0 v9	10 0 h9		
77	0 0022	0 0022	0 96	0	1	1	2 3 h1	2 0 v1	7 0 h4	3 0 v4	1 5 v1	1 3 h1	7 0 v2	8 0 h3	8 0 h7	12 0 h9	12 0 v1	12 0 v4	9 0 v1	9 0 v4		
78	0 0022	0 0066	1 03	0	1	3	2.3 h1	2 0 v1	7 0 h4	3 0 v4	2 7 h1	2 7 v1	5 0 v3	7 0 v7	10 4 v9	10 4 h2						
79	0 0022	0 0022	1 48	0	1	1	2 3 h1	2 0 v1	7 0 h4	3 0 v4	2 7 h1	2 7 v1	5 0 v3	7 0 v7	10 4 v9	10 4 h2	6 0 h1	6 0 v1	9 0 h4	6 0 v4		
80	0 0022	0 0022	0 93	0	1	1	2 3 h1	2 0 v1	7 0 h4	3 0 v4	2 7 h1	2 7 v1	5 0 v3	7 0 v7	10 4 v9	10 4 h2	8 0 v1	5 0 v4				
81	0 0022	0 0022	0 84	0	1	1	2 3 h1	2 0 v1	4 0 v2	11 0 h2	3 0 v1	3 0 h1	8 0 h4	4 0 v4								
82	0 0546	0 0546	1 27	0	25	25	2 3 h1	4 6 v3	6 8 v7	9 7 v9	9 9 h2	5 3 v1	5 5 v4	2 7 v1	2 7 h1	5 5 h4	3 8 v4	1 7 v1				
83	0 0066	0 0066	1 11	0	3	3	2 3 h1	4 6 v3	6 8 v7	9 7 v9	9 9 h2	5 3 v1	5 5 v4	3 0 h1	3 0 v1	6 7 h4	4 0 v4	1 7 v1				
84	0 0088	0 0983	1 50	0	4	43	2 3 h1	4 6 v3	6 8 v7	9 7 v9	9 9 h2	5 3 v1	3 4 h1	6 0 h4								
85	0 0787	0.0808	1 26	0	36	37	2 3 h1	4 6 v3	6 8 v7	9 7 v9	9 9 h2	5 3 v1	3 4 h1	6 0 h4	4 0 v4	1 7 v1						
86	0 0022	0 0022	1 24	0	1	1	2 3 h1	4 6 v3	6 8 v7	9 7 v9	9 9 h2	5 3 v1	3 4 h1	6 0 h4	4 0 v4	1 7 v1	2 0 h1	7.0 h4	4 0 v4	2 0 v1		
87	0 0044	0.0044	1 08	0	2	2	2 3 h1	4 6 v3	6 8 v7	9 7 v9	9 9 h2	5 3 v1	3 4 h1	6 0 h4	4 5 h1	5 0 h4	4 0 v4	2.0 v1				
88	0 0022	0 0022	0.96	0	1	1	2 3 h1	4 6 v3	6 8 v7	9 7 v9	9 9 h2	3 0 h1	3 0 v1	4 0 h4	4 0 v4	2 0 v1						

Digit 4 (continued)

89	0 0044	0 0044	1 20	0	2	2	2.3 h1	4 6 v3	6 8 v7	9 7 v9	8 0 h3	7 7 h7	9 0 h9	9 0 v1	6 5 v4	3 0 v1	3 0 h1	5 0 h4	4 0 v4	1 5 v1		
90	0 0022	0 0022	1 10	0	1	1	2 3 h1	4 6 v3	6 8 v7	9 7 v9	8 0 h3	7 7 h7	12.0 h10	12 0 h7	12.0 h9	12.0 v1	3 0 h1	3 0 v3	9 0 v7	12.0 h4	7.0 v6	4 0 v1
91	0 0022	0 0022	1 03	0	1	1	2 3 h1	4 6 v3	6 8 v7	9 7 v9	8 0 h3	4 0 v1	4 0 v4	4 0 h7	4 5 h9	4 5 v1	2 5 v4	1 5 v1	1 5 h1	2.5 h4	2 0 v4	2 0 v1
92	0 0022	0 0022	1 16	0	1	1	2.3 h1	4 6 v3	6 8 v7	7 0 v10	8 0 v7	10 0 v9	10 0 h2	7 0 v1	3 0 h1	5 0 h4	1 0 v4	1 0 v1				
93	0 0022	0 0022	1 34	0	1	1	2.3 h1	4 6 v3	6 8 v7	7 0 v10	8 0 v7	10.0 v9	10 0 h2	7 0 v1	11 0 v4	6 0 v1	6 0 v4	3 0 v1	3 0 h1	5 0 h4	4 0 v4	2.0 v1
94	0 0022	0 0022	2 31	0	1	1	2.3 h1	4 6 v3	6 8 v7	10 0 h2	10 0 v9	6 0 v1	6 0 h1	8 0 h4	4 0 v4	1 0 v1						
95	0 0022	0 0044	1 44	0	1	2	2.3 h1	4 6 v3	6 8 v7	6 4 h4	1 0 h1	4 0 v9	12.0 h2	9 0 v1								
96	0 0022	0 0022	1 69	0	1	1	2 3 h1	4 6 v3	6 8 v7	6 4 h4	1 0 h1	4 0 v9	12.0 h2	9 0 v1	9 0 v4	9 0 v1						
97	0 0022	0 0022	1.37	0	1	1	2 3 h1	4 6 v3	6 8 v7	6 4 h4	1 0 h1	4 0 v9	7 0 h3	7 0 h7	12.0 h9	12 0 v1						
98	0 0022	0 0022	1 03	0	1	1	2 3 h1	4 6 v3	6 8 v7	10 0 h3	10 0 v9	8 0 v1	8 0 v4	8 0 h7	9 0 h9	9 0 v1	5 0 v4	3 0 v1	3 0 h1	5 0 h4	4 0 v4	2 0 v1
99	0 0394	0 0415	1 06	0	18	19	2 3 h1	4 6 v3	6 3 h3	5 6 h7	6 8 v7	10 1 v9	9 7 h9	4 5 v1	2.9 h1	5 4 h4	4 5 v4	1 9 v1				
100	0 0022	0 0022	1 14	0	1	1	2 3 h1	4 6 v3	6 3 h3	5 6 h7	6 8 v7	10 1 v9	9 7 h9	4 5 v1	2 9 h1	5 4 h4	4 5 v4	1 9 v1	3 0 h1	8 0 h4	4 0 v4	2 0 v1
101	0 0022	0 0022	1 00	0	1	1	2 3 h1	4 6 v3	6 3 h3	5 6 h7	6 8 v7	10 1 v9	9 7 h9	4 5 v1	2.9 h1	5 4 h4	1 0 h1	2 0 h4	2 0 v4	2.0 v1		
102	0 0153	0 0153	1 20	0	7	7	2 3 h1	4 6 v3	6 3 h3	5 6 h7	6 8 v7	10 1 v9	9 7 h9	4 5 v1	7 7 v4	3 0 v1	3 0 h1	6 9 h4	4 9 v4	1 9 v1		
103	0 0022	0 0022	1 11	0	1	1	2 3 h1	4 6 v3	6 3 h3	5 6 h7	6 8 v7	10 1 v9	9 7 h9	4 5 v1	7 7 v4	3 0 v1	3 0 h1	6 9 h4	7 0 h1	7 0 h4	7 0 v4	2 0 v1
104	0 0022	0 0022	1 00	0	1	1	2 3 h1	4 6 v3	6 3 h3	5 6 h7	6 8 v7	10 1 v9	9 7 h9	3 0 h1	3 0 v1	5 0 h4	2 0 h1	4 0 h4	4 0 v4	2.0 v1		
105	0 0044	0 0044	0 98	0	2	2	2.3 h1	4 6 v3	6 3 h3	5 6 h7	6 8 v7	10 1 v9	10 5 h10	7 5 h7	7 5 h9	7 5 v1	6 0 v4	3 0 v1	3 0 h1	4 5 h4	4 0 v4	2 0 v1
106	0 0022	0 0022	1 03	0	1	1	2 3 h1	4 6 v3	6 3 h3	5 6 h7	6 8 v7	10 0 h9	10 0 v9	3 0 v1	3 0 h1	8 0 h4	4 0 v4	2 0 v1				
107	0 0022	0 0022	0 95	0	1	1	2.3 h1	5 1 v2	7 3 h3	6 8 h7	11 8 h9	6 8 v1	6 0 h1	6 7 h4	4 0 v4	2.0 v						
108	0 0022	0 0022	1 38	0	1	1	2 3 h1	5 1 v2	7 3 h3	6 8 h7	11 8 h9	6 8 v1	6 0 h1	6 7 h4	2.5 h1	2 0 v3	9 0 v7	8 0 h4	4 0 v6	1 0 v1		
109	0 0022	0 0022	0 93	0	1	1	2 3 h1	5 1 v2	7 3 h3	6 8 h7	11 8 h9	6 [illegible] v1	6 0 h1	6 7 h4	2 5 h1	4 0 h4	4 0 v4	1 0 v1				
110	0 0022	0 0022	1 34	0	1	1	2 3 h1	5 1 v2	7 3 h3	6 8 h7	11 8 h9	6 8 v1	6 0 v4	6 0 v1	3 0 h1	7 0 h4	4 0 v4	1 0 v1				
111	0 0110	0 0110	1 22	0	5	5	2 3 h1	5 1 v2	11 5 h2	8 5 v1	2.7 h1	8 2 h4	4 6 v4	1 2 v1								
112	0 0022	0 0022	0 95	0	1	1	2.3 h1	5 1 v2	11 5 h2	8 5 v1	2 7 h1	2 0 v3	5 0 v7	8 0 h4	4 0 v6	1 0 v1						
113	0 0022	0 0044	1 48	0	1	2	2 3 h1	5 1 v2	11 5 h2	8 5 v1	9 5 v4	5 8 v1	3 0 h1	5 5 h4								
114	0 0022	0 0022	1 33	0	1	1	2 3 h1	5 1 v2	11 5 h2	8 5 v1	9 5 v4	5 8 v1	3 0 h1	5 5 h4	7 0 v4	1 0 v1						
115	0 0044	0 0044	1 03	0	2	2	2 3 h1	5 1 v2	11 5 h2	8 5 v1	9 5 v4	5 8 v1	8 0 v4	3 0 v1	3 0 h1	7 0 h4	5 5 v4	2 0 v1				
116	0 0088	0 0088	1 23	0	4	4	2 3 h1	4 0 v12	11 6 h2	6 8 v12	3 8 h1	8 3 h4										
117	0 0022	0 0022	1 77	0	1	1	2 3 h1	4 0 v12	11 6 h2	3 0 h1	3 0 v12	5 0 h4										
118	0 0022	0 0022	1 23	0	1	1	2 3 h1	4 0 v12	7 0 h3	5 0 h7	11 0 h9	2 0 v12										
119	0 0022	0 0022	1 06	0	1	1	2 3 h1	4 0 v9	12 0 h2	12.0 v1	9 0 v4	9 0 v1	6 0 h1	9 0 h4	2.0 h1	2.0 v3	8 0 v7	8 0 h4				
120	0 0066	0 0066	0 94	0	3	3	1 4 v1	1 4 h1	2.3 v3	3 7 v7	5 4 v9	5 4 h2	1 5 v1	1 5 h1	2 7 h4	4 0 v4						
121	0 0022	0 0022	1 25	0	1	1	1 4 v1	1 4 h1	2 3 v3	3 7 v7	5 0 h2	5 0 v9	1 5 h1	1 5 v1	4 0 h4	4 0 v4						
122	0 0022	0 0022	1 50	0	1	1	1 4 v1	1 4 h1	2.3 v3	2 8 h3	2.3 h7	4 0 v7	5 3 v9	5 3 h9	3 0 v1	3 0 h1	3 0 h4	2 5 v4	1 5 v1	1 5 h1	2.5 h4	4 0 v4
123	0 0022	0 0022	0 81	0	1	1	1 4 v1	1 4 h1	2.3 v3	2 8 h3	2.3 h7	4 0 v7	5 3 v9	5 3 h9	3 0 v1	2.5 v4	1 5 v1	1 5 h1	2.0 h4	4 0 v4		
124	0 0022	0 0110	0 67	0	1	3	1 4 v1	1 4 h1	3 7 h4	2 1 v4	1 0 v1	0 8 h1	2 8 v3	4 0 h3	3 7 h7	3 9 v7	5 0 v9	6 3 h9				
125	0 0044	0 0044	0 89	0	2	2	1 4 v1	1 4 h1	3 7 h4	2.1 v4	1 0 v1	0 8 h1	2.8 v3	4 0 h3	3 7 h7	3 9 v7	5 0 v9	6 3 h9	4 3 v1	6 5 v4		
126	0 0110	0 0415	1 13	0	5	12	1 4 v1	1 4 h1	3 7 h4	2 1 v4	1 0 v1	0 8 h1	2 8 v3	3 7 v7	5 2 v9	6 6 h2						
127	0 0088	0 0132	0 94	0	4	5	1 4 v1	1 4 h1	3 7 h4	2 1 v4	1 0 v1	0 8 h1	2.8 v3	3 7 v7	5 2 v9	6 6 h2	4 3 v1	5 9 v4				
128	0 0022	0 0022	1 00	0	1	1	1 4 v1	1 4 h1	3 7 h4	2.1 v4	1 0 v1	0 8 h1	2.8 v3	3 7 v7	5 2 v9	6 6 h2	4 3 v1	5 9 v4	4 5 v1	8 0 v4		
129	0 0022	0 0022	0 91	0	1	1	1 4 v1	1 4 h1	3 7 h4	2.1 v4	1 0 v1	0 8 h1	2.8 v3	3 7 v7	5 2 v9	6 6 h2	4 3 v1	4 5 h1	4 0 h4	8 0 v4		
130	0 0022	0 0022	1 48	0	1	1	1 4 v1	1 4 h1	3 7 h4	2 1 v4	1 0 v1	0 8 h1	2 8 v3	3 7 v7	5 2 v9	6 6 h2	3 0 h1	3 0 v1	4 5 h4	6 0 v4		
131	0 0022	0 0022	0 91	0	1	1	1 4 v1	1 4 h1	3 7 h4	2.1 v4	1 0 v1	0 8 h1	2.8 v3	3 7 v7	2.0 v10	3 5 h3	2.5 h7	2.5 v7	5 0 v9	10 0 h9		
132	0 0022	0 0022	0 96	0	1	1	1 4 v1	1 4 h1	3 7 h4	2 1 v4	1 0 v1	0 8 h1	3 5 v2	4 0 h3	4 0 h7	6 0 h9	6 0 v1	6 0 v4	4 5 v1	9 0 v4		
133	0 0022	0 0022	0 84	0	1	1	1 4 v1	1 4 h1	2.0 v2	5 5 h2	1 5 v1	1 5 h1	4 0 h4	4 0 v4								

Digit 4 (continued)

134	0 0044	0 0088	1 08	0	2	4	3 0 h12	5 5 v3	8 0 v7	10 0 v9	10 3 h12	6 0 v1		
135	0 0044	0 0044	1 04	0	2	2	3 0 h12	5 5 v3	8 0 v7	10 0 v9	10 3 h12	6 0 v1	6 5 v4	3 0 v1

Extended sample set size 458

B.6 Feature Strings for Digit 5

j	Term/Ext	Pass/Ext	H/W	Hole	Term	Pass	Feature String															
1	0.0358	0.0454	1.00	0	15	19	2.7 h1	4.1 v3	8.1 v7	9.9 h4	7.5 h1	8.5 v9	10.0 h3	8.3 v1	3.4 v4	2.0 h7	3.0 h9	2.9 v1				
2	0.0048	0.0072	0.77	0	2	3	2.7 h1	4.1 v3	8.1 v7	9.9 h4	7.5 h1	8.5 v9	10.0 h3	8.3 v1	3.4 v4	2.0 h7	3.0 h9	2.9 v1	3.0 h1	3.0 h4		
3	0.0024	0.0024	0.72	0	1	1	2.7 h1	4.1 v3	8.1 v7	9.9 h4	7.5 h1	8.5 v9	10.0 h3	8.3 v1	3.4 v4	2.0 h7	3.0 h9	2.9 v1	3.0 h1	3.0 h4	2.0 v4	2.0 v1
4	0.0024	0.0024	0.82	0	1	1	2.7 h1	4.1 v3	8.1 v7	9.9 h4	7.5 h1	8.5 v9	10.0 h3	8.3 v1	3.4 v4	2.0 h7	3.0 h9	2.9 v1	2.0 v4	3.0 v1		
5	0.0024	0.0024	1.00	0	1	1	2.7 h1	4.1 v3	8.1 v7	9.9 h4	7.5 h1	8.5 v9	10.0 h3	8.3 v1	3.4 v4	2.0 h7	1.5 v1	3.0 h9				
6	0.0024	0.0024	1.06	0	1	1	2.7 h1	4.1 v3	8.1 v7	9.9 h4	7.5 h1	8.5 v9	10.0 h3	8.3 v1	3.4 v4	2.0 v1	2.0 v4	3.0 h7	3.0 h9	3.0 v1		
7	0.3748	0.3891	0.98	0	157	163	2.7 h1	4.1 v3	8.1 v7	9.9 h4	7.5 h1	8.5 v9	10.5 h2	8.6 v1	3.9 v4	3.1 v1						
8	0.0072	0.0096	0.75	0	3	4	2.7 h1	4.1 v3	8.1 v7	9.9 h4	7.5 h1	8.5 v9	10.5 h2	8.6 v1	3.9 v4	3.1 v1	3.0 h1	2.3 h4				
9	0.0024	0.0024	0.70	0	1	1	2.7 h1	4.1 v3	8.1 v7	9.9 h4	7.5 h1	8.5 v9	10.5 h2	8.6 v1	3.9 v4	3.1 v1	3.0 h1	2.3 h4	1.0 v4	2.0 v1		
10	0.0048	0.0048	1.00	0	2	2	2.7 h1	4.1 v3	8.1 v7	9.9 h4	7.5 h1	8.5 v9	10.5 h2	8.6 v1	3.9 v4	3.1 v1	3.5 v4	2.5 v1				
11	0.0096	0.0096	1.15	0	4	4	2.7 h1	4.1 v3	8.1 v7	9.9 h4	7.5 h1	8.5 v9	10.5 h2	8.6 v1	5.5 h1	5.8 h4	3.0 v4	2.8 v1				
12	0.0024	0.0024	1.24	0	1	1	2.7 h1	4.1 v3	8.1 v7	9.9 h4	7.5 h1	8.5 v9	5.5 v1	5.5 h2	5.5 v4	4.5 v1	2.5 v4	3.0 v1				
13	0.0024	0.0048	0.70	0	1	2	2.7 h1	4.1 v3	8.1 v7	9.9 h4	7.5 h1	9.4 h4	8.0 h1	9.0 v9	10.0 h3	8.5 v1	4.0 v4	1.5 h7	3.0 h9	3.0 v1		
14	0.0024	0.0024	1.04	0	1	1	2.7 h1	4.1 v3	8.1 v7	9.9 h4	7.5 h1	9.4 h4	8.0 h1	9.0 v9	10.0 h3	8.5 v1	4.0 v4	1.5 h7	3.0 h9	3.0 v1	3.0 h1	2.0 h4
15	0.0024	0.0024	1.03	0	1	1	2.7 h1	4.1 v3	8.1 v7	9.9 h4	7.5 h1	9.4 h4	8.0 h1	9.0 v9	10.0 h2	9.0 v1	5.0 v4	3.0 v1				
16	0.0072	0.0072	1.18	0	3	3	2.7 h1	4.1 v3	8.1 v7	9.9 h4	7.5 h1	7.3 v10	10.4 v7	10.0 v9	10.4 h2	7.7 v1	4.7 v4	3.0 v1				
17	0.0048	0.0048	1.39	0	2	2	2.7 h1	4.1 v3	8.1 v7	9.9 h4	7.5 h1	7.3 v10	6.0 h3	5.5 h7	9.0 v7	11.0 h6	7.0 h1	8.5 v9	11.5 h2	9.0 v1	3.5 v4	3.0 v1
18	0.0382	0.0430	0.98	0	16	18	2.7 h1	4.1 v3	8.1 v7	9.9 h4	6.6 v6	6.2 v1	6.0 h1	7.7 v2	9.1 h2	7.5 v1	3.8 v4	3.0 v1				
19	0.0024	0.0024	0.77	0	1	1	2.7 h1	4.1 v3	8.1 v7	9.9 h4	6.6 v6	6.2 v1	6.0 h1	7.7 v2	9.1 h2	7.5 v1	3.8 v4	3.0 v1	2.0 v4	2.0 v1		
20	0.0024	0.0024	0.83	0	1	1	2.7 h1	4.1 v3	8.1 v7	9.9 h4	6.6 v6	6.2 v1	6.0 h1	7.7 v2	9.1 h2	7.5 v1	3.8 v4	3.0 v1	3.0 h1	3.0 h4		
21	0.0048	0.0048	0.78	0	2	2	2.7 h1	4.1 v3	8.1 v7	9.9 h4	6.6 v6	6.2 v1	6.0 h1	7.7 v2	10.5 h3	8.5 v1	3.0 v4	2.5 h7	3.0 h9	3.0 v1		
22	0.0072	0.0072	1.09	0	3	3	2.7 h1	4.1 v3	8.1 v7	9.9 h4	6.6 v6	7.0 h1	7.0 v1	10.0 v2	10.4 h2	8.4 v1	4.7 v4	3.0 v1				
23	0.0024	0.0024	0.82	0	1	1	2.7 h1	4.1 v3	8.1 v7	5.9 v10	9.6 v7	10.5 h4	7.0 h1	7.8 v9	10.7 h2	8.0 v1	3.0 h1	2.0 h4				
24	0.0048	0.0048	0.86	0	2	2	2.7 h1	4.1 v3	8.1 v7	5.9 v10	9.6 v7	10.5 h4	7.0 h1	7.8 v9	10.7 h2	8.0 v1	4.5 v4	3.0 v1				
25	0.0024	0.0024	1.00	0	1	1	2.7 h1	4.1 v3	8.1 v7	5.9 v10	9.6 v7	10.5 h4	7.0 h1	7.8 v9	10.0 h3	8.0 v1	5.0 v4	2.0 h7	3.0 h9	3.0 v1		
26	0.0024	0.0024	1.00	0	1	1	2.7 h1	4.1 v3	8.1 v7	5.9 v10	9.6 v7	10.5 h4	10.0 v6	7.0 v1	7.0 h1	10.0 v2	11.0 h2	12.0 v1	4.0 v4	3.0 v1		
27	0.0024	0.0024	0.89	0	1	1	2.7 h1	4.1 v3	8.1 v7	5.9 v10	7.5 h3	5.0 h7	8.5 v7	10.0 h6	10.0 h1	10.0 v9	10.0 h2	9.0 v1	5.0 v4	3.0 v1		
28	0.0024	0.0024	0.95	0	1	1	2.7 h1	4.1 v3	8.1 v7	5.9 v10	7.5 h3	5.0 h7	8.5 v7	10.0 h6	10.0 v6	10.0 v1	7.0 h1	10.0 v2	10.0 h3	6.0 v1	5.0 v4	3.0 h7
							3.0 h9	3.0 v1														
29	0.0096	0.0096	0.83	0	4	4	2.7 h1	4.1 v3	8.1 v7	10.3 v9	10.5 h3	7.8 v1	2.0 v4	1.8 h7	2.8 h9	2.8 v1						
30	0.0024	0.0024	1.14	0	1	1	2.7 h1	4.1 v3	8.1 v7	10.3 v9	10.0 h2	8.3 v1	5.0 h1	4.0 h4	4.0 v4	3.0 v1						
31	0.0048	0.0048	0.82	0	2	2	2.7 h1	4.1 v3	8.1 v7	10.3 v9	10.0 h2	8.3 v1	4.7 v4	3.0 v1	3.0 h1	2.0 h4						
32	0.0024	0.0024	0.75	0	1	1	2.7 h1	4.1 v3	8.1 v7	10.3 v9	10.0 h2	8.3 v1	4.7 v4	3.0 h1	3.0 v1	3.0 h4						
33	0.0168	0.0168	1.21	0	7	7	2.7 h1	4.1 v3	5.4 h3	5.0 h7	8.1 v7	9.4 h6	7.8 h1	8.8 v9	11.2 h3	9.2 v1	3.3 v4	1.9 h7	3.3 h9	3.3 v1		
34	0.0716	0.0812	1.07	0	30	34	2.7 h1	4.1 v3	5.4 h3	5.0 h7	8.1 v7	9.4 h6	7.8 h1	8.8 v9	10.1 h2	8.0 v1	4.3 v4	3.3 v1				
35	0.0048	0.0048	1.06	0	2	2	2.7 h1	4.1 v3	5.4 h3	5.0 h7	8.1 v7	9.4 h6	7.8 h1	8.8 v9	10.1 h2	8.0 v1	4.3 v4	3.3 v1	4.5 v4	2.5 v1		
36	0.0048	0.0048	0.83	0	2	2	2.7 h1	4.1 v3	5.4 h3	5.0 h7	8.1 v7	9.4 h6	7.8 h1	8.8 v9	10.1 h2	8.0 v1	4.3 v4	3.3 v1	3.0 h1	2.5 h4		
37	0.0191	0.0215	1.06	0	8	9	2.7 h1	4.1 v3	5.4 h3	5.0 h7	8.1 v7	9.4 h6	7.8 h1	8.8 v9	10.1 h2	8.0 v1	5.3 h1	5.0 h4	4.1 v4	3.3 v1		
38	0.0024	0.0024	0.50	0	1	1	2.7 h1	4.1 v3	5.4 h3	5.0 h7	8.1 v7	9.4 h6	7.8 h1	8.8 v9	10.1 h2	8.0 v1	5.3 h1	5.0 h4	4.1 v4	3.3 v1	5.0 v4	3.0 v1
39	0.0024	0.0024	1.26	0	1	1	2.7 h1	4.1 v3	5.4 h3	5.0 h7	8.1 v7	9.4 h6	7.8 h1	8.8 v9	10.1 h2	8.0 v1	5.3 h1	4.0 h5	4.0 v4	3.0 h7	6.0 h9	3.0 v1
40	0.0024	0.0024	1.08	0	1	1	2.7 h1	4.1 v3	5.4 h3	5.0 h7	8.1 v7	9.4 h6	7.8 h1	8.8 v9	10.1 h2	9.0 h1	9.0 v1	8.0 h4	5.0 v4	3.0 v1		
41	0.0024	0.0024	0.75	0	1	1	2.7 h1	4.1 v3	5.4 h3	5.0 h7	8.1 v7	9.4 h6	7.8 h1	10.0 h4	7.0 h1	7.0 v9	10.0 h2	10.0 v1	10.0 v4	8.0 v1	8.0 v4	8.0 v1
							5.0 v4	3.0 v1														
42	0.0096	0.0144	0.89	0	4	6	2.7 h1	4.1 v3	5.4 h3	5.0 h7	8.1 v7	9.4 h6	10.0 v6	8.0 v1	5.7 h1	9.5 v2	10.4 h2	7.9 v1	3.9 v4	3.0 v1		

Digit 5 (continued)

43	0 0048	0 0048	1 24	0	2	2	2 7 h1	4 1 v3	5 4 h3	5 0 h7	8 1 v7	9 4 h6	10 0 v6	8 0 v1	6 7 h1	9 5 v2	10 4 h2	7 9 v1	3 9 v4	3 0 v1	3 0 h1	2 5 h4
44	0 0072	0 0072	1 10	0	3	3	2 7 h1	4 1 v3	5 4 h3	5 0 h7	8 1 v7	9 4 h6	5 0 v9	5 0 h1	5 2 h2	4 2 v1	2 4 v4	3 0 v1				
45	0 0335	0 0335	1.19	0	14	14	2.7 h1	4 1 v3	5 4 h3	5 0 h7	8 1 v7	10 1 v9	10 5 h9	8 0 v1	4 5 v4	3 0 v1						
46	0 0120	0 0144	1 23	0	5	6	2 7 h1	4 1 v3	5 4 h3	5 0 h7	8 1 v7	10 1 v9	10 5 h9	8 0 v1	5 7 h1	6 0 h4	4 9 v4	4 0 v1				
47	0 0024	0 0024	1 00	0	1	1	2.7 h1	4 1 v3	5 4 h3	5 0 h7	8 1 v7	10.1 v9	10 5 h9	8 0 v1	5 7 h1	6 0 h4	4 9 v4	4 0 v1	5 0 v4	3 0 v1		
48	0 0024	0 0024	1 13	0	1	1	2 7 h1	4 1 v3	5 4 h3	5 0 h7	8 1 v7	10 1 v9	10 0 h10	8 0 v1	1 0 v4	2 0 h7	3 0 h9	3 0 v1				
49	0 0024	0 0024	0 81	0	1	1	2.7 h1	4 1 v3	5 4 h3	5 0 h7	8 1 v7	8 0 v10	9 0 v7	11 0 h6	7 0 h1	7 0 v9	11 0 h2	9 0 v1	5 0 v4	3 0 v1		
50	0 0024	0 0024	1 72	0	1	1	2 7 h1	4 1 v3	5 4 h3	5 0 h7	8 1 v7	11 0 h8	10 0 v6	10 0 h7	11 0 h9	12 0 v1	7 0 h1	10 0 v2	11 0 h2	9 0 v1	6 0 v4	3 0 v1
51	0 0120	0 0120	1 12	0	5	5	2.7 h1	2 7 v1	3 9 v3	8 9 v7	10 5 h4	8 2 h1	8 9 v9	10 6 h2	8 9 v1	3 8 v4						
52	0 0024	0 0024	0 96	0	1	1	2.7 h1	2 7 v1	3 9 v3	8 9 v7	10 5 h4	10 0 v6	9 0 v1	7 0 h1	10 0 v2	11 0 h2	9 0 v1	2.0 v4				
53	0 0024	0 0024	1 46	0	1	1	2.7 h1	2 7 v1	3 9 v3	5 5 h3	5 0 h7	9 0 v7	11 0 h6	10 0 h1	10 0 v9	11 0 h2	9 0 v1	4 0 v4				
54	0 0024	0 0024	1 55	0	1	1	2 7 h1	2 7 v1	3 9 v3	5 5 h3	5 0 h7	9 0 v7	11 0 h6	10 0 h1	10 0 v9	11 0 h2	9 0 v1	6 0 h1	7 0 h4	4 0 v4		
55	0 0024	0 0024	0 66	0	1	1	2 7 h1	2 7 v1	2 0 h4	1 0 h1	1 0 v3	7 0 v7	10 0 h4	7 0 h1	7 0 v9	10 0 h2	8 0 v1	4 0 v4				
56	0 0144	0 0144	0 84	0	6	6	2 7 h1	3 6 h4	2.7 h1	4 2 v3	7 8 v7	10 0 h4	8 8 h1	9 2 v9	10 2 h2	8 5 v1	4 2 v4	3 0 v1				
57	0 0024	0 0024	0 69	0	1	1	2 7 h1	3 6 h4	2 7 h1	4 2 v3	7 8 v7	10 0 h4	8 8 h1	9 2 v9	10 0 h3	8 0 v1	2 0 v4	2 0 h7	2 0 h9	3 0 v1		
58	0 0024	0 0024	0 90	0	1	1	2 7 h1	3 6 h4	2 7 h1	4 2 v3	7 8 v7	10 0 h4	7 0 v6	7 0 v1	7 0 h1	7 0 v2	11 0 h2	9 0 v1	5 0 v4	3 0 v1		
59	0 0024	0 0024	0 74	0	1	1	2 7 h1	3 6 h4	2.7 h1	4 2 v3	7 8 v7	6 0 v10	7 5 h3	7 0 h7	8 5 v7	10 0 h6	8 5 h1	10 0 v9	10 0 h2	8 0 v1	4 0 v4	3 0 v1
60	0 0024	0 0024	0 86	0	1	1	2 7 h1	3 6 h4	2 7 h1	4 2 v3	7 8 v7	6 0 v10	7 5 h3	7 0 h7	8 5 v7	10 0 h6	8 5 h1	10 0 v9	11 0 h3	9 0 v1	5 0 v4	2 0 h7
							6 0 h9	3 0 v1														
61	0 0048	0 0048	0 68	0	2	2	2 7 h1	3 6 h4	2 7 h1	4 2 v3	7 8 v7	10 0 v9	10 0 h3	8 0 v1	4 5 v4	2 0 h7	2 5 h9	3 0 v1				
62	0 0048	0 0048	0 94	0	2	2	2.7 h1	3 6 h4	2.7 h1	4 2 v3	7 8 v7	10 0 v9	10 5 h2	8 5 v1	4 5 v4	3 0 v1						
63	0 0120	0 0120	1 06	0	5	5	2 7 h1	3 6 h4	2.7 h1	4 2 v3	5 5 h3	5 0 h7	8 4 v7	10 5 h6	7 9 h1	8 8 v9	10 5 h2	8 5 v1	4 6 v4	3 0 v1		
64	0 0048	0 0048	1 01	0	2	2	2.7 h1	3 6 h4	2 7 h1	4 2 v3	5 5 h3	5 0 h7	8 4 v7	10 5 h6	7 9 h1	8 8 v9	10 5 h2	8 5 v1	5 0 h1	6 0 h4	4 0 v4	3 0 v1
65	0 0024	0 0024	0 95	0	1	1	2 7 h1	3 6 h4	2 7 h1	4 2 v3	5 5 h3	5 0 h7	8 4 v7	10 0 v9	10 0 h9	8 0 v1	5 0 v4	3 0 v1				
66	0 0096	0 0096	0 75	0	4	4	2 7 h1	3 6 h4	2 7 h1	7 8 v12	10 3 h2	3 0 v12										
67	0 1218	0 1242	1 11	0	51	52	2 7 h12	3 8 v3	8 4 v7	10 1 v9	10 3 h12	8 9 v1	3 8 v4	3 1 v1								
68	0 0024	0 0024	1 33	0	1	1	2 7 h12	3 8 v3	8 4 v7	10 1 v9	10 3 h12	8 9 v1	3 8 v4	3 1 v1	1 0 v4	3 0 v1						
69	0 0024	0 0024	0 94	0	1	1	2 7 h12	3 8 v3	8 4 v7	4 0 v10	8 0 v7	10 0 v9	10 0 h12	8 0 v1	4 0 v4	3 0 v1						
70	0 0024	0 0024	1 42	0	1	1	2 7 h12	2 0 v1	4 0 v3	9 0 v7	10 0 v9	10 0 h12	9 0 v1	4 0 v4								
71	0 0120	0 0120	1 12	0	5	5	1 4 v1	1 4 h1	2 0 v3	4 5 v7	5 3 h4	4 1 h1	4 5 v9	5 3 h2	4 5 v1	3 8 v4						
72	0 0024	0 0024	0 96	0	1	1	1 4 v1	1 4 h1	2.0 v3	4 5 v7	5 3 h4	5 0 v6	4 5 v1	3 5 h1	5 0 v2	5 5 h2	4 5 v1	2 0 v4				
73	0 0024	0 0024	1 46	0	1	1	1 4 v1	1 4 h1	2.0 v3	2 8 h3	2.5 h7	4 5 v7	5 5 h6	5 0 h1	5 0 v9	5 5 h2	4 5 v1	4 0 v4				
74	0 0024	0 0024	1 55	0	1	1	1 4 v1	1 4 h1	2.0 v3	2 8 h3	2.5 h7	4 5 v7	5 5 h6	5 0 h1	5 0 v9	5 5 h2	4 5 v1	3 0 h1	3 5 h4	4 0 v4		
75	0 0024	0 0024	0 66	0	1	1	1 4 v1	1 4 h1	1 0 h4	0 5 h1	0 5 v3	3 5 v7	5 0 h4	3 5 h1	3 5 v9	5 0 h2	4 0 v1	4 0 v4				
76	0 0024	0 0024	1 42	0	1	1	1 4 v1	1 0 h12	2.0 v3	4 5 v7	5 0 v9	5 0 h12	4 5 v1	4 0 v4								

Extended sample set size 419

B.7 Feature Strings for Digit 6

j	Term/Ext	Pass/Ext	H/W	Hole	Term	Pass	Feature String															
1	0.0737	0.0737	1.36	1	31	31	2.4 h1	7.9 h11	8.6 v11	9.6 v11	9.8 h11	9.7 v2	10.0 h2	8.7 v1	7.1 h1	8.7 h4	7.8 v4	2.8 v1				
2	0.0167	0.0167	1.29	1	7	7	2.4 h1	7.9 h11	8.6 v11	9.6 v11	9.8 h11	9.7 v2	10.0 h2	8.7 v1	11.2 v4	8.2 v1	7.5 h1	9.9 h4	8.8 v4	2.8 v1		
3	0.0072	0.0072	1.45	1	3	3	2.4 h1	7.9 h11	8.6 v11	9.6 v11	9.8 h11	9.7 v2	10.0 h3	10.0 h7	11.0 h9	9.0 v1	8.7 h1	7.7 h4	7.4 v4	3.0 v1		
4	0.0024	0.0024	1.55	1	1	1	2.4 h1	7.9 h11	8.6 v11	9.6 v11	9.8 h11	10.0 h2	10.0 v2	6.0 v1	6.0 h1	7.0 h4	7.0 v4	2.0 v1				
5	0.0784	0.0784	1.35	1	33	33	2.4 h1	7.9 h11	8.6 v11	9.6 v11	9.5 v2	10.7 h11	10.4 h2	9.0 v1	7.2 h1	9.1 h4	7.8 v4	2.7 v1				
6	0.0024	0.0024	1.70	1	1	1	2.4 h1	7.9 h11	8.6 v11	9.6 v11	9.5 v2	10.7 h11	10.4 h2	9.0 v1	7.2 h1	8.0 v3	11.0 v7	10.0 h4	7.0 v6	2.0 v1		
7	0.0024	0.0024	1.65	1	1	1	2.4 h1	7.9 h11	8.6 v11	9.6 v11	9.5 v2	10.7 h11	10.4 h2	9.0 v1	7.2 h1	10.0 h5	7.0 v4	2.0 h7	6.0 h9	3.0 v1		
8	0.0072	0.0072	1.23	1	3	3	2.4 h1	7.9 h11	8.6 v11	9.6 v11	9.5 v2	10.7 h11	10.4 h2	9.0 v1	11.3 v4	9.0 v1	5.8 h1	8.7 h4	7.0 v4	2.7 v1		
9	0.0024	0.0024	1.44	1	1	1	2.4 h1	7.9 h11	8.6 v11	9.6 v11	9.5 v2	10.7 h11	10.4 h2	9.0 v1	11.3 v4	9.0 v1	5.8 h1	8.0 v3	11.0 v7	10.0 h4	7.0 v6	3.0 v1
10	0.0024	0.0024	1.29	1	1	1	2.4 h1	7.9 h11	8.6 v11	9.6 v11	9.5 v2	10.7 h11	10.0 h3	10.0 h7	11.0 h9	6.0 v1	6.0 h1	7.0 h4	7.0 v4	2.0 v1		
11	0.2613	0.2661	1.41	1	110	112	2.4 h1	7.9 h11	8.6 v11	8.5 v2	9.8 v11	10.4 h11	10.7 h2	9.0 v1	7.6 h1	9.2 h4	7.6 v4	2.8 v1				
12	0.0024	0.0024	1.92	1	1	1	2.4 h1	7.9 h11	8.6 v11	8.5 v2	9.8 v11	10.4 h11	10.7 h2	9.0 v1	7.6 h1	9.2 h4	7.6 v4	2.8 v1	6.0 h1	10.0 h4	7.0 v4	2.0 v1
13	0.0024	0.0024	1.03	1	1	1	2.4 h1	7.9 h11	8.6 v11	8.5 v2	9.8 v11	10.4 h11	10.7 h2	9.0 v1	7.6 h1	9.2 h4	7.6 v4	2.8 v1	7.0 v4	2.0 v1		
14	0.0024	0.0024	1.21	1	1	1	2.4 h1	7.9 h11	8.6 v11	8.5 v2	9.8 v11	10.4 h11	10.7 h2	9.0 v1	7.6 h1	10.0 h5	10.0 v4	3.0 h7	3.0 h9	3.0 v1		
15	0.0096	0.0096	1.57	1	4	4	2.4 h1	7.9 h11	8.6 v11	8.5 v2	9.8 v11	10.4 h11	10.7 h2	9.0 v1	7.6 h1	9.3 v3	10.3 v7	10.5 h4	7.0 v6	2.3 v1		
16	0.0333	0.0357	1.42	1	14	15	2.4 h1	7.9 h11	8.6 v11	8.5 v2	9.8 v11	10.4 h11	10.7 h2	9.0 v1	10.7 v4	8.0 v1	6.4 h1	9.4 h4	6.8 v4	2.0 v1		
17	0.0024	0.0024	1.20	1	1	1	2.4 h1	7.9 h11	8.6 v11	8.5 v2	9.8 v11	10.4 h11	10.7 h2	9.0 v1	10.7 v4	8.0 v1	6.4 h1	9.4 h4	6.8 v4	2.0 v1	2.0 v4	2.0 v1
18	0.0024	0.0024	1.19	1	1	1	2.4 h1	7.9 h11	8.6 v11	8.5 v2	9.8 v11	10.4 h11	5.0 h3	5.5 v1	4.0 v5	3.0 h7	1.0 v7	6.0 h9	6.0 v9	3.0 v1		
19	0.0024	0.0024	1.19	1	1	1	2.4 h1	7.9 h11	8.6 v11	8.5 v2	9.8 v11	10.4 h11	5.0 h3	5.5 v1	4.0 v5	3.0 h7	1.0 v7	3.0 v9	3.0 h9	3.0 v1		
20	0.0024	0.0024	1.57	1	1	1	2.4 h1	7.9 h11	8.6 v11	8.5 v2	9.8 v11	10.4 h11	5.0 v1	5.0 h2	5.0 v4	4.5 v1	3.0 h1	5.0 h4	3.5 v4	2.0 v1		
21	0.0024	0.0024	0.78	1	1	1	2.4 h1	7.9 h11	8.6 v11	8.5 v2	9.8 v11	10.0 h3	11.0 h11	10.0 h7	11.0 h9	8.0 v1	8.0 v4	3.0 v1				
22	0.0048	0.0048	1.05	1	2	2	2.4 h1	7.9 h11	8.6 v11	7.0 v12	8.0 v11	11.0 h11	11.0 h2	7.5 v12	4.0 h1	10.0 h4						
23	0.0024	0.0024	1.62	1	1	1	2.4 h1	7.9 h11	8.6 v11	7.0 v3	11.0 v11	11.0 h11	10.0 v7	10.0 v9	11.0 h2	9.0 v1	9.0 h1	10.0 h4	7.0 v4	3.0 v1		
24	0.0832	0.0832	1.44	1	35	35	2.4 h1	7.9 h11	7.6 v2	9.4 v11	9.8 v11	10.9 h11	10.8 h2	9.5 v1	7.9 h1	8.8 h4	7.3 v4	2.5 v1				
25	0.0048	0.0048	1.20	1	2	2	2.4 h1	7.9 h11	7.6 v2	9.4 v11	9.8 v11	10.9 h11	10.8 h2	9.5 v1	7.9 h1	10.0 h5	7.0 v4	4.0 h7	4.0 h9	3.0 v1		
26	0.0024	0.0024	1.13	1	1	1	2.4 h1	7.9 h11	7.6 v2	9.4 v11	9.8 v11	10.9 h11	10.8 h2	9.5 v1	7.9 h1	8.0 v3	9.0 v7	11.0 h4	4.0 v6	1.0 v1		
27	0.0024	0.0024	1.38	1	1	1	2.4 h1	7.9 h11	7.6 v2	9.4 v11	9.8 v11	10.9 h11	10.8 h2	9.5 v1	11.5 v4	10.5 v1	7.0 h1	11.0 h4				
28	0.0024	0.0024	1.31	1	1	1	2.4 h1	7.9 h11	7.6 v2	9.4 v11	9.8 v11	10.9 h11	10.8 h2	9.5 v1	11.5 v4	10.5 v1	7.0 h1	8.0 v3	11.0 v7	10.0 h4	7.0 v6	3.0 v1
29	0.0072	0.0072	1.46	1	3	3	2.4 h1	7.1 v2	8.1 h11	9.1 v11	9.4 v11	10.9 h11	11.2 h2	10.3 v1	7.6 h1	9.0 v3	11.4 v7	11.0 h4	5.0 v6	2.0 v1		
30	0.0547	0.0547	1.44	1	23	23	2.4 h1	7.1 v2	8.1 h11	9.1 v11	9.4 v11	10.9 h11	11.2 h2	10.3 v1	7.6 h1	8.9 h4	6.1 v4	2.4 v1				
31	0.0048	0.0048	1.48	1	2	2	2.4 h1	7.1 v2	8.1 h11	9.1 v11	9.4 v11	10.9 h11	11.2 h2	10.3 v1	7.6 h1	7.0 h5	7.0 v4	4.0 h7	4.0 h9	3.0 v1		
32	0.0096	0.0167	1.31	1	4	7	2.4 h1	7.1 v2	8.1 h11	9.1 v11	9.4 v11	10.9 h11	11.2 h2	10.3 v1	11.6 v4	9.0 v1	5.8 h1	8.6 h4				
33	0.0072	0.0072	1.36	1	3	3	2.4 h1	7.1 v2	8.1 h11	9.1 v11	9.4 v11	10.9 h11	11.2 h2	10.3 v1	11.6 v4	9.0 v1	5.8 h1	8.6 h4	4.0 v4	2.4 v1		
34	0.0024	0.0024	1.45	1	1	1	2.4 h1	7.1 v2	8.1 h11	9.1 v11	9.4 v11	10.9 h11	11.0 v1	11.0 h2	8.0 v4	6.0 v1	3.0 h1	8.0 h4				
35	0.0024	0.0024	2.25	1	1	1	2.4 h1	7.1 v2	8.1 h11	9.1 v11	9.4 v11	10.9 h11	11.0 h3	11.0 h7	11.0 h9	9.0 v1	9.0 h1	10.0 h4	7.0 v4	3.0 v1		
36	0.0024	0.0024	1.75	1	1	1	2.4 h1	7.1 v2	8.1 h11	9.1 v11	9.4 v11	10.0 h2	3.4 h11	12.0 h1	12.0 v1	10.0 h5	10.0 v5	9.0 h7	9.0 v7	12.0 v9	12.0 h9	9.0 v1
							9.0 h1	10.0 h4	7.0 v4	3.0 v1												
37	0.0024	0.0024	1.75	1	1	1	2.4 h1	7.1 v2	8.1 h11	9.1 v11	9.4 v11	10.0 h2	3.4 h11	6.0 v1	6.0 h1	5.0 h5	5.0 v5	4.5 h7	4.5 v7	6.0 v9	6.0 h9	4.5 v1
							4.5 h1	5.0 h4	3.5 v4	3.0 v1												
38	0.0024	0.0024	1.47	0	1	1	2.4 h1	7.1 v2	9.6 h2	9.0 h1	9.0 v1	11.0 h5	10.0 v4	6.0 h7	9.0 h9	6.0 v1	6.0 h1	7.0 h4	7.0 v4	2.0 v1		
39	0.0024	0.0096	1.20	0	1	3	2.4 h1	7.1 v2	9.6 h2	9.0 v1	7.5 h1	8.0 h5	6.3 v4	5.0 h7	6.5 h9	5.3 v1	4.3 h1	6.3 h4				
40	0.0048	0.0048	1.39	0	2	2	2.4 h1	7.1 v2	9.6 h2	9.0 v1	7.5 h1	8.0 h5	6.3 v4	5.0 h7	6.5 h9	5.3 v1	4.3 h1	6.3 h4	4.7 v4	2.5 v1		
41	0.0214	0.0309	1.34	0	9	13	2.4 h1	7.1 v2	9.6 h2	9.0 v1	7.5 h1	9.3 h4	8.1 v4	4.4 v1								
42	0.0024	0.0072	1.19	0	1	3	2.4 h1	7.1 v2	9.6 h2	9.0 v1	7.5 h1	9.3 h4	8.1 v4	4.4 v1	7.0 h1	9.4 h4						

Digit 6 (continued)

43	0 0048	0 0048	1 56	0	2	2	2 4 h1	7 1 v2	9 6 h2	9 0 v1	7 5 h1	9 3 h4	8 1 v4	4 4 v1	7 0 h1	9 4 h4	8 5 v4	3 0 v1				
44	0 0024	0 0024	1 45	0	1	1	2 4 h1	7 1 v2	9 6 h2	9 0 v1	7 5 h1	9 3 h4	8 1 v4	4 4 v1	7 0 h1	10 0 h5	7 0 v4	3 0 h7	3 0 h9	3 0 v1		
45	0 0167	0 0214	1 32	0	7	8	2 4 h1	7 1 v2	9 6 h2	9 0 v1	7 5 h1	7 5 v3	7 0 h3	7 1 h7	7 9 v7	9 4 h6	7 6 v6	3 3 v1				
46	0 0024	0 0024	1 34	0	1	1	2 4 h1	7 1 v2	9 6 h2	9 0 v1	7 5 h1	7 5 v3	7 0 h3	7 1 h7	7 9 v7	9 4 h6	7 6 v6	3 3 v1	3 5 v4	3 0 v1		
47	0 0024	0 0024	1 26	0	1	1	2 4 h1	7 1 v2	9 6 h2	9 0 v1	7 5 h1	7 5 v3	7 0 h3	7 1 h7	7 9 v7	5 0 h8	5 0 v8	3 0 h7	1 0 v7	3 0 h9	3 0 v9	3 0 v1
48	0 0024	0 0024	1 26	0	1	1	2 4 h1	7 1 v2	9 6 h2	9 0 v1	7 5 h1	7 5 v3	7 0 h3	7 1 h7	7 9 v7	5 0 h8	5 0 v8	3 0 h7	1 0 v7	1 5 v9	1 5 h9	3 0 v1
49	0 0072	0 0191	1 36	0	3	8	2 4 h1	7 1 v2	9 6 h2	9 0 v1	7 5 h1	7 5 v3	9 5 v7	10 9 h4	8 7 v6	6 0 v1						
50	0 0048	0 0048	1 82	0	2	2	2 4 h1	7 1 v2	9 6 h2	9 0 v1	7 5 h1	7 5 v3	9 5 v7	10 9 h4	8 7 v6	6 0 v1	8 0 h1	10 0 h4	8 5 v4	3 0 v1		
51	0 0072	0 0072	1 52	0	3	3	2 4 h1	7 1 v2	9 6 h2	9 0 v1	7 5 h1	7 5 v3	9 5 v7	10 9 h4	8 7 v6	6 0 v1	7 0 v4	3 0 v1				
52	0 0048	0 0048	1 25	0	2	2	2 4 h1	7 1 v2	9 6 h2	9 0 v1	7 5 h1	9 0 v2	9 5 h3	9 5 v1	9 5 v5	8 5 h7	9 0 v7	10 5 h6	8 5 v6	3 0 v1		
53	0 0024	0 0024	1 34	0	1	1	2 4 h1	7 1 v2	9 6 h2	9 0 v1	7 5 h1	8 0 h3	8 0 v3	9 0 h7	9 0 v7	11 0 h6	10 0 v6	8 0 v1	7 0 v4	3 0 v1		
54	0 0024	0 0024	1 35	0	1	1	2 4 h1	7 1 v2	9 6 h2	9 0 v1	11 0 v4	9 0 v1	9 0 h1	9 5 h4	8 0 v4	7 5 v1	9 0 h1	11 0 h4	4 0 v4	1 0 v1		
55	0 0024	0 0024	1 34	0	1	1	2 4 h1	7 1 v2	9 6 h2	9 0 v1	11 0 v4	9 0 v1	9 0 h1	9 5 h4	8 0 v4	7 5 v1	5 0 v4	3 0 v1				
56	0 0024	0 0024	1 15	0	1	1	2 4 h1	7 1 v2	3 7 v1	11 0 h2	11 0 v4	9 0 v1	3 0 h1	6 0 v3	9 0 v7	11 0 h4	6 0 v6	2 0 v1	2 0 h1	10 0 h4		
57	0 0024	0 0024	1 15	0	1	1	2 4 h1	7 1 v2	3 7 v1	5 5 v4	5 5 h2	4 5 v1	1 5 h1	3 0 v3	4 5 v7	5 5 h4	4 0 v6	1 0 v1	1 0 h1	10 0 h4		
58	0 0024	0 0024	1 11	0	1	1	2 4 h1	7 1 v2	11 0 h3	12 0 h7	12 0 h9	9 0 v1	6 0 h1	9 0 h4	6 0 h1	8 0 v2	8 0 h3	8 0 v1	8 0 v5	6 0 h7	9 0 h10	9 0 h7
							9 0 v7	9 0 v10	9 0 v7	11 0 h6	8 0 v6	8 0 v1										
59	0 0024	0 0024	1 43	0	1	1	2 4 h1	2 1 v1	8 2 v2	11 0 h2	10 0 v1	8 4 h1	10 0 h4	7 0 v4								
60	0 0024	0 0048	1 42	0	1	2	2 4 h1	2 1 v1	8 2 v2	11 0 h2	10 0 v1	8 4 h1	9 5 v3	10 5 v7	11 0 h4	7 0 v6						
61	0 0024	0 0024	1 42	0	1	1	2 4 h1	2 1 v1	8 2 v2	11 0 h2	10 0 v1	8 4 h1	9 5 v3	10 5 v7	11 0 h4	7 0 v6	8 0 v1	7 0 v4				
62	0 0024	0 0024	1 46	1	1	1	2 4 h1	2 1 v1	8 2 v2	9 0 h11	9 0 v11	11 0 v11	11 0 h11	11 0 h2	9 0 v1	9 0 h1	7 0 h4	7 0 v4				
63	0 0024	0 0024	1 77	0	1	1	2 4 h1	2 1 v1	8 2 v2	11 0 h3	12 0 v1	8 0 v4	8 0 h7	9 0 h9	9 0 v1	7 0 v4						
64	0 0024	0 0024	0 95	1	1	1	2 4 h1	2 1 v1	6 8 h11	7 0 v2	9 0 v11	11 0 v11	11 0 h11	11 0 h2	9 0 v1	6 0 h1	11 0 h4	4 0 v4				
65	0 0048	0 0048	1 30	1	2	2	2 4 h1	2 1 v1	6 8 h11	8 2 v11	8 7 v11	8 5 v2	10 0 h11	11 0 h2	9 0 v1	6 0 h1	9 0 h4	7 0 v4				
66	0 0024	0 0024	1 35	1	1	1	2 4 h1	2 1 v1	6 8 h11	8 2 v11	8 7 v11	9 0 h11	10 0 v2	11 0 h2	9 0 v1	6 0 h1	11 0 h4	7 0 v4				
67	0 0096	0 0096	1 18	1	4	4	2 4 h1	2 1 v1	6 8 h11	8 2 v11	7 8 v2	10 3 v11	11 0 h11	10 8 h2	7 5 v1	6 0 h1	10 3 h4	7 0 v4				
68	0 0096	0 0096	1 31	1	4	4	2 4 h1	4 3 v3	3 9 v7	7 3 h11	8 0 v11	8 5 v9	10 5 v11	10 8 h11	10 5 h2	8 0 v1	7 0 h1	10 0 h4	8 5 v4	2 8 v1		
69	0 0024	0 0024	1 37	1	1	1	2 4 h1	4 3 v3	3 9 v7	7 3 h11	8 0 v11	10 0 v11	10 0 h11	10 0 v9	10 0 h2	9 0 v1	8 0 h1	10 0 h4	10 0 v4	3 0 v1		
70	0 0024	0 0024	1 37	1	1	1	2 4 h1	4 3 v3	3 9 v7	8 0 v11	7 0 v11	7 0 h11	10 0 v9	10 0 h11	10 0 h2	9 0 v1	6 0 h1	8 0 h4	5 0 v4	3 0 v1		
71	0 0024	0 0024	1 38	0	1	1	2 4 h1	4 3 v3	3 9 v7	7 0 v9	11 0 h2	10 5 v1	9 0 h1	11 0 h5	11 0 v5	6 0 h7	9 0 v7	9 0 v9	9 0 h9	9 0 v1	6 0 h1	10 0 h4
							7 0 v4	2 0 v1														
72	0 0024	0 0024	1 43	0	1	1	2 4 h1	4 3 v3	3 9 v7	7 0 v9	11 0 h2	10 5 v1	9 0 h1	7 0 v3	8 0 h3	9 0 h7	9 0 v7	10 0 h6	7 0 v6	3 0 v1		
73	0 0024	0 0024	1 75	1	1	1	2 4 h1	4 3 v3	3 9 v7	4 0 v10	7 0 v7	8 0 h11	9 0 v11	10 0 v9	10 0 v11	11 0 h11	10 0 h2	9 0 v1	8 0 h1	7 0 h4	7 0 v4	3 0 v1
74	0 0024	0 0024	0 97	1	1	1	2 4 h1	4 3 v3	8 0 h11	11 0 v11	10 0 v7	10 0 v11	10 0 v9	11 0 h11	11 0 h2	12 0 v1	8 0 h1	10 0 h4	7 0 v4	2 0 v1		
75	0 0024	0 0024	0 98	1	1	1	2 4 h1	1 0 v9	5 0 h11	5 0 v11	9 0 v11	12 0 h11	12.0 h2	12 0 v1	5 0 h1	5 0 v3	12 0 v7	12 0 h4				
76	0 0119	0 0119	1 15	1	5	5	2 4 h1	3 4 v12	6 3 h11	8 6 v11	8 9 v11	11 2 h11	11 0 h2	9 0 v12	5 8 h1	8 9 h4						
77	0 0119	0 0119	1 26	1	5	5	2 8 h12	7 5 v2	8 0 h11	9 6 v11	10 0 v11	11 2 h11	11 0 h12	11 2 v1	6 3 v4	2 8 v1						
78	0 0024	0 0024	1 47	0	1	1	2 8 h12	7 5 v2	11 0 h12	9 0 v1	8 0 v4	3 0 v1										
79	0 0214	0 0214	1 47	1	9	9	2 8 h12	8 0 h11	8 7 v11	9 1 v11	9 4 v2	10 5 h11	10 6 h12	8 7 v1	6 0 v4	3 0 v1						
80	0 0119	0 0119	1 46	1	5	5	2 8 h12	8 0 h11	8 7 v11	9 1 v11	10 0 h11	10 0 v2	10 2 h12	8 6 v1	6 6 v4	3 0 v1						
81	0 0214	0 0214	1 46	1	9	9	2 8 h12	8 0 h11	8 7 v11	8 7 v2	9 4 v11	10 8 h11	10 9 h12	9 4 v1	5 6 v4	2 8 v1						
82	0 0119	0 0119	1 17	1	5	5	2 8 h12	8 0 h11	7 6 v2	8 5 v11	9 5 v11	11 2 h11	10 5 h12	9 6 v1	6 6 v4	3 0 v1						
83	0 0024	0 0024	1 50	1	1	1	2 8 h12	3 0 v1	11 0 h11	10 0 v2	11 0 v11	10 0 v11	11 0 h11	11 0 h12	12 0 v1	7 0 v4						
84	0 0024	0 0024	1 19	1	1	1	2 8 h12	1 0 v12	8 0 h11	8 0 v11	12 0 v11	12 0 h11	12 0 h12	12 0 v12								
85	0 0024	0 0072	1 42	0	1	2	1 1 v1	1 0 h1	3 9 v2	5 5 h2	5 3 v1	4 0 h1	4 8 v3	5 3 v7	5 5 h4	4 7 v6						
86	0 0024	0 0024	1 42	0	1	1	1 1 v1	1 0 h1	3 9 v2	5 5 h2	5 3 v1	4 0 h1	4 8 v3	5 3 v7	5 5 h4	4 7 v6	4 0 v1	7 0 v4				

Digit 6 (continued)

87	0 0024	0 0024	1 46	1	1	1	1 1 v1	1 0 h1	3 9 v2	4 5 h11	4 5 v11	5 5 v11	5 5 h11	5 5 h2	4 5 v1	4 5 h1	3 5 h4	7 0 v4
88	0 0024	0 0024	1 77	0	1	1	1 1 v1	1 0 h1	3 9 v2	5 5 h3	6 0 v1	4 0 v4	4 0 h7	4 5 h9	4 5 v1	7 0 v4		
89	0 0024	0 0024	0 95	1	1	1	1 1 v1	1 0 h1	3 4 h11	3 5 v2	4 5 v11	5 5 v11	5.5 h11	5 5 h2	4.5 v1	3 0 h1	5 5 h4	4 0 v4
90	0 0048	0 0040	1 30	1	2	2	1 1 v1	1 0 h1	3 4 h11	4 1 v11	4 4 v11	4 3 v2	5 0 h11	5 5 h2	4 5 v1	3 0 h1	4 5 h4	7 0 v4
91	0 0024	0 0024	1 35	1	1	1	1.1 v1	1 0 h1	3 4 h11	4 1 v11	4 4 v11	4 5 h11	5 0 v2	5 5 h2	4 5 v1	3 0 h1	5 5 h4	7 0 v4
92	0 0096	0 0096	1 18	1	4	4	1 1 v1	1 0 h1	3 4 h11	4 1 v11	3 9 v2	5 2 v11	5 5 h11	5 4 h2	3 8 v1	3 0 h1	5 2 h4	7 0 v4
93	0 0024	0 0024	1 50	1	1	1	1 1 v1	1 5 h12	5 5 h11	5 0 v2	5 5 v11	5 0 v11	5 5 h11	5 5 h12	6 0 v1	7 0 v4		

Extended sample set size 421

B.8 Feature Strings for Digit 7

j	Term/Ext	Pass/Ext	H/W	Hole	Term	Pass	Feature String															
1	0.1768	0.1884	1.30	0	76	81	1.8 h12	1.2 v3	4.0 v7	10.1 v9	10.3 h12	3.9 v1										
2	0.0117	0.0117	1.44	0	5	5	1.8 h12	1.2 v3	4.0 v7	10.1 v9	10.3 h12	3.9 v1	10.6 v4	3.7 v1								
3	0.0024	0.0024	1.21	0	1	1	1.8 h12	1.2 v3	4.0 v7	10.0 h12	10.0 v9	3.0 v1										
4	0.0047	0.0047	1.40	0	2	2	1.8 h12	1.0 v12	12.0 h12	4.5 v12												
5	0.5070	0.6233	1.34	0	218	227	2.2 h1	2.5 v3	2.8 h3	2.5 h7	3.1 v7	9.5 v9	9.7 h9	3.6 v1								
6	0.0442	0.0745	1.36	0	19	32	2.2 h1	2.5 v3	2.8 h3	2.5 h7	3.1 v7	9.5 v9	9.7 h9	3.6 v1	3.0 h1	2.1 h4						
7	0.0303	0.0303	1.25	0	13	13	2.2 h1	2.5 v3	2.8 h3	2.5 h7	3.1 v7	9.5 v9	9.7 h9	3.6 v1	3.0 h1	2.1 h4	1.6 v4	1.8 v1				
8	0.0326	0.0396	1.41	0	14	17	2.2 h1	2.5 v3	2.8 h3	2.5 h7	3.1 v7	9.5 v9	9.7 h9	3.6 v1	9.4 v4	3.0 v1						
9	0.0070	0.0070	1.30	0	3	3	2.2 h1	2.5 v3	2.8 h3	2.5 h7	3.1 v7	9.5 v9	9.7 h9	3.6 v1	9.4 v4	3.0 v1	3.0 h1	2.7 h4				
10	0.0024	0.0024	1.54	0	1	1	2.2 h1	2.5 v3	2.8 h3	2.5 h7	3.1 v7	9.5 v9	10.0 h10	8.0 h7	8.0 h10	6.0 h7	6.0 h9	3.0 v1				
11	0.0024	0.0024	1.56	0	1	1	2.2 h1	2.5 v3	2.8 h3	2.5 h7	3.1 v7	9.5 v9	6.0 v1	6.0 h9	4.5 v4	1.5 v1	1.5 h1	3.0 h4				
12	0.0187	0.0187	1.47	0	8	8	2.2 h1	2.5 v3	2.8 h3	2.5 h7	3.1 v7	10.0 h9	10.0 v9	3.0 v1								
13	0.0024	0.0070	1.21	0	1	3	2.2 h1	2.5 v3	2.8 h3	2.5 h7	3.1 v7	4.6 v10	8.0 v7	10.4 v9	10.7 h9	7.7 v1						
14	0.0047	0.0047	1.40	0	[illegible]	2	2.2 h1	2.5 v3	2.8 h3	2.5 h7	3.1 v7	4.6 v10	8.0 v7	10.4 v9	10.7 h9	7.7 v1	9.5 v4	3.0 v1				
15	0.0024	0.0024	1.12	0	1	1	2.2 h1	2.5 v3	2.8 h3	2.5 h7	3.1 v7	4.6 v10	2.0 h10	1.0 h7	1.5 v7	5.0 v9	5.0 h9	3.0 v1				
16	0.0024	0.0024	1.21	0	1	1	2.2 h1	2.5 v3	2.8 h3	2.5 h7	3.1 v7	10.0 h6	7.0 h1	10.0 v9	10.0 h2	3.0 v1						
17	0.0024	0.0024	1.23	0	1	1	2.2 h1	2.5 v3	2.8 h3	2.5 h7	3.5 h10	4.5 h7	6.0 v7	11.0 v9	11.5 h9	7.5 v1	9.0 v4	3.0 v1	3.0 h1	2.0 h4		
18	0.0024	0.0024	1.28	0	1	1	2.2 h1	2.5 v3	2.8 h3	2.5 h7	3.5 h10	4.5 h7	6.0 v7	11.0 v9	11.5 h9	7.5 v1	3.0 h1	2.0 h4				
19	0.0163	0.0163	1.27	0	7	7	2.2 h1	2.5 v3	3.3 v7	10.2 v9	10.2 h2	3.0 v1	3.0 h1	2.6 h4								
20	0.0047	0.0047	1.46	0	2	2	2.2 h1	2.5 v3	3.3 v7	4.0 v10	4.0 h3	2.5 h7	4.5 v7	10.5 v9	10.5 h9	4.5 v1						
21	0.0024	0.0024	1.18	0	1	1	2.2 h1	2.5 v3	3.3 v7	2.0 h4	2.0 h1	4.0 v10	4.0 h3	2.0 h7	3.0 v7	10.0 v9	10.0 h9	3.0 v1				
22	0.0349	0.0349	1.15	0	15	15	2.2 h1	1.7 h4	1.1 h1	2.6 v3	2.5 h3	2.7 h7	3.4 v7	10.4 v9	10.5 h9	3.0 v1						
23	0.0024	0.0024	1.14	0	1	1	2.2 h1	1.7 h4	1.1 h1	2.6 v3	2.5 h3	2.7 h7	4.0 h10	2.0 h7	3.0 v7	10.0 v9	10.0 h9	3.0 v1				
24	0.0047	0.0047	1.33	0	2	2	2.2 h1	1.7 h4	1.1 h1	2.6 v3	2.5 h3	2.0 v7	2.0 h7	5.0 v9	5.0 h9	3.0 v1						
25	0.0094	0.0094	1.19	0	4	4	2.2 h1	1.7 h4	1.1 h1	2.6 v3	3.5 v7	10.5 v9	10.5 h2	3.0 v1								
26	0.0024	0.0024	1.50	0	1	1	2.2 h1	1.7 h4	1.1 h1	4.0 v2	4.0 h3	4.0 v1	4.0 v5	1.0 h7	2.0 h10	3.0 h7	3.0 v7	5.0 v10	6.0 v7	11.0 v9	11.0 h9	3.0 v1
27	0.0024	0.0024	1.23	0	1	1	2.2 h1	1.7 h4	0.8 v4	1.0 v1	0.8 h1	1.5 v3	2.3 h3	3.0 h7	1.9 v7	10.0 h9	10.0 v9	3.0 v1				
28	0.0047	0.0070	1.18	0	2	3	2.2 h1	1.7 h4	0.8 v4	1.0 v1	0.8 h1	1.5 v3	2.3 h3	3.0 h7	1.9 v7	7.8 v9	7.8 h9	5.7 v1				
29	0.0024	0.0024	0.81	0	1	1	2.2 h1	1.7 h4	0.8 v4	1.0 v1	0.8 h1	1.5 v3	2.3 h3	3.0 h7	1.9 v7	7.8 v9	7.8 h9	5.7 v1	10.0 v4	3.0 v1		
30	0.0070	0.0070	1.61	0	3	3	2.2 h1	1.0 v12	3.0 h3	1.4 h7	12.0 h9	4.0 v12										
31	0.0280	0.0303	1.34	0	12	13	2.2 h1	2.1 h3	2.1 v3	2.8 h7	2.5 v7	9.5 v9	9.6 h9	3.7 v1								
32	0.0024	0.0024	1.18	0	1	1	2.2 h1	2.1 h3	2.1 v3	2.8 h7	2.5 v7	9.5 v9	9.6 h9	3.7 v1	11.0 v4	3.0 v1						
33	0.0024	0.0024	1.40	0	1	1	2.2 h1	2.1 h3	2.1 v3	2.8 h7	2.5 v7	10.0 h9	10.0 v9	3.0 v1								
34	0.0024	0.0024	1.12	0	1	1	2.2 h1	2.1 h3	2.1 v3	2.8 h7	2.5 v7	4.0 v10	4.0 h10	2.0 h7	3.0 v7	10.0 v9	10.0 h9	3.0 v1				
35	0.0047	0.0047	1.15	0	2	2	2.2 h1	3.0 v2	4.4 h3	4.4 v1	1.5 v5	3.0 h7	3.0 v7	10.0 v9	10.0 h9	3.0 v1						
36	0.0024	0.0024	1.45	0	1	1	2.2 h1	3.0 v2	4.4 h3	4.4 v1	1.0 v4	2.0 h7	12.0 h9	6.0 v1								
37	0.0024	0.0024	1.10	0	1	1	2.2 h1	2.5 v1	2.0 h4	2.0 h1	4.0 v3	4.0 h3	2.0 h7	3.0 v7	10.0 v9	10.0 h9						
38	0.0024	0.0024	1.33	0	1	1	2.2 h1	2.5 v1	1.0 v3	1.0 h3	3.0 h7	3.0 v7	10.0 v9	10.0 h9	3.0 v1	3.0 h1	2.0 h4	1.0 v4				
39	0.0024	0.0024	1.10	0	1	1	1.3 v1	1.3 h1	1.0 h4	1.0 h1	2.0 v3	2.0 h3	1.0 h7	1.5 v7	5.0 v9	10.0 h9						
40	0.0024	0.0024	1.33	0	1	1	1.3 v1	1.3 h1	0.5 v3	0.5 h3	1.5 h7	1.5 v7	5.0 v9	5.0 h9	1.5 v1	1.5 h1	1.0 h4	1.0 v4				

Extended sample set size 430

B.9 Feature Strings for Digit 8

i	Term/Ext	Pass/Ext	H/W	Hole	Term	Pass	Feature String															
1	0 0024	0 0308	1 28	1	1	12	2 2 h1	2 3 v3	4 7 v7	6 5 h11	7 7 v11	9 0 v9	9 5 v11	10 0 h11	9 8 h2	8 6 v1	5 0 v4	2 8 v1	2 8 h1	4 9 h4		
2	0 0261	0 0261	1 45	1	11	11	2 2 h1	2.3 v3	4 7 v7	6 5 h11	7 7 v11	9 0 v9	9 5 v11	10 0 h11	9 8 h2	8 6 v1	5 0 v4	2.8 v1	2.8 h1	4 9 h4	1 5 v4	2.6 v1
3	0 0024	0 0024	1 61	1	1	1	2.2 h1	2 3 v3	4 7 v7	6 5 h11	7 7 v11	9 0 v9	9 5 v11	10 0 h11	9 8 h2	8 6 v1	5.0 v4	2 8 v1	2.8 h1	5 0 h5	1 0 v4	2.0 h7
							3 0 h9	3 0 v1														
4	0 0024	0 0024	1 38	1	1	1	2 2 h1	2 3 v3	4 7 v7	6 5 h11	7 7 v11	9 0 v9	9 5 v11	10 0 h11	9 8 h2	8 6 v1	5 0 v4	2 8 v1	2.8 h1	3 0 v3	3 0 v7	5 0 h4
							2 0 v6	2.0 v1														
5	0 0024	0 0024	0 94	1	1	1	2 2 h1	2 3 v3	4 7 v7	6 5 h11	7 7 v11	9 0 v9	9 5 v11	10 0 h11	9 8 h2	8 6 v1	5 0 v4	3 0 h1	3 0 v1	5 0 h4	4 0 v4	2.0 v1
6	0 0024	0 0024	1 63	1	1	1	2 2 h1	2 3 v3	4 7 v7	6 5 h11	7 7 v11	9 0 v9	9 5 v11	10 0 h11	9 8 h2	8 6 v1	5 3 h1	8 0 h5	4 0 v5	3 0 h7	3 0 v7	5 0 v9
							5 0 h9	3 0 v1														
7	0 0024	0 0024	1 34	1	1	1	2 2 h1	2 3 v3	4 7 v7	6 5 h11	7 7 v11	9 0 v9	9 5 v11	10 0 h11	9 8 h2	8 6 v1	5 3 h1	8 0 h5	5 0 v4	3 0 h7	3 0 h9	3 0 v1
8	0 0048	0 0048	1 29	1	2	2	2 2 h1	2 3 v3	4 7 v7	6 5 h11	7 7 v11	9 0 v9	9 5 v11	10 0 h11	9 8 h2	8 6 v1	5 3 h1	5 0 h4	1 5 v4	2.5 v1		
9	0 0024	0 0024	1 21	1	1	1	2 2 h1	2 3 v3	4 7 v7	6 5 h11	7 7 v11	9 0 v9	9 5 v11	10 0 h11	11 0 h3	9 0 v1	4 0 v4	3 0 h7	3 0 h9	3 0 v1		
10	0 0095	0 0119	1 30	1	4	5	2 2 h1	2 3 v3	4 7 v7	6 5 h11	7 7 v11	8 8 v11	10 0 h11	10 0 v9	10 0 h2	4 0 v1	3 6 h1	5 6 h4	4 0 v4	3 0 v1		
11	0 0024	0 0024	0 89	1	1	1	2 2 h1	2 3 v3	4 7 v7	6 5 h11	7 7 v11	8 8 v11	10 0 h11	10 0 v9	10 0 h2	4 0 v1	3 6 h1	5 6 h4	4 0 v4	3 0 v1	3 0 h1	8 0 h5
							5 0 v4	3 0 h7	3 J h9	3 0 v1												
12	0 0024	0 0024	1 13	1	1	1	2 2 h1	2 3 v3	4 7 v7	6 5 h11	7 7 v11	8 8 v11	10 0 h11	10 0 v9	10 0 h2	4 0 v1	3 6 h1	2 0 v3	6 0 v7	5 0 h4	5 0 v6	2 0 v1
13	0 0024	0 0024	1 09	1	1	1	2 2 h1	2.3 v3	4 7 v7	6 5 h11	7 7 v11	8 8 v11	10 0 h11	10 0 v9	10 0 h2	4 0 v1	3 6 h1	5 0 h5	2 0 v4	2 0 h7	3 0 h9	3 0 v1
14	0 0024	0 0284	1 20	1	1	12	2 2 h1	2 3 v3	4 7 v7	6 5 h11	7 7 v11	8 8 v11	9 0 v9	9 7 h11	8 9 h2	6 0 v1	3 6 h1	5 3 h4				
15	0 0261	0 0261	1 43	1	11	11	2 2 h1	2 3 v3	4 7 v7	6 5 h11	7 7 v11	8 8 v11	9 0 v9	9 7 h11	8 9 h2	6 0 v1	3 6 h1	5 3 h4	2 0 v4	2 8 v1		
16	0 0095	0 0095	1 47	1	4	4	2.2 h1	2 3 v3	4 7 v7	6 5 h11	7 7 v11	8 8 v11	9 0 v9	9 7 h11	8 9 h2	6 0 v1	3 6 h1	3 3 h5	1 5 v4	1 0 h7	1 9 h9	2.8 v1
17	0 0024	0 0024	1 56	1	1	1	2 2 h1	2 3 v3	4 7 v7	6 5 h11	7 7 v11	8 8 v11	9 0 v9	9 7 h11	8 9 h2	6 0 v1	3 6 h1	3 3 h5	1 5 v4	1 0 h7	1 5 v1	3 0 h9
18	0 0024	0 0024	1 39	1	1	1	2.2 h1	2 3 v3	4 7 v7	6 5 h11	7 7 v11	8 8 v11	9 0 v9	9 7 h11	8 9 h2	6 0 v1	6 3 v4	3 5 v1	3 5 h1	5 0 h5	1 0 v4	2 0 h7
							3 0 h9	3 0 v1														
19	0 0308	0 0308	1 52	1	13	13	2.2 h1	2 3 v3	4 7 v7	6 5 h11	7 7 v11	8 8 v11	9 0 v9	9 7 h11	8 9 h2	6 0 v1	6 3 v4	3 5 v1	3 5 h1	5 0 h4	1 8 v4	2 5 v1
20	0 0048	0 0048	1 47	1	2	2	2 2 h1	2 3 v3	4 7 v7	6 5 h11	7 7 v11	8 8 v11	9 0 v9	9 7 h11	8 9 h2	6 0 h1	6 0 v1	6 5 h5	2.5 v4	2 0 h7	2 5 h9	2 5 v1
21	0 0024	0 0024	1 44	1	1	1	2 2 h1	2 3 v3	4 7 v7	6 5 h11	7 7 v11	8 9 v11	9 0 v9	9 7 h11	5 0 h3	3 0 v1	2 0 v4	0 7 h7	3 0 h9	3 0 v1		
22	0 0024	0 0024	1 44	1	1	1	2 2 h1	2 3 v3	4 7 v7	6 5 h11	7 7 v11	8 8 v11	9 0 v9	9 7 h11	5 0 h3	3 0 v1	2 0 v4	0 7 h7	1 5 v1	3 0 h9		
23	0 0024	0 0024	1 44	1	1	1	2 2 h1	2 3 v3	4 7 v7	6 5 h11	7 7 v11	8 8 v11	9 0 v9	11 0 h2	11 0 h11	8 0 v1	5 0 v4	3 0 v1	3 0 h1	5 0 h4	1 0 v4	2.0 v1
24	0 0024	0 0024	1 62	1	1	1	2 2 h1	2 3 v3	4 7 v7	6 5 h11	7 4 v9	7 4 v11	9 9 v11	10 9 h11	11 3 h2	10 8 v1	5 8 v4	4 3 v1	4 2 h1	7 0 h5	4 0 v4	2.0 h7
							2 0 h9	2 0 v1														
25	0 0142	0 0142	1 51	1	6	6	2 2 h1	2 3 v3	4 7 v7	6 5 h11	7 4 v9	7 4 v11	9 9 v11	10 9 h11	11 3 h2	10 8 v1	5 8 v4	4 3 v1	4 2 h1	4 5 h4	3 0 v4	2.2 v1
26	0 0024	0 0024	1 05	1	1	1	2 2 h1	2 3 v3	4 7 v7	6 5 h11	7 4 v9	7 4 v11	9 9 v11	10 9 h11	11 3 h2	10 8 v1	6 0 h1	5 0 h5	2.0 v4	2 0 h7	3 0 h9	3 0 v1
2"	0 0024	0 0024	1 42	1	1	1	2 2 h1	2 3 v3	4 7 v7	6 5 h11	7 4 v9	7 4 v11	9 9 v11	10 9 h11	10 0 h3	5 0 h7	6 0 h9	6 0 v1	5 0 v4	3 0 v1		
28	0 0024	0 0024	1 62	1	1	1	2 2 h1	2.3 v3	4 7 v7	8 0 h5	4 0 v6	3 5 h7	5 5 h9	5 5 v1	2.0 h1	7 0 h11	7 0 v2	7 0 v11	11 0 v11	11 0 h11	11 0 h2	11 0 v1
							8 0 v4	3 0 v1														
29	0 0024	0 0024	1 62	1	1	1	2 2 h1	2 3 v3	4 7 v7	8 0 h5	4 0 v6	3 5 h7	5 5 h9	5 5 v1	2.0 h1	4 0 v3	8 0 v7	8 0 h11	11 0 v11	10 0 v11	11 0 h11	10 0 v9
							11 0 h2	12.0 v1	8 0 v4	3 0 v1												
30	0 0024	0 0024	1 10	1	1	1	2 2 h1	2 3 v3	4 7 v7	5 7 h4	3 7 v6	2.9 v1	2.5 h1	7 0 v2	8 0 h11	8 0 v11	12.0 v11	12.0 h11	12.0 h2	12 0 v1	5 0 v4	2.0 v1
31	0 0024	0 0024	0 94	0	1	1	2.2 h1	2 3 v3	4 7 v7	5 7 h4	3 7 v6	2.9 v1	2.5 h1	7 0 v2	10 0 h2	3 0 v1	3 0 h1	3 0 v3	3 0 v7	5 0 h4	4 0 v6	2.0 v1
32	0 0024	0 0024	1 53	1	1	1	2.2 h1	2 3 v3	4 7 v7	5 7 h4	3 7 v6	2.9 v1	2.5 h1	3 5 v3	5 5 v7	7 0 h11	7 0 v9	7 0 v11	8 0 v11	11 0 h11	11 0 h2	3 0 v1
							5 0 v4	3 0 v1														
33	0 0024	0 0024	2 44	1	1	1	2 2 h1	2.3 v3	4 7 v7	5 7 h4	3 7 v6	2.9 v1	2.5 h1	3 5 v3	5 5 v7	7 0 h11	8 7 v11	10 0 v11	10 0 v3	11 0 h11	1' 0 h2	3 0 v1
34	0 0048	0 0048	1 11	1	2	2	2.2 h1	2 3 v3	4 7 v7	5 7 h4	3 7 v6	2.9 v1	2.5 h1	3 5 v3	5 5 v7	7 0 h11	8 7 v11	10 0 v9	10 5 v11	10 5 h11	10 5 h2	10 0 v1
							6 5 v4	3 0 v1														

Digit 8 (continued)

35	0 0024	0 0024	1 57	1	1	1	2 2 h1	2 3 v3	4 7 v7	5 7 h4	3 7 v6	2.9 v1	2 5 h1	3 5 v3	5 0 h11	8 0 v7	9 0 v11	10 0 v9	10 0 v11	11 0 h11	10 0 h2	3 0 v1
36	0 0024	0 0024	1 37	0	1	1	2 2 h1	2.3 v3	4 7 v7	5 7 h4	3 7 v6	2 9 v1	2.5 h1	3 5 v3	10 0 h3	7 0 h7	8 0 v7	10 0 v9	10 0 h9	3 0 v1		
37	0 0024	0 0024	1 04	1	1	1	2 2 h1	2 3 v3	4 7 v7	5 7 h4	3 7 v6	2.9 v1	2.5 h1	6 7 h11	7 4 v11	10 0 v2	10 0 v11	10 0 h11	10 0 h2	11 0 v1	7 0 v4	3 0 v1
38	0 0024	0 0024	0 97	1	1	1	2 2 h1	2.3 v3	4 7 v7	5 7 h4	3 7 v6	2 9 v1	2.5 h1	6 7 h11	7 4 v11	7 5 v11	10 0 h11	10 0 v2	10 0 h2	3 0 v1		
39	0 0024	0 0024	1 10	1	1	1	2 2 h1	2 3 v3	4 7 v7	5 7 h4	3 7 v6	2 9 v1	2.5 h1	6 7 h11	7 4 v11	7 5 v11	10 0 v2	11 0 h11	11 0 h2	3 0 v1			
40	0 0024	0 0048	1 54	1	1	2	2 2 h1	2 3 v3	4 7 v7	5 7 h4	2 0 h1	7 0 h11	8 7 v11	10 5 v11	10 0 v9	10 5 h11	10 5 h2	7 0 v1				
41	0 0024	0 0024	1 35	1	1	1	2.2 h1	2 3 v3	4 7 v7	5 7 h4	2 0 h1	7 0 h11	8 7 v11	10 5 v11	10 0 v9	10 5 h11	10 5 h2	7 0 v1	8 0 v4	3 0 v1			
42	0 0024	0 0024	1 48	1	1	1	2 2 h1	2 3 v3	4 7 v7	5 7 h4	2 0 h1	7 0 h11	8 7 v11	7 0 v9	7 0 v11	10 0 h11	11 0 h2	3 0 v1					
43	0 0048	0 0048	2 28	1	2	2	2 2 h1	2 3 v3	4 7 v7	5 7 h4	2 0 h1	3 2 v10	6 5 v7	7 8 h11	8 5 v9	9 0 v11	10 5 v11	10 5 h11	10 5 h2	11 5 v1	8 0 v4	3 0 v1
44	0 0071	0 0071	1 82	1	3	3	2 2 h1	2 3 v3	4 7 v7	5 7 h4	2 0 h1	3 2 v10	6 5 v7	7 8 h11	8 0 v11	10 0 v11	10 0 v9	10 4 h11	10 0 h2	3 0 v1		
45	0 0024	0 0024	1 25	0	1	1	2 2 h1	2 3 v3	4 7 v7	5 7 h4	2 0 h1	3 2 v10	6 5 v7	10 0 v9	10 0 h2	8 0 v1	8 0 h1	10 0 h4	10 0 v4	3 0 v1		
46	0 0024	0 0024	1 46	0	1	1	2 2 h1	2 3 v3	4 7 v7	5 3 v10	4 7 h3	4 4 h7	6 4 v7	6 7 h6	5 7 h1	5 7 v9	6 7 h2	5 0 v1	8 0 v4	6 0 v1	6 0 h1	8 0 h4
							4 0 v4	3 0 v1														
47	0 0024	0 0024	1 43	0	1	1	2 2 h1	2 3 v3	4 7 v7	5 3 v10	4 7 h3	4 4 h7	6 4 v7	6 7 h6	5 7 h1	5 7 v9	6 7 h2	5 0 v1	1 5 h1	2 5 h4	0 5 v4	2 0 v1
48	0 0024	0 0024	1 22	0	1	1	2 2 h1	2 3 v3	4 7 v7	5 3 v10	8 0 v7	10 0 h4	10 0 v6	7 0 v1	7 0 h1	10 0 v2	10 0 h2	3 0 v1	3 0 h1	5 0 h4	5 0 v4	3 0 v1
49	0 0024	0 0024	0 98	0	1	1	2 2 h1	2.3 v3	4 7 v7	10 0 v9	3 4 h2	8 0 h1	8 0 v1	10 0 h5	10 0 v4	5 0 h7	8 0 h9	3 0 v1	3 0 h1	5 0 h4	2 0 v4	3 0 v1
50	0 0024	0 0024	0 98	0	1	1	2 2 h1	2 3 v3	4 7 v7	10 0 v9	3 4 h2	4 0 v1	4 0 h1	5 0 h5	5 0 v4	2 5 h7	4 0 h9	1 5 v1	1 5 h1	2 5 h4	1 0 v4	3 0 v1
51	0 0024	0 0024	1 43	0	1	1	2 2 h1	2 3 v3	4 7 v7	7 0 h3	7 0 v10	5 0 h7	8 0 v7	10 0 h6	7 0 h1	7 0 v9	10 0 h2	3 0 v1	3 0 h1	5 0 h4	1 0 v4	2 0 v1
52	0 0024	0 0024	1 46	2	1	1	2 2 h1	2 3 v3	2 5 h11	3 0 v11	2 4 v11	3 7 h11	3 4 v7	7 0 h22	11 0 v22	10 0 v22	10 0 v9	11 0 h22	11 0 h2	3 0 v1	3 0 h1	4 0 h4
53	0 0024	0 0024	1 41	1	1	1	2 2 h1	2.3 v3	2 5 h11	3 0 v11	2 4 v11	3 7 h11	3 4 v7	4 0 h4	0 5 v6	0 5 v1	0 5 h1	2 0 v3	8 0 v7	3 4 v9	11 0 h3	11 0 v1
							8 0 v5	8 0 h7	12 0 v7	11 0 v9	12 0 h9	12 0 v1	8 0 v4	3 0 v1								
54	0 0024	0 0024	1 41	1	1	1	2 2 h1	2 3 v3	2 5 h11	3 0 v11	2 4 v11	3 7 h11	3 4 v7	4 0 h4	0 5 v6	0 5 v1	0 5 h1	2 0 v3	8 0 v7	3 4 v9	5 5 v1	5 5 h3
							4 0 v5	4 0 h7	6 0 v7	5 5 v9	6 0 h9	6 0 v1	4 0 v4	3 0 v1								
55	0 0024	0 0024	1 58	1	1	1	2 2 h1	2 3 v3	2 5 h11	5 0 v7	9 0 v11	10 0 v9	11 0 v11	11 0 h11	11 0 h2	9 0 v1	5 0 h1	5 0 h4	4 0 v4	3 0 v1		
56	0 0024	0 0048	1 64	1	1	2	2 2 h1	2 3 v3	2 3 h3	2 2 h7	3 9 v7	6 3 h6	2 9 h1	4 0 v10	6 8 v7	8 0 h11	8 8 v11	10 5 v9	10 5 v11	11 0 h11	11 0 h2	7 5 v1
57	0 0024	0 0024	1 20	1	1	1	2 2 h1	2 3 v3	2 3 h3	2 2 h7	3 9 v7	6 3 h6	2 9 h1	4 0 v10	6 8 v7	8 0 h11	8 8 v11	10 5 v9	10 5 v11	11 0 h11	11 0 h2	7 5 v1
							6 0 v4	3 0 v1														
58	0 0048	0 0048	1 78	1	2	2	2 2 h1	2 3 v3	2 3 h3	2 2 h7	3 9 v7	6 3 h6	2 9 h1	4 0 v10	6 8 v7	8 0 h11	8 8 v11	9 0 v11	10 0 v9	11 0 h11	11 0 h2	9 5 v1
							6 5 v4	3 0 v1														
59	0 0024	0 0024	1 25	1	1	1	2.2 h1	2 3 v3	2 3 h3	2 2 h7	3 9 v7	6.3 h6	2 9 h1	7 5 h11	8 0 v11	10 0 v11	10 0 v9	10 0 h11	10 0 h3	5 0 h7	5 0 h9	3 0 v1
60	0 0024	0 0024	1 08	1	1	1	2 2 h1	2 3 v3	2 3 h3	2 2 h7	3 9 v7	6 3 h6	2 9 h1	7 5 h11	10 0 v9	10 0 v11	11 0 v11	10 0 h11	10 0 h2	11 0 v1	8 0 v4	3 0 v1
61	0 0024	0 0024	1 53	1	1	1	2 2 h1	2 3 v3	2 3 h3	2 2 h7	3 9 v7	6 3 h6	4 0 v6	5 0 v1	4 0 h1	4 0 v3	8 0 v7	8 0 h11	11 0 v11	10 0 v9	10 0 v11	11 0 h11
							11 0 h2	12 0 v1	8 0 v4	3 0 v1												
62	0 0119	0 0119	1 52	1	5	5	2 2 h1	4 2 h11	5 2 v11	7 0 v11	9 4 v2	9 6 h11	9 6 h2	4 8 v1	4 3 v4	2 5 v1	2 5 h1	3 9 h4	3 4 v4	2 7 v1		
63	0 0024	0 0024	0 97	1	1	1	2 2 h1	4 2 h11	5 2 v11	7 0 v11	9 4 v2	9 6 h11	9 6 h2	4 8 v1	4 3 v4	3 0 h1	3 0 v1	5 0 h4	5 0 v4	3 0 v1		
64	0 0237	0 0237	1 01	1	10	10	2 2 h1	4 2 h11	5 2 v11	7 0 v11	9 4 v2	9 6 h11	9 6 h2	4 8 v1	3 6 h1	5 1 h4	3 7 v4	2 8 v1				
65	0 0095	0 0095	0 99	1	4	4	2 2 h1	4 2 h11	5 2 v11	7 0 v11	9 4 v2	9 6 h11	9 6 h2	4 8 v1	3 6 h1	4 8 h5	3 8 v4	2 8 h7	3 8 h9	3 0 v1		
66	0 0024	0 0024	0 69	1	1	1	2 2 h1	4 2 h11	5 2 v11	7 0 v11	9 4 v2	9 6 h11	9 6 h2	4 8 v1	3 6 h1	3 0 v3	3 0 v7	8 0 h4	4 0 v6	2.0 v1		
67	0 0024	0 0024	1 13	2	1	1	2 2 h1	4 2 h11	5 2 v11	7 0 v11	3 0 v3	2 5 h3	1 0 h7	5 0 h11	5 0 v7	6 5 h22	8 0 v22	10 0 v22	11 0 h22	10 0 v9	10 0 h9	9 0 v1
							5 0 v4	3 0 v1														
68	0 0024	0 0024	1 38	2	1	1	2 2 h1	4 2 h11	5 2 v11	7 0 v11	3 0 v3	2.5 h3	1 0 h7	5 0 h11	5 0 v7	6 5 h22	8 0 v22	10 0 v22	10 0 v9	11 0 h22	11 0 h9	9 0 v1
							6 0 v4	3 0 v1														
69	0 0024	0 0024	1 53	1	1	1	2 2 h1	4 2 h11	5 2 v11	7 0 v11	3 0 v3	5 0 h11	5 0 v7	10 0 v10	10 0 h3	8 0 h7	8 0 v7	10 0 v9	10 0 h9	8 0 v1	5 0 v4	3 0 v1
70	0 0024	0 0024	0 98	1	1	1	2 2 h1	4 2 h11	5 2 v11	7 0 v11	3 9 h11	4 3 v3	5 0 v7	5 0 v9	5 0 h2	5 0 v1	5 0 h1	5 0 h5	10 0 v4	2.4 h7	10 0 h9	10 0 v1
							10 0 v4	3 0 v1														

Digit 8 (continued)

71	0 0024	0 0024	0 98	1	1	1	2 2 h1	4 2 h11	5 2 v11	7 0 v11	3 9 h11	4 3 v3	5 0 v7	5 0 v9	5 0 h2	5 0 v1	5 0 h1	5 0 h5	10 0 v4	2.4 h7	5 0 v1	5 0 h9
							5 0 v4	3 0 v1														
72	0 0024	0 0024	1 07	1	1	1	2.2 h1	4 2 h11	5 2 v11	7 0 v11	3 9 h11	4 3 v3	5 0 h3	3 5 h7	4 0 v7	5 0 v9	5 0 h9	3 0 v1				
73	0 0024	0 0024	1 07	1	1	1	2 2 h1	4 2 h11	5 2 v11	7 0 v11	3 9 h11	5 0 h3	5 0 v3	7 0 h7	2 7 v7	10 0 h9	10 0 v9	3 0 v1				
74	0 0024	0 0024	1 07	1	1	1	2 2 h1	4 2 h11	5 2 v11	7 0 v11	3 9 h11	5 0 h3	5 0 v3	7 0 h7	2.7 v7	5 0 v9	5 0 h9	3 0 v1				
75	0 0048	0 0048	0 89	2	2	2	2 2 h1	4 2 h11	5 2 v11	7 0 v11	3 9 h11	7 5 h22	8 5 v22	10 0 v22	10 0 v12	10 0 h22	10 0 h2	3 0 v12	3 0 h1	3 0 h4		
76	0 0024	0 0024	0 98	2	1	1	2 2 h1	4 2 h11	5 2 v11	7 0 v11	3 9 h11	7 5 h22	8 5 v22	10 0 v12	10 0 v22	10 0 h22	10 0 h2	3 0 v12	3 0 h1	3 0 h4		
77	0 0024	0 0024	2 05	2	1	1	2 2 h1	4 2 h11	5 2 v11	7 0 v11	3 9 h11	7 5 h22	8 5 v22	10 0 v2	10 0 v22	10 0 h22	10 0 h3	11 0 v1	8 0 v4	6 0 h7	6 0 h9	6 0 v1
78	0 0024	0 0024	1 09	1	1	1	2 2 h1	4 2 h11	5 2 v11	7 0 v11	3 9 h11	10 0 v2	10 0 h2	3 0 v1	3 0 h1	5 0 h5	5 0 v4	2 0 h7	2 0 h9	2 0 v1		
79	0 0024	0 0024	1 00	1	1	1	2 2 h1	4 2 h11	5 2 v11	7 0 v11	3 9 h11	10 0 h4	10 0 v4	7 0 v1	7 0 h1	10 0 v2	10 0 h2	3 0 v1				
80	0 0166	0 0166	1 17	1	7	7	2 2 h1	4 2 h11	5 2 v11	7 6 v2	8 0 v11	8 9 h11	9 0 h2	4 0 v1	3 0 h1	5 0 h4	4 2 v4	2 8 v1				
81	0 0071	0 0071	1 03	1	3	3	2 2 h1	4 2 h11	5 2 v11	7 6 v2	8 0 v11	8 9 h11	9 0 h2	4 0 v1	3 0 h1	3 4 h5	4 0 v4	1 7 h7	3 0 h9	3 0 v1		
82	0 0024	0 0024	1 31	1	1	1	2 2 h1	4 2 h11	5 2 v11	7 6 v2	8 0 v11	8 9 h11	9 0 h2	4 0 v1	3 0 h1	3 4 h5	4 0 v4	1 7 h7	1 5 v1	3 0 h9		
83	0 0024	0 0024	0 94	1	1	1	2 2 h1	4 2 h11	5 2 v11	7 6 v2	8 0 v11	8 9 h11	9 0 h2	4 0 v1	3 0 h1	3 4 h5	1 0 v5	2 0 h7	0 7 v7	2.0 h3	2 0 v9	2 0 v1
84	0 0024	0 0024	0 94	1	1	1	2 2 h1	4 2 h11	5 2 v11	7 6 v2	8 0 v11	8 9 h11	9 0 h2	4 0 v1	3 0 h1	3 4 h5	1 0 v5	2 0 h7	0 7 v7	1 0 v9	1 0 h9	2 0 v1
85	0 0048	0 0048	1 91	1	2	2	2 2 h1	4 2 h11	5 2 v11	7 6 v2	8 0 v11	8 9 h11	9 0 h2	4 0 v1	4 5 v4	4 5 v1	4 5 h1	4 0 h4	4 0 v4	2 5 v1		
86	0 0048	0 0048	1 02	1	2	2	2 2 h1	4 2 h11	5 2 v11	7 6 v2	8 0 v11	8 9 h11	10 0 h3	7 0 v1	3 5 v4	2 5 h7	3 0 h9	3 0 v1				
87	0 0024	0 0024	1 05	1	1	1	2 2 h1	4 2 h11	5 2 v11	7 6 v2	8 0 v11	5 0 h3	5 5 h11	4 0 v1	2 5 v4	3 0 v1	1 0 v4	0 7 h7	2 0 h9	2 0 v1		
88	0 0024	0 0024	1 05	1	1	1	2 2 h1	4 2 h11	5 2 v11	7 6 v2	8 0 v11	5 0 h3	5 5 h11	4 0 v1	2 5 v4	3 0 v1	1 0 v4	0 7 h7	1 0 v1	2 0 h9		
89	0 0024	0 0024	0 90	1	1	1	2 2 h1	4 2 h11	5 2 v11	7 6 v2	8 0 v11	5 0 h2	2 5 h11	1 5 h1	1 5 v1	2 5 h5	5 0 v4	1 0 h7	3 0 h9	3 0 v1		
90	0 0024	0 0024	0 90	1	1	1	2 2 h1	4 2 h11	5 2 v11	7 6 v2	8 0 v11	5 0 h2	2 5 h11	1 5 h1	1 5 v1	2 5 h5	5 0 v4	1 0 h7	1 5 v1	3 0 h9		
91	0 0024	0 0024	0 90	1	1	1	2 2 h1	4 2 h11	5 2 v11	7 6 v2	8 0 v11	5 0 h2	2 5 h11	1 5 v1	1 5 h1	2 5 h5	2 5 v4	1 5 h7	1 5 v1	3 0 h9		
92	0 0024	0 0024	1 35	2	1	1	2 2 h1	4 2 h11	5 2 v11	2 9 v3	3 3 v11	5 1 h11	6 0 v7	6 9 h22	6 9 v22	8 0 v22	8 0 v9	10 3 h22	11 0 h3	8 0 v1	8 0 v4	5 0 h7
							9 0 h9	6 0 v1	5 0 v4	3 0 v1												
93	0 0071	0 0071	1 19	2	3	3	2 2 h1	4 2 h11	5 2 v11	2 9 v3	3 3 v11	5 1 h11	6 0 v7	6 9 h22	6 9 v22	8 0 v22	8 0 v9	10 3 h22	6 0 h2	2 3 v1	2 3 h1	3 0 h4
94	0 0024	0 0024	1 36	2	1	1	2 2 h1	4 2 h11	5 2 v11	2 9 v3	3 3 v11	5 1 h11	6 0 v7	6 9 h22	6 9 v22	8 0 v22	8 0 v9	10 3 h22	6 0 h2	3 0 h1	3 0 v1	3 0 h4
95	0 0024	0 0024	1 20	2	1	1	2 2 h1	4 2 h11	5 2 v11	2 9 v3	3 3 v11	5 1 h11	6 0 v7	6 9 h22	6 9 v22	10 0 v9	10 0 v22	10 0 h22	10 0 h2	3 0 v1	3 0 h1	3 0 h4
96	0 0024	0 0024	1 20	2	1	1	2 2 h1	4 2 h11	5 2 v11	2 9 v3	3 3 v11	5 1 h11	6 0 v7	6 9 h22	6 9 v22	10 0 v9	10 0 v22	10 0 h22	10 0 h3	3 0 h7	3 0 h9	3 0 v1
97	0 0024	0 0024	1 18	1	1	1	2 2 h1	4 2 h11	5 2 v11	2 9 v3	3 3 v11	5 1 h11	6 0 v7	7 8 v10	7 8 h3	8 0 h7	8 8 v7	10 0 h6	7 0 h1	10 0 v9	10 0 h2	3 0 v1
98	0 0048	0 0048	1 25	1	2	2	2.2 h1	4 2 h11	5 2 v11	2 9 v3	3 3 v11	5 1 h11	6 0 v7	7 8 v10	7 8 h3	8 0 h7	8 8 v7	10 0 h6	10 0 v6	10 0 v1	10 0 h1	10 0 v2
							10 0 h2	3 0 v1														
99	0 0024	0 0024	1 11	1	1	1	2 2 h1	4 2 h11	5 2 v11	2 9 v3	3 3 v11	5 1 h11	6 0 v7	7 8 v10	7 8 h3	8 0 h7	8 8 v7	10 0 v9	10 0 h9	3 0 v1		
100	0 0024	0 0048	1 50	1	1	2	2 2 h1	4 2 h11	5 2 v11	2 9 v3	3 3 v11	5 1 h11	6 0 v7	10 0 h4	10 0 v6	7 5 v1	7 0 h1	10 0 v2	10 0 h2	8 5 v1	7 0 v4	3 0 v1
101	0 0024	0 0024	1 64	1	1	1	2.2 h1	4 2 h11	5 2 v11	2 9 v3	3 3 v11	5 1 h11	6 0 v7	10 0 h4	10 0 v6	7 5 v1	7 0 h1	10 0 v2	10 0 h2	8 5 v1	7 0 v4	3 0 v1
							3 0 h1	3 0 h4														
102	0 0024	0 0024	1 50	1	1	1	2.2 h1	4 2 h11	5 2 v11	2 9 v3	3 3 v11	5 1 h11	6 0 v7	5 0 v6	5 0 h4	3 5 v1	3 5 h1	5 0 v2	5 0 h2	4 0 v1	4 0 v4	3 0 v1
103	0 0024	0 0024	1 32	2	1	1	2 2 h1	4 2 h11	5 2 v11	2 0 h4	2 0 h1	1 0 v3	1 0 v11	5 0 h11	4 0 v7	5 0 h22	8 0 v22	7 0 v22	10 0 v9	10 0 h22	10 0 h2	8 0 v1
							5 0 v4	3 0 v1														
104	0 0024	0 0024	1 19	1	1	1	2 2 h1	4 2 h11	5 7 v2	5 7 v11	7 4 v11	7 4 h11	7 4 h2	11 0 v1	3 0 v4	3 0 h1	3 0 v1	5 0 h4	4 0 v4	3 0 v1		
105	0 0024	0 0024	1 19	1	1	1	2 2 h1	4 2 h11	5 7 v2	5 7 v11	7 4 v11	7 4 h11	7 4 h2	11 0 v1	3 0 v4	2.0 v1	2.0 h1	2.5 h4	2.0 v4	3 0 v1		
106	0 0024	0 0024	1 19	1	1	1	2.2 h1	4 2 h11	5 7 v2	5 7 v11	7 4 v11	7 4 h11	7 4 h2	11 0 v1	3 0 v4	2.0 v1	2.0 h1	5 0 h5	5 0 v4	2.0 h7	5 0 h9	3 0 v1
107	0 0024	0 0024	1 10	2	1	1	2 2 h1	4 2 h11	1 0 v3	2.4 v11	4 4 v11	5 5 h11	6 5 v7	8 0 h22	8 0 v22	10 0 v9	10 0 v22	10 0 h22	10 0 h3	6 0 v1	3 0 v4	3 0 h7
							3 0 h9	3 0 v1														
108	0 0024	0 0024	1 29	1	1	1	2 2 h1	4 2 h11	1 0 v3	2 4 v11	4 4 v11	5 5 h11	6 5 v7	7 0 h4	7 0 h1	10 0 v9	10 0 h3	7 0 h7	11 0 h9	12 0 v1	8 0 h1	8 0 v3
							12.0 v[illegible]	11 0 h4	[illegible] 0 v6	3 0 v1												

Digit 8 (continued)

109	0 0024	0 0024	1 30	2	1	1	22 h1	42 h11	10 v3	24 v11	44 v11	50 v7	50 h11	50 h22	80 v22	100 v9	100 v22	110 h22	110 h2	90 v1	50 v4	30 v1
							30 h1	20 h4														
110	0 0024	0 0024	1 33	2	1	1	22 h1	42 h11	10 v3	10 v22	50 v22	50 h11	80 v7	80 h22	80 v11	80 v9	90 v11	12.0 h22	12.0 h2	120 v1	50 v4	30 v1
							30 h1	20 h4														
111	0 0024	0 0024	1 36	2	1	1	22 h1	42 h11	20 v22	14 v22	10 v3	50 h11	40 v7	50 h22	80 v11	70 v9	100 v11	110 h22	110 h3	90 v1	50 v4	30 h7
							30 h9	30 v1														
112	0 0024	0 0024	1 03	2	1	1	22 h1	42 h11	20 v22	14 v22	10 v2	50 h11	50 h22	80 v11	90 v11	120 h22	120 h3	90 v1	50 v4	30 h7	30 h9	30 v1
113	0 0024	0 0024	1 05	2	1	1	22 h1	42 h11	20 v22	14 v22	50 h11	50 h22	90 v11	70 v11	110 h22	100 h2	110 v9	60 h1	90 v1	90 h4	90 v3	60 v7
114	0 0024	0 0024	1 80	2	1	1	22 h1	42 h11	20 v22	10 v3	30 v22	10 h3	10 h7	60 h11	50 v7	50 h22	90 v11	100 v9	100 v11	110 h22	110 h9	90 v1
							60 v4	30 v1														
115	0 0024	0 0024	1 27	2	1	1	22 h1	42 h11	30 h4	20 h1	30 v11	40 v3	40 v11	50 h11	40 v7	70 h22	70 v9	70 v22	80 v22	110 h22	100 h2	90 v1
							80 v4	30 v1														
116	0 0024	0 0024	1 34	1	1	1	22 h1	80 v2	70 h11	100 v11	100 v11	100 h11	100 h2	110 v1	70 v4	30 v1	30 h1	40 h4	10 v4	20 v1		
117	0 0024	0 0024	1 21	0	1	1	22 h1	80 v2	110 h2	60 v1	60 h1	80 h5	50 v5	30 h7	30 v7	50 v9	60 h9	30 v1				
118	0 0024	0 0024	1 04	0	1	1	22 h1	80 v2	100 h3	100 v1	100 v4	70 h7	110 h9	60 v1	60 h1	50 h4	50 v4	30 v1				
119	0 0024	0 0024	1 72	1	1	1	22 h1	56 h4	44 v4	33 v1	25 h1	39 v3	73 v7	83 h11	87 v11	100 v9	100 v11	100 h11	100 h2	30 v1		
120	0 0048	0 0048	1 62	1	2	2	22 h1	56 h4	44 v4	33 v1	25 h1	39 v3	73 v7	83 h11	87 v11	100 v11	100 v9	100 h11	100 h2	80 v1	80 v4	30 v1
121	0 0024	0 0024	2.19	1	1	1	22 h1	56 h4	44 v4	33 v1	25 h1	39 v3	73 v7	83 h11	100 v9	100 v11	100 v11	100 h11	100 h2	30 v1		
122	0 0024	0 0024	0 95	0	1	1	22 h1	56 h4	44 v4	33 v1	25 h1	39 v3	35 h3	40 h7	40 v7	50 h6	50 v6	35 v1	35 h1	50 v2	50 h2	30 v1
123	0 0095	0 0095	1 43	1	4	4	22 h1	56 h4	44 v4	33 v1	25 h1	78 h11	87 v11	100 v11	100 v2	100 h11	103 h2	30 v1				
124	0 0024	0 0024	1 00	1	1	1	22 h1	56 h4	44 v4	33 v1	25 h1	78 h11	87 v11	100 v11	100 h11	100 v2	100 h2	80 v1	80 v4	30 v1		
125	0 0024	0 0024	1 05	1	1	1	22 h1	56 h4	44 v4	33 v1	25 h1	78 h11	87 v11	100 v2	100 v11	100 h11	100 h2	30 v1				
126	0 0024	0 0024	1 30	1	1	1	22 h1	56 h4	44 v4	33 v1	25 h1	78 h11	100 v2	100 v11	100 v11	100 h11	100 h2	30 v1				
127	0 0024	0 0024	0 95	0	1	1	22 h1	56 h4	44 v4	33 v1	25 h1	70 h3	70 v3	80 h7	80 v7	100 h6	100 v6	70 v1	70 h1	100 v2	100 h2	30 v1
128	0 0024	0 0024	1 79	2	1	1	22 h1	56 h4	15 h1	30 h11	50 v22	40 v22	40 v3	70 h11	70 v7	80 h22	100 v11	120 v11	100 v9	110 h22	110 h2	120 v1
							80 v4	30 v1														
129	0 0024	0 0024	1 47	2	1	1	22 h1	56 h4	15 h1	30 h11	60 v11	40 v3	40 v11	50 h11	80 v7	80 h22	80 v22	70 v22	100 v9	100 h22	100 h2	30 v1
130	0 0048	0 0048	0 91	1	2	2	22 h1	20 v1	64 h4	30 v4	24 v1	20 h1	25 v3	60 v7	75 h11	80 v11	100 v9	100 v11	100 h11	100 h2		
131	0 0024	0 0024	0 83	1	1	1	22 h1	20 v1	64 h4	30 v4	24 v1	20 h1	70 h11	70 v11	100 v11	100 v2	100 h11	100 h2				
132	0 0024	0 0024	1 36	1	1	1	22 h1	20 v1	80 h11	80 v11	100 v11	100 v2	100 h11	100 h2	30 h1	30 v1	80 h4	50 v4				
133	0 0024	0 0024	1 63	1	1	1	22 h1	20 v1	30 v3	20 v7	40 h11	40 v11	50 v9	50 v11	50 h11	50 h2	80 v1	17 v4	30 h1	30 v1	50 h4	10 v4
134	0 0024	0 0024	1 63	1	1	1	22 h1	20 v1	30 v3	20 v7	40 h11	40 v11	50 v9	50 v11	50 h11	50 h2	80 v1	17 v4	15 v1	15 h1	25 h4	10 v4
135	0 0024	0 0024	1 36	0	•	1	22 h1	20 v1	30 v3	20 v7	70 h3	70 v10	50 h7	110 v7	100 h6	70 h1	100 v9	100 h2	80 v1	50 v4	30 h1	30 v1
							50 h4	20 v4														
136	0 0024	0 0024	1 36	0	1	1	22 h1	20 v1	30 v3	20 v7	35 v10	35 h3	25 h7	55 /7	50 h6	35 h1	50 v9	50 h2	40 v1	25 v4	15 h1	15 v1
							25 h4	20 v4														
137	0 0024	0 0024	0 65	2	1	1	22 h1	30 v12	30 h11	30 h4	20 h1	30 v11	50 v11	50 h11	70 h22	80 v22	100 v12	100 v22	100 h22	100 h2		
138	0 0024	0 0024	1 47	1	1	1	22 h1	60 h5	40 v5	20 h7	20 v7	20 v9	20 h9	20 v1	20 h1	40 v3	70 v7	70 h11	110 v11	100 v11	100 v9	100 h11
							100 h2	110 v1	80 v4	30 v1												
139	0 0024	0 0024	1 50	1	1	1	22 h1	60 h5	40 v4	20 h7	50 h9	20 v1	20 h1	40 v3	70 v7	70 h11	110 v11	100 v9	100 v11	100 h11	100 h2	110 v1
							80 v4	30 v1														
140	0 0544	0 0544	1 25	2	23	23	25 h12	25 h11	32 v11	47 v11	52 h11	71 h22	83 v22	98 v12	98 v22	101 h22	101 h12	30 v12				
141	0 0142	0 0142	1 73	2	6	6	25 h12	25 h11	32 v11	47 v11	52 h11	71 h22	83 v22	95 v2	99 v22	107 h22	105 h12	104 v1	75 v4	30 v1		
142	0 0662	0 0662	1 17	2	28	28	25 h12	25 h11	32 v11	47 v11	52 h11	71 h22	83 v22	90 v22	98 v12	100 h22	101 h12	30 v12				
143	0 0071	0 0095	1 33	2	3	4	25 h12	25 h11	32 v11	47 v11	52 h11	71 h22	83 v22	90 v22	100 v2	103 h22	105 h12	103 v1	70 v4	38 v1		
144	0 0024	0 0024	1 85	2	1	1	25 h12	25 h11	32 v11	47 v11	52 h11	71 h22	83 v22	90 v22	100 v2	103 h22	105 h12	103 v1	70 v4	38 v1	60 v4	30 v1

Digit 8 (continued)

145	0.0119	0.0119	1.03	2	5	5	2.5 h12	2.5 h11	3.2 v11	4.7 v11	5.2 h11	7.1 h22	8.3 v22	9.0 v22	10.0 h22	10.0 v12	10.0 h12	3.0 v12				
146	0.0048	0.0048	1.63	2	2	2	2.5 h12	2.5 h11	3.2 v11	4.7 v11	5.2 h11	7.1 h22	7.0 v2	7.0 v22	11.0 v22	11.0 h22	11.0 h12	10.0 v1	7.5 v4	3.0 v1		
147	0.0024	0.0024	2.30	2	1	1	2.5 h12	2.5 h11	3.2 v11	4.7 v11	5.2 h11	4.0 v3	7.0 v7	8.0 h22	10.0 v22	11.0 v22	10.0 v9	11.0 h22	11.0 h12	12.0 v1	8.0 v4	3.0 v1
148	0.0048	0.0071	1.17	2	2	3	2.5 h12	2.5 h11	3.2 v11	4.7 v11	3.8 v3	5.6 h11	6.1 v7	7.6 h22	8.6 v22	9.2 v22	10.4 h22	10.0 v9	10.4 h12	6.0 v1		
149	0.0024	0.0024	1.50	2	1	1	2.5 h12	2.5 h11	3.2 v11	4.7 v11	3.8 v3	5.6 h11	6.1 v7	7.6 h22	8.6 v22	9.2 v22	10.4 h22	10.0 v9	10.4 h12	6.0 v1	8.0 v4	6.0 v1
							3.0 v4	3.0 v1														
150	0.0071	0.0142	1.23	2	3	6	2.5 h12	2.5 h11	3.2 v11	4.7 v11	3.8 v3	5.6 h11	6.1 v7	7.6 h22	8.6 v22	9.2 v22	9.5 v9	9.9 h22	10.4 h12	5.7 v1		
151	0.0071	0.0071	1.37	2	3	3	2.5 h12	2.5 h11	3.2 v11	4.7 v11	3.8 v3	5.6 h11	6.1 v7	7.6 h22	8.6 v22	9.2 v22	9.5 v9	9.9 h22	10.4 h12	5.7 v1	5.0 v4	3.0 v1
152	0.0119	0.0142	1.31	2	5	6	2.5 h12	2.5 h11	3.2 v11	4.7 v11	3.8 v3	5.6 h11	6.1 v7	7.6 h22	8.6 v22	10.0 v9	10.0 v22	10.2 h22	10.2 h12	4.5 v1		
153	0.0024	0.0024	1.57	2	1	1	2.5 h12	2.5 h11	3.2 v11	4.7 v11	3.8 v3	5.6 h11	6.1 v7	7.6 h22	8.6 v22	10.0 v9	10.0 v22	10.2 h22	10.2 h12	4.5 v1	5.0 v4	3.0 v1
154	0.0024	0.0024	0.78	2	1	1	2.5 h12	2.5 h11	3.2 v11	4.7 v11	3.8 v3	5.0 v7	5.0 h11	8.0 h22	8.0 v22	7.0 v22	10.0 h22	10.0 v9	10.0 h12	3.0 v1		
155	0.0024	0.0024	1.59	2	1	1	2.5 h12	2.5 h11	3.2 v11	4.7 v11	5.5 v2	7.5 h11	8.0 h22	8.0 v22	8.0 v22	11.0 h22	11.0 h12	9.0 v1	5.0 v4	3.0 v1		
156	0.0024	0.0024	1.05	1	1	1	2.5 h12	2.5 h11	3.2 v11	4.7 v11	5.5 v2	7.5 h11	10.0 h12	6.0 v1	5.0 v4	3.0 v1						
157	0.0166	0.0402	1.25	2	7	17	2.5 h12	2.5 h11	3.2 v11	3.3 v3	4.0 v11	5.4 h11	6.3 v7	7.5 h22	8.7 v22	9.9 v9	9.9 v22	10.3 h22	10.5 h12	7.4 v1		
158	0.0237	0.0237	1.68	2	10	10	2.5 h12	2.5 h11	3.2 v11	3.3 v3	4.0 v11	5.4 h11	6.3 v7	7.5 h22	8.7 v22	9.9 v9	9.9 v22	10.3 h22	10.5 h12	7.4 v1	6.1 v4	3.3 v1
159	0.0261	0.0592	1.36	2	11	25	2.5 h12	2.5 h11	3.2 v11	3.3 v3	4.0 v11	5.4 h11	6.3 v7	7.5 h22	8.7 v22	9.8 v22	9.8 v9	10.3 h22	10.4 h12	6.8 v1		
160	0.0331	0.0331	1.51	2	14	14	2.5 h12	2.5 h11	3.2 v11	3.3 v3	4.0 v11	5.4 h11	6.3 v7	7.5 h22	8.7 v22	9.8 v22	9.8 v9	10.3 h22	10.4 h12	6.8 v1	6.5 v4	3.0 v1
161	0.0119	0.0166	1.22	2	5	7	2.5 h12	2.5 h11	3.2 v11	3.3 v3	4.0 v11	5.4 h11	6.3 v7	7.5 h22	8.7 v22	9.8 v22	10.3 h22	10.0 v9	10.2 h12	5.9 v1		
162	0.0048	0.0048	1.71	2	2	2	2.5 h12	2.5 h11	3.2 v11	3.3 v3	4.0 v11	5.4 h11	6.3 v7	7.5 h22	8.7 v22	9.8 v22	10.3 h22	10.0 v9	10.2 h12	5.9 v1	6.5 v4	3.0 v1
163	0.0142	0.0142	1.66	2	6	6	2.5 h12	2.5 h11	3.2 v11	3.3 v3	4.0 v11	5.4 h11	6.3 v7	7.5 h22	9.5 v9	9.5 v22	11.2 v22	10.9 h22	10.9 h12	11.4 v1	6.0 v4	3.0 v1
164	0.0024	0.0024	1.84	1	1	1	2.5 h12	2.5 h11	3.2 v11	3.3 v3	4.0 v11	5.4 h11	6.3 v7	10.0 v9	10.0 h12	3.0 v1						
165	0.0024	0.0024	1.56	2	1	1	2.5 h12	2.5 h11	3.2 v11	3.3 v3	4.0 v11	5.4 h11	5.0 h22	7.0 v7	8.0 v22	7.0 v22	10.0 v9	11.0 h22	11.0 h12	9.0 v1	5.0 v4	3.0 v1
166	0.0024	0.0024	1.11	2	1	1	2.5 h12	2.5 h11	3.2 v11	3.3 v3	4.0 v11	4.5 v7	5.0 h11	7.0 h22	8.0 v22	10.0 v22	10.0 v9	10.0 h22	10.0 h12	3.0 v1		
167	0.0024	0.0024	1.26	2	1	1	2.5 h12	2.5 h11	3.2 v11	3.3 v3	4.0 v11	4.5 v7	5.0 h11	7.0 h22	8.0 v22	7.0 v9	7.0 v22	10.0 h22	10.0 h12	3.0 v1		
168	0.0071	0.0071	1.42	2	3	3	2.5 h12	2.5 h11	3.2 v11	4.0 v2	4.0 v11	6.0 h11	8.0 h22	7.7 v22	12.0 v22	11.4 h22	11.4 h12	12.0 v1	7.4 v4	3.0 v1		
169	0.0024	0.0048	1.69	2	1	2	2.5 h12	2.5 h11	1.3 v3	2.3 v11	4.0 v11	5.2 h11	7.0 v7	7.6 h22	8.8 v22	9.8 v22	10.0 v9	11.0 h22	11.0 h12	9.0 v1		
170	0.0024	0.0024	1.87	2	1	1	2.5 h12	2.5 h11	1.3 v3	2.3 v11	4.0 v11	5.2 h11	7.0 v7	7.6 h22	8.8 v22	9.8 v22	10.0 v9	11.0 h22	11.0 h12	9.0 v1	8.0 v4	6.0 v1
171	0.0024	0.0048	0.96	2	1	2	2.5 h12	2.5 h11	1.3 v3	2.3 v11	4.0 v11	5.2 h11	7.0 v7	7.6 h22	8.8 v22	9.8 v22	10.5 h22	10.0 v9	10.5 h12	9.0 v1		
172	0.0024	0.0024	1.95	2	1	1	2.5 h12	2.5 h11	1.3 v3	2.3 v11	4.0 v11	5.2 h11	7.0 v7	7.6 h22	8.8 v22	9.8 v22	10.5 h22	10.0 v9	10.5 h12	9.0 v1	8.0 v4	6.0 v1
173	0.0048	0.0071	1.39	2	2	3	2.5 h12	2.5 h11	1.3 v3	2.3 v11	4.0 v11	5.2 h11	7.0 v7	7.6 h22	8.8 v22	10.0 v9	10.0 v22	10.4 h22	10.0 h12	6.0 v1		
174	0.0024	0.0024	1.86	2	1	1	2.5 h12	2.5 h11	1.3 v3	2.3 v11	4.0 v11	5.2 h11	7.0 v7	7.6 h22	8.8 v22	10.0 v9	10.0 v22	10.4 h22	10.0 h12	6.0 v1	6.0 v4	3.0 v1
175	0.0024	0.0048	1.40	2	1	2	2.5 h12	2.5 h11	1.3 v3	2.3 v11	4.0 v11	5.0 v7	5.0 h11	7.0 h22	8.0 v22	8.5 v22	8.5 v9	10.5 h22	10.5 h12	6.0 v1		
176	0.0024	0.0024	1.74	2	1	1	2.5 h12	2.5 h11	1.3 v3	2.3 v11	4.0 v11	5.0 v7	5.0 h11	7.0 h22	8.0 v22	8.5 v22	8.5 v9	10.5 h22	10.5 h12	6.0 v1	5.0 v4	6.0 v1
							2.0 v4	3.0 v1														
177	0.0024	0.0024	1.45	2	1	1	2.5 h12	2.5 h11	1.3 v3	2.3 v11	4.0 v11	5.0 v7	5.0 h11	7.0 h22	8.0 v22	10.0 v9	10.0 v22	10.0 h22	10.0 h12	8.0 v1	5.0 v4	3.0 v1
178	0.0024	0.0024	1.36	2	1	1	2.5 h12	2.5 h11	1.3 v3	3.0 h22	3.0 v11	5.0 v11	5.0 h11	5.0 h22	5.0 v7	7.0 v9	7.0 v22	9.0 v22	11.0 h12	9.0 v1	6.0 v4	3.0 v1
179	0.0095	0.0095	1.52	2	4	4	2.5 h12	2.5 h11	1.3 v3	1.9 v22	3.2 v22	5.5 h11	5.0 v7	7.0 h22	8.5 v11	8.3 v9	9.5 v11	11.5 h22	11.5 h12	10.5 v1	5.3 v4	3.5 v1
180	0.0048	0.0048	1.41	2	2	2	2.5 h12	2.5 h11	1.3 v3	1.9 v22	3.2 v22	5.5 h11	5.0 v7	7.0 h22	8.5 v9	10.0 v11	9.5 v11	11.5 h22	11.5 h12	10.5 v1	7.0 v4	6.0 v1
181	0.0024	0.0024	1.16	2	1	1	2.5 h12	2.5 h11	1.3 v3	1.9 v22	3.2 v22	4.0 v7	5.0 h11	4.0 v10	5.0 v7	5.0 h22	8.0 v9	9.0 v11	8.0 v11	11.0 h22	11.0 h12	9.0 v1
							5.0 v4	3.0 v1														
182	0.0048	0.0048	1.94	2	2	2	2.5 h12	2.5 h11	3.0 v22	2.5 v3	2.5 v22	5.5 h11	6.8 v7	7.0 h22	8.5 v9	10.0 v11	12.0 v11	11.0 h22	12.0 h12	12.0 v1	5.0 v4	3.0 v1
183	0.0048	0.0048	1.55	2	2	2	2.5 h12	2.5 h11	3.0 v22	2.5 v3	2.5 v22	5.5 h11	6.8 v7	7.0 h22	9.0 v11	5.5 v9	9.0 v11	11.0 h22	11.0 h12	9.0 v1	7.5 v4	3.0 v1
184	0.0024	0.0024	0.97	2	1	1	2.5 h12	2.5 h11	3.0 v22	6.0 h22	4.0 v12	4.0 v22	4.0 h11	9.0 v11	8.0 v11	11.0 h22	11.0 h12	9.0 v12				
185	0.0024	0.0024	1.90	2	1	1	2.5 h12	2.5 h11	3.0 v22	4.0 v2	4.0 v22	5.0 h11	8.0 h22	8.0 v11	9.0 v11	11.0 h22	11.0 h12	9.0 v1	5.0 v4	3.0 v1		
186	0.0024	0.0024	1.50	2	1	1	2.5 h12	2.5 h11	3.0 v22	4.0 v22	4.0 v3	5.0 h11	7.0 v7	8.0 h22	8.0 v11	10.0 v9	11.0 v11	11.0 h22	11.0 h12	9.0 v1	5.0 v4	3.0 v1
187	0.0024	0.0024	1.53	2	1	1	2.5 h12	2.5 h11	1.0 v2	2.0 v22	4.0 v22	5.0 h11	8.0 h22	8.0 v11	9.0 v11	12.0 h22	12.0 h12	12.0 v1	5.0 v4	3.0 v1		

Digit 8 (continued)

188	0 0024	0 0024	1.36	2	1	1	2.5 h12	2.5 h11	1 0 v12	1.0 v22	2.0 v22	5 0 h11	8 0 h22	8 0 v11	12.0 v11	12 0 h22	12.0 h12	12 0 v12				
189	0 0024	0 0024	0 84	2	1	1	2.5 h12	2.5 h11	2.0 h22	2.0 v11	6 0 v11	6 0 h11	8 0 h22	7 0 v12	8 0 v22	7 0 v22	11 0 h12	6 0 v12				
190	0 0024	0 0024	1 25	2	1	1	2.5 h12	2 0 v2	5 7 h11	1 0 v22	2.0 v22	5 0 h11	5.0 h22	8 0 v11	12.0 v11	12 0 h22	12.0 h12	12.0 v1	5 0 v4	3 0 v1		
191	0 0048	0 0048	1 81	1	2	2	2 5 h12	2.0 v2	5 7 h11	8 5 v11	10 0 v11	11 0 h11	11 0 h12	9 0 v1	1 0 v4	2 0 v1						
192	0 0048	0 0048	1 81	1	2	2	2 5 h12	1 9 v3	3 8 v7	4.0 h11	6 0 v11	8 5 v9	8 5 v11	10 5 h11	10 5 h12	8 5 v1	3 5 v4	2.5 v1				
193	0 0024	0 0024	1 36	2	1	1	2 5 h12	1 9 v3	3 8 v7	4 0 h11	6 0 v11	4 5 v10	5 0 v11	8 5 h11	8 0 v7	8 0 h22	9 5 v22	10 0 v9	10 0 v22	10 0 h22	10 0 h12	6 0 v1
194	0 0024	0 0024	1 89	2	1	1	2.5 h12	1 9 v3	3 8 v7	4 0 h11	6 0 v11	4 5 v10	5 0 v11	8 5 h11	8 0 v7	8 0 h22	9 5 v22	10 0 v22	10 0 v9	10 0 h22	11 0 h12	3 0 v1
195	0 0048	0 0048	1 76	1	2	2	2.5 h12	1 9 v3	3 8 v7	4 0 h11	6 0 v11	5 8 v11	8 5 v9	10 5 h11	11 0 h12	7 0 v1	3 5 v4	3 0 v1				
196	0 0048	0 0071	1 61	2	2	3	2.5 h12	1 9 v3	3 8 v7	4 0 h11	6 0 v11	5 8 v11	5 0 h11	8 0 h22	9 0 v22	10 0 v9	10 0 v22	10 0 h22	10 4 h12	6 7 v1		
197	0 0024	0 0024	1 40	2	1	1	2 5 h12	1 9 v3	3 8 v7	4 0 h11	6 0 v11	5 8 v11	5 0 h11	8 0 h22	9 0 v22	10 0 v9	10 0 v22	10 0 h22	10 4 h12	6 7 v1	8 0 v4	3 0 v1
198	0 0024	0 0024	1 77	1	1	1	2 5 h12	1 9 v3	3 8 v7	4 0 h11	7 0 v9	9 0 v11	10 0 v11	11 0 h11	11 0 h12	9 0 v1	5 0 v4	5 0 v1	1 0 v4	2 0 v1		
199	0 0024	0 0024	1 58	2	1	1	2 5 h12	1 9 v3	3 8 v7	5 0 h22	4 0 v10	5 0 v22	5 0 v22	5 0 h22	7 0 v7	7 0 h11	8 0 v11	10 0 v11	10 0 v9	10 0 h11	10 0 h12	3 0 v1
200	0 0024	0 0024	1 21	2	1	1	2 5 h12	1 9 v3	2.0 h11	2 0 v11	4 5 v11	6 0 h11	5 0 v7	8 0 h22	7 5 v22	7 0 v9	10 0 v22	11 0 h22	11 0 h12	3 0 v1		
201	0 0024	0 0024	1 12	2	1	1	2 5 h12	1 9 v3	2.0 h11	2 0 v11	4 5 v11	6 0 h11	5 0 v7	8 0 h22	7 5 v22	8 0 v22	10 0 v9	11 0 h22	11 0 h12	3 0 v1		
202	0 0024	0 0024	1 64	2	1	1	2 5 h12	1 9 v3	2.0 h11	1 0 v22	3 5 v22	4 5 h11	5 0 h22	4 0 v7	7 0 v11	7 0 v9	12 0 v11	12 0 h22	12 0 h12	12.0 v1		
203	0 0024	0 0024	1.61	2	1	1	2 5 h12	1 9 v3	2 0 h11	1 0 v22	3 5 v22	4 5 h11	4 0 v7	8 0 h22	10 0 v9	10 0 v11	12.0 v11	12 0 h22	11 0 h12	12 0 v1	6 0 v4	3 0 v1
204	0 0024	0 0024	0 93	2	1	1	2.5 h12	1 9 v3	2 0 h11	2.0 v7	3 0 v11	5 0 v11	5 0 h11	7 0 h22	7 0 v22	10 0 v22	10 0 v9	10 0 h22	10 0 h12	3 0 v1		
205	0 0024	0 0024	1 10	2	1	1	2 5 h12	1 9 v3	2.0 h11	2 0 v7	3 0 v11	5 0 v10	5 0 v11	5 0 h11	5 0 v7	8 0 h22	8 0 v22	10 0 v22	10 0 v9	10 0 h22	10 0 h12	3 0 v1
206	0 0024	0 0024	1 31	2	1	1	2.5 h12	2.5 h22	4 5 v22	5 0 v22	5 0 h22	8 0 h11	11 0 v11	10 0 v2	10 0 v11	10 0 h11	10 0 h12	11 0 v1	8 0 v4	3 0 v1		
207	0 0024	0 0024	1 12	2	1	1	2.5 h12	2 5 h22	4 5 v22	5 0 v3	5 0 v22	5 0 h22	5 0 v7	8 0 h11	8 0 v11	10 0 v11	10 0 v9	10 0 h11	10 0 h12	3 0 v1		
208	0 0048	0 0048	0 91	1	2	2	1 4 v1	1 4 h1	3 2 h4	1 5 v4	1 2 v1	1.0 h1	1 3 v3	3 0 v7	3 8 h11	4 0 v11	5 0 v9	5 0 v11	5 0 h11	10 0 h2		
209	0 0024	0 0024	0 83	1	1	1	1 4 v1	1 4 h1	3 2 h4	1 5 v4	1 2 v1	1 0 h1	3 5 h11	3 5 v11	5 0 v11	5 0 v2	5 0 h11	10 0 h2				
210	0.0024	0 0024	1.63	1	1	1	1 4 v1	1 4 h1	2.0 v3	2.5 v7	4 0 h11	4 0 v11	5 0 v9	5 0 v11	5 0 h11	5 0 h2	4 0 v1	2 5 v4	1 5 v1	1 5 h1	2 5 h4	1 0 v4
211	0 0024	0 0024	0 65	2	1	1	1 5 v12	1 5 h1	1 5 h11	1 5 h4	1.0 h1	1 5 v11	2.5 v11	2 5 h11	3 5 h22	4 0 v22	5 0 v12	5 0 v22	5 0 h22	10 0 h2		

Extended sample set size 423

B.10 Feature Strings for Digit 9

J	Term/Ext	Pass/Ext	H/W	Hole	Term	Pass	Feature String															
1	0.0681	0.0681	1.35	0	29	29	2.5 h1	3.8 v3	5.8 v7	9.6 v9	9.5 h2	5.0 v1	4.1 h1	4.8 h4	3.5 v4	2.9 v1						
2	0.0423	0.0423	1.42	0	18	18	2.5 h1	3.8 v3	5.8 v7	9.6 v9	9.5 h2	5.0 v1	4.1 h1	4.6 h5	3.4 v4	2.1 h7	4.2 h9	3.5 v1				
3	0.0047	0.0047	1.77	0	2	2	2.5 h1	3.8 v3	5.8 v7	9.6 v9	9.5 h2	5.0 v1	4.1 h1	4.6 h5	3.4 v4	2.1 h7	1.3 v1	2.5 h9				
4	0.0024	0.0024	1.50	0	1	1	2.5 h1	3.8 v3	5.8 v7	9.6 v9	9.5 h2	5.0 v1	8.7 v4	5.0 v1	3.9 h1	2.0 v3	2.0 v7	5.0 h4	1.0 v6	2.0 v1		
5	0.0047	0.0047	1.55	0	2	2	2.5 h1	3.0 v3	5.8 v7	9.6 v9	9.5 h2	5.0 v1	8.7 v4	5.0 v1	3.9 h1	5.0 h4	4.0 v4	3.0 v1				
6	0.0047	0.0047	1.58	0	[illegible]	2	2.5 h1	3.8 v3	5.8 v7	9.6 v9	9.5 h2	5.0 v1	8.7 v4	5.0 v1	3.9 h1	3.7 h5	2.5 v4	1.0 h7	3.0 h9	3.0 v1		
7	0.0024	0.0024	1.74	0	1	1	2.5 h1	3.8 v3	5.8 v7	9.6 v9	9.5 h2	5.0 v1	8.7 v4	5.0 v1	3.9 h1	3.7 h5	2.5 v4	1.0 h7	1.5 v1	3.0 h9		
8	0.0047	0.0047	1.58	0	2	2	2.5 h1	3.8 v3	5.8 v7	9.6 v9	10.6 h3	6.5 v1	1.0 v5	2.5 h7	3.0 v7	3.0 v9	3.0 h9	3.0 v1				
9	0.0235	0.0235	1.34	0	10	10	2.5 h1	3.8 v3	5.8 v7	9.6 v9	10.6 h3	6.5 v1	2.7 v4	2.3 h7	4.3 h9	3.0 v1						
10	0.0024	0.0024	1.87	0	1	1	2.5 h1	3.8 v3	5.8 v7	9.6 v9	10.6 h3	8.0 h7	8.0 h9	6.0 v1	3.0 h1	5.0 h5	4.0 v4	3.0 h7	3.0 h9	3.0 v1		
11	0.0024	0.0024	1.62	0	1	1	2.5 h1	3.8 v3	5.8 v7	4.4 h4	1.0 h1	4.0 v10	4.0 h3	6.0 h7	6.0 v7	11.0 v9	11.0 h9	3.0 v1				
12	0.0024	0.0024	1.15	0	1	1	2.5 h1	3.8 v3	5.8 v7	4.4 h4	4.0 v6	2.5 v1	2.0 h1	4.0 v3	8.0 v7	10.0 v9	10.0 h2	3.0 v1				
13	0.0024	0.0024	1.90	0	1	1	2.5 h1	3.8 v3	5.8 v7	4.4 h4	4.0 v6	2.5 v1	2.0 h1	4.0 v3	7.0 h3	5.0 h7	5.0 v7	10.0 v9	10.0 h9	3.0 v1		
14	0.0024	0.0024	1.48	0	1	1	2.5 h1	3.8 v3	5.8 v7	10.0 h2	10.0 v9	3.0 v1	3.0 h1	4.0 h4	4.0 v4	3.0 v1						
15	0.0047	0.0047	1.37	0	2	2	2.5 h1	3.8 v3	4.9 h3	5.2 h7	5.3 v7	7.0 h9	7.0 v9	3.0 v1	3.0 h1	4.4 h5	4.0 v4	1.3 h7	3.0 h9	3.0 v1		
16	0.0024	0.0024	1.13	0	1	1	2.5 h1	3.8 v3	4.9 h3	5.2 h7	5.3 v7	7.0 h9	7.0 v9	3.0 v1	3.0 h1	4.4 h5	4.0 v4	1.3 h7	1.5 v1	3.0 h9		
17	0.0517	0.0517	1.52	0	22	22	2.5 h1	3.8 v3	4.9 h3	5.2 h7	5.3 v7	9.4 v9	9.4 h9	5.1 v1	3.8 h1	4.2 h5	3.7 v4	2.3 h7	3.0 h9	3.0 v1		
18	0.0047	0.0047	1.51	0	2	2	2.5 h1	3.8 v3	4.9 h3	5.2 h7	5.3 v7	9.4 v9	9.4 h9	5.1 v1	3.8 h1	4.2 h5	3.7 v4	2.3 h7	1.5 v1	3.0 h9		
19	0.0071	0.0071	1.23	0	3	3	2.5 h1	3.8 v3	4.9 h3	5.2 h7	5.3 v7	9.4 v9	9.4 h9	5.1 v1	3.8 h1	4.2 h5	3.0 v5	3.0 h7	1.9 v7	3.8 v9	3.8 h9	3.0 v1
20	0.0024	0.0024	0.92	0	1	1	2.5 h1	3.8 v3	4.9 h3	5.2 h7	5.3 v7	9.4 v9	9.4 h9	5.1 v1	3.8 h1	4.2 h5	3.0 v5	3.0 h7	1.9 v7	3.0 h9	3.0 v9	3.0 v1
21	0.0376	0.0423	1.45	0	16	18	2.5 h1	3.8 v3	4.9 h3	5.2 h7	5.3 v7	9.4 v9	9.4 h9	5.1 v1	3.8 h1	4.7 h4	4.0 v4	3.0 v1				
22	0.0024	0.0024	1.35	0	1	1	2.5 h1	3.8 v3	4.9 h3	5.2 h7	5.3 v7	9.4 v9	9.4 h9	5.1 v1	3.8 h1	4.7 h4	4.0 v4	3.0 v1	3.0 h1	2.0 h5	2.0 v5	3.0 h7
							2.0 v7	6.0 h9	6.0 v9	3.0 v1												
23	0.0024	0.0024	1.35	0	1	1	2.5 h1	3.8 v3	4.9 h3	5.2 h7	5.3 v7	9.4 v9	9.4 h9	5.1 v1	3.8 h1	4.7 h4	4.0 v4	3.0 v1	3.0 h1	2.0 h5	2.0 v5	3.0 h7
							2.0 v7	3.0 v9	3.0 h9	3.0 v1												
24	0.0094	0.0094	1.44	0	4	4	2.5 h1	3.8 v3	4.9 h3	5.2 h7	5.3 v7	9.4 v9	9.4 h9	5.1 v1	10.4 v4	5.5 v1	4.5 h1	6.5 h4	5.5 v4	3.0 v1		
25	0.0024	0.0024	1.13	0	1	1	2.5 h1	3.8 v3	4.9 h3	5.2 h7	5.3 v7	9.4 v9	9.4 h9	5.1 v1	10.4 v4	5.5 v1	4.5 h1	4.0 h5	4.0 v5	3.0 h7	3.0 v7	6.0 v9
							6.0 h9	3.0 v1														
26	0.0024	0.0024	1.48	0	1	1	2.5 h1	3.8 v3	4.9 h3	5.2 h7	5.3 v7	9.4 v9	9.4 h9	5.1 v1	10.4 v4	5.5 v1	4.5 h1	4.0 h5	4.0 v4	3.0 h7	3.0 h9	3.0 v1
27	0.0047	0.0047	1.63	0	2	2	2.5 h1	3.8 v3	4.9 h3	5.2 h7	5.3 v7	9.0 h6	8.5 h1	10.0 v9	10.5 h2	6.0 v1	4.5 h1	4.0 h5	4.0 v4	2.0 h7	3.0 h9	3.0 v1
28	0.0024	0.0024	1.41	1	1	1	2.5 h1	3.8 v3	5.0 h11	4.0 h3	5.0 h7	5.0 v7	5.0 v11	5.0 v11	8.0 h11	10.0 v9	10.0 h9	10.0 v1	10.0 v4	6.0 v1	2.0 h1	4.0 h5
							4.0 v4	3.0 h7	3.0 h9	3.0 v1												
29	0.0094	0.0094	1.74	1	4	4	2.5 h1	2.3 h11	2.8 v11	3.8 v11	4.0 v12	4.5 h11	6.8 h3	6.3 h7	12.0 h9	9.0 v12						
30	0.0047	0.0047	1.44	1	2	2	2.5 h1	2.3 h11	2.8 v11	3.8 v11	3.9 v3	4.4 h11	5.1 h3	5.4 h7	5.2 v7	6.0 v10	6.5 v7	10.0 v9	10.5 h9	3.0 v1		
31	0.0775	0.0822	1.47	1	33	35	2.5 h1	2.3 h11	2.8 v11	3.8 v11	3.9 v3	4.4 h11	5.1 h3	5.4 h7	5.2 v7	9.5 v9	9.5 h9	3.7 v1				
32	0.0047	0.0047	1.23	1	2	2	2.5 h1	2.3 h11	2.8 v11	3.8 v11	3.9 v3	4.4 h11	5.1 h3	5.4 h7	5.2 v7	9.5 v9	9.5 h9	3.7 v1	7.0 v4	3.0 v1		
33	0.0047	0.0047	1.12	1	2	2	2.5 h1	2.3 h11	2.8 v11	3.8 v11	3.9 v3	4.4 h11	5.1 h3	5.4 h7	5.2 v7	9.5 v9	10.0 h10	6.0 h7	6.0 h9	3.0 v1		
34	0.0071	0.0071	1.42	1	3	3	2.5 h1	2.3 h11	2.8 v11	3.8 v11	3.9 v3	4.4 h11	5.1 h3	5.4 h7	5.2 v7	10.0 h9	10.0 v9	3.0 v1				
35	0.0024	0.0024	1.32	1	1	1	2.5 h1	2.3 h11	2.8 v11	3.8 v11	3.9 v3	4.4 h11	2.5 v7	10.0 v9	3.4 h2	3.0 h1	3.0 v1	6.0 h4	3.0 v4	3.0 v1		
36	0.0024	0.0024	1.32	1	1	1	2.5 h1	2.3 h11	2.8 v11	3.8 v11	3.9 v3	4.4 h11	2.5 v7	10.0 v9	3.4 h2	1.5 v1	1.5 h1	3.0 h4	1.5 v4	3.0 v1		
37	0.0447	0.0517	1.29	1	19	22	2.5 h1	2.3 h11	2.8 v11	3.8 v11	4.5 h11	4.8 v3	5.5 h3	5.2 h7	5.8 v7	10.2 v9	10.2 h9	3.7 v1				
38	0.0024	0.0024	1.13	1	1	1	2.5 h1	2.3 h11	2.8 v11	3.8 v11	4.5 h11	4.8 v3	5.5 h3	5.2 h7	5.8 v7	10.2 v9	10.2 h9	3.7 v1	10.0 v4	3.0 v1		
39	0.0024	0.0047	1.69	1	1	2	2.5 h1	2.3 h11	2.8 v11	3.8 v11	4.5 h11	4.8 v3	5.5 h3	5.2 h7	5.8 v7	10.2 v9	10.2 h9	3.7 v1	6.5 h1	6.5 h4		
40	0.0024	0.0024	1.09	1	1	1	2.5 h1	2.3 h11	2.8 v11	3.8 v11	4.5 h11	4.8 v3	5.5 h3	5.2 h7	5.8 v7	10.2 v9	10.2 h9	3.7 v1	6.5 h1	6.5 h4	10.0 v4	3.0 v1

Digit 9 (continued)

41	0.1339	0.1573	1.51	1	57	67	2.5 h1	2.3 h11	2.8 v11	4.1 v3	4.2 v11	4.8 h11	5.3 h3	5.5 h7	5.6 v7	9.9 v9	10.0 h9	4.2 v1				
42	0.0024	0.0118	1.58	1	1	5	2.5 h1	2.3 h11	2.8 v11	4.1 v3	4.2 v11	4.8 h11	5.3 h3	5.5 h7	5.6 v7	9.9 v9	10.0 h9	4.2 v1	5.5 h1	6.3 h4		
43	0.0094	0.0094	1.40	1	4	4	2.5 h1	2.3 h11	2.8 v11	4.1 v3	4.2 v11	4.8 h11	5.3 h3	5.5 h7	5.6 v7	9.9 v9	10.0 h9	4.2 v1	5.5 h1	6.3 h4	5.8 v4	3.0 v1
44	0.0094	0.0118	1.64	1	4	5	2.5 h1	2.3 h11	2.8 v11	4.1 v3	4.2 v11	4.8 h11	5.3 h3	5.5 h7	5.6 v7	9.9 v9	10.0 h9	4.2 v1	9.9 v4	3.0 v1		
45	0.0024	0.0024	1.40	1	1	1	2.5 h1	2.3 h11	2.8 v11	4.1 v3	4.2 v11	4.8 h11	5.3 h3	5.5 h7	5.6 v7	9.9 v9	10.0 h9	4.2 v1	9.9 v4	3.0 v1	3.0 h1	3.0 h4
46	0.0024	0.0024	1.29	1	1	1	2.5 h1	2.3 h11	2.8 v11	4.1 v3	4.2 v11	4.8 h11	5.3 h3	5.5 h7	5.6 v7	9.9 v9	11.0 h10	11.0 v1	11.0 v4	3.0 h7	6.0 h9	3.0 v1
47	0.0071	0.0071	1.55	1	3	3	2.5 h1	2.3 h11	2.8 v11	4.1 v3	4.2 v11	4.8 h11	5.3 h3	5.5 h7	5.6 v7	10.0 h9	10.0 v9	3.0 v1				
48	0.0024	0.0024	1.23	1	1	1	2.5 h1	2.3 h11	2.8 v11	4.1 v3	4.2 v11	4.8 h11	5.3 h3	5.5 h7	5.6 v7	4.8 v10	8.0 v7	11.0 v9	11.0 h9	3.0 v1		
49	0.0024	0.0047	1.42	1	1	2	2.5 h1	2.3 h11	2.8 v11	4.1 v3	4.2 v11	4.8 h11	5.3 h3	5.5 h7	5.6 v7	4.8 v10	4.0 h10	4.4 h7	4.7 v7	6.7 v9	7.0 h9	7.0 v1
50	0.0024	0.0024	1.40	1	1	1	2.5 h1	2.3 h11	2.8 v11	4.1 v3	4.2 v11	4.8 h11	5.3 h3	5.5 h7	5.6 v7	4.8 v10	4.0 h10	4.4 h7	4.7 v7	6.7 v9	7.0 h9	7.0 v1
							11.0 v4	3.0 v1														
51	0.0024	0.0024	1.42	1	1	1	2.5 h1	2.3 h11	2.8 v11	4.1 v3	4.2 v11	4.8 h11	5.3 h3	5.5 h7	5.6 v7	5.0 h10	5.0 v10	5.0 h7	6.0 v7	10.0 v9	10.0 h9	3.0 v1
52	0.0024	0.0024	1.13	1	1	1	2.5 h1	2.3 h11	2.8 v11	4.1 v3	4.2 v11	4.8 h11	5.3 h3	5.5 h7	10.0 h10	5.0 h7	8.0 v7	10.0 v9	10.0 h9	3.0 v1		
53	0.0024	0.0024	1.37	1	1	1	2.5 h1	2.3 h11	2.8 v11	4.1 v3	4.2 v11	4.8 h11	5.3 h3	3.0 v7	3.0 h7	5.0 v9	5.0 h9	3.0 v1				
54	0.0024	0.0024	1.24	1	1	1	2.5 h1	2.3 h11	2.8 v11	4.1 v3	4.2 v11	4.8 h11	5.0 v7	10.0 v9	10.0 h3	3.0 h7	6.0 h9	6.0 v1				
55	0.0024	0.0024	1.31	1	1	1	2.5 h1	2.3 h11	2.8 v11	4.1 v3	4.2 v11	4.8 h11	5.0 v7	10.0 h4	7.0 h1	10.0 v9	10.0 h2	3.0 v1				
56	0.0024	0.0024	1.44	1	1	1	2.5 h1	2.3 h11	2.8 v11	4.1 v3	2.0 v7	4.0 v11	5.0 h11	4.0 v10	4.0 h3	5.0 h7	5.0 v7	10.0 v9	10.0 h9	3.0 v1		
57	0.0047	0.0047	1.48	1	2	2	2.5 h1	2.3 h11	2.8 v11	4.0 v12	4.0 v11	6.5 h11	8.0 h3	7.0 h7	12.0 h9	4.5 v12						
58	0.0024	0.0024	1.47	1	1	1	2.5 h1	2.3 h11	2.8 v11	1.0 h4	1.0 h1	4.0 v3	4.0 v11	4.0 h11	4.0 h3	5.0 h7	5.0 v7	10.0 v9	10.0 h9	6.0 v1	6.0 v4	3.0 v1
59	0.0047	0.0047	1.27	1	2	2	2.5 h1	2.3 h11	2.5 v12	2.5 v11	3.5 v11	6.0 h11	6.0 h3	7.0 h7	12.0 h9	12.0 v12						
60	0.0047	0.0047	1.35	1	2	2	2.5 h1	2.3 h11	3.0 h4	2.0 h1	4.0 v11	4.0 v11	5.5 v3	5.5 h11	5.5 h3	6.5 h7	7.0 v7	10.0 v9	10.0 h9	4.5 v1		
61	0.0024	0.0024	1.53	1	1	1	2.5 h1	2.3 h11	1.0 v3	1.0 v11	3.0 v11	5.0 h11	5.0 v7	10.0 v9	10.0 h2	3.0 v1	3.0 h1	3.0 h4				
62	0.0024	0.0047	1.16	0	1	2	2.5 h1	2.9 v2	7.0 h2	7.3 v1	4.3 h1	4.3 h5	2.5 v4	0.8 h7	5.5 h9	4.5 v1						
63	0.0024	0.0024	1.28	0	1	1	2.5 h1	2.9 v2	7.0 h2	7.3 v1	4.3 h1	4.3 h5	2.5 v4	0.8 h7	5.5 h9	4.5 v1	3.0 h1	2.0 h4				
64	0.0024	0.0024	1.16	0	1	1	2.5 h1	2.9 v2	7.0 h2	7.3 v1	4.3 h1	4.3 h5	2.5 v4	0.8 h7	3.0 v1	6.0 h9						
65	0.0024	0.0024	1.33	0	1	1	2.5 h1	2.9 v2	7.0 h2	7.3 v1	4.3 h1	4.3 h5	4.0 v5	3.0 h7	3.0 v7	2.0 v10	3.0 v7	10.0 v9	10.0 h9	3.0 v1	3.0 v4	3.0 v1
66	0.0047	0.0047	1.43	0	2	2	2.5 h1	2.9 v2	5.3 h3	5.0 v1	3.0 v5	2.3 h7	2.6 v7	10.0 v9	10.0 h9	3.0 v1						
67	0.0047	0.0094	1.41	0	2	3	2.5 h1	2.9 v2	5.3 h3	5.0 v1	3.0 v5	2.3 h7	2.6 v7	4.0 v10	5.0 v7	10.7 v9	6.5 h9	2.3 v1				
68	0.0024	0.0024	0.97	0	1	1	2.5 h1	2.9 v2	5.3 h3	5.0 v1	3.0 v5	2.3 h7	2.6 v7	4.0 v10	5.0 v7	10.7 v9	6.5 h9	2.3 v1	1.5 h1	3.0 h4		
69	0.0024	0.0024	0.97	0	1	1	2.5 h1	2.9 v2	5.3 h3	5.0 v1	3.0 v5	2.3 h7	2.6 v7	4.0 v10	5.0 v7	10.7 v9	6.5 h9	3.0 h1	3.0 v1	3.0 h4		
70	0.0024	0.0024	1.62	0	1	1	2.5 h1	2.9 v2	5.3 h3	5.0 v1	3.0 v5	2.3 h7	2.6 v7	4.0 v10	5.0 h10	5.0 h7	6.0 v7	10.0 v9	10.0 h9	3.0 v1		
71	0.0024	0.0024	1.66	0	1	1	2.5 h1	2.9 v2	5.3 h3	5.0 v1	4.0 v4	1.0 v1	1.0 v5	3.0 h7	3.0 v7	5.0 v10	6.0 v7	10.0 v9	10.0 h9	3.0 v1		
72	0.0071	0.0071	1.74	0	3	3	2.5 h1	2.9 v2	5.3 h3	5.8 h7	12.0 h9	9.0 v1	3.4 h1	5.0 h5	3.0 v4	2.4 h7	4.0 h9	3.0 v1				
73	0.0047	0.0047	1.42	0	2	2	2.5 h1	2.9 v2	5.3 h3	5.8 h7	12.0 h9	9.0 v1	3.4 h1	4.5 h4	4.0 v4	2.5 v1						
74	0.0024	0.0024	1.56	0	1	1	2.5 h1	2.9 v2	3.5 v1	3.5 h3	2.0 v5	1.5 h7	1.5 v7	5.0 v9	5.0 h9	3.0 v1						
75	0.0024	0.0024	1.50	0	1	1	2.5 h1	2.0 v1	4.0 v3	5.0 h3	6.0 h7	6.0 v7	10.0 v9	10.0 h9	3.0 v1	3.0 h1	5.0 h4	1.0 v4				
76	0.0024	0.0024	2.48	0	1	1	2.5 h1	2.0 v1	4.0 v3	6.0 v7	11.0 v9	11.0 h2	6.0 v1	6.0 h1	5.0 h4	1.0 v4						
77	0.0024	0.0024	1.64	0	1	1	2.5 h1	2.0 h4	2.0 v4	1.0 v1	1.0 h1	4.0 v3	1.4 h3	6.0 h7	6.0 v7	10.0 v9	11.0 h9	6.0 v1				
78	0.0024	0.0024	1.64	0	1	1	2.5 h1	2.0 h4	2.0 v4	1.0 v1	1.0 h1	4.0 v3	1.4 h3	3.0 v7	3.0 h7	5.0 v9	5.5 h9	6.0 v1				
79	0.1479	0.1526	1.55	1	63	65	2.5 h12	2.4 h11	3.0 v11	3.8 v3	3.9 v11	5.1 h11	6.4 v7	10.2 v9	10.3 h12	3.7 v1						
80	0.0047	0.0047	1.78	1	2	2	2.5 h12	2.4 h11	3.0 v11	3.8 v3	3.9 v11	5.1 h11	6.4 v7	10.2 v9	10.3 h12	3.7 v1	11.0 v4	3.0 v1				
81	0.0024	0.0024	1.53	1	1	1	2.5 h12	2.4 h11	3.0 v11	3.8 v3	3.9 v11	5.1 h11	6.4 v7	7.0 v10	2.4 v7	10.0 h12	10.0 v9	3.0 v1				
82	0.0024	0.0024	1.53	1	1	1	2.5 h12	2.4 h11	3.0 v11	3.8 v3	3.9 v11	5.1 h11	6.4 v7	7.0 v10	2.4 v7	5.0 v9	5.0 h12	3.0 v1				
83	0.0728	0.0752	1.45	1	31	32	2.5 h12	2.4 h11	3.0 v11	4.0 v11	4.0 v3	4.9 h11	6.2 v7	10.1 v9	10.2 h12	3.8 v1						
84	0.0024	0.0024	1.27	1	1	1	2.5 h12	2.4 h11	3.0 v11	4.0 v11	4.0 v3	4.9 h11	6.2 v7	10.1 v9	10.2 h12	3.8 v1	11.0 v4	6.0 v1	6.0 v4	3.0 v1		
85	0.0024	0.0024	1.29	1	1	1	2.5 h12	2.4 h11	3.0 v11	4.0 v11	4.0 v3	4.9 h11	6.2 v7	5.0 v10	5.0 v7	10.0 v9	10.0 h12	3.0 v1				

Digit 9 (continued)

86	0 0118	0 0141	1 29	1	5	6	2 5 h12	2.4 h11	3 0 v11	4 0 v11	4 5 h11	5 2 v3	7 4 v7	10 0 v9	10 0 h12	3 5 v1		
87	0 0024	0 0024	1 18	1	1	1	2 5 h12	2 4 h11	3 0 v11	4 0 v11	4 5 h11	5 2 v3	7.4 v7	10 0 v9	10 0 h12	3 5 v1	3 0 v4	3 0 v1
88	0 0024	0 0024	1 15	1	1	1	2.5 h12	2.4 h11	3 0 v11	4 0 v11	4.0 v2	8 0 h11	12 0 h12	12.0 v1	12.0 v4	6 0 v1		
89	0 0024	0 0024	1 94	1	1	1	2 5 h12	2.4 h11	3 0 v11	4 0 v11	4 0 v12	5 0 h11	12.0 h12	6 0 v12				
90	0 0047	0 0047	1 44	1	2	2	2.5 h12	2.4 h11	3 0 v11	4 0 v12	4 0 v11	8 0 h11	11.5 h12	4 5 v12				
91	0 0071	0.0071	1 82	1	3	3	2.5 h12	2.4 h11	2 0 v3	2 0 v11	3 7 v11	4 4 h11	6.4 v7	10 7 v9	10 7 h12	5 0 v1		
92	0 0024	0 0024	1 56	0	1	1	2 5 h12	1 0 v3	5 0 v7	10 0 v9	10 0 h12	3 0 v1	2 0 v4	3 0 v1				
93	0 0024	0 0024	1 50	0	1	1	1.0 v1	1 0 h1	2.0 v3	2.5 h3	3 0 h7	3 0 v7	5 0 v9	5 0 h9	1 5 v1	1 5 h1	2 5 h4	1 0 v4
94	0 0024	0 0024	2.48	0	1	1	1 0 v1	1 0 h1	2 0 v3	3 0 v7	5 5 v9	5.5 h2	3 0 v1	3 0 h1	2 5 h4	1 0 v4		

Extended sample set size 426

APPENDIX C

TREES

C.1 Tree for Digit 0

405 Samples

297 Nodes

43 Paths [Number of Terminal Nodes]

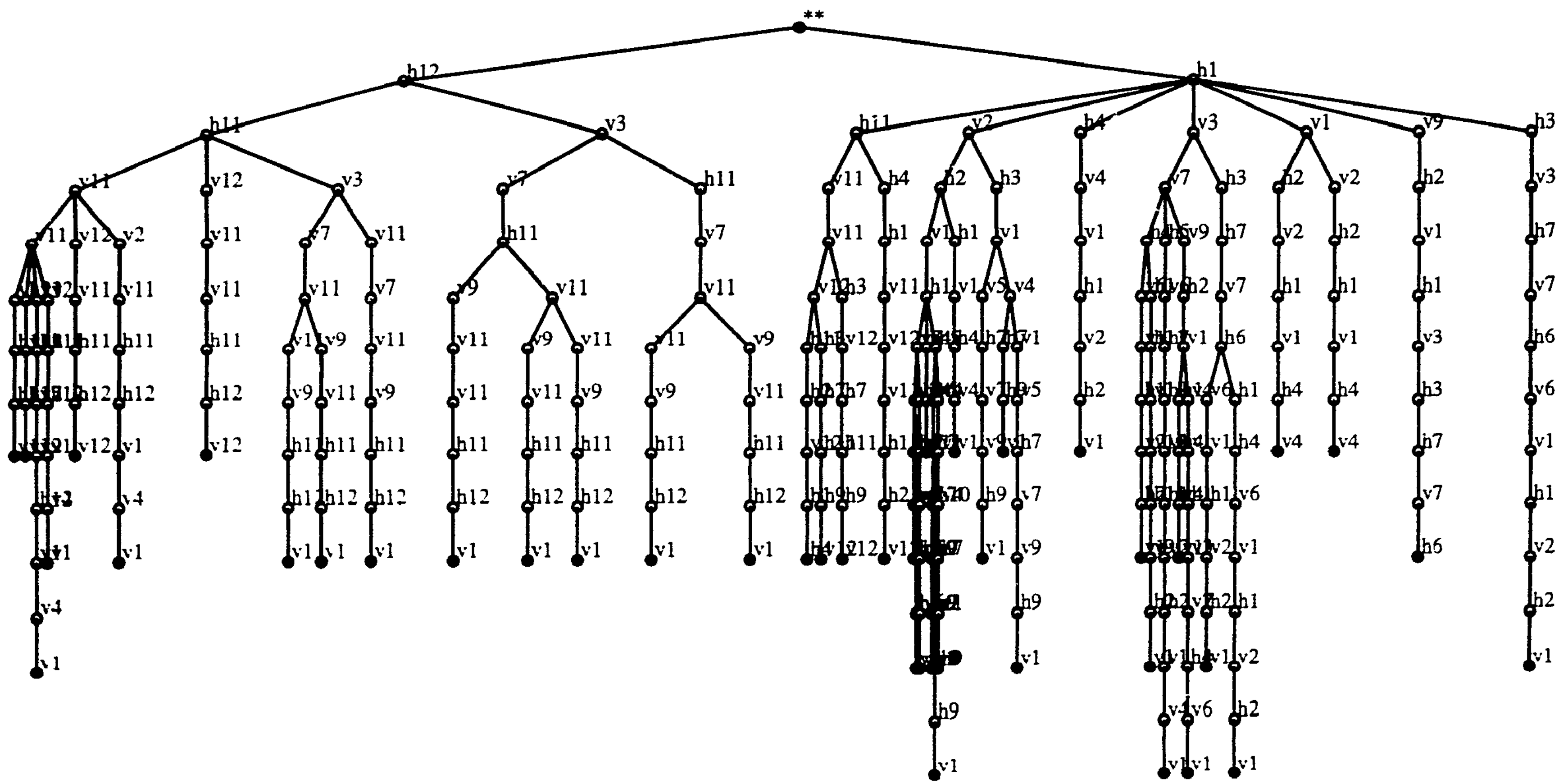

C.2 Tree for Digit 1

416 Samples

51 Nodes

13 Paths [Number of Terminal Nodes]

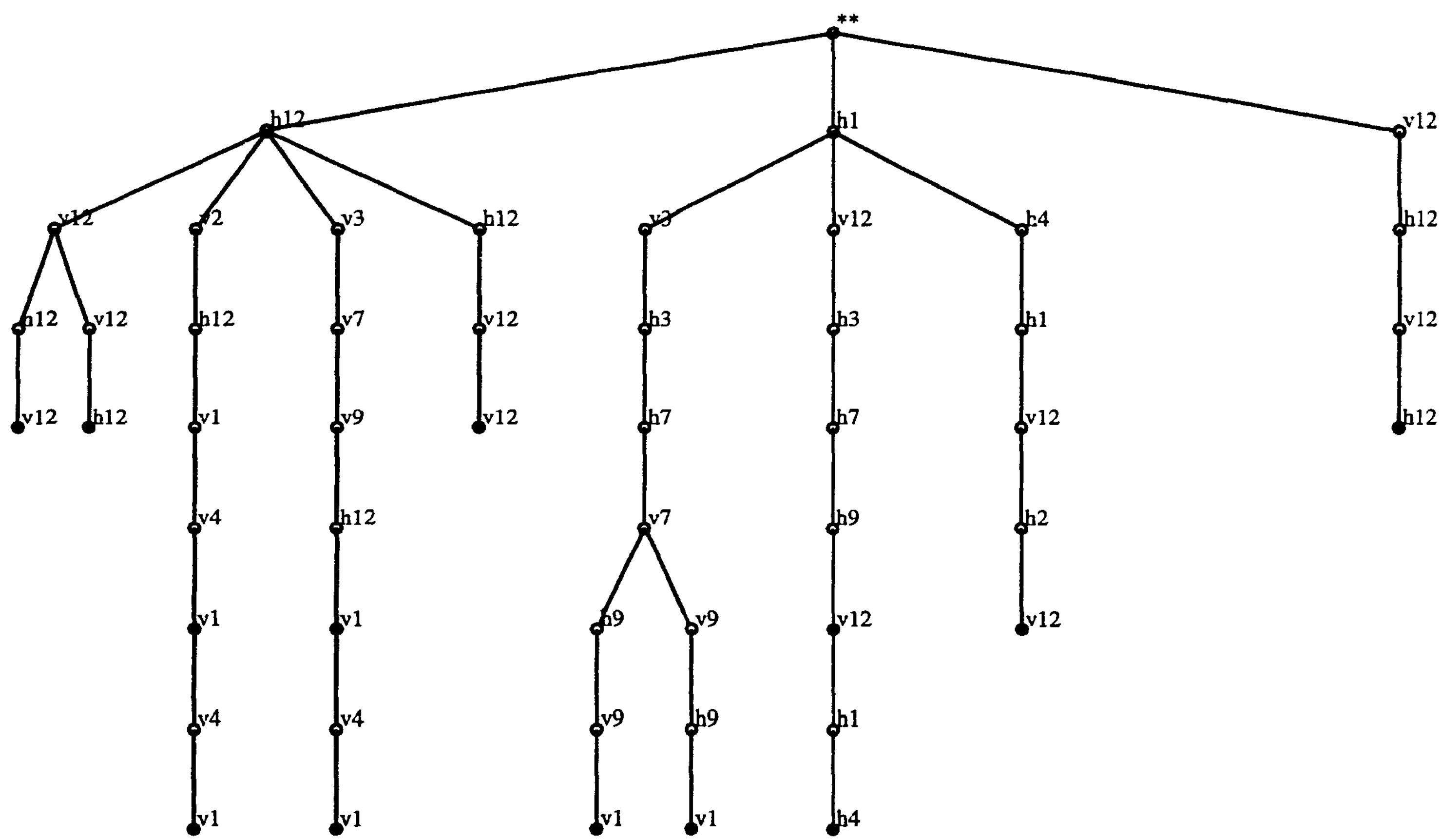

C.3 Tree for Digit 2

422 Samples
1026 Nodes
167 Paths [Number of Terminal Nodes]

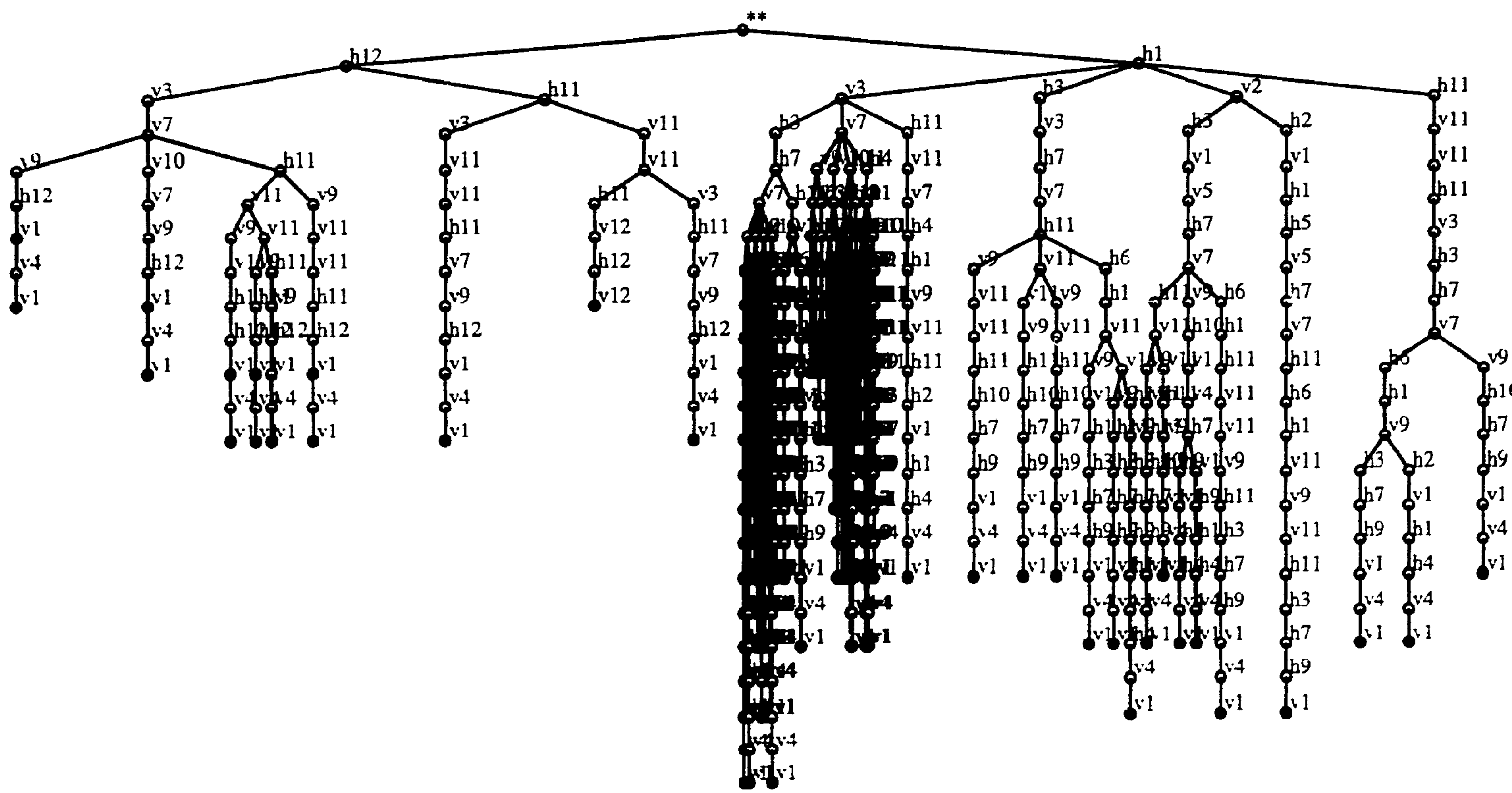

C.4 Tree for Digit 3

408 Samples

376 Nodes

66 Paths [Number of Terminal Nodes]

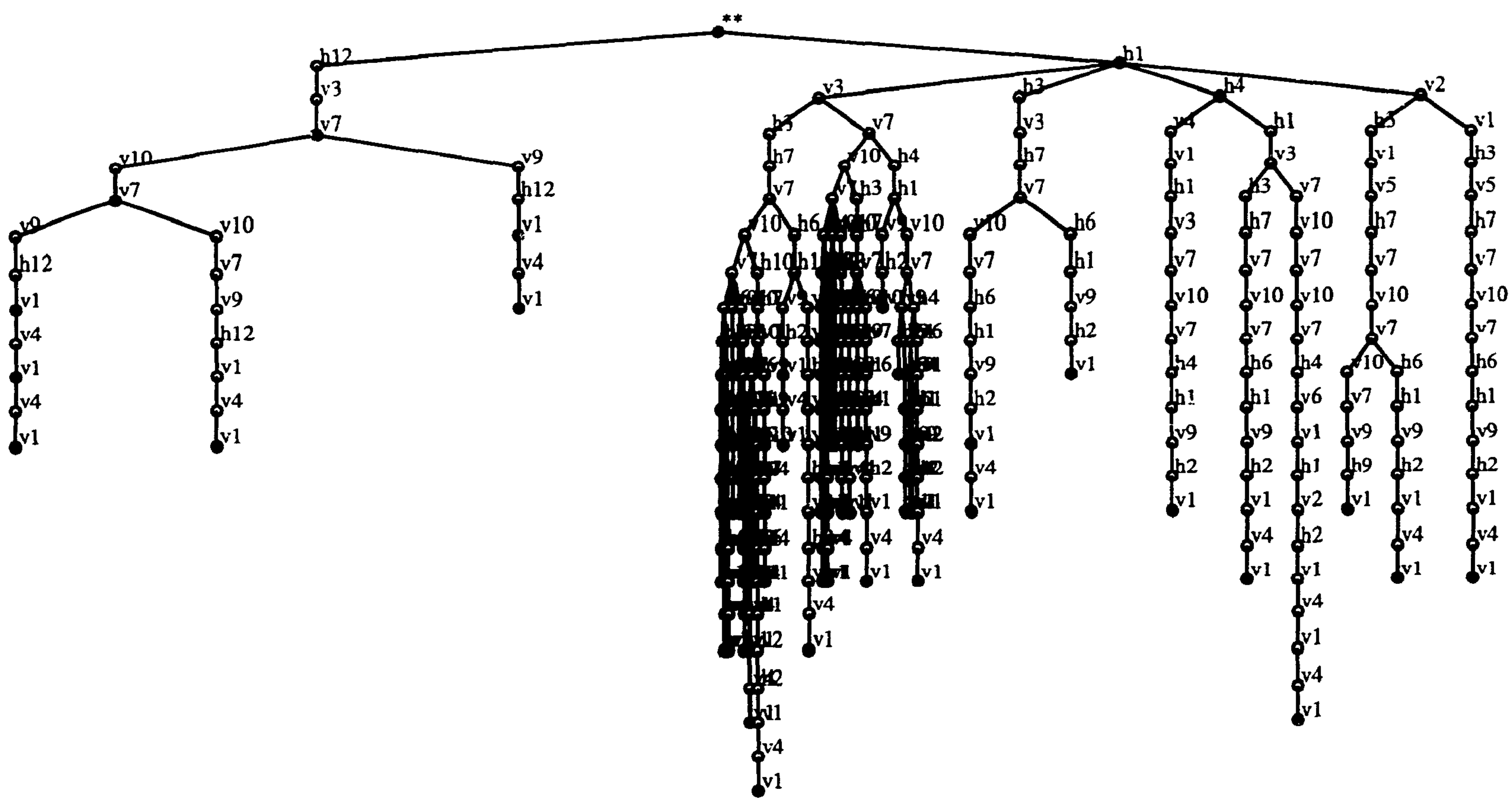

C.5 Tree for Digit 4

458 Samples

697 Nodes

135 Paths [Number of Terminal Nodes]

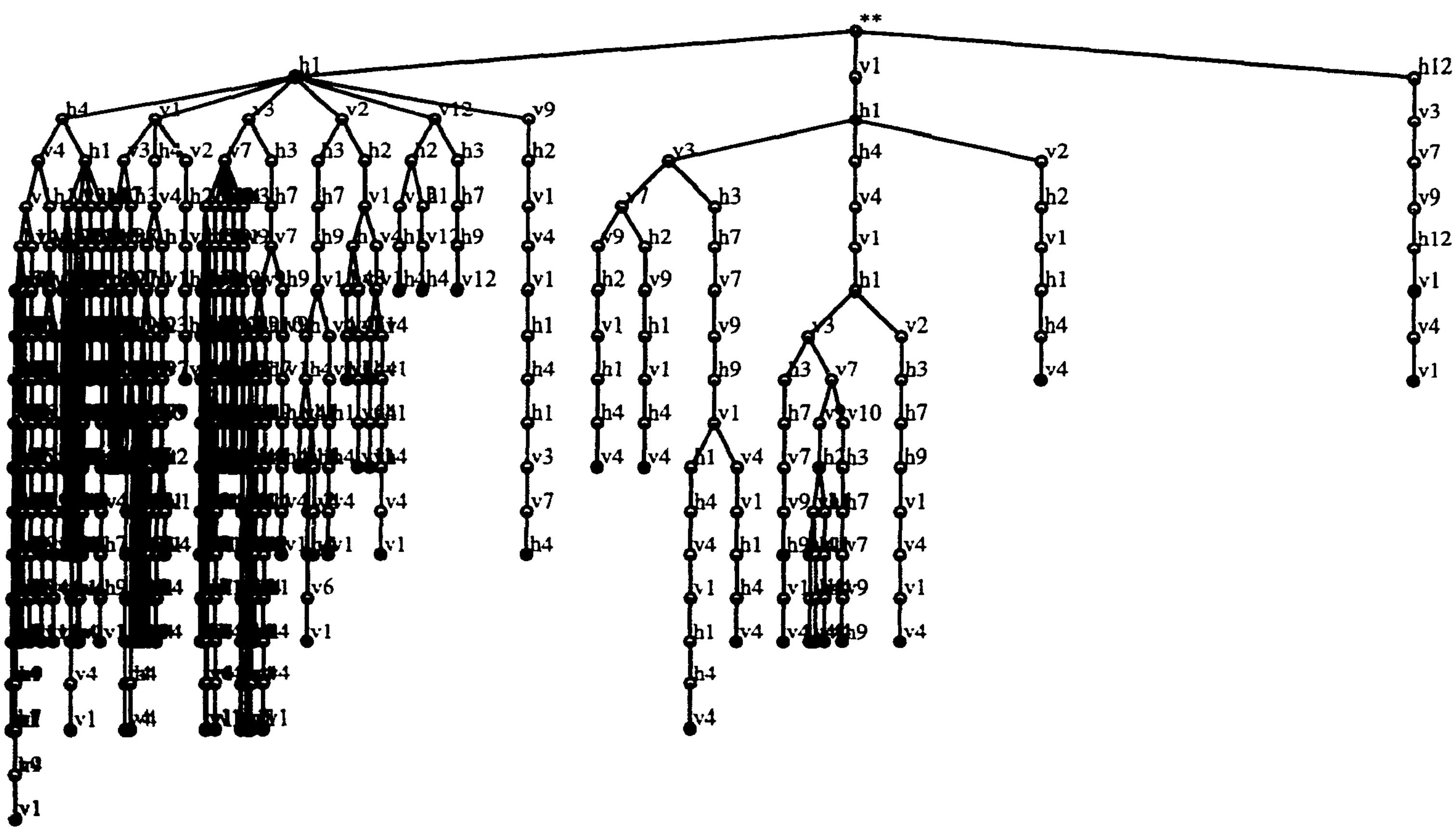

C.6 Tree for Digit 5

419 Samples
451 Nodes
76 Paths [Number of Terminal Nodes]

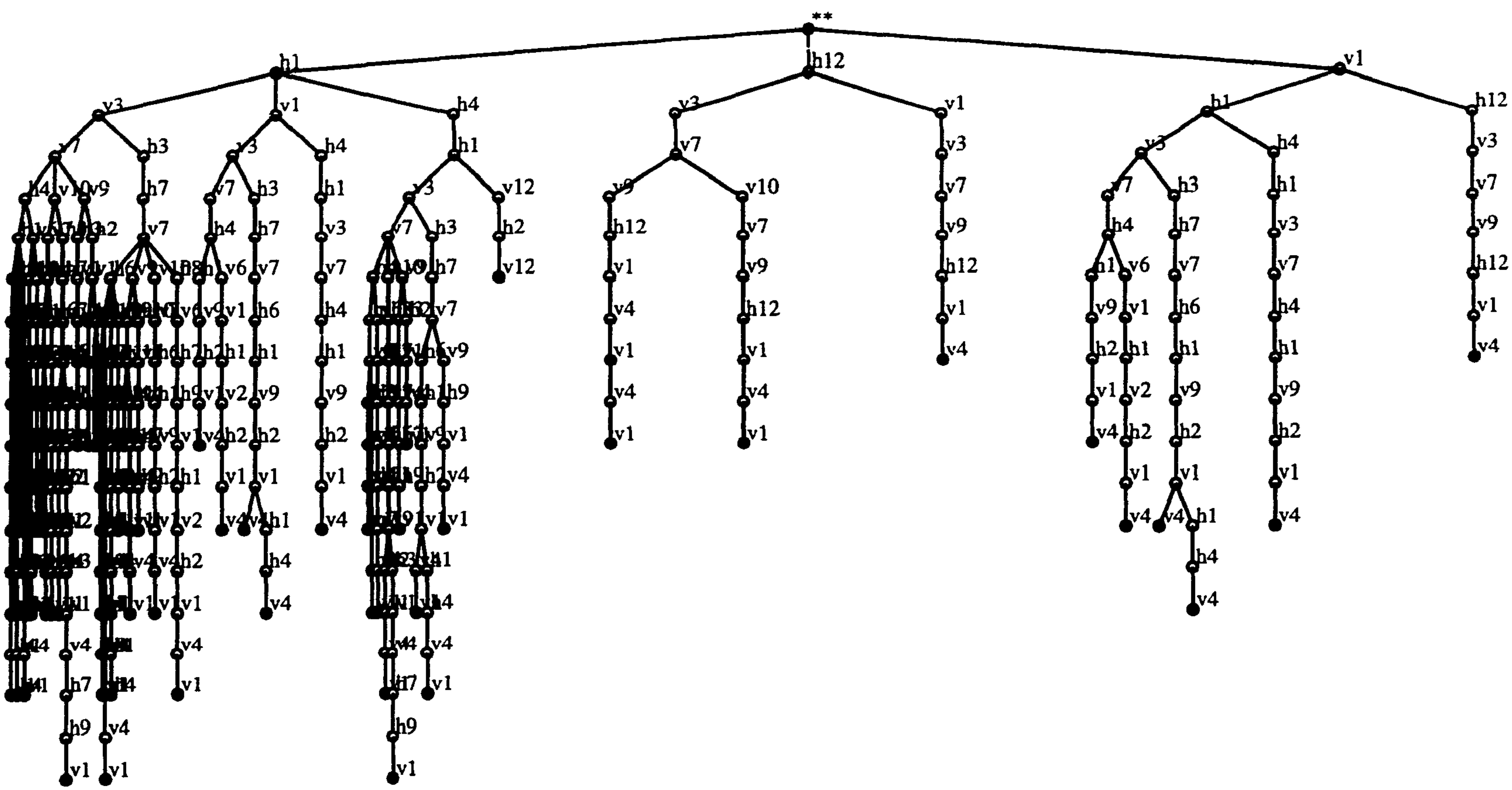

C.7 Tree for Digit 6

421 Samples

677 Nodes

93 Paths [Number of Terminal Nodes]

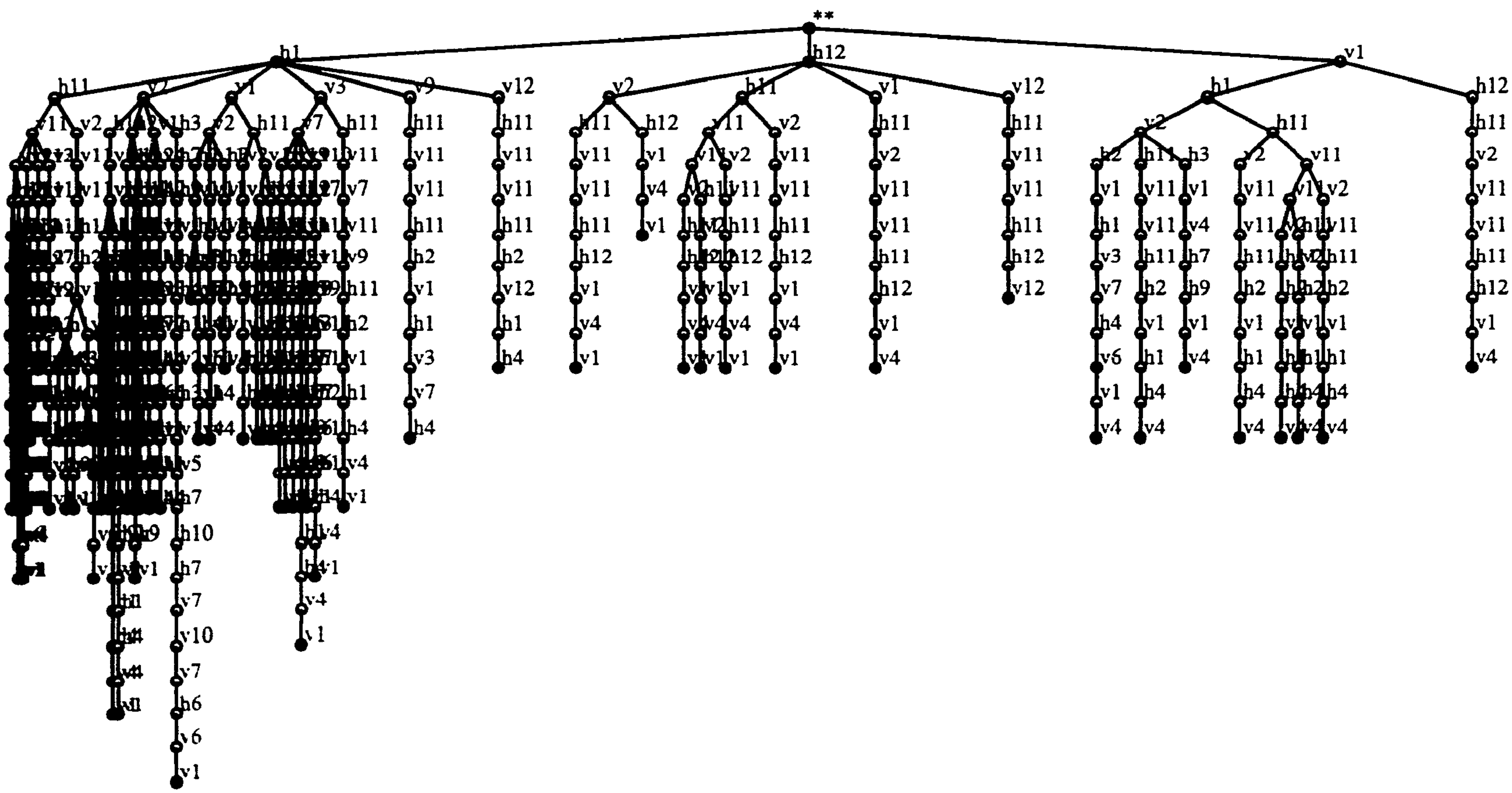

C.8 Tree for Digit 7

430 Samples

226 Nodes

40 Paths [Number of Terminal Nodes]

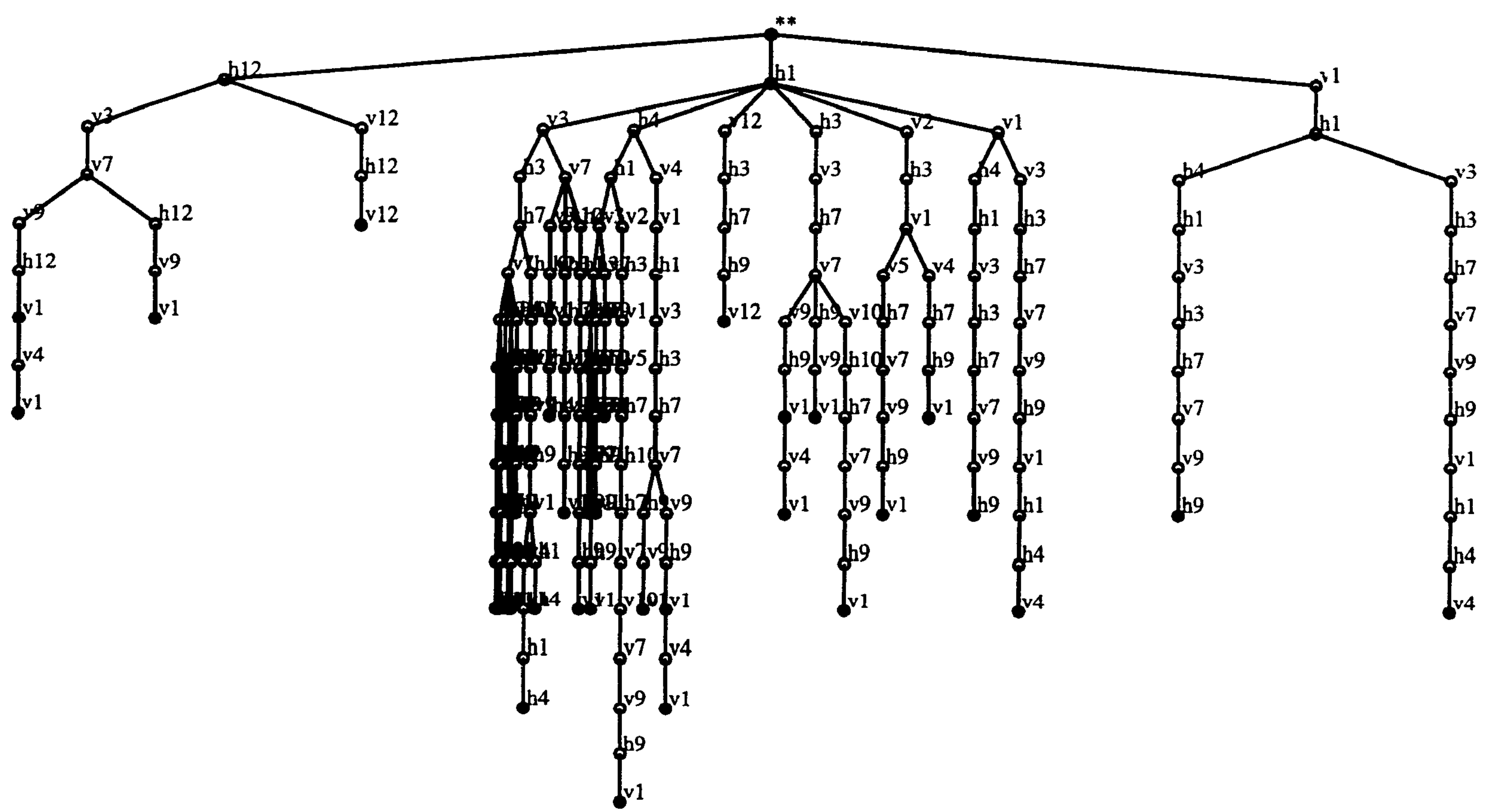

C.9 Tree for Digit 8

423 Samples

1747 Nodes

211 Paths [Number of Terminal Nodes]

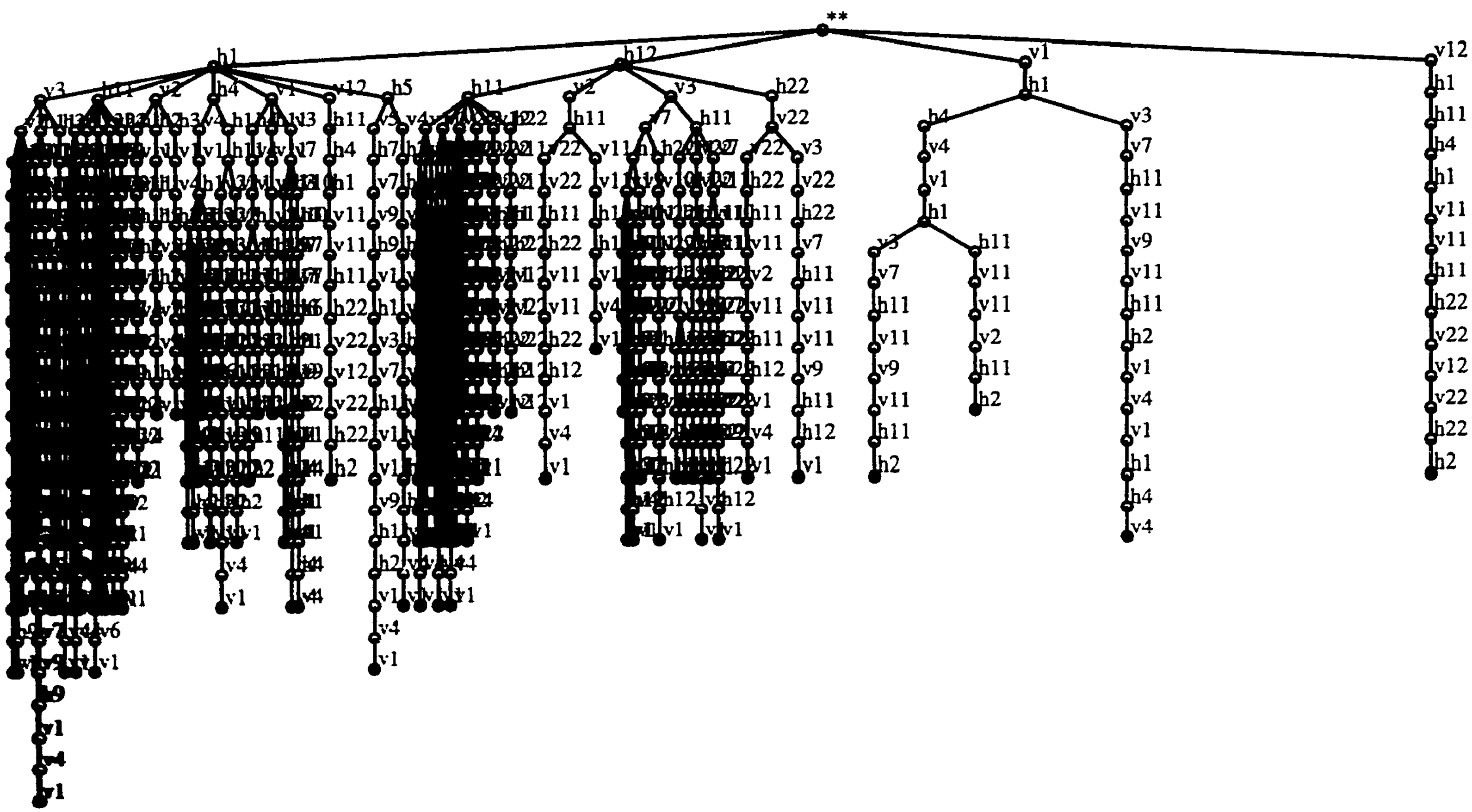

C.10 Tree for Digit 9

426 Samples
571 Nodes
94 Paths [Number of Terminal Nodes]

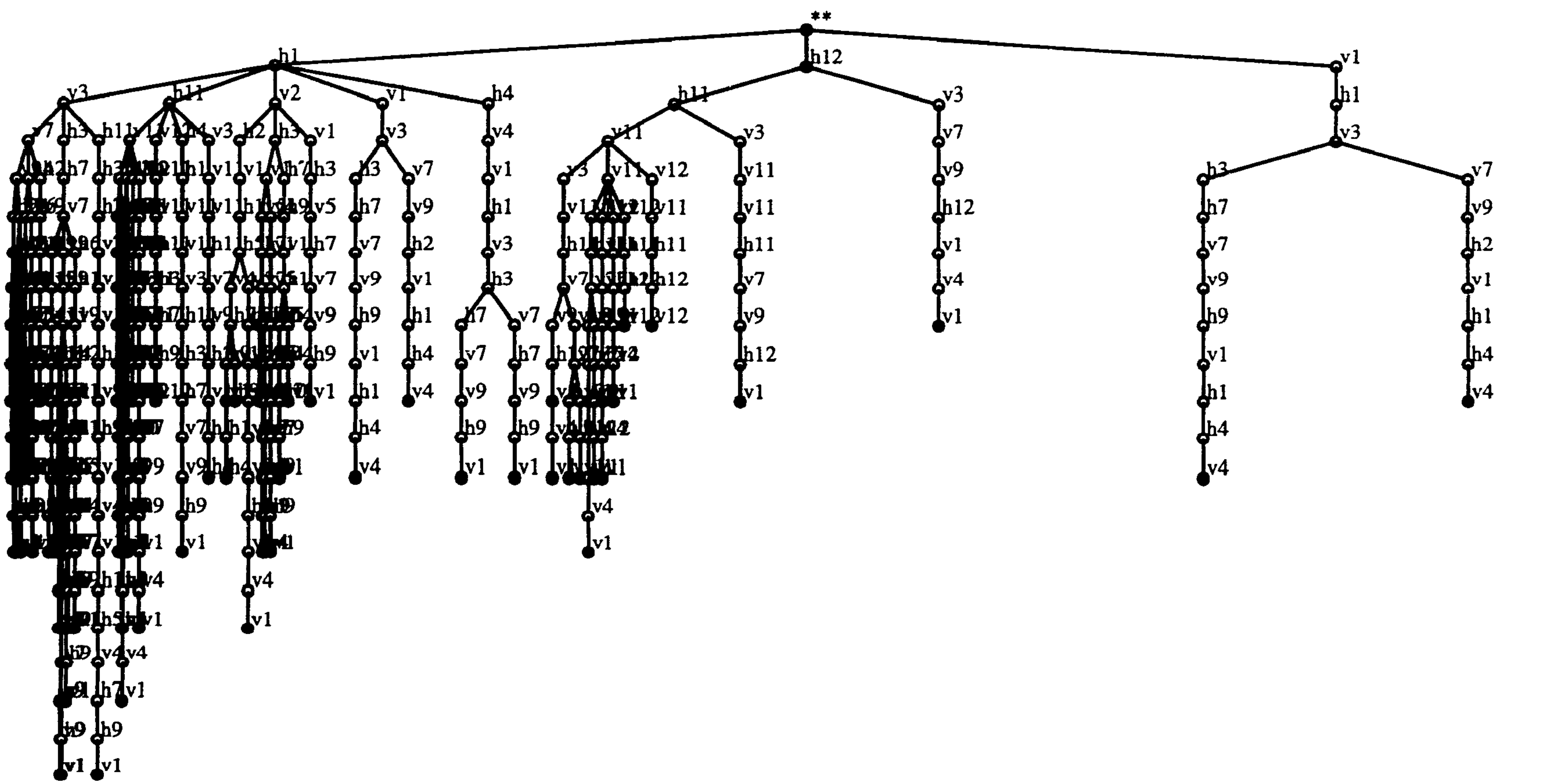

SUBTREES

C.11 First Level Subtrees for Digit 0

405 Samples

297 Nodes

15 Paths [Number of SubTree Terminal Nodes]

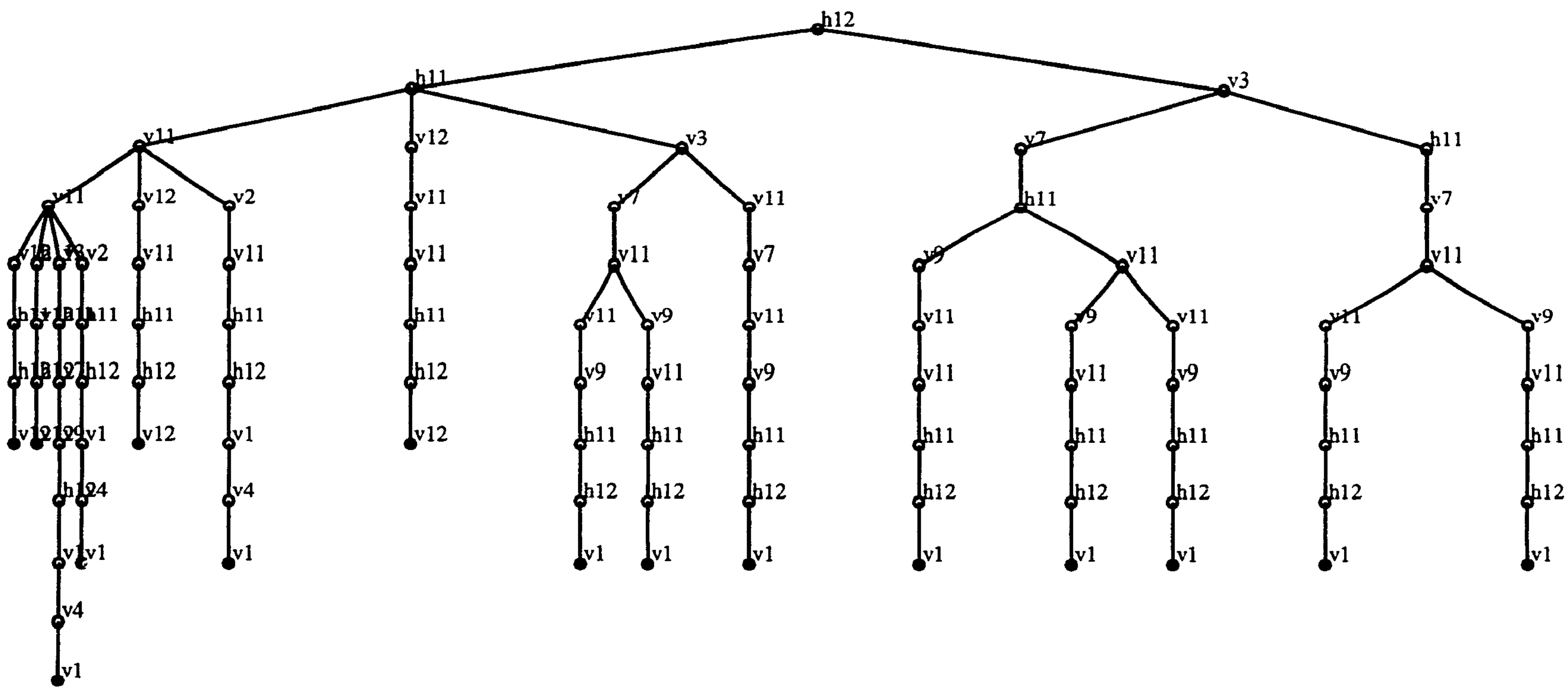

Digit 0 [continued]

405 Samples

297 Nodes

28 Paths [Number of SubTree Terminal Nodes]

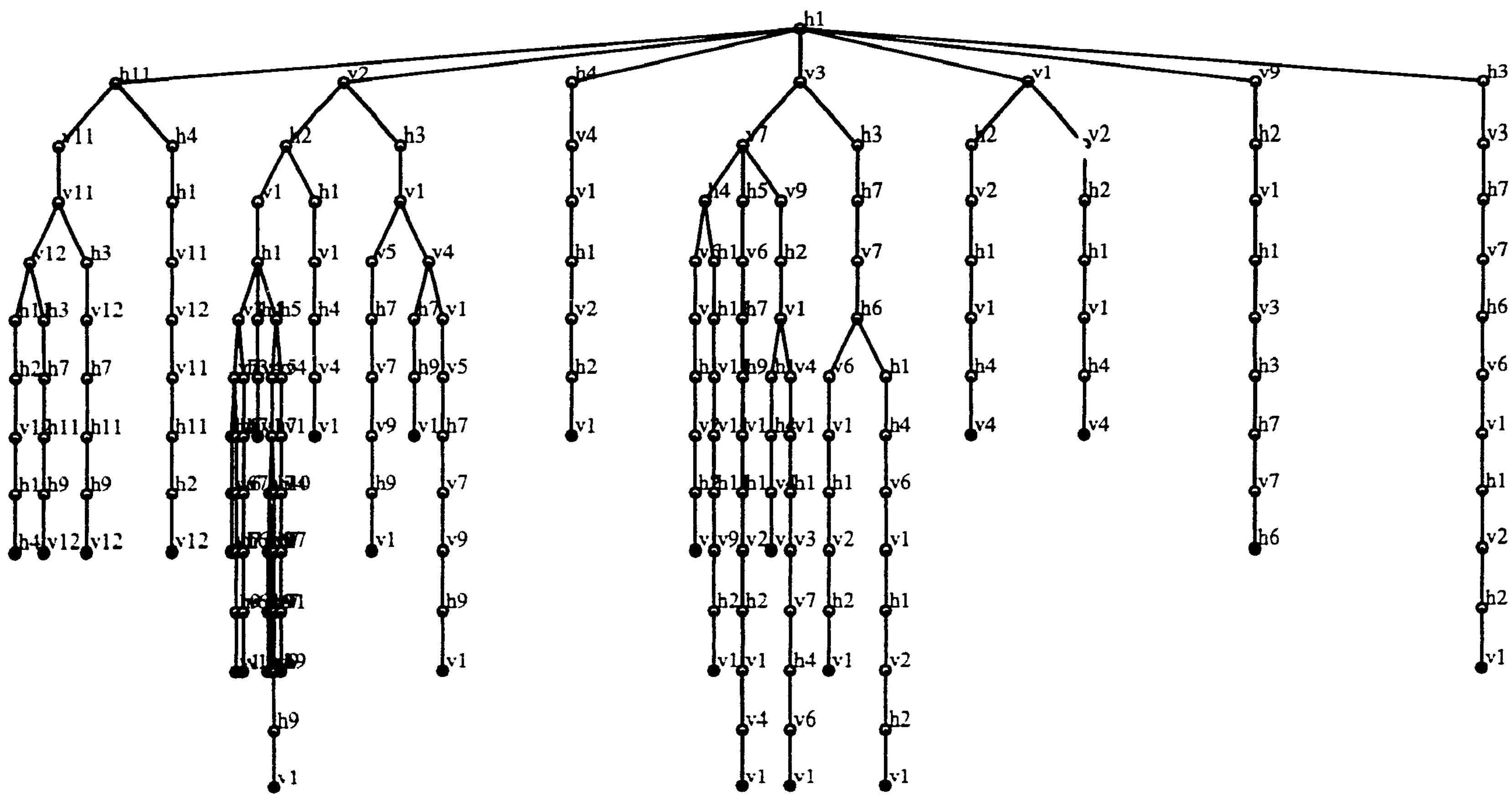

C.12 First Level Subtrees for Digit 1

416 Samples

51 Nodes

7 Paths [Number of SubTree Terminal Nodes]

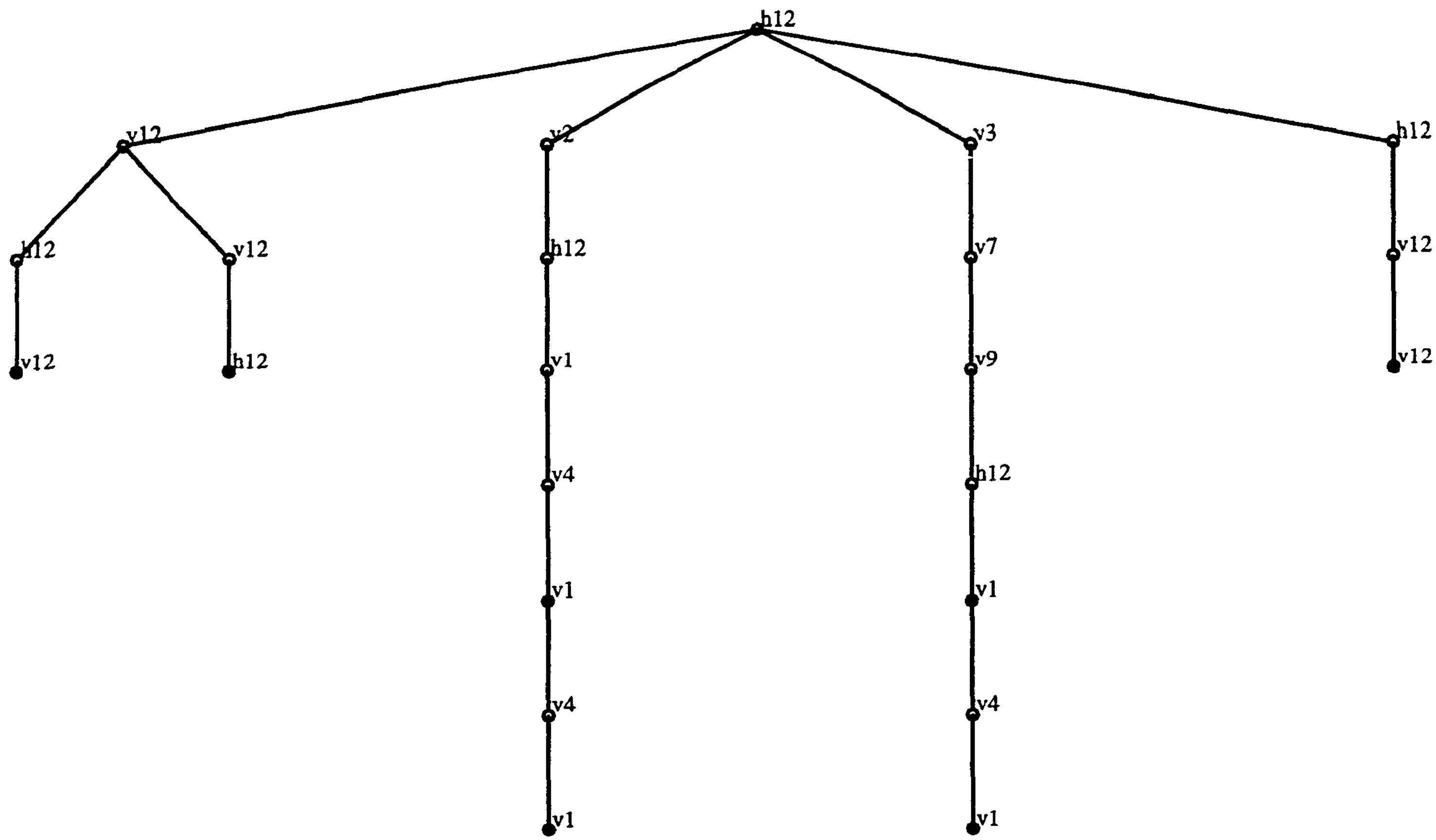

Digit 1 [continued]

416 Samples
51 Nodes
5 Paths [Number of SubTree Terminal Nodes]

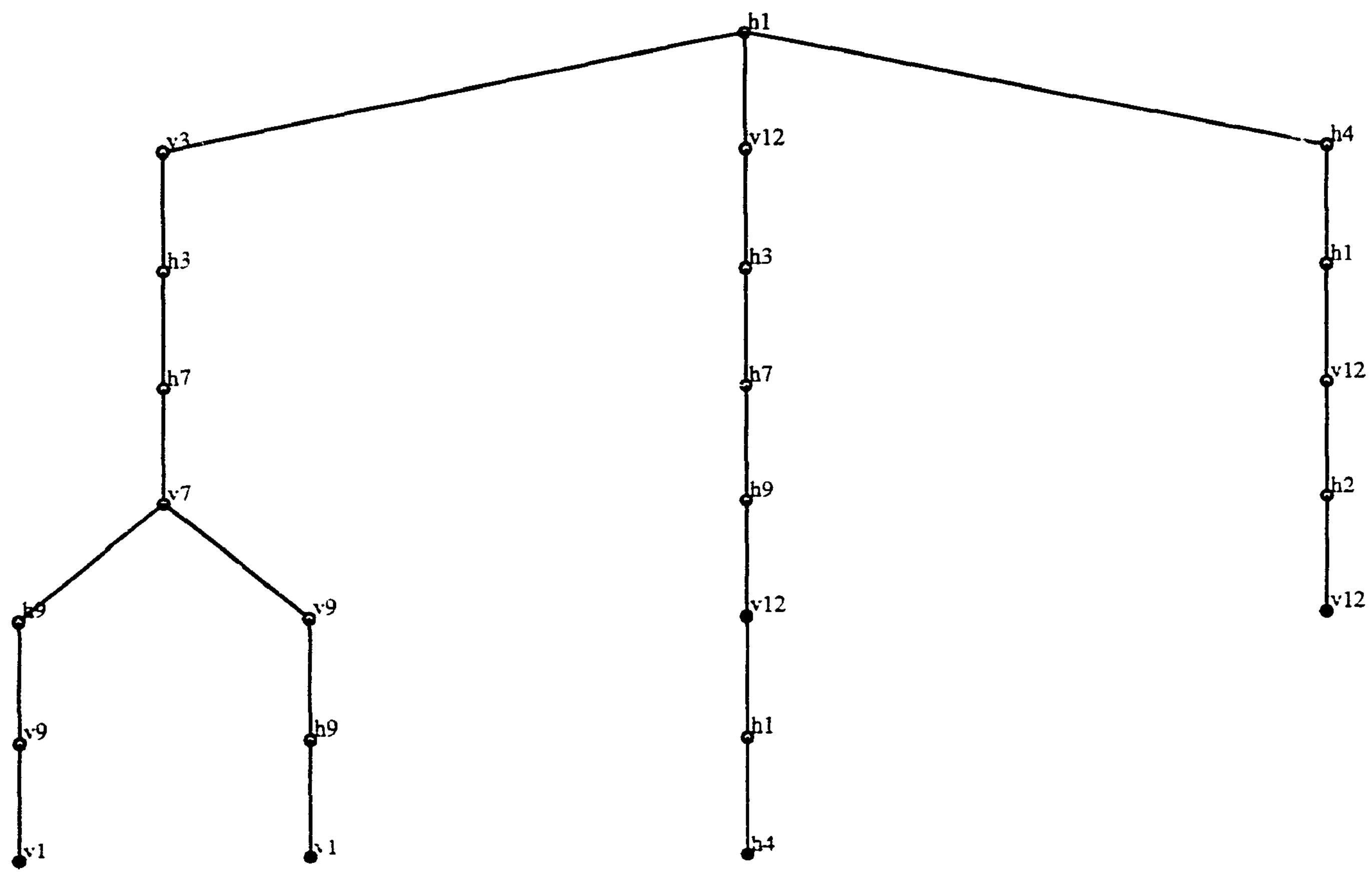

Digit 1 [continued]

416 Samples

51 Nodes

1 Paths [Number of SubTree Terminal Nodes]

C.13 First Level Subtrees for Digit 2

422 Samples

1026 Nodes

14 Paths [Number of SubTree Terminal Nodes]

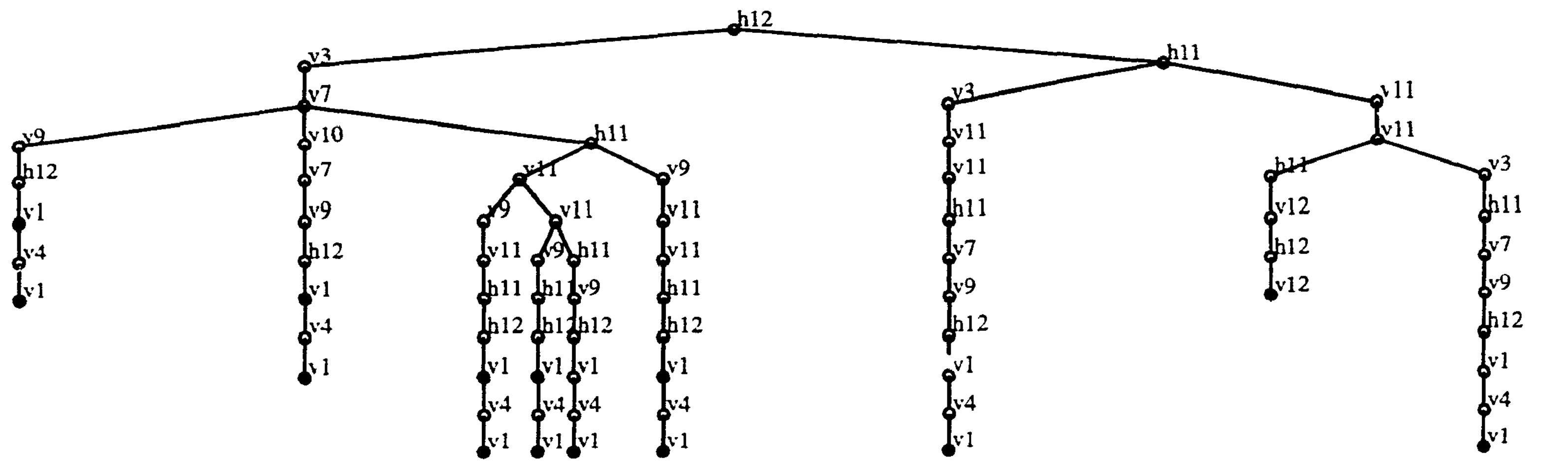

Digit 2 [continued]

422 Samples

1026 Nodes

153 Paths [Number of SubTree Terminal Nodes]

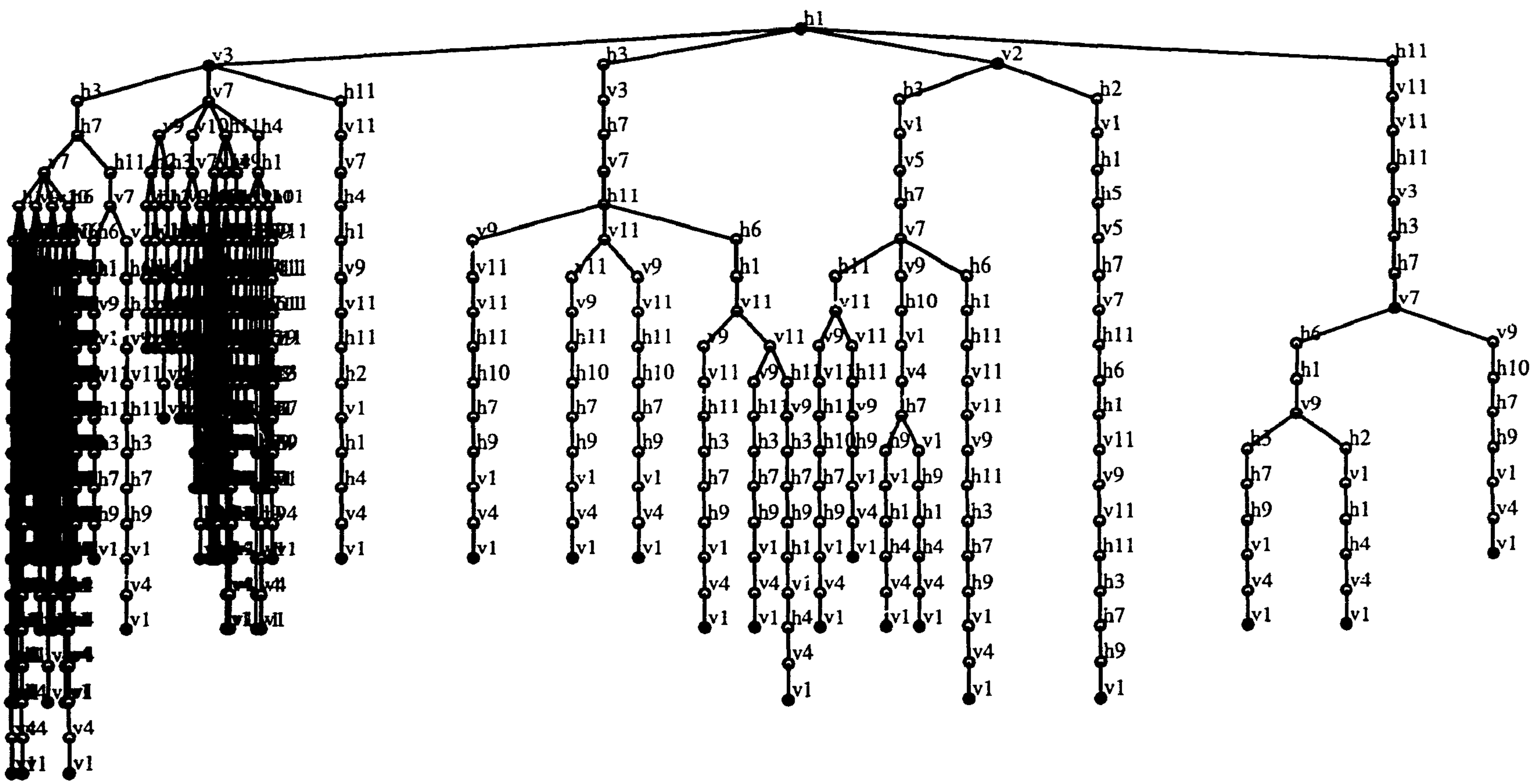

C.14 First Level Subtrees for Digit 3

408 Samples

376 Nodes

6 Paths [Number of SubTree Terminal Nodes]

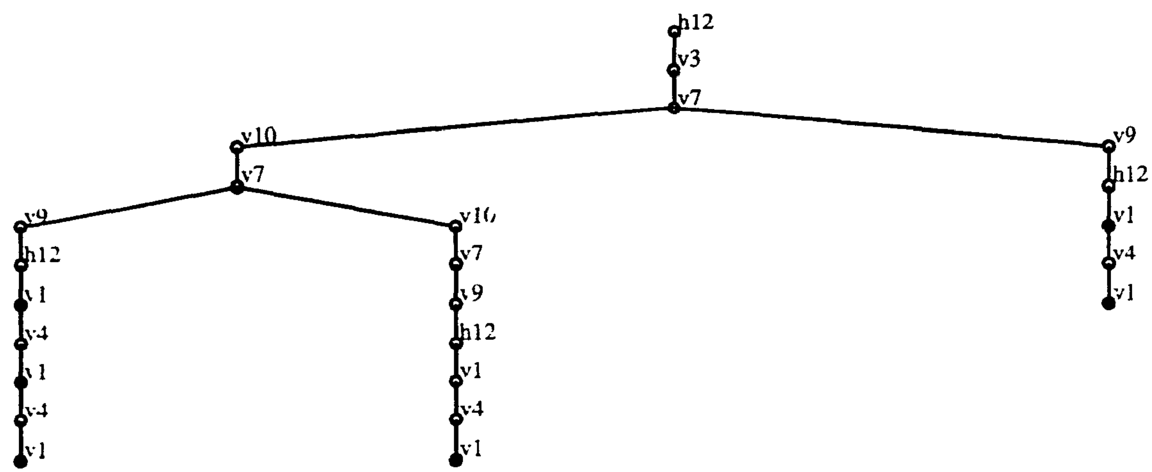

Digit 3 [continued]

408 Samples
376 Nodes
60 Paths [Number of SubTree Terminal Nodes]

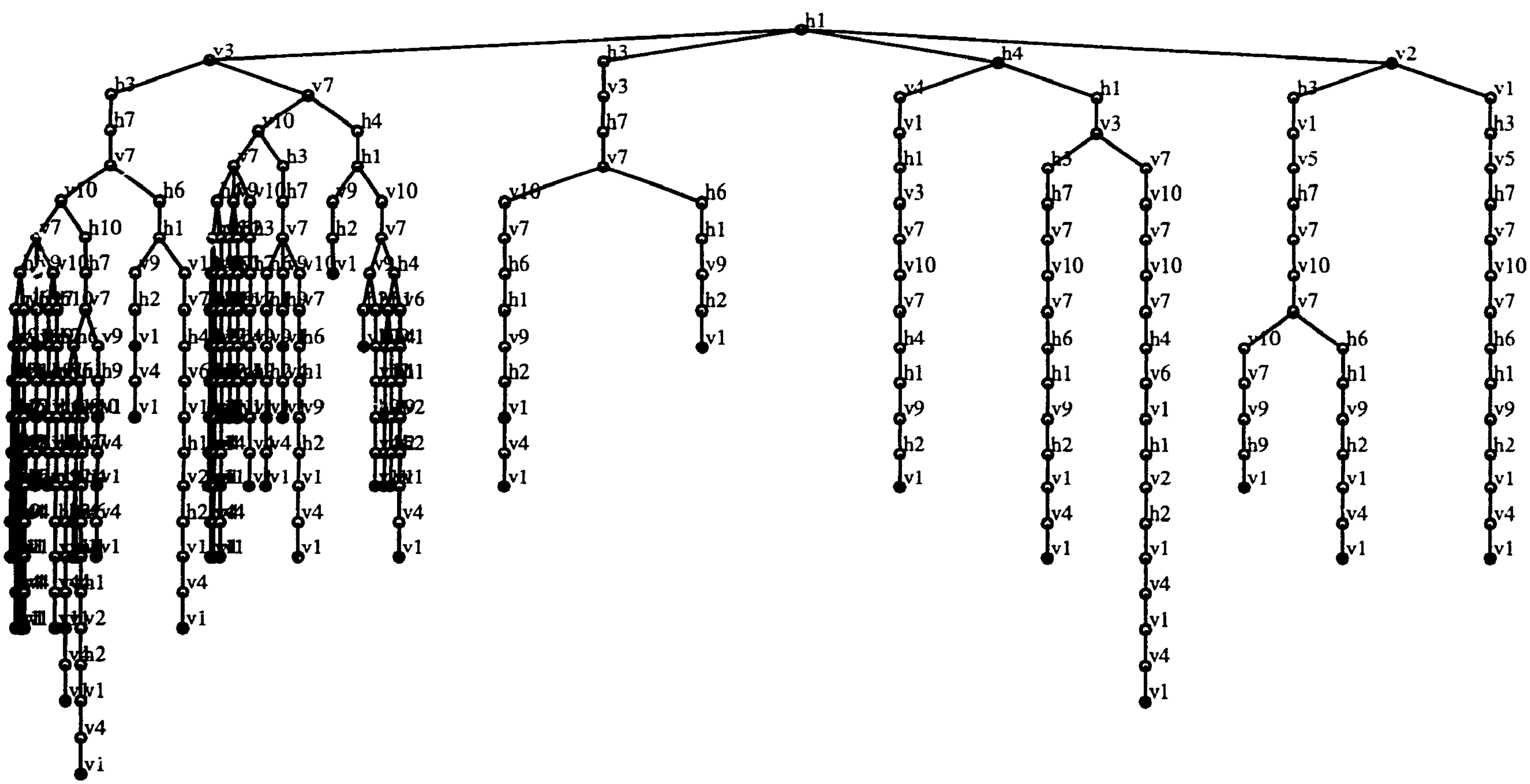

C.15 First Level Subtrees for Digit 4

458 Samples

697 Nodes

119 Paths [Number of SubTree Terminal Nodes]

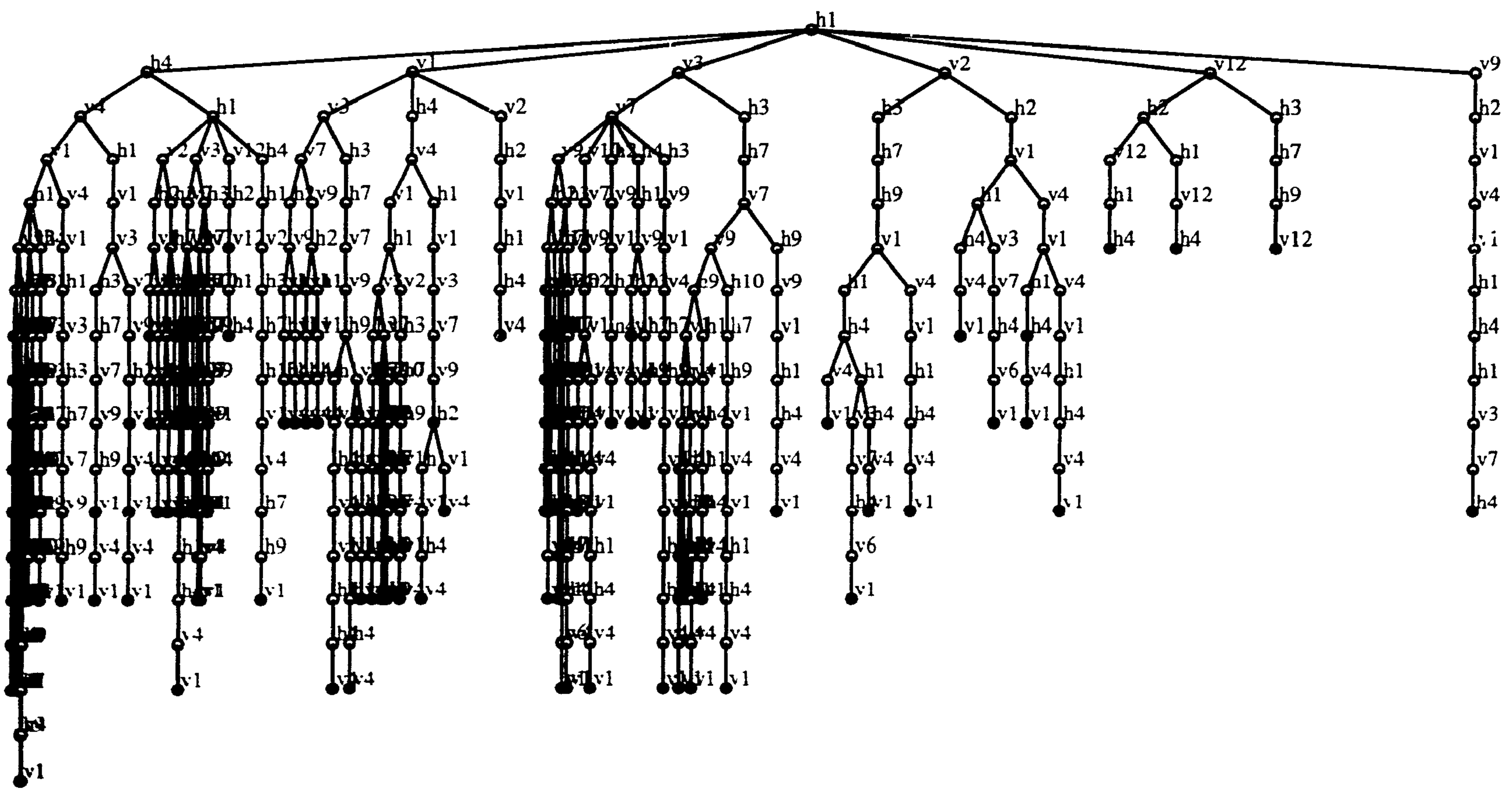

Digit 4 [continued]

458 Samples

697 Nodes

14 Paths [Number of SubTree Terminal Nodes]

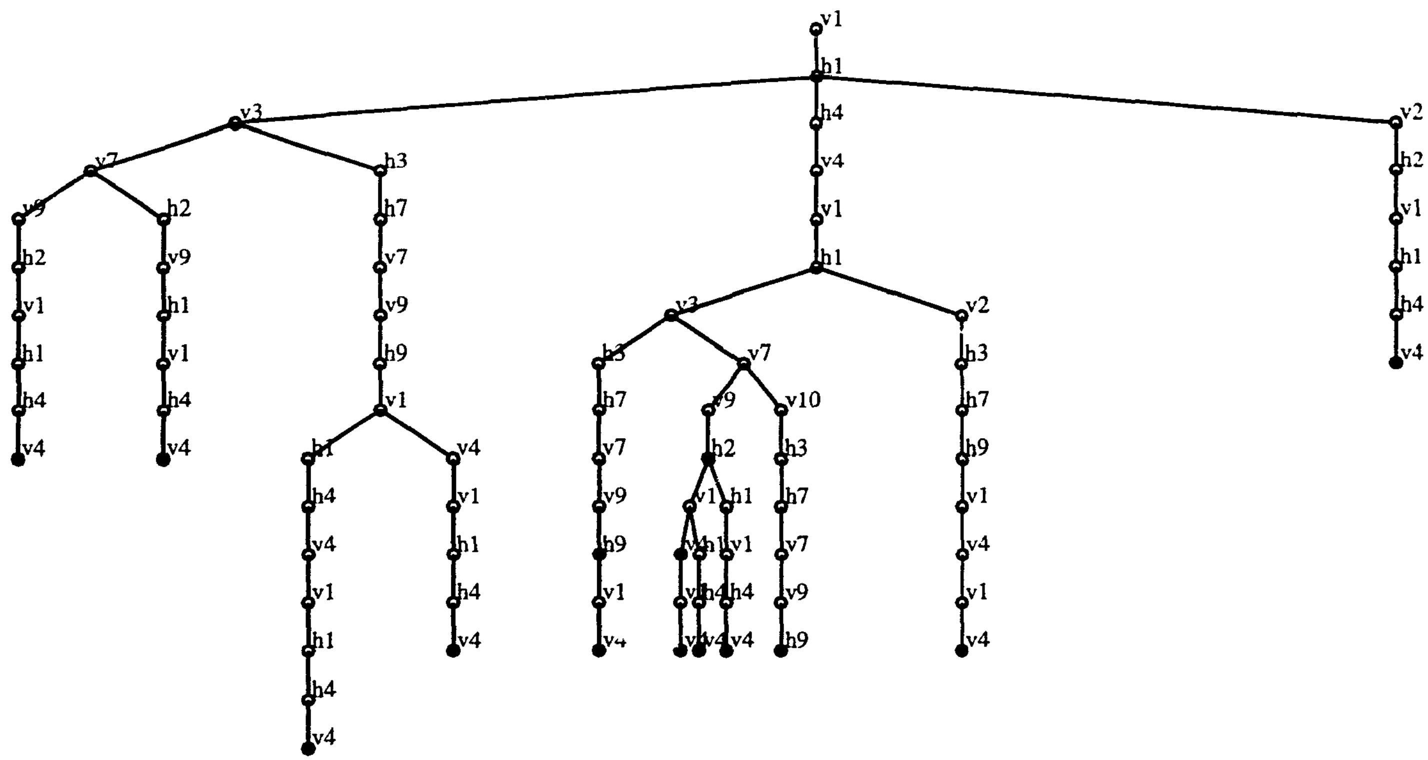

Digit 4 [continued]

458 Samples

697 Nodes

2 Paths [Number of SubTree Terminal Nodes]

C.16 First Level Subtrees for Digit 5

419 Samples

451 Nodes

66 Paths [Number of SubTree Terminal Nodes]

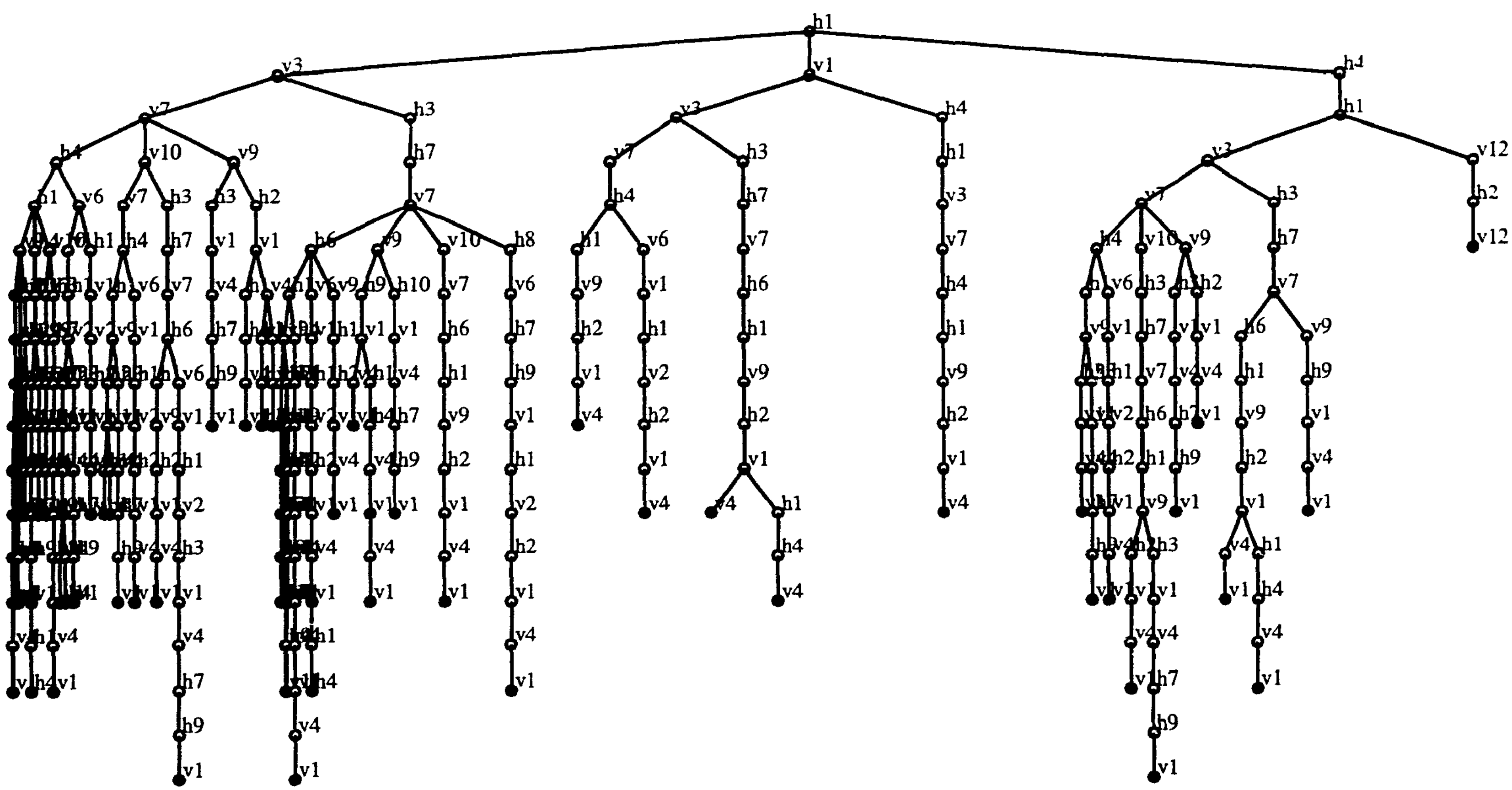

Digit 5 [continued]

419 Samples

451 Nodes

4 Paths [Number of SubTree Terminal Nodes]

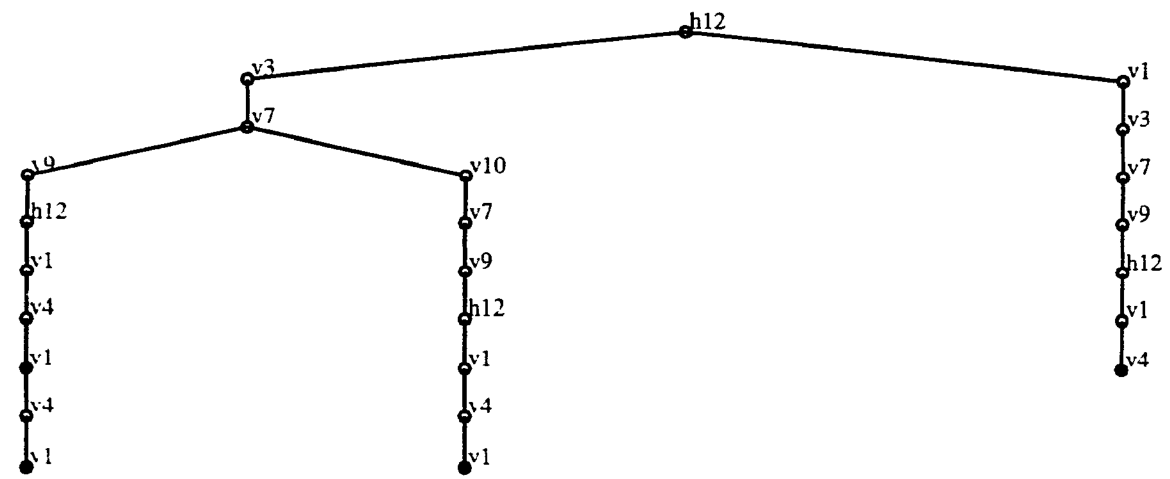

Digit 5 [continued]

419 Samples

451 Nodes

6 Paths [Number of SubTree Terminal Nodes]

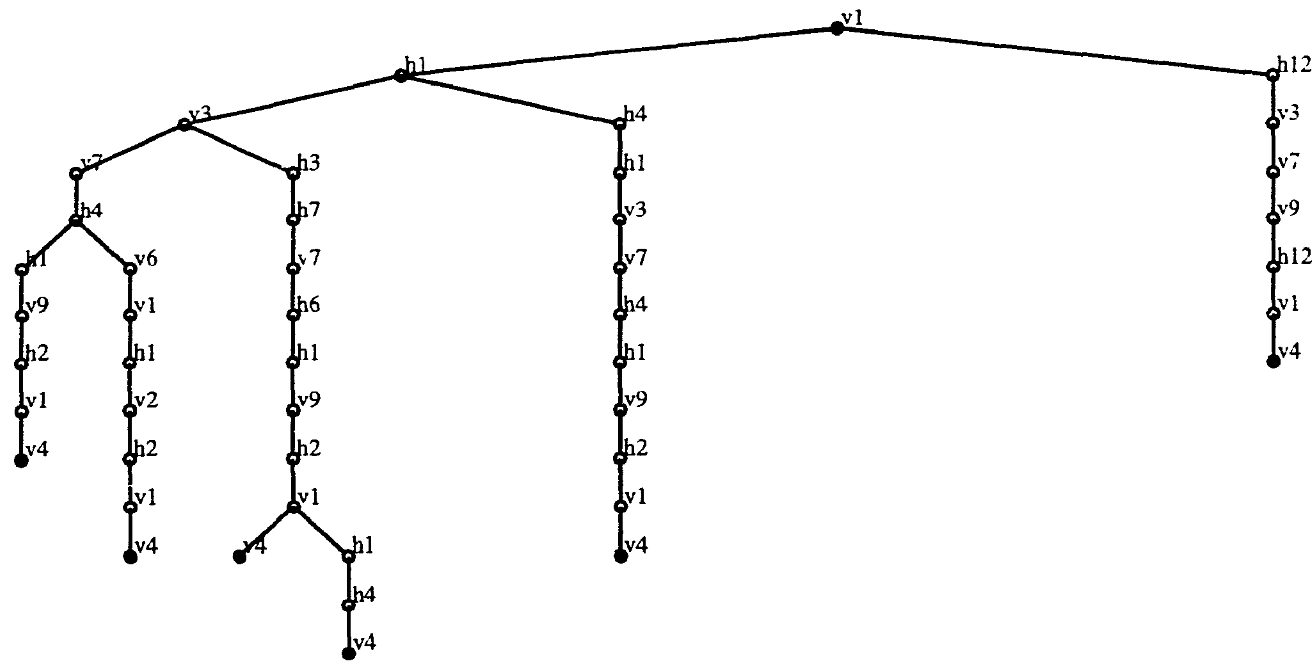

C.17 First Level Subtrees for Digit 6

421 Samples

677 Nodes

76 Paths [Number of SubTree Terminal Nodes]

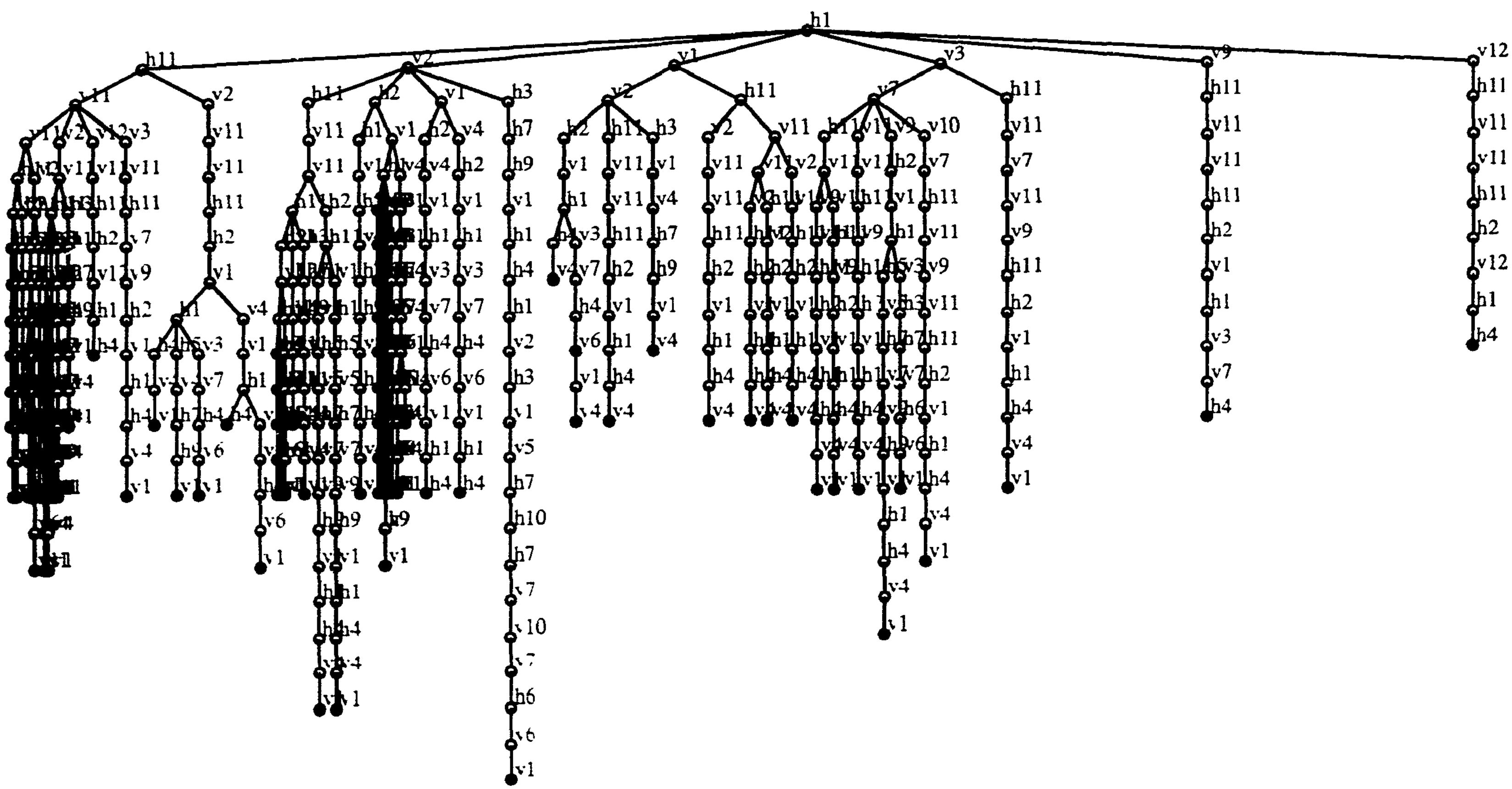

Digit 6 [continued]

421 Samples

677 Nodes

8 Paths [Number of SubTree Terminal Nodes]

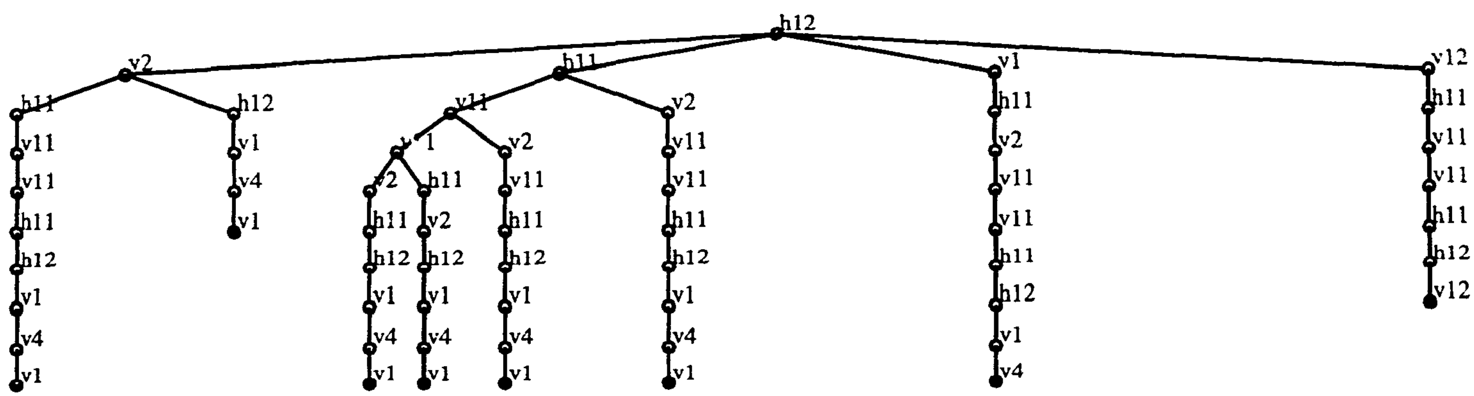

Digit 6 [continued]

421 Samples

677 Nodes

9 Paths [Number of SubTree Terminal Nodes]

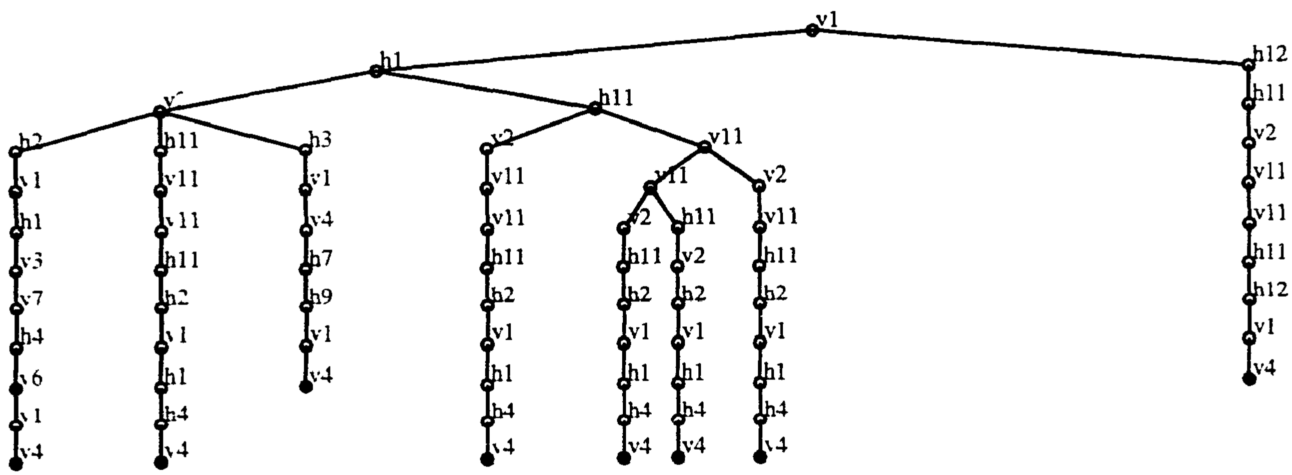

C.18 First Level Subtrees for Digit 7

430 Samples

226 Nodes

4 Paths [Number of SubTree Terminal Nodes]

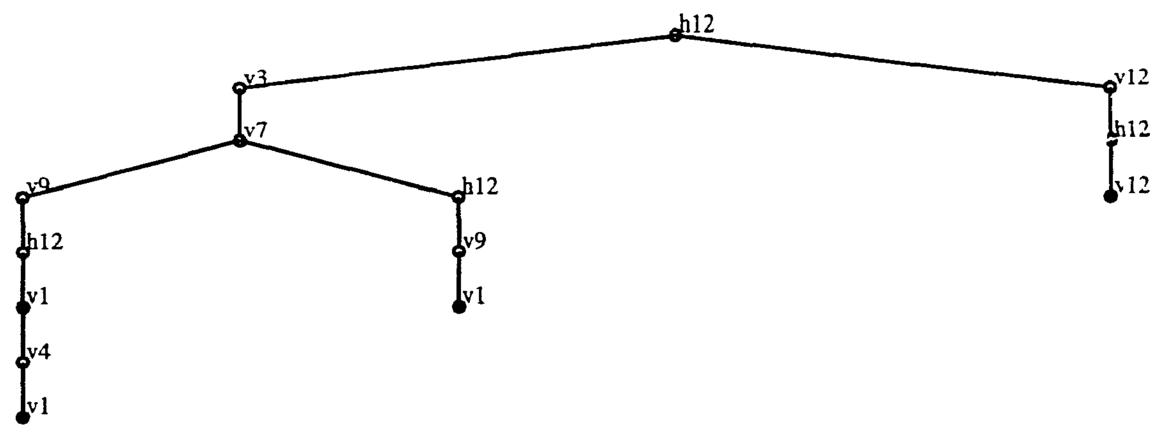

Digit 7 [continued]

430 Samples
226 Nodes
34 Paths [Number of SubTree Terminal Nodes]

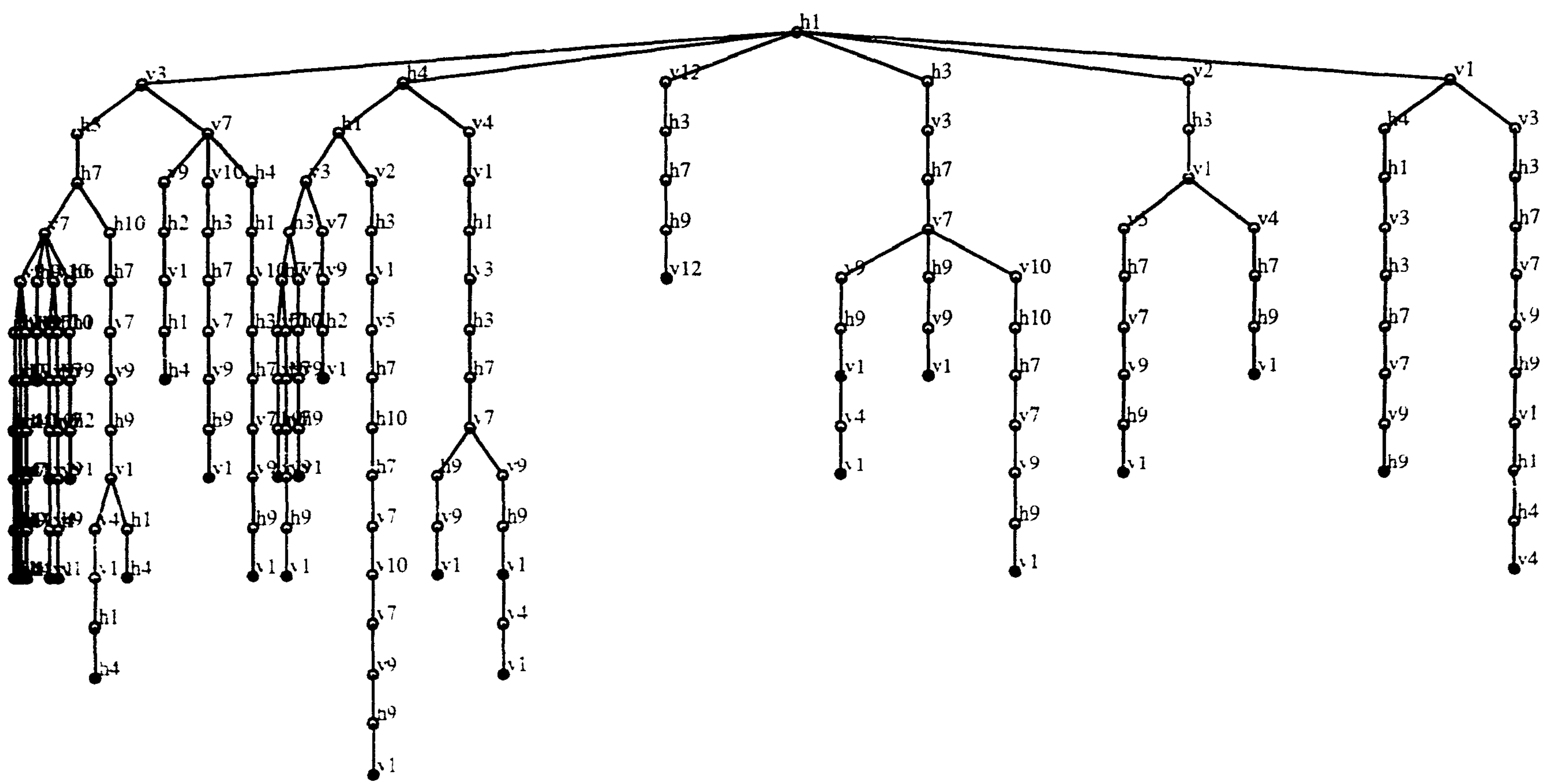

Digit 7 [continued]

430 Samples

226 Nodes

2 Paths [Number of SubTree Terminal Nodes]

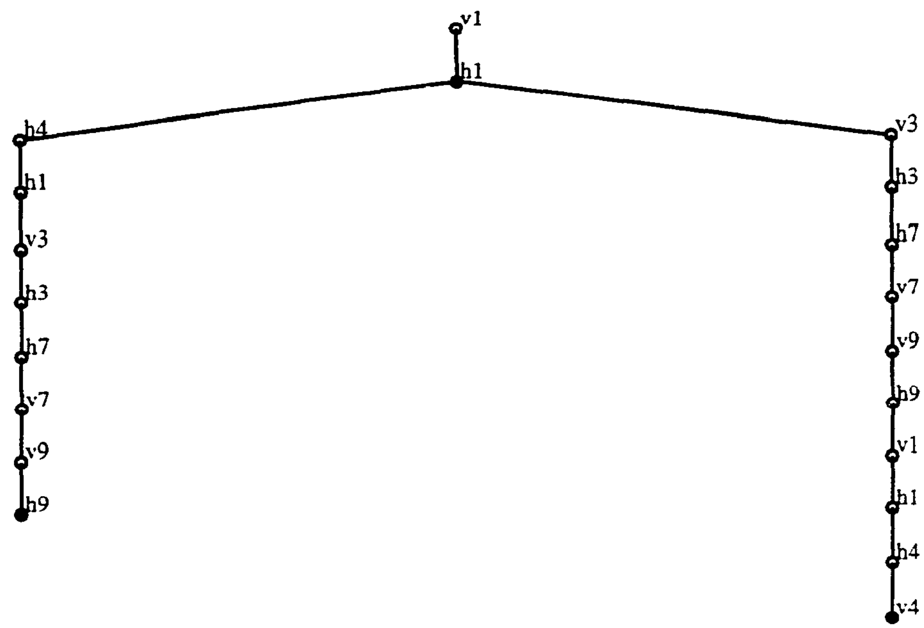

C.19 First Level Subtrees for Digit 8

423 Samples

1747 Nodes

139 Paths [Number of SubTree Terminal Nodes]

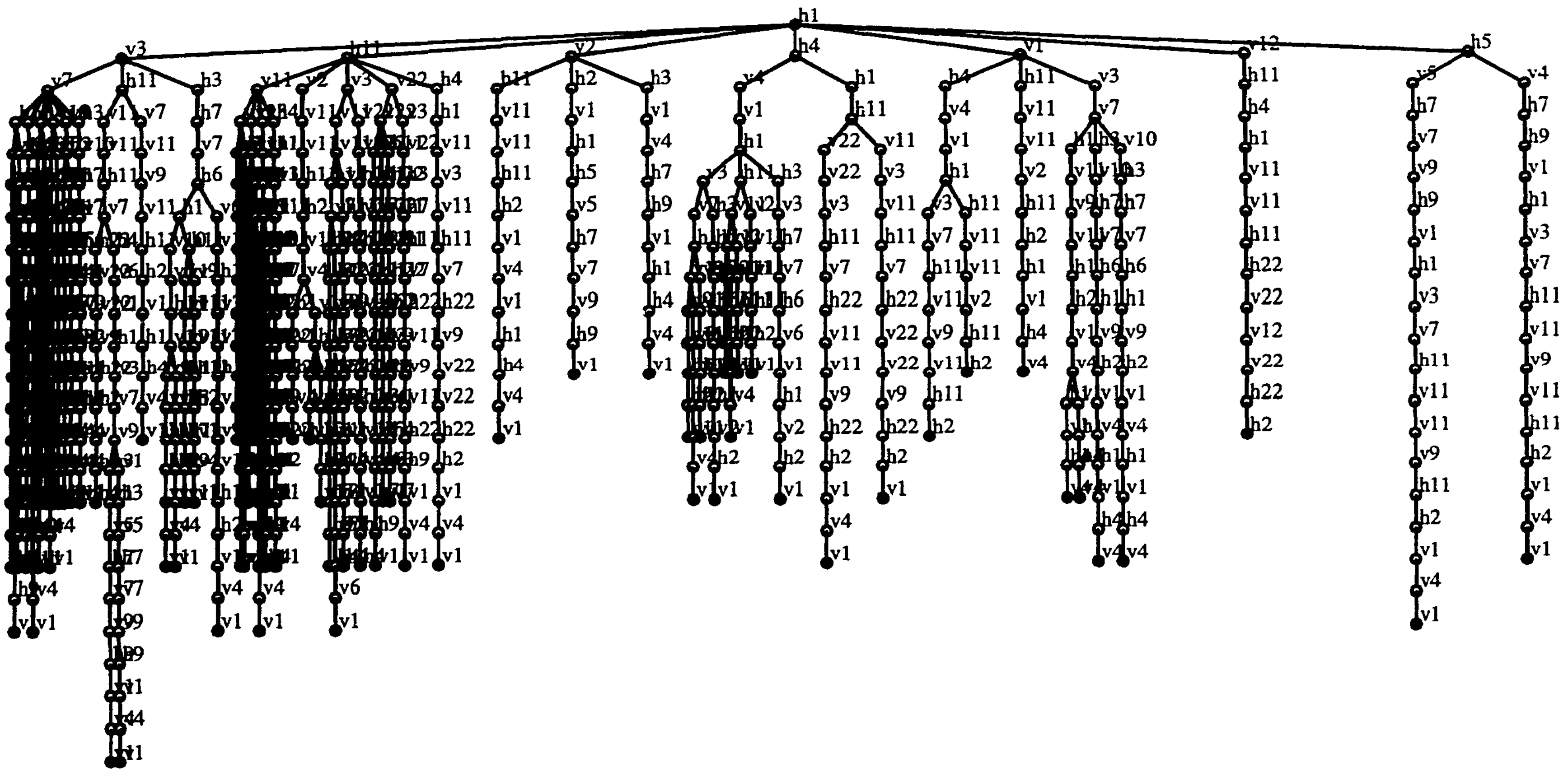

Digit 8 [continued]

423 Samples

1747 Nodes

68 Paths [Number of SubTree Terminal Nodes]

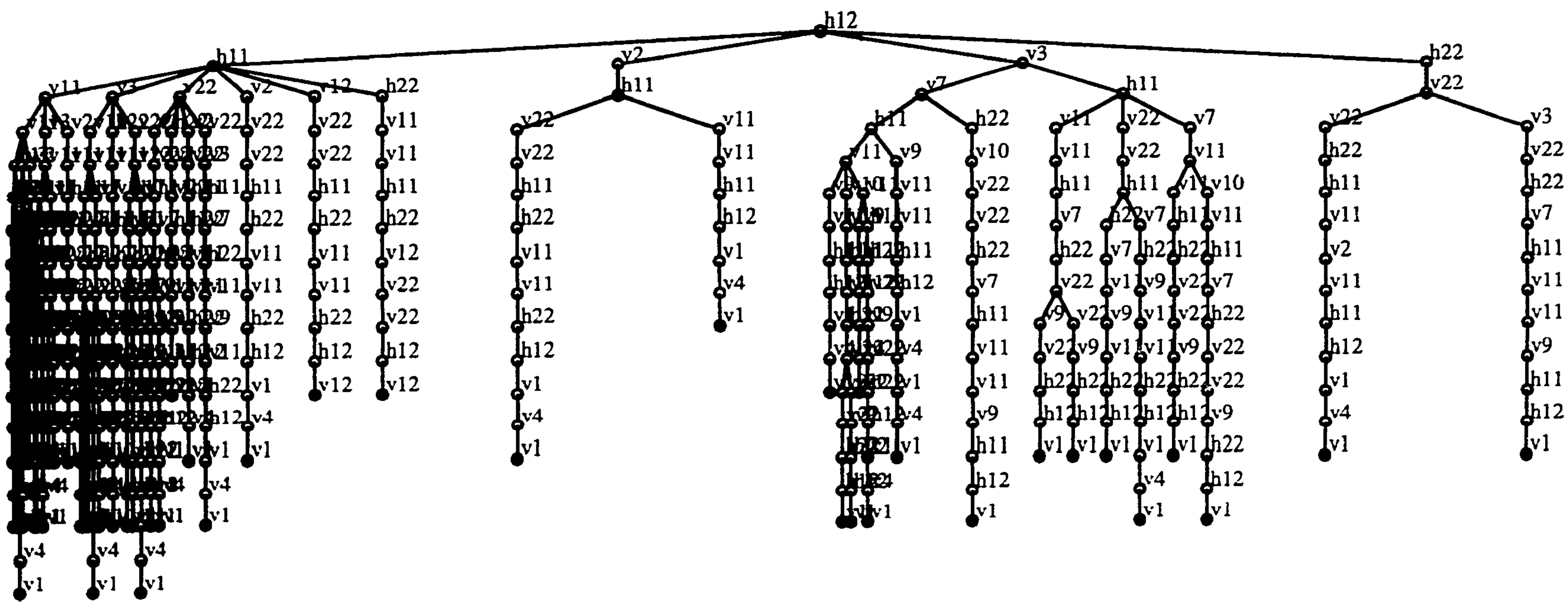

Digit 8 [continued]

423 Samples

1747 Nodes

3 Paths [Number of SubTree Terminal Nodes]

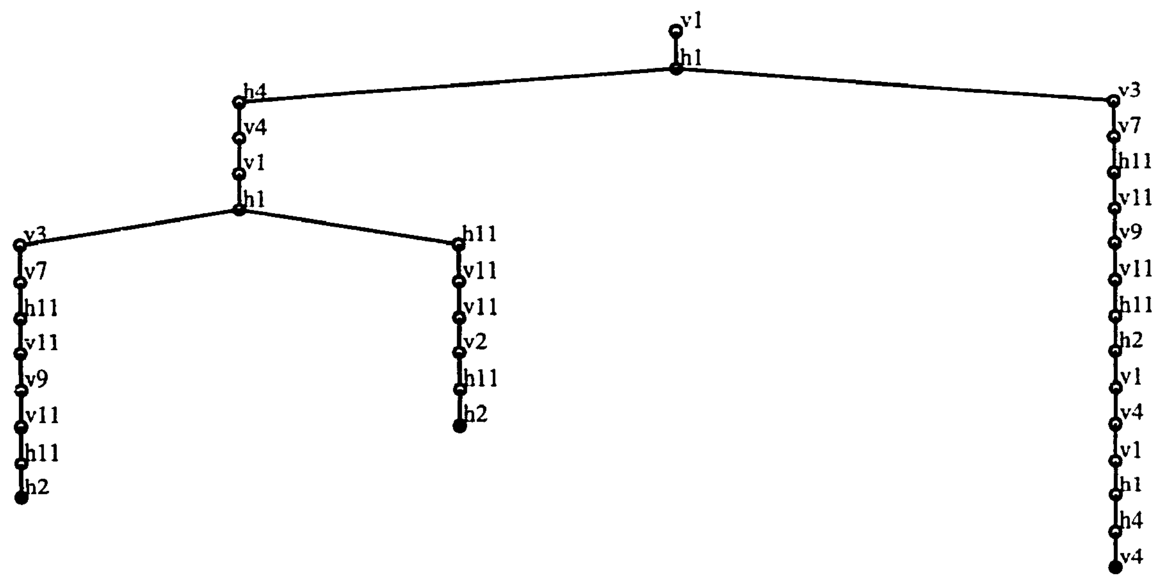

Digit 8 [continued]

423 Samples

1747 Nodes

1 Paths [Number of SubTree Terminal Nodes]

C.20 First Level Subtrees for Digit 9

426 Samples

571 Nodes

78 Paths [Number of SubTree Terminal Nodes]

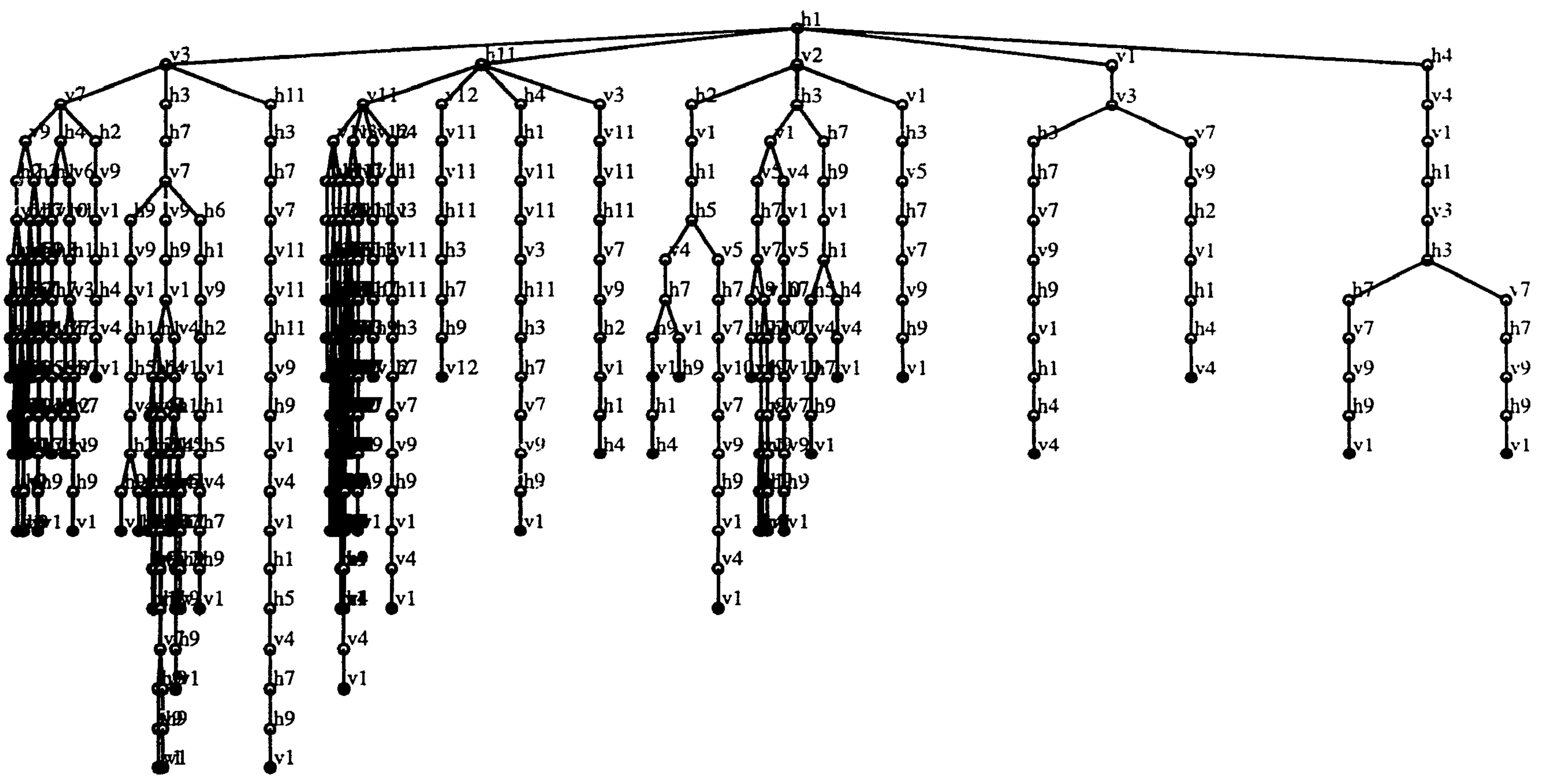

Digit 9 [continued]

426 Samples

571 Nodes

14 Paths [Number of SubTree Terminal Nodes]

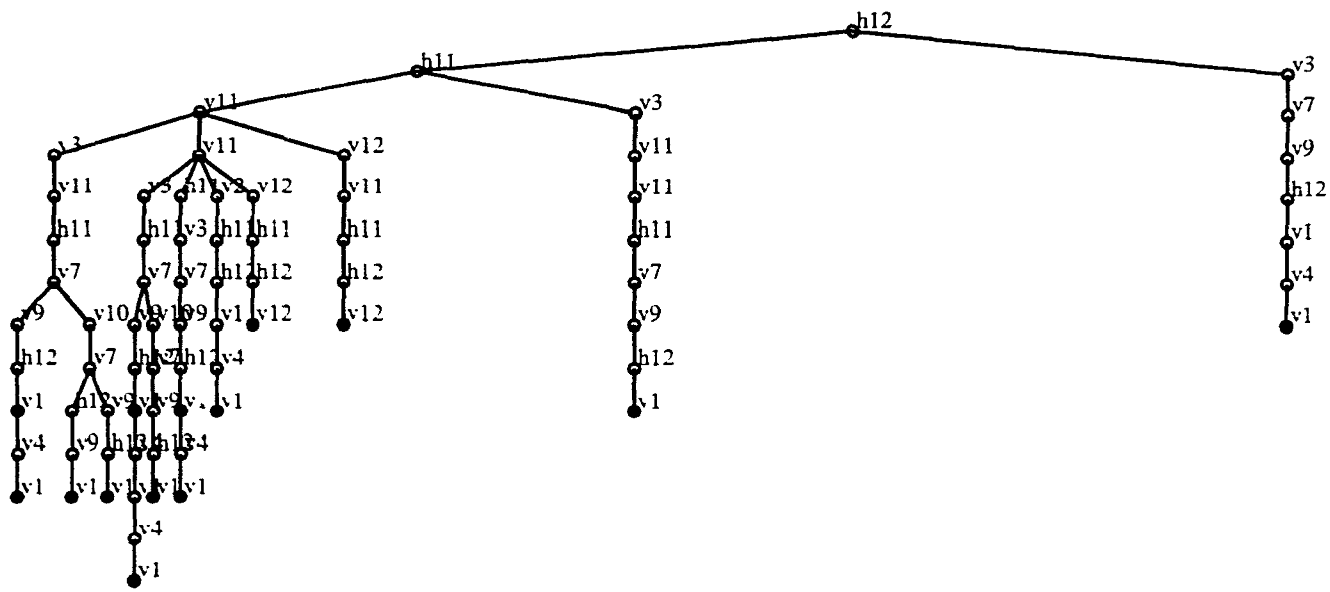

Digit 9 [continued]

426 Samples

571 Nodes

2 Paths [Number of SubTree Terminal Nodes]